Nuclear Factor I in Malignant Glioma

by

Miranda Brun

A thesis submitted in partial fulfillment of the requirements for the degree of

Doctor of Philosophy

in

Experimental Oncology

Department of Oncology
University of Alberta

Abstract

Malignant glioma (MG), comprised of grade III (anaplastic astrocytoma) and grade IV (glioblastoma) astrocytoma, is the most common adult brain tumour, with an incidence of ~4 in 100 000 people. Despite aggressive treatment with surgery, radiation, and chemotherapy, survival remains dismal, with median survival of 2-3 years for grade III, and 14.6 months for grade IV astrocytomas. MGs are hypothesized to arise from cells in the glial cell lineage based on expression of glial genes including glial fibrillary acidic protein (GFAP) and brain fatty acid-binding protein (B-FABP, FABP7). In MG, B-FABP expression correlates with poor prognosis, and increased migratory activity in MG cell lines. During development, B-FABP is expressed in a type of neural stem cells called radial glial cells. Following the onset of gliogenesis, expression of GFAP is activated in these cells. The Nuclear factor I (NFI) family of transcription factors, consisting of four family members (NFIA, B, C, X), are expressed in the developing brain, and are necessary for normal glial cell differentiation, including expression of GFAP.

NFI binding sites are present in the promoters of both *B-FABP* and *GFAP*, and NFI family members are expressed in MG cells. We examined the role of NFI family members in regulating expression of *B-FABP* and *GFAP* in MG cell lines. We show that NFIs bind to the promoters of the *B-FABP* and *GFAP* genes and regulate their expression, with all four NFIs contributing to their regulation. Of note, we show that NFI-dependent regulation is promoter and promoter-context dependent. We also observe compensation between NFI family members, which suggests cross-talk between NFIs.

Given the vital role of NFI in gliogenesis, and expression of NFI in MG cells, we sought to identify additional NFI target genes in MG. Using chromatin immunoprecipitation (ChIP)-on-chip, we identified 403 putative NFI target genes, including the Notch effector *HEY1*. HEY1 promotes maintenance of neural progenitor cells during development, and its expression correlates with decreased survival in MG. Here, we show that NFI binds to NFI binding sites in the *HEY1* promoter, and represses expression of *HEY1* in MG cells.

NFI is differentially phosphorylated in MG cell lines, and hypophosphorylated NFI correlates with expression of B-FABP and GFAP in these cells. Previously, a phosphatase activity was identified in cells with hypophosphorylated NFI that was absent in cells with hyperphosphorylated NFI. We show that the phosphatase calcineurin regulates NFI dephosphorylation and activation in MG cells. Furthermore, we identify a cleaved, activated form of calcineurin that localizes to the nucleus and is specifically found in MG cells with hypophosphorylated NFI. Immunohistochemical analysis of grade IV astrocytoma tumour tissues reveals the presence of calcineurin in the nucleus of cells found in areas of infiltration/migration. Taken together, our findings demonstrate an important role for NFI in regulation of genes involved in glial cell differentiation in MG cells, and reveal a novel calcineurin-NFI regulatory axis that further regulates NFI-dependent promoter activity in these cells.

Preface

The research in this thesis was conducted with assistance or in collaboration as noted below.

Chapter 2 has been published as Brun M*, Coles JE*, Monckton EA, Glubrecht DD, Bisgrove D, Godbout R. Nuclear Factor I regulates brain fatty acid-binding protein and glial fibrillary acidic protein gene expression in malignant glioma cell lines. Journal of Molecular Biology. 2009 391(2):282-300. *These authors contributed equally to this work. Constructs were prepared by Dr. Dwayne Bisgrove and Elizabeth Monckton. Gel shift assays were performed by Jeff Coles and Elizabeth Monckton. Elizabeth Monckton also provided assistance with reporter gene assays. Darryl Glubrecht provided technical assistance. I performed chromatin immunoprecipitations, reporter gene assays, western blot analysis and quantitative RT-PCR. I was responsible for data analysis, preparing the model, and writing the manuscript. Dr. Roseline Godbout carried out the Northern blot analysis, was involved in all stages of the project, and in writing the manuscript.

Chapter 4 has been published as Brun M, Glubrecht DD, Baksh S, Godbout R. Calcineurin regulates nuclear factor I activity in malignant glioma cell lines. Journal of Biological Chemistry. 2013 288(33):24104-24115. Darryl Glubrecht performed immunohistochemistry. Dr. Shairaz Baksh performed calcineurin activity assays. I was responsible for all other experimental procedures, experimental design, data analysis, imaging, and writing the manuscript. Dr. Roseline Godbout was involved in all stages of the project and in writing the manuscript.

Acknowledgements

This work would not have been possible without the unending support and guidance of Dr. Roseline Godbout. On the day she accepted me as her newest student, I joked that she could be stuck with me for ten years. That came close to being true. She gave me the freedom to pursue this project in the many directions it led, and throughout this journey her knowledge, encouragement, and patience were unfailing. Dr. Godbout's dedication to students extends far beyond expectation and requirement. I count myself tremendously fortunate to have had Roseline as my supervisor, and a mentor in the years to come.

This work has been supported by the numerous members of the Godbout Lab. Liz Monckton, Darryl Glubrecht, and Stanley Poon were invaluable for their help with experiments, especially Liz, for stepping in for radioactive experiments when I found myself unable. I was also lucky to have the company of many students in the lab. My ability to respond quickly, and debate on an array of subjects was sharpened through discussions with fellow students Devon, Matthew, Raja, Mike, and Tina. In addition, my time in the lab would not have been complete without the entire Godbout team; Lei, Lucy, Rong-Zong, Saket, Indrani, David, Elizabeth, Amit, Kevin, Erin, Jack and Xia.

I am in also in debt to my supervisory committee, Dr. Alan Underhill and Dr. Gordon Chan, for their advice and assistance throughout my PhD. Their questions and ideas helped shape the direction of this project. Their expertise and insight into many aspects of this project are greatly appreciated. This work was completed at the Cross Cancer Institute in the Department of Oncology In this environment I was

privileged to have the technical support of the Cell Imaging Facility, including Dr. Sun and Gerry Barron, the Gene Analysis Facility, and the Experimental Oncology support team. In addition, I was fortunate to meet and interact with many students in the Experimental Oncology graduate program, where I made many friends with whom I was able to share this experience, including David Sharon, Manik Chahal, and Sheena Macleod, who has been and continues to be my sounding board.

Finally, it is with heartfelt gratitude that I thank my family for their unwavering belief in me. My parents Eldon and Susan, and my brother and sisters, whose confidence in me surpassed my own, and my entire extended family, who offered support and encouragement in so many ways throughout my degree. I am very lucky to have the steadfast commitment of Ray Fendelet, who has felt the pain of this thesis as acutely as I have. He has patiently listened to countless one-sided scientific debates, and given me balance throughout this journey. Lastly, I am grateful to Myelle and Cormac, this thesis may have been finished sooner without them, but it wouldn’t have been nearly as much fun.

Table of Contents

List of Tables

List of Figures

Abbreviations

2-HG	2-Hydroxyglutarate
AA	Anaplastic astrocytoma
aa	Amino acids
ADAM	A disintegrin and metalloproteinase
a.k.a.	Also known as
AKAP	Protein A-kinase anchoring protein
AMPA	α-amino-3-hydoxy-5-methyl-4-isoxazolepropionic acid
AP2	Activating protein 2
ASCL1	Achaete-scute homolog 1
ATF5	Activating transcription factor 5
BCNU	Carmustine (bis-chloroethylnitrosourea)
B-FABP/FABP7	Brain fatty acid-binding protein
bHLH	Basic helix-loop-helix
BLBP	Brain lipid binding protein (B-FABP)
BMP	Bone morphogenetic protein
bp	Base pair
br	Binding region
BTSC	Brain tumour stem cell
CaM	Calmodulin
CAMKIV	Calcium/calmodulin-dependent kinase IV
cAMP	Cyclic adenosine monophosphate
CAT	Chloramphenicol acetyltransferase
CBP	CREB-binding protein
CCNU	Lomustine (chloroethyl-cyclohexyl-nitrosourea
CDK	Cyclin-dependent kinase
CDKN1A	Cyclin-dependent kinase inhibitor IA (p21)
CDKN2A	Cyclin-dependent kinase inhibitor 2A ($p14^{ARF}$ and $p16^{INK4A}$)
CDKN2B	Cyclin-dependent kinase inhibitor 2B
CDKN2C	Cyclin-dependent kinase inhibitor 2C
CGN	Cerebellar granular neuron
CHF	Cardiovascular helix-loop-helix factor
ChIP	Chromatin immunoprecipitation
CKI	Casein kinase 1
CNA	Calcineurin A
CNA-CA	Constitutively active calcineurin A
CNA-IN	Catalytically inactive calcineurin A
CNB	Calcineurin B
CNS	Central nervous system
CNTF	Ciliary neurotrophic factor

COUP-TF	Chicken ovalbumin upstream promoter-transcription factor
cpm	Counts per minute
CRAC	Ca^{2+} release activated Ca^{2+}
CREB	Cyclic AMP response element binding protein
CsA	Cyclosporin A
CT	Computerized tomography scan
CT-1	Cardiotropin 1
CTD	C-terminal domain
CTF	CCAAT-binding transcription factor
DAPI	4'6-diamidino-2-phenylindole
DDX1	Dead box 1
DLL	Delta like ligand
DMEM	Dulbecco's modification of Eagle's minimum essential medium
DMSO	Dimethyl sulfoxide
DNA	Deoxyribonucleic acid
DNA-PK	DNA-dependent protein kinase
DNMT1	DNA methyltransferase 1
dNTP	deoxyribose nucleotide triphosphate
DREAM	Downstream regulatory element antagonist modulator
DSCR	Down syndrome critical region
DTT	Dithiothreitol
E2F	E2 promoter binding factor
ECL	Enhanced chemiluminescence
ECM	Extracellular matrix
EDTA	Ethylenediaminetetraacetic acid
EGF	Epidermal growth factor
EGFR	Epidermal growth factor receptor
EGTA	Ethylene glycol tetraacetic acid
EMSA	Electrophoretic mobility shift assay
EMT	Epithelial-mesenchymal transition
ERBB2	Avian erythroblastic leukemia viral oncogene homolog 2
ERK	Extracellular signal-regulated kinase
EZH2	Enhancer of zeste homolog 2
FGFR3	Fibroblast growth factor receptor 3
FRAP	Fluorescence recovery after photobleaching
GABRA6	Gamma-aminobutyric acid type a receptor 6
GAPDH	Glyceraldehyde 3-phosphate dehydrogenase
GBM	Glioblastoma multiforme
G-CIMP	Glioma-CpG island methylator phenotype
GE	Ganglionic eminence
GFAP	Glial fibrillary acidic protein
GLAST	Glutamate aspartate transporter
GLDC	Glycine decarboxylase

GO	Gene ontology
GSK3	Glycogen synthase kinase 3
GTP	Guanine triphosphate
GTR	Gross total resection
Gy	Gray
h	Hour(s)
HA	Hemagglutinin
HER2	Human epidermal growth factor receptor 2
HES	Hairy and enhancer of split
HEY	Hairy/E(spl)-related with YPRW motif
HIF-1α	Hypoxia inducible factor 1α
HMG-CoA	3-Hydroxy-3-methyl-glutaryl-CoA
HRP	Horseradish peroxidase
HRT	Hairy-related transcription factor
IB	Immunoblot
ID4	Inhibitor of differentiation 4
IDH	Isocitrate dehydrogenase
IFRT	Involved field radiotherapy
IgG	Immunoglobulin G
IL	Interleukin
IP	Immunoprecipitation
JAG-1	Jagged-1
JAK	Janus kinase
KSR2	Kinase suppressor of Ras 2
LIF	Leukemia inhibitor factor
LM-PCR	Ligation mediated-polymerase chain reaction
MADM	Mosaic analysis of double markers
MAG	Myelin-associated glycoprotein
MAML	Mastermind-like protein
MASH1	Mammalian homolog of achaete-scute homolog 1 (ASCL1)
MBP	Myelin binding protein
MCIP	Myocyte-enriched calcineurin interacting protein
MDM2/4	Mouse double minute 2/4 homolog
MEK	Mitogen-activated protein kinase kinase
MG	Malignant glioma
MGMT	O^6-methylguanine-DNA methyltransferase
min	Minute(s)
MMP	Matrix metalloproteinase
MMTV	Mouse mammary tumour virus
MRI	Magnetic resonance imaging
mRNA	Messenger ribonucleic acid
N-CoR	Nuclear receptor co-repressor
NEB	New England Biolabs
NEUROD4	Neuronal differentiation 4
NICD	Notch intracellular domain

NF1	Neurofibromatosis 1
NFAT	Nuclear factor of activated T cells
NFI	Nuclear factor I
NFκB	Nuclear factor kappa-light-chain-enhancer of activated B cells
NEFL	Neurofilament light polypeptide
NES	Nuclear export sequence
NLS	Nuclear localization sequence
PAI1	Plasminogen activator inhibitor
PBS	Phosphate buffered saline
PcG	Polycomb group complex
PRC2	Polycomb repressive complex 2
PDGFRA	Platelet derived growth factor receptor alpha
PEI	Polyethylenimine
PI3K	Phosphoinositide 3-kinase
PI3KCA	Phosphoinositide 3-kinase catalytic subunit alpha
PI3KR1	Phosphoinositide 3-kinase regulatory subunit alpha
PKA	Protein kinase A
PKC	Protein kinase C
PLP1	Proteolipid protein 1
PMSF	Phenylmethylsulfonyl fluoride
PNS	Peripheral nervous system
PP2B	Protein phosphatase 2B
PPase	Phosphatase
PPP3	Protein phosphatase 3
pRB	Retinoblastoma protein
PTEN	Phosphatase and tensin homolog
PVDF	Polyvinylidene fluoride
qPCR	Quantitative real-time polymerase chain reaction
RB	Retinoblastoma
RBP-Jκ	Recombining binding protein suppressor of hairless
RCAN	Regulator of calcineurin
REST	RE1 silencing transcription factor
RIPA	Radioimmunoprecipitation assay
RNA	Ribonucleic acid
RT	Radiotherapy
RT-PCR	Reverse transcriptase polymerase chain reaction
RTK	Receptor tyrosine kinase
s	Second(s)
SCLC	Small cell lung cancer
SDS	Sodium dodecyl sulfate
SHH	Sonic hedgehog
SHMT2	Serine hydroxymethyltransferase
siRNA	Small interfering ribonucleic acid
STR	Subtotal resection
STAT	Signal transducer and activator of transcription

TBE	Tris-borate-EDTA buffer
TBP	TATA-binding protein
TCGA	The Cancer Genome Atlas Research Network
TFIIB	Transcription factor II B
TGF-β	Transforming growth factor beta
TMA	Tissue microarray
TMZ	Temozolomide
TNF-α	Tumour necrosis factor alpha
TRESK	TWIK-related spinal cord potassium channel
TSC1/2	Tuberous sclerosis 1/2
UK	United Kingdom
uPA	Urokinase plasminogen activator
VEGF	Vascular endothelial growth factor
VEGFR	Vascular endothelial growth factor receptor
VZ	Ventricular zone
WBRT	Whole-brain radiotherapy
WHO	World Health Organization

Chapter 1

INTRODUCTION

1.1 Malignant Glioma

1.1.1 Malignant glioma classification and epidemiology

In the central nervous system (CNS), there are two main types of cells: neurons and glia. Tumours of the CNS are classified based on histological identification of the prevalent cell type. Gliomas, which can arise from glial cells, account for 81% of malignant brain tumours (Ostrom et al., 2014a). Gliomas are further subdivided based on prevalent cell type: astrocytomas are primarily composed of neoplastic astrocytes, oligodendrogliomas are predominantly composed of neoplastic oligodendrocytes, ependymomas of cells with ependymal characteristics (Louis et al., 2007). Tumours of mixed cell types, such as oligoastrocytomas, contain a combination of two distinct neoplastic cell types (Louis et al., 2007; Ostrom et al., 2014a; Zhu and Parada, 2002). These tumours are further classified into grades (I to IV) based on histopathological and clinical presentation parameters established by the World Health Organization (WHO) (Louis et al., 2007). Accurate grading of tumours is important for two reasons: (i) to predict biological behavior, and treat appropriately, and (ii) to facilitate international communication and research (Louis et al., 2007). Astrocytomas are by far the most common glioma subtype, accounting for more than 80% of gliomas (Dolecek et al., 2012).

Astrocytomas are graded based on mitotic activity, infiltration, nuclear atypia, microvascularization and necrosis. Grade I astrocytoma, also known as pilocytic astrocytoma, is a brain tumour that normally affects children or young adults. These tumours have a low proliferative potential, are often well-

circumscribed, rarely recur at a higher grade, and can commonly be cured solely by surgical resection (Dunham, 2010; Louis et al., 2007; Marko and Weil, 2012). Similar to pilocytic astrocytoma, diffuse astrocytomas (grade II) are characterized by low proliferative potential; however, grade II astrocytomas are commonly infiltrative, may display occasional nuclear atypia, and often recur at a higher grade (Louis et al., 2007). Anaplastic astrocytoma (AA) (grade III) and glioblastoma (GBM) (grade IV), collectively referred to as high grade astrocytoma or malignant glioma (MG), display nuclear atypia, mitotic activity, and widespread infiltration. In addition, glioblastoma tumours exhibit microvascular proliferation and/or necrosis (Figure 1-1) (Louis et al., 2007; Ostrom et al., 2014a).

Increasing the complexity of MG, GBM can be further separated into primary and secondary GBM. Primary GBM arise *de novo*, while secondary GBM occurs from malignant transformation of a lower-grade tumour (DeAngelis, 2001). Primary GBM commonly occurs in an older population (mean age 55), while secondary GBM presents in patients ≤45 (DeAngelis, 2001; Kleihues et al., 2000). In addition, alternative genetic pathways are detected in these two subtypes (discussed in Section 1.1.3). Although MG accounts for the majority of adult human brain tumours, incidence is rare, affecting approximately ~3-5/100 000 people/year (Deorah et al., 2006; Kleihues and Sobin, 2000). These tumours are more common in males than females (3:2), and as with many malignancies, incidence increases with age, with highest incidence in the 75-84 age group (Dubrow and Darefsky, 2011; Ostrom et al., 2014a).

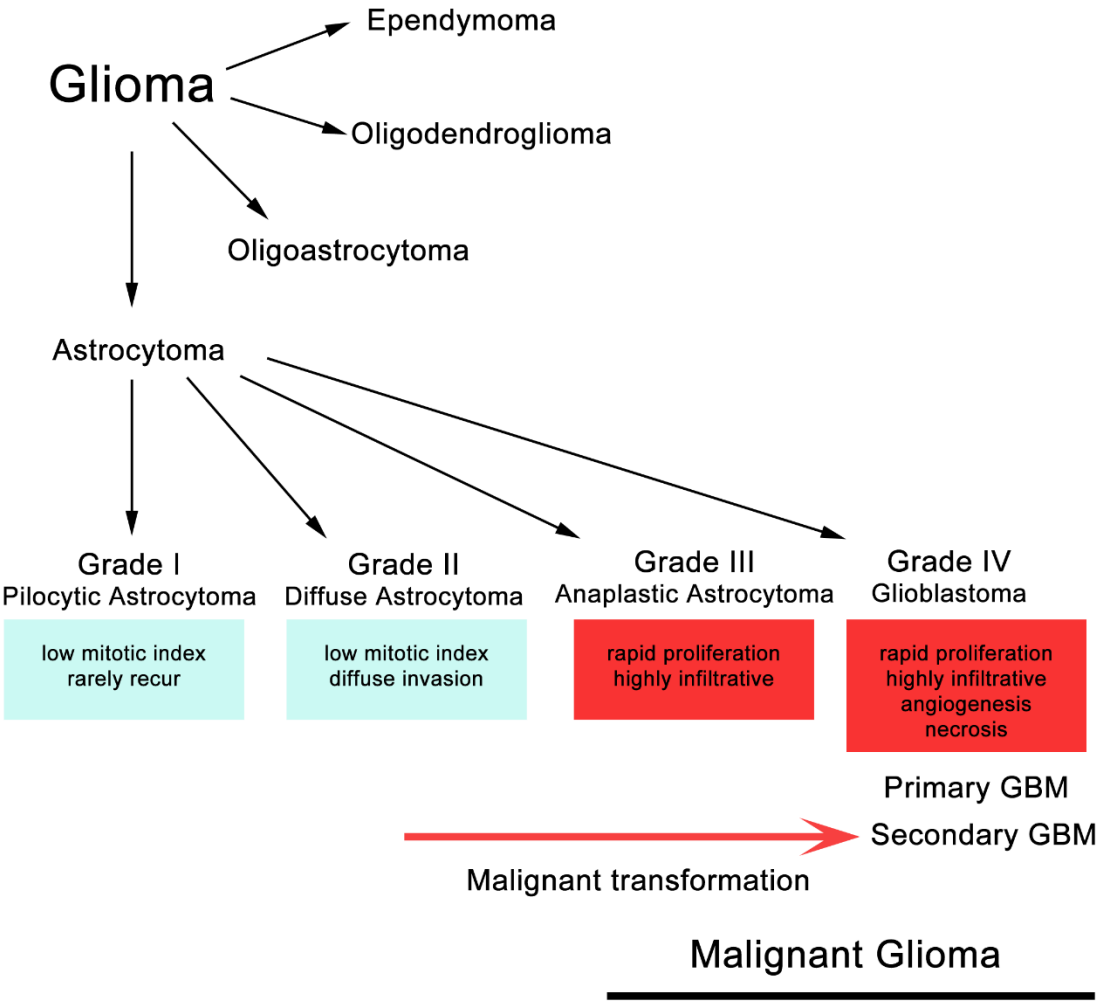

Figure 1-1: Glioma classification

Genetic risk factors can contribute to an increased risk for all glioma. Li-Fraumeni syndrome, characterized by germline mutation of *TP53,* encoding p53 protein, results in predisposition to a number of cancers, with 10% of patients developing glioma, predominantly astrocytoma, commonly at an early age (<45) (Hottinger and Khakoo, 2009; Kleihues et al., 1995). Tuberous sclerosis, resulting from disruption of tuberous sclerosis 1 (*TSC1)* or *TSC2,* is associated with a 5-15% incidence of grade I astrocytoma; however, these tumours rarely recur or undergo malignant transformation (Hottinger and Khakoo, 2009; Ostrom et al., 2014a). Patients with Neurofibromatosis 1 (NF1), caused by disruption of the *NF1* gene which encodes neurofibromin, have a high incidence (15% of patients) of developing pilocytic (grade I) astrocytomas (Lewis et al., 1984; Zhu and Parada, 2001). Together, these syndromes account for only a very small proportion of all glioma cases.

Additional risk factors for gliomas include exposure to ionizing radiation. Exposure to therapeutic doses of ionizing radiation results in increased glioma risk, which has been clearly characterized in children treated for acute lymphoblastic leukemia (Neglia et al., 1991; Ohgaki, 2009; Ostrom et al., 2014b). Use of mobile cell phones has been widely investigated as a putative risk factor for glioma. Multiple studies have failed to find a significant association between cell phone use and glioma (Deltour et al., 2012; Little et al., 2012; Swerdlow et al., 2011); however, as cell phones have only become widely used in the last 20 years, the effects of long term usage remain to be seen.

1.1.2 Malignant glioma treatment and survival

MG is treated aggressively with a combination of surgery, radiation, and chemotherapy. Despite this aggressive approach, long term survival remains elusive, with median survival times of 2-3 years for grade III, and 9-15 months for grade IV patients (Louis et al., 2007; Ohgaki and Kleihues, 2005b). Malignant transformation of grade II astrocytomas is common, and approximately 70% of these tumours recur as higher grade disease within 10 years of initial diagnosis despite treatment (Furnari et al., 2007; Louis et al., 2007).

Following identification of a brain tumour by CT or MRI imaging, surgery is planned. The aim of surgery is three-fold: (i) identification and diagnosis by histopathological and cytogenetic analysis of tumour tissue, (ii) debulking of tumour to relieve symptoms, and (iii) increase survival time by removing as much of the tumour as possible to achieve minimal residual disease. Depending on the location of the tumour, surgery may be a biopsy, subtotal resection (STR), or gross total resection (GTR). GTR is advised whenever possible to increase survival time, as greater extent of resection correlates strongly with patient survival. However, this must be balanced with preservation of functional brain regions (Hardesty and Sanai, 2012; Sanai and Berger, 2008; Simpson et al., 1993; Stummer et al., 2008). As MG is highly infiltrative, even aggressive surgery such as GTR is not curative and tumours invariably recur. Despite the significant tumour infiltration seen in MG, metastasis outside the brain is exceedingly rare (Lun et al., 2011).

Following definitive diagnosis of MG following surgery, the standard of care for newly diagnosed MG is radiotherapy (RT) with concurrent chemotherapy with

the alkylating agent temozolomide TMZ). RT with a total dose of 60 Gy is delivered as involved field RT (IFRT), in fractions of 1.8-2 Gy over the course of ~6 weeks (Mason et al., 2007). Post-operative RT was first used as standard of care starting in the 1970s, given as whole-brain RT (WBRT). Studies by the Brain Tumor Cooperative Group identified a significant increase in survival time for patients treated with WBRT compared to no RT control (Walker et al., 1976; Walker et al., 1978; Walker et al., 1980). Doses beyond 60 Gy did not produce increased survival time, and resulted in radiation necrosis of normal brain (Nelson et al., 1988; Salazar et al., 1979). WBRT was replaced by IFRT as the standard of care following studies that found no difference in survival between patients treated with WBRT and IFRT (Onoyama et al., 1976; Phillips et al., 2003; Sharma et al., 2003).

Emerging techniques in radiotherapy aim to increase efficacy, decrease side-effects, and/or improve delivery methods. Accelerated fractionation delivers more than one fraction of radiation per day to decrease total treatment time, and hyperfractionation refers to smaller fractions delivered more frequently to allow for a higher total dose without added toxicity (Withers et al., 1982). Clinical trials examining both accelerated fractionation and hyperfractionation showed no advantage over current practices (Fiveash and Spencer, 2003; Fulton et al., 1992; Mason et al., 2007; Prados et al., 2001). Stereotactic radiosurgery to deliver high radiation doses specifically to tumours over the course of one to five fractions, and fractionated stereotactic radiosurgery, whereby smaller doses are delivered over the course of more fractions, have also been investigated, especially for recurrent glioblastoma (Larson et al., 1990). Though clinical trials have yet to demonstrate

improved outcomes, additional research in this field may yield more promising results (Barani and Larson, 2015; Cardinale et al., 2006; Souhami et al., 2004).

The current Canadian standard of care calls for concurrent administration of the alkylating agent TMZ with radiotherapy at a daily dose of 75 mg/m^2 for 42 days. Following completion of radiotherapy, adjuvant TMZ is given at a dose of 150 to 200 mg/m^2 per day for 5 consecutive days over a 28-day schedule for six cycles if well tolerated (Mason et al., 2007). The addition of TMZ to the standard of care resulted in an increase in the median survival of GBM from 12.1 months to 14.6 months, the largest increase in survival time since the introduction of radiotherapy (Stupp et al., 2005). In addition, the two year survival for GBM increased from 10.4% to 26.5%, and five year survival from 1.9% to 9.8% (Stupp et al., 2009).

TMZ is a prodrug produced through rational drug design by the UK Cancer Research Campaign (Newlands et al., 1997). TMZ alkylates N^7 guanine, O^3 adenine and O^6 guanine positions in DNA (Denny et al., 1994). The cytotoxic lesion is the 0^6 methylguanine, which results in futile cycling of the mismatch repair pathway and signaling for apoptosis (Stupp et al., 2001). Prior to the introduction of TMZ, other alkylating drugs including the nitrosoureas carmustine (BCNU) and lomustine (CCNU), as well as procarbazine, were used but did not significantly improve survival (Shapiro et al., 1989). Interestingly, although the increase in median survival following concurrent and adjuvant treatment with TMZ was only ~2.5 months, a subset of patients whose tumours showed epigenetic silencing of the O^6-methylguanine-DNA methyltransferase (*MGMT*) gene had a 21.7 month

median survival in the TMZ-treated cohort compared to 15.3 months for the cohort treated with radiation only (Hegi et al., 2005). Comparatively, in patients with tumours that had unmethylated MGMT promoters, treatment with TMZ only increased median survival to 12.7 months compared to 11.8 months for radiation only (Hegi et al., 2005). MGMT removes the alkyl group from the O^6 position of guanine in a stoichiometric reaction, repairing the lesion (Fukushima et al., 2009). Methylation of the *MGMT* promoter results in promoter silencing, and loss of MGMT expression (Watts et al., 1997), and the *MGMT* gene is methylated in 30-40% of MG (Esteller et al., 1999; Mellai et al., 2012). Thus, while patients with methylation of the *MGMT* promoter respond well to TMZ, the drug has little impact on survival for patients with an unmethylated *MGMT* promoter (Hegi et al., 2005).

New therapies, included targeted therapies, are currently being investigated for the treatment of MG. GBM tumours are highly vascularized and anti-angiogenic therapy is a potential therapy. Bevacizumab is a humanized monoclonal antibody to vascular endothelial growth factor A (VEGF-A). Addition of bevacizumab to the current radiotherapy and TMZ protocol in newly diagnosed GBM does not significantly increase overall survival (Chinot et al., 2014), but is used for recurrent MG, and may increase progression-free survival (Easaw et al., 2011; Friedman et al., 2009). Cilengitide, which selectively inhibits $\alpha_v\beta_3$ and $\alpha_v\beta_5$ integrins, recently failed to show benefit in a phase III clinical study despite early promise (Stupp et al., 2014). Additional drugs targeting multiple signaling pathways are also currently being investigated including multiple drugs targeting receptor tyrosine kinases. Unfortunately, the redundancy of signaling pathways, activation of multiple

signaling pathways in MG, the heterogeneous nature of these tumours, and the need to cross the blood-brain barrier vastly complicate successful drug development (Hamza and Gilbert, 2014; Jordan and Wen, 2015).

Immunotherapy may show the most promise for significant increases in survival in MG by using the immune system to identify and destroy tumour cells. Multiple immunotherapy approaches including vaccines are currently being investigated for MG. Tumour vaccines are designed to present tumour specific antigens to the host immune system to stimulate a tumour-specific response. Multiple methods of delivery and design are currently in the early stages of investigation (Bloch, 2015; Oh et al., 2015).

1.1.3 Molecular biology of malignant glioma

MG is a molecularly heterogeneous disease, consisting of multiple subtypes based on both clinical presentation and genetic characterization. Increasing this complexity, there is significant intratumoural heterogeneity. Within this diversity, recurrent chromosomal abnormalities have been identified, and three core signaling pathways have emerged as regularly dysregulated: p53, retinoblastoma (pRB), and receptor tyrosine kinase (RTK)/RAS/phosphoinositide 3-kinase (PI3K) signaling (Furnari et al., 2007; Louis et al., 2007). All three genetic pathways are disrupted in the majority of MG tumours, resulting in increased cell survival, proliferation, disruption of cell cycle checkpoints and apoptotic signaling (Chen et al., 2012). The Cancer Genome Atlas Research Network (TCGA) has undertaken comprehensive genomic, epigenomic, transcriptomic, and proteomic analysis of

GBMs. This study has highlighted the significance of these pathways in GBM, with 74% of GBM tumours containing genomic alterations in all three pathways (2008; Brennan et al., 2013; Noushmehr et al., 2010; Verhaak et al., 2010). In addition, numerous additional genetic alterations have been revealed that contribute to the heterogeneity and aggressiveness that characterize MG (Parsons et al., 2008).

The p53 signaling pathway regulates the cellular response to stress signals. When activated, this pathway blocks cell cycle progression by inhibiting cell proliferation and/or promoting apoptosis (Vousden and Prives, 2009). *TP53* encodes the transcription factor p53. In the absence of stress signaling, the E3 ubiquitin ligase MDM2 binds and degrades p53 ensuring that p53 is maintained at low levels (Honda et al., 1997; Kubbutat et al., 1997). Upon genotoxic stress, the MDM2-p53 interaction is disrupted, p53 is up-regulated and post-translationally modified, resulting in transcription of p53 target genes including the cell cycle regulator p21(*CDKN1A*) (el-Deiry et al., 1994; Horn and Vousden, 2007; Shieh et al., 1997). The tumour suppressor $p14^{ARF}$, which is transcribed from the *CDKN2A* locus, also regulates p53 by sequestering MDM2 to promote p53 activation (Horn and Vousden, 2007; Toledo and Wahl, 2006). Molecular profiling of MG has revealed disruption of the p53 signaling pathway in 87% of tumours (2008; Dunn et al., 2012). Disruption occurs through mutation or deletion of the *TP53* gene (35%), amplification of *MDM2* (14%) and closely related *MDM4* (7%), and mutation or deletion of *CDKN2A* (encoding $p14^{ARF}$) (49%) (2008). Interestingly, alterations in this pathway are mutually exclusive, such that a mutation is only found in one component of this pathway (Brennan et al., 2013; Ciriello et al., 2012). Mutation or

deletion of *TP53* is more common in secondary tumours, indicating that disruption of *TP53* may be an early event in tumourigenesis in lower grade astrocytomas (Dunn et al., 2012; Louis, 1994).

The RB pathway regulates cell proliferation. When pRB is phosphorylated, it interacts with and sequesters the E2F family of transcription factors. E2F family members regulate genes involved in DNA synthesis and cell cycle progression. pRB is phosphorylated by activated cyclin-dependent kinase (CDK) 4 and 6 (CDK4 and CDK6), releasing E2F transcription factors (Dick and Rubin, 2013). CDK4 and CDK6 are inhibited by cyclin dependent kinase inhibitors, including CDKN2B, CDKN2C, and $p16^{INK4A}$, which is transcribed from *CDKN2A*, the same locus as $p14^{ARF}$ (Dick and Rubin, 2013). Similar to p53 signaling, the RB pathway can be disrupted through multiple mechanisms; *RB1* mutation or deletion (11%), *CDK4* amplification (14%), *CDK6* amplification (1%), deletion or mutation of *CDKN2A* (52%), deletion of *CDKN2B* (47%), or deletion of *CKDN2C* (2%), resulting in uncontrolled cellular proliferation (2008; Knudsen and Wang, 2010).

The third core pathway frequently disrupted in MG is signaling through RTK/RAS/PI3K, encompassing signaling through growth factor receptors and downstream effectors including the PI3K pathway. The TCGA found mutations or amplification of the epidermal growth factor receptor (*EGFR*) in 45% of GBM tumours. One common mutation is deletion of exons 2-7 encoding a portion of the EGFR extracellular domain. This EGFRvIII mutant, which is constitutively active, accounts for approximately 50% of genetic disruptions involving *EGFR* (Dunn et al., 2012; Frederick et al., 2000; Huang et al., 1997; Narita et al., 2002). Other

RTKs are altered to a lesser extent, including mutation of *ERBB2* [also known as human epidermal growth factor receptor 2 (HER2)] (8%), and amplification of platelet derived growth factor alpha (*PDGFRA)* (13%) and *MET* (4%) (2008). The most commonly altered downstream effectors are phosphatase and tensin homolog (*PTEN)* (mutated or deleted in 36% of GBM tumours), *PIK3R1* (10%), *PIK3CA* (7%), and *NF1* (18%) (2008; Parsons et al., 2008). While alterations in downstream effectors of the PI3K pathway are mutually exclusive, similar to the p53 and RB pathways, alterations in RTKs are not mutually exclusive (Brennan et al., 2013).

Outside of the three core signaling pathways implicated in MG, a novel recurrent mutation of R132 in *IDH1* was identified by Parsons e*t al.* (2008) in 12% of the GBM genomes sequenced (Parsons et al., 2008). *IDH1* encodes isocitrate dehydrogenase I, a metabolic enzyme that catalyzes the oxidative decarboxylation of isocitrate to α-ketoglutarate, and production of NAPDH (Reitman et al., 2010). The R132 mutation is in the active site of the enzyme, is monoallelic, and confers ability to produce 2-hydroxyglutarate (2-HG) (Parsons et al., 2008; Ward et al., 2010). Mutation of *IDH2* at R172, analogous to the *IDH1* R132 mutation, has also been reported.

IDH1 mutations are more prevalent in younger patients whose MG tumours are characterized by *TP53* mutations. These *IDH1* mutations are associated with a better prognosis, even after correcting for confounding factors including age (Parsons et al., 2008). *IDH1/2* mutations are more common in grade III astrocytomas (73%) and secondary GBM (85%) than in primary GBM (5%), and

may identify a specific subset of MG tumours (Noushmehr et al., 2010; Yan et al., 2009). The mechanism of how IDH mutations contribute to MG remains unclear, but may be due to production of 2-HG. 2-HG is a competitive inhibitor of α-ketoglutarate-dependent dioxygenases, and consequently, elevated 2-HG results in inhibition of histone demethylases and the TET family of 5-methylcytosine hydroxylases (Xu et al., 2011). Studies using immortalized astrocytes demonstrate that *IDH1* R132 alters DNA methylation, resulting in widespread CpG island hypermethylation (Turcan et al., 2012). Promoter hypermethylation in MG tumours has been previously observed (Kim et al., 2006; Martinez et al., 2009), including hypermethylation of *MGMT* (Hegi et al., 2005). MG with widespread methylation is referred to as 'glioma-CpG island methylator phenotype (G-CIMP) (Noushmehr et al., 2010). There is strong correlation between *IDH1/2* mutations and G-CIMP, given that 98% of MG tumours with G-CIMP harbour mutations in *IDH1/2* (Turcan et al., 2012). In addition, as seen with IDH mutations, patients with G-CIMP tumours have significantly improved survival, independent of tumour grade (Noushmehr et al., 2010).

Extensive molecular profiling of MG has resulted in identification of 3-5 subtypes of disease, based on integration of genomic data (Brennan et al., 2013; Noushmehr et al., 2010; Phillips et al., 2006; Verhaak et al., 2010). These subtypes include mesenchymal, classical (proliferative), neural, proneural, and proneural with G-CIMP (Table 1-1). The mesenchymal subtype is characterized by increased incidence of NF1 disruption, expression of mesenchymal markers, high levels of necrosis, expression of NFκB pathway genes, and a gene expression profile

similar to cultured astrocytes (Brennan et al., 2013; Phillips et al., 2006; Verhaak et al., 2010). Classical tumours commonly show loss of PTEN and high levels of *EGFR* amplification or activation, no *TP53* mutations, and homozygous deletion of the *CDKN2A* locus, thereby disrupting p53 and RB signaling. These tumours also express markers of neural precursor cells, and gene expression profiling resembles an astrocyte specific gene expression profile (Brennan et al., 2013; Dunn et al., 2012; Verhaak et al., 2010). Neural subtype tumours express neuronal markers and are most similar to normal adult brain, while proneural tumours have the highest similarity to fetal brain, express genes involved in oligodendrocytic development, and harbour amplifications of *PDGFRA* and mutations in *TP53* (Phillips et al., 2006; Verhaak et al., 2010). In addition, a subset of proneural tumours also have *IDH1/2* mutations, and display G-CIMP (Noushmehr et al., 2010). Importantly, RNA-sequencing of single cells isolated from GBM tumours revealed that cells within the same tumour have molecular profiles correlating to different subtypes (Patel et al., 2014). This suggests that molecular subtyping of tumours may not reflect the entire tumour.

Secondary GBM and grade III tumours are virtually all classified as proneural, and many have *IDH1/2* mutations (Noushmehr et al., 2010; Phillips et al., 2006). Many of these tumours also display G-CIMP phenotype, which is tightly linked to IDH mutations (Noushmehr et al., 2010). This suggests that mutation of *TP53* and *IDH1/2* are early events in tumourigenesis, and other subtypes may develop as distinct diseases via alternative pathways. As characterization

Proneural	**Neural**	**Classical**	**Mesenchymal**
Oligodendrocytic signature	Oligodendrocyte, astrocytic, and neural gene expression	Astrocytic signature	Cultured astrocyte gene signature
PDGFRA amplification	neuronal markers	*EGFR* amplified/overexpressed	*NF1* loss/mutation
TP53 mutations		*PTEN* loss	mesenchymal markers
		CDKN2A loss	
Proneural +G-CIMP			
IDH1/2 mutation			
Secondary GBM			

Table 1-1: Malignant glioma subtypes

becomes increasingly specific, additional classifications may be added. These and future classifications may help improve design and testing of new therapies, predict survival and disease progression.

Invasion is a defining feature of MG, resulting in dismal survival due to tumour recurrence. Invasion of surrounding tissue follows a progression that mirrors cell migration during development (Dirks, 2001), with the most frequent routes of invasion being white matter tracts and the basement membranes of blood vessels (Parsa et al., 2005). Despite their migratory nature, MG metastasis outside the brain is exceedingly rare, occurring in less than 0.5% of cases (Hamilton et al., 2014; Lun et al., 2011). Invasion requires adhesion to the extracellular matrix (ECM), modification of the ECM, changes in cell contractility, cytoskeletal reorganization, and migration (Westphal and Lamszus, 2011). MG cells adhere to the ECM through multiple effectors including integrins, cadherins, and neural cell adhesion molecules (Cuddapah et al., 2014). Cells then detach from the ECM, remodel the ECM, and migrate. Cells remodel the ECM through expression of secreted matrix metalloproteinases (e.g. MMP-1, MMP-2 and MMP-9), the serine protease uPA, and membrane anchored ADAM proteases (Cuddapah et al., 2014; Rao, 2003). Expression of MMP-2, MMP-9, uPA, and ADAM12 is increased in MG tumours (Forsyth et al., 1999; Kodama et al., 2004; Wang et al., 2003; Yamamoto et al., 1994a; Yamamoto et al., 1994b). Cytoskeletal reorganization and migration is regulated by the Rho GTPases Rac1 and Rac3 which have been linked to MG cell migration (Chan et al., 2005; Nakada et al., 2007). Additional signaling

pathways and molecules also contribute to infiltration and migration, with new molecules continuously being identified.

Microvascular proliferation is a hallmark of disease progression, and an identifying feature of GBM tumours (Louis et al., 2007). Transformation of grade II/III astrocytomas to grade IV GBM is characterized by the presence of microvascular proliferation. Angiogenesis results from a network of interacting signaling pathways, including signaling through hypoxia inducible factor 1α (HIF-1α) that is stabilized in low oxygen conditions. The ensuing expression of HIF-1α downstream target genes, including vascular endothelial growth factors (VEGFs), results in activation of VEGF receptors (VEGFRs) and their downstream effectors (Kaur et al., 2005). HIF-1α can also be regulated downstream of EGFR, via the PI3K pathway, which is commonly activated in MG (Clarke et al., 2001). A number of additional factors also contribute to angiogenesis and microvascular proliferation in GBM (Dunn et al., 2012). Tumour vasculature is poorly organized, resulting in areas of hypoxia and edema. The latter upregulate angiogenic signaling and are often accompanied by areas of necrosis, an additional hallmark of GBM tumours (Furnari et al., 2007; Kaur et al., 2005; Kaur et al., 2004).

1.1.4 Gliomagenesis

Understanding the process of gliomagenesis has focused on identifying the critical steps that result in malignant transformation and determining in what cells these changes occur. Based on the glial nature of MG tumours, as exemplified by expression of glial fibrillary acidic protein (GFAP), MG was originally hypothesized

to arise from astrocytes in the adult brain (Kleihues et al., 1995). The cell-of-origin has come under extensive debate following the identification of neural stem cells in the adult brain, the detection of possible brain tumour stem cells, and findings from mouse models of glioma. There are now three main hypotheses for the cell-of-origin of MG: (i) neural stem cells within the postnatal/adult brain, (ii) progenitor cells, and (iii) de-differentiated astrocytes (Liu and Zong, 2012; Quinones-Hinojosa and Chaichana, 2007; Siebzehnrubl et al., 2011).

In the adult mouse brain, neurogenesis is restricted to two main compartments: the subventricular zone and the subgranular zone (Doetsch, 2003a). In the subventricular zone, neuroblast (type A) cells migrate as chains through tunnels formed by subventricular zone astrocytes (type B cells), and transit amplifying (type C) cells are scattered along these neuroblast chains (Doetsch, 2003a; Doetsch et al., 1997; Lois et al., 1996). Subventricular zone astrocytes act as neural stem cells, give rise to neurospheres and repopulate the subventricular zone after ablation of type A and type C cells (Doetsch et al., 1999a). Subventricular zone astrocytes express GFAP and maintain stem cell characteristics including extensive proliferative potential, ability to differentiate into multiple cell types, and self-renewal (Doetsch et al., 1999a). These cells are an attractive cell-of-origin for MG as they exist in a stem cell niche that is permissive for cell proliferation, located near blood vessels and the basal lamina, and exposed to growth factors. In addition, subventricular zone astrocytic neural stem cells are able to give rise to a heterogeneous population of cells, similar to what is observed

within a MG tumour, and these cells have the capacity for migration and invasion (Doetsch, 2003b).

Brain tumour stem cells (BTSCs), first identified by Singh *et al. (*Singh et al., 2003) in pediatric brain tumours, and in GBM by Galli *et al.* (Galli et al., 2004), refer to a small subset of tumour cells that are able to proliferate, self-renew, and differentiate, similar to neural stem cells, and to give rise to heterogeneous tumours, mirroring the tumours from which they are isolated. These cells have been hypothesized to be responsible for tumour growth, recurrence, and treatment resistance (Stiles and Rowitch, 2008). The nature of BTSCs has been widely debated. While CD133+ was initially used as a marker for these cells, there are reports indicating that CD133- cells can also act as BTSCs (Beier et al., 2007). More recent work suggests that MG tumours can harbour multiple cell populations with different phenotypes, expressing different markers, and showing different growth patterns, while maintaining the ability to self-renew and regenerate tumours (Chen et al., 2010).

In mouse models, different combinations of genetic mutations in subventricular zone astrocytes (adult neural stem cells) result in different types of brain tumours. Deletion of *PTEN* and *TP53* in subventricular zone astrocytes gives rise to gliomas, but these same mutations do not result in tumours when targeted to mature astrocytes (Jacques et al., 2010). Another mouse model where both *NF1* and *TP53* are deleted showed tumour formation when these deletions were targeted to the subventricular zone of adult mice; however, no tumours were observed when deletions were targeted specifically to the cortex or striatum, which

do not contain neural stem cells. These models suggest that neural stem cells or progenitor cells found in the subventricular zone (type C cells), but not mature astrocytes, are the cell-of-origin of MG.

Mosaic analysis of double markers (MADM) facilitates the analysis of changes in individual cell lineages prior to emergence of a tumour. In a MADM mouse model, inactivation of *TP53* and *NF1* in neural stem cells did not result in expansion of the neural stem cell population; however, there was substantial expansion of downstream progeny, specifically NG2+ oligodendrocyte precursor cells, which act as progenitor cells (Liu et al., 2011). Transcriptome analyses of these tumours revealed a molecular signature that matched the proneural subtype (Liu et al., 2011; Verhaak et al., 2010).

Recent work targeting differentiated cells in the CNS suggests that mature astrocytes and neurons can also give rise to MG in mice under specific conditions. Targeted knockdown of *TP53* and *NF1* or knockdown of *TP53* and expression of activated H-Ras in mature neurons of adult mice results in development of large tumours (Friedmann-Morvinski et al., 2012). Microarray analysis of these tumours reveals a molecular signature that corresponds closely with the mesenchymal subtype of GBM. Disruption of the same targets in mature astrocytes also results in tumours with a mesenchymal molecular signature (Friedmann-Morvinski et al., 2012). Knockdown of *TP53* and activation of H-Ras in neural stem cells using the same system also results in tumours; however, these tumours have a neural subtype molecular signature. These results support work done *in vitro* with astrocytes and neural stem cells demonstrating that both mature neurons and

mature astrocytes can form tumours following disruption of specific signaling pathways (Rich et al., 2001; Stiles and Rowitch, 2008; Uhrbom et al., 2005). Importantly, astrocytes can de-differentiate following genetic mutations commonly seen in MG, including deletion of the gene encoding $p16^{INK4A}$ and $p19^{ARF}$ (mirroring disruption of the *CDKN2A* locus) and activation of EGFR (Bachoo et al., 2002). Taken together, these results suggest that there may be more than one cell-of-origin for MG.

Mouse models and *in vitro* work have also revealed complexity regarding the genetic pathways leading to tumour formation, which is mirrored by the cellular and molecular heterogeneity seen in MG tumours. Genetically engineered mouse models reveal that multiple combinations of genetic disruptions can result in MG formation. For example, disruption of *NF1* alone does not lead to tumour formation; however, when combined with loss of *TP53,* MG tumours occur at high penetrance, but only when *TP53* inactivation occurs before or with *NF1* inactivation (Zhu et al., 2005). *PTEN* loss hastens tumour formation in this model, but loss of *PTEN* and *NF1* are not sufficient to cause tumours without *TP53* disruption (Kwon et al., 2008). Concomitant loss of *PTEN* and *TP53* in the mouse CNS results in aggressive MG tumours (Zheng et al., 2008). Loss of *RB1* in mouse astrocytes results in MG tumours with long latency. When combined with loss of *TP53*, there is no change in latency: however, when combined with loss of *PTEN*, tumours developed much more quickly (Xiao et al., 2002; Xiao et al., 2005).

EGFR is commonly overexpressed in MG tumours. Even so, overexpression of EGFR (wild-type or EGFRvIII) in adult mouse brain is insufficient

to produce MG tumours (Zhu et al., 2009). However, when EGFRvIII overexpression is combined with loss of $p16^{INK4A}$, $p19^{ARF}$ and PTEN, highly aggressive tumours are formed with high penetrance and short latency, compared to low penetrance and longer latency when wild-type EGFR is overexpressed (Zhu et al., 2009). Multiple additional mouse models of MG have been generated with combinations of alterations to mirror different genetic disruptions found in human MG tumours (Janbazian et al., 2014). These mouse models illustrate that different genetic alterations work in tandem, and the timing and combination of these alterations, in conjunction with the cells in which these alterations arise, contribute to the fundamental heterogeneity and complexity of gliomagenesis.

1.2 Gliogenesis

1.2.1 Development of the brain

During gastrulation, complex signaling between migrating cells specifies a population of cells in the ectoderm as neuroectodermal cells. These neuroectodermal cells are stem cells that give rise to neural tissue including the CNS and peripheral nervous system (PNS) (Stiles, 2008). The neural tube forms from the neural plate with neural precursor cells lining the surface of the hollow tube. As the brain grows, the hollow tube forms the basis of the ventricles, with the neural precursor cells lining the surface, referred to as the ventricular zone (Stiles, 2008; Stiles and Jernigan, 2010). The neural tube develops into the spinal cord, whereas the anterior end of the neural tube expands, and forms three brain vesicles which are precursors to the forebrain, midbrain, and hindbrain (Clark,

2002). Specification of the CNS occurs through neural patterning via exposure to morphogen gradients which are converted into transcription factor codes resulting in defined boundaries (Stiles and Jernigan, 2010). This spatial patterning results in neural precursor cells that give rise to different types of neurons and glia based on location within the developing brain (Briscoe et al., 2000; Jessell, 2000).

Neural precursor cells generate neurons and glia within proliferative regions of the developing brain including the ventricular zone and the ganglionic eminences. In the ventricular zone, neural precursor cells, also referred to as neural stem cells, first proliferate via symmetrical cell division to exponentially increase the pool of proliferating cells (Stiles, 2008). Brain cells are produced in a temporally controlled fashion, with neurons produced first, and glial cells second (Miller and Gauthier, 2007). At the onset of neurogenesis, neural precursor cells transition from neuroepithelial cells to radial glial cells (Pinto and Gotz, 2007). This occurs through loss of some epithelial characteristics, including loss of tight junctions, and gain of glial characteristics, including expression of brain fatty acid-binding protein (B-FABP, FABP7) (Anthony et al., 2004; Gotz and Huttner, 2005). Radial glial cells were originally believed to act solely as a scaffold for migrating neurons, but are now known to be the predominant neural precursor cell after the onset of neurogenesis (Anthony et al., 2004; Noctor et al., 2002) (Figure 1-2A). Along with B-FABP, radial glial cells are characterized by the expression of the intermediate filament proteins vimentin and nestin (Noctor et al., 2002; Park et al., 2009).

During neurogenesis a subset of radial glial cells undergo asymmetric division, giving rise to two daughter cells. One daughter cell remains in the ventricular zone, while the second migrates out of the ventricular zone and differentiates into a neuron (Figure 1-2A). In the neocortex, there are six layers of cells that form in an inside out manner, with the deepest layer containing the first neurons that are formed, and later-stage neurons found in progressively more superficial layers (Stiles, 2008). Later in development, radial glial cells also produce an intermediate progenitor cell that migrates to the subventricular zone, and symmetrically divides to produce either two neurons or two progenitor cells. In the adult subventricular zone, astrocytes (type B cells), acting as neural stem cells, asymmetrically divide to produce transit amplifying cells (type C cells), which in turn produce neuroblasts (see Section 1.1.3) (Doetsch, 2003a; Doetsch et al., 1999a; Doetsch et al., 1999b) (Figure 1-2B).

1.2.2 The gliogenic switch

There are three main types of glia cells found in brain: astrocytes, oligodendrocytes, and microglia. Glia cells account for 90% of the cells within the human brain. Astrocytes are heterogeneous and play many roles in the brain including structural support, metabolism, injury response, formation of the blood-brain barrier, and synapse formation (Allen and Barres, 2009). Astrocytes are also important for regulation of synaptic activity, including bidirectional signaling between neurons and astrocytes (Araque et al., 2014; Panatier et al., 2011). Oligodendrocytes form the myelin sheath that surrounds neuronal axons, acting

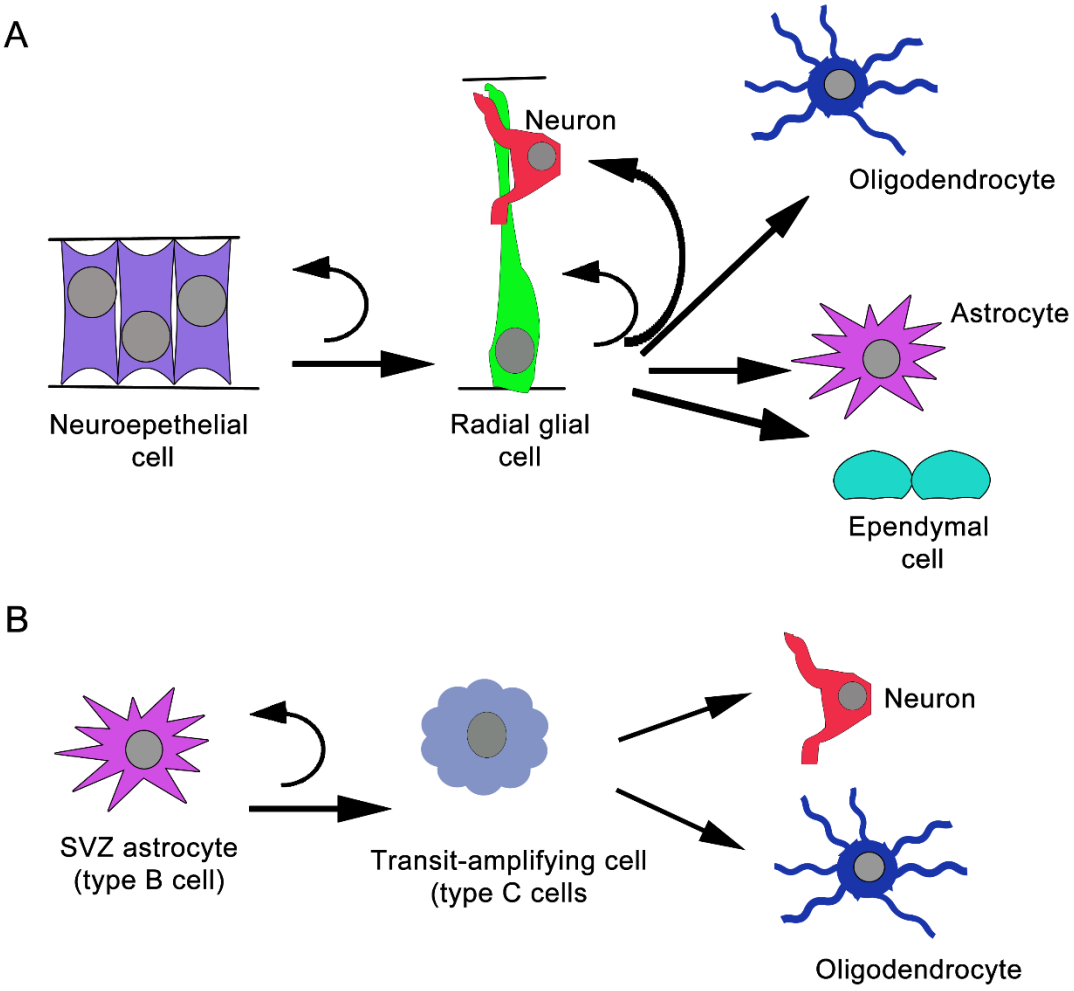

Figure 1-2: Neural precursor cell differentiation. (A) During development, neuroepithelial cells produce radial glial cells, which act as neural precursor cells giving rise to neurons and glial cells. (B) In the adult subventricular zone, subventricular zone (SVZ) astrocytes act as neural stem cells giving rise to neurons and glial cells.

as insulators for the efficient transmission of electrical impulses in neurons (Freeman and Rowitch, 2013). Microglia are the resident immune cells in the brain (Aguzzi et al., 2013). Microglia originate in the yolk sac and migrate to the neural tube during development (Aguzzi et al., 2013). During gliogenesis, first astrocytes and then oligodendrocytes arise from progenitor cells in the developing central nervous system following neurogenesis (Rowitch and Kriegstein, 2010).

The switch from neurogenesis to gliogenesis depends on both extrinsic and intrinsic signals that are temporally controlled (Okano and Temple, 2009). During neurogenesis, gliogenesis is repressed by limited progenitor cell competence and repression of necessary signaling and transcriptional pathways. During neurogenesis, epigenetic silencing of glial genes by CpG methylation inhibits transcription factor binding and activation (Namihira et al., 2004; Takizawa et al., 2001). In neural precursor cells, the DNA methyltransferase DNMT1 associates with the promoter of the glial gene *Gfap* to silence transcription (Namihira et al., 2009). In addition, expression of proneural basic helix-loop-helix (bHLH) proteins further inhibits gliogenesis (Ross et al., 2003; Sun et al., 2001b), and overexpression of proneural bHLH results in increased neurogenesis, and decreased gliogenesis (Cai et al., 2000; Miller and Gauthier, 2007). The proneural bHLH, neurogenin 1 (Ngn-1) binds and sequesters the transcriptional activator complex p300/CBP, which plays a vital role in gliogenic transcription through the Janus kinase-signal transducer and activator of transcription (JAK-STAT) pathway (Sun et al., 2001b). The JAK-STAT pathway is also repressed by inactivation

through the tyrosine phosphatase SHP-2-MEK-ERK pathway (Gauthier et al., 2007).

Independent of neurogenesis, gliogenic transcription is also inhibited in precursor cells to maintain undifferentiated cell populations. The nuclear receptor co-repressor (N-CoR), in complex with the Notch effector RBP-Jκ, binds to the promoter of *GFAP* and represses transcription. Brains from *Ncor1-/-* mice exhibit premature astrocyte differentiation (Hermanson et al., 2002). Activating transcription factor 5 (ATF5) is also important for maintenance of progenitor cells, and inhibits both neural and glial differentiation, preserving neural precursor cells (Angelastro et al., 2003; Angelastro et al., 2005; Mason et al., 2005).

Near the end of neurogenesis, radial glial cells become permissive to glial differentiation. Young neurons express Notch ligands, activating Notch signaling in radial glial cells (Namihira et al., 2009). Notch signaling induces expression of nuclear factor IA (NFIA), which binds to the promoters of astrocyte-specific genes, resulting in the dissociation of DNMT1, and demethylation of these astrocytic genes (Namihira et al., 2009). Chicken ovalbumin upstream promoter-transcription factor I and II (COUP-TFI and II) also contribute to glial competency: knock-down of *Coup-tfI/II* in neurospheres results in maintenance of *Gfap* promoter methylation, and a decrease in glial cells in the developing mouse brain (Naka et al., 2008). As radial glial cells gain glial competence, neurogenesis is inhibited. The proneural bHLH *Ngn1* is epigenetically inhibited by the polycomb group complex (PcG) (Hirabayashi et al., 2009), and proneural bHLHs are also inhibited

by negative bHLH proteins (Imayoshi and Kageyama, 2014; Nakashima et al., 2001).

The onset of gliogenesis is regulated by multiple signaling pathways. Activation of the JAK-STAT signaling pathway in radial glial cells by the IL-6 family of cytokines, which includes ciliary neurotrophic factor (CNTF), leukemia inhibitory factor (LIF), and cardiotropin 1 (CT-1), induces astrocyte formation (Barnabe-Heider et al., 2005; Bonni et al., 1997; Miller and Gauthier, 2007; Rajan and McKay, 1998). Young neurons secrete CT-1, which binds to the cytokine receptor gp130 and its co-receptor LIFR, activating JAK-STAT signaling (Barnabe-Heider et al., 2005). Upon phosphorylation of STAT1/3 by JAK, STAT1/3 translocates to the nucleus (Cattaneo et al., 1999) where it interacts with the transcriptional coactivator complex p300/CBP (Paulson et al., 1999), and activates transcription of astrocyte genes including *GFAP* and *S100β* (He et al., 2005). Bone morphogenetic protein (BMP) signaling also contributes to gliogenesis via activation of SMADs which synergistically interact with the STAT-p300/CBP complex (Nakashima et al., 1999). This occurs only once Ngn1 is repressed, as Ngn1 sequesters this complex during neurogenesis (Sun et al., 2001b). The MEK/ERK pathway also plays an important regulatory role. Deletion of *Mek1/2* in radial glial cells results in loss of gliogenic differentiation, with dramatic loss of astrocytes and oligodendrocytes, while overactivation of MEK increases the number of glial cells (Li et al., 2012).

Production of astrocytes and oligodendrocytes following induction of gliogenesis is regulated in a spatiotemporal manner with numerous gliogenic

regulators contributing to differentiation (Rowitch and Kriegstein, 2010). Expression of the bHLH factors Olig 1 and 2 are critical for oligodendrocyte specification and differentiation (Emery, 2010; Imayoshi and Kageyama, 2014; Zhou and Anderson, 2002). Sox9 promotes gliogenesis, while Sox10 specifically promotes oligodendrocyte specification and differentiation (Stolt et al., 2003; Stolt et al., 2002; Wang et al., 2014). Sox9 and Sox10 can both form complexes with NFIA and Olig2, and depending on expression of these components, modify astrocytic and oligodendrocytic genes and cell fate (Glasgow et al., 2014; Kang et al., 2012). The role of NFIA in gliogenesis and glial differentiation will be discussed further in Section 1.3.4

1.3 Nuclear Factor I (NFI)

1.3.1 The NFI transcription factor family

The transcription factor Nuclear Factor I (NFI) was first identified as a host-encoded DNA binding factor necessary for viral gene replication (Nagata et al., 1982; Nagata et al., 1983). Upon further examination, NFI was found to be identical in polypeptide composition and biochemical properties to the CCAAT-binding transcription factor (CTF) (Jones et al., 1987) that was first identified as a factor binding to CCAAT elements in various gene promoters (Cohen et al., 1986; Jones et al., 1985). This revealed that in addition to its role in viral gene replication, NFI is a sequence-specific transcription factor (Jones et al., 1987; Santoro et al., 1988). NFI binds to the palindromic consensus sequence TTGGC(N_5)GCCAA on double-stranded DNA (Borgmeyer et al., 1984; Gronostajski, 1986; Gronostajski et al.,

1985; Leegwater et al., 1986), and putative and validated NFI binding sites have been identified in a large variety of genes, including genes expressed in mammary, lung, and muscle tissue, and in the CNS (Amemiya et al., 1992; Hebbar and Archer, 2007; Lajoie et al., 2014; Messina et al., 2010; Murtagh et al., 2003).

The NFI transcription factor family consists of four family members in vertebrates: NFIA, NFIB, NFIC and NFIX (Gronostajski, 2000; Kruse et al., 1991; Rupp et al., 1990). Both *C. elegans* and *D. melanogaster* have a single NFI gene (Fletcher et al., 1999). NFI contains an N-terminal DNA binding and dimerization domain, and a C-terminal transactivation domain (Figure 1-3) (Mermod et al., 1989). The N-terminal domain is highly conserved (~80-90%) among NFI family members, while the C-terminus shows much more variability, ranging from 39-60% sequence homology at the protein level (Mason et al., 2009). All four NFI RNAs undergo alternative splicing, resulting in additional complexity and control. NFIs contain 11-12 exons, with the largest exon, exon two, containing the DNA binding and dimerization domain (Fletcher et al., 1999; Grunder et al., 2003). Splicing occurs primarily in the C-terminus, resulting in multiple isoforms with varying transactivational activity (Apt et al., 1994; Grunder et al., 2003; Kruse and Sippel, 1994a; Prado et al., 2002).

NFI dimerization is essential for DNA binding (Armentero et al., 1994), with NFIs binding DNA as both homodimers and heterodimers. Homodimers and heterodimers bind the NFI consensus binding site with the same apparent affinity (Kruse and Sippel, 1994b; Mason et al., 2009) and specificity *in vitro* (Osada et al., 1999). However, each NFI demonstrates different binding affinities to NFI binding

sites identified in different promoters (Osada et al., 1999). For example, NFIB and NFIX bind to the NFI binding site in the whey acidic protein gene with greater affinity than NFIA, whereas NFIA and NFIX have greater affinity for NFI binding sites in the HMG-CoA reductase and glutathione transferase P genes than NFIB and NFIC (Mukhopadhyay et al., 2001; Osada et al., 1999).

The C-terminal transactivation domain varies widely among family members, such that each family member has unique transactivation potential (Chaudhry et al., 1998). NFIs are also able to repress expression of genes (Cooke and Lane, 1999a; Cooke and Lane, 1999b). A proline-rich domain, first identified in NFIC (399-499 aa), potently activates transcription (Mermod et al., 1989). Additional residues between 220-399 aa further drive transcription in cooperation with this proline-rich domain (Mermod et al., 1989). Proline-rich domains were subsequently found in NFIA, NFIB and NFIX (Gronostajski, 2000; Osada et al., 1999). Within the proline-rich domain of NFIC there is a repeat of the C-terminal domain (CTD) heptapeptide repeat (PTSPSYS) found in RNA polymerase II that, when mutated or deleted from the NFIC C-terminus, results in loss of transcriptional activity in a reporter assay in yeast (Wendler et al., 1994; Xiao et al., 1994). The proline-rich domain of NFIC has been shown to interact with general transcription factors TFIIB (Kim and Roeder, 1994) and TATA-binding protein (TBP) (dependent on presence of CTD) (Xiao et al., 1994). Notably, alternatively spliced NFIC isoforms lacking this repeat still activate transcription, and NFIA, NFIB and NFIX do not have a well conserved heptapeptide repeat (Altmann et al., 1994; Gronostajski, 2000), indicating that NFI transcription activity can be

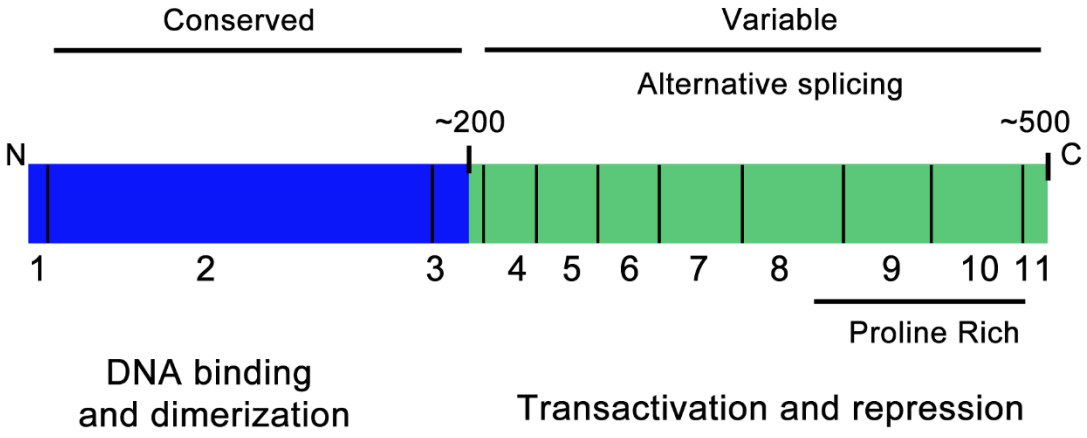

Figure 1-3: NFI protein organization. Approximate size in kDa listed above. Exons marked by lines, with exon numbers below. Shown is largest identified splice variant, additional isoforms contain alternative spliced exons. Adapted from *Gronostajski et al.* (Gronostajski, 2000).

mediated through different mechanisms.

NFIC has been shown to relieve histone H1-mediated repression of transcription (Dusserre and Mermod, 1992) and interact with histone H3 to contribute to chromatin remodeling at target binding sites (Alevizopoulos et al., 1995). In the context of the chromosome, NFI binding to a consensus recognition element in the mouse mammary tumour virus (MMTV) promoter stabilizes an open nucleosome conformation thereby facilitating binding and transactivation by additional factors (Di Croce et al., 1999). Of note, this action requires only the N-terminal DNA binding domain of NFI, suggesting multiple roles for NFI in regulating transcription (Di Croce et al., 1999). NFIC can prevent silencing of telomeric genes by maintaining chromatin in an open configuration (Esnault et al., 2009). NFI regulatory activity can also be facilitated through interaction with additional factors, including the transactivation complex p300/CBP (Leahy et al., 1999), and other site-specific transcription factors such as FOXA1 (Grabowska et al., 2014), hepatocyte nuclear factor 1 alpha (Satoh et al., 2005), thyroid transcription factor 1 (Bachurski et al., 2003), Sox9 (Kang et al., 2012), and Sox10 (Glasgow et al., 2014).

1.3.2 Regulation of NFI activity

Phosphorylation of NFI in response to multiple signaling pathways has been reported, suggesting that regulation of NFI activity through post-translational modification provides an additional layer of regulatory control on the expression of NFI target genes. NFI phosphorylation by DNA-PK was first reported by Jackson

et al. (Jackson et al., 1990) who also reported that NFI can undergo O-glycosylation (Jackson and Tjian, 1988). Kawamura *et al.* further demonstrated that NFI could be phosphorylated by Cdk1 *in vitro*, and phosphorylation did not appear to alter its *in vitro* DNA binding affinity (Kawamura et al., 1993). Multiple phosphorylated forms of NFI were observed in actively growing 3T3-L1 cells, as well as in quiescent 3T3-L1 cells upon overexpression of c-Myc (Yang et al., 1993). NFI-dependent promoter activity was decreased in cells overexpressing c-Myc and in actively growing cells compared to quiescent cells, suggesting an association between phosphorylated NFI and decreased promoter activity (Yang et al., 1993). Additional work in 3T3-L1 adipocytes revealed that NFI is rapidly phosphorylated in response to insulin signaling (Cooke and Lane, 1999b).

Multiple phosphorylated forms of NFI have also been identified in MG cell lines, with phosphorylation correlating with decreased expression of NFI target genes (Bisgrove et al., 2000), consistent with the findings in adipocytes. In contrast, tyrosine phosphorylation of NFIC in mammary epithelial cells by nuclear Jak2 results in increased activity. In these cells, prolactin activates Jak2, which phosphorylates NFI-C2, the dominant isoform in these cells, protecting NFI-C2 from proteasomal degradation, and resulting in increased transcriptional activation of target genes (Nilsson et al., 2006).

NFI activity is regulated by transforming growth factor beta (TGF-β) and tumour necrosis factor alpha (TNF-α), suggesting that NFI is a mediator of the opposing actions of these two signaling molecules (Alevizopoulos and Mermod, 1996). TGF-β induces activity of the NFIC C-terminus proline-rich transactivation

domain, with the TGF-β responsive domain in NFIC located in the extreme C-terminus (472-499 aa) (Alevizopoulos et al., 1995). This same domain is repressed by TNF-α (Alevizopoulos and Mermod, 1996). Mutation of putative phosphorylation sites in the 472-499 aa domain does not affect response to TGF-β and TNF-α, suggesting that regulation of NFIC by these two factors is not through direct NFIC phosphorylation (Alevizopoulos and Mermod, 1996). Of considerable interest, TGF-β induction of NFI activity is calcium-dependent, and expression of constitutively active calcium/calmodulin-dependent phosphatase calcineurin or calcium/calmodulin-dependent kinase IV (CaMKIV) in fibroblasts also activates the NFIC transactivation domain (Alevizopoulos et al., 1997).

1.3.3 NFI knockout mice

In the adult mouse, all four NFIs are expressed at the mRNA level in the brain, heart, lung, liver, kidney, and muscle, with varying expression in the spleen and testis. During development, *NFIA* mRNA is detected first in the brain and heart, followed by *NFIB* in the developing lungs, and *NFIC* in the aortic arch and dorsal root ganglia (Chaudhry et al., 1997). As development progresses, *NFIA*, *NFIB*, and *NFIX* are all expressed in the developing brain, including the neocortex, and ventricular zone (Chaudhry et al., 1997). *NFIC* and *NFIX* RNA levels are higher in liver than *NFIA* and *NFIB* RNA levels. In the lung, *NFIB* is more highly expressed than *NFIA*, *NFIC*, and *NFIX*. In developing skeletal muscle, *NFIX* is expressed first, followed by *NFIA* and *NFIC*. The only NFI detected in the gonads is *NFIA*

(Chaudhry et al., 1997). This work reveals distinct but overlapping expression patterns in specific tissues throughout development and differentiation.

To identify the specific roles of each NFI family member, mouse knockouts of each member have been generated. These mouse models reveal unique but overlapping roles for NFIs, with the phenotypes observed in *Nfia-/-*, *Nfib-/-*, and *Nfix-/-* mice demonstrating important roles for all three NFIs in brain development (das Neves et al., 1999a; Driller et al., 2007; Shu et al., 2003). *Nfia-/-* mice exhibit perinatal lethality, with 95% of mice dying within two weeks of birth. Examination of the brains of *Nfia-/-* mice revealed agenesis of the corpus callosum, hydrocephalus, disruption of midline glial structures, and delayed neuronal and glial differentiation (das Neves et al., 1999a; Shu et al., 2003; Wong et al., 2007). *Nfia-/-* mice also display kidney and ureteral defects (Lu et al., 2007). *Nfib-*/- mice die at birth due to severe lung hyperplasia as a result of delayed lung maturation (Hsu et al., 2011; Steele-Perkins et al., 2005). *Nfib-/-* mice also display brain phenotypes similar to those of *Nfia-*/- mice, with additional loss of neural precursor cells leading to disruption of neurogenesis in the cortex (Barry et al., 2008; Betancourt et al., 2014; Piper et al., 2014; Steele-Perkins et al., 2005).

In contrast to *Nfia-/-* and *Nfib-/-* mice, *Nfic-/-* mice are viable, but have defects in tooth root development (Steele-Perkins et al., 2003). Disruption of *Nfix* results in postnatal lethality in mice, and similar to *Nfia-/-* and *Nfib-/-* mice, *Nfix-/-* mice display delayed maturation of neuronal and glial lineages (Driller et al., 2007; Heng et al., 2014; Piper et al., 2011). Reports vary on whether loss of *Nfix* results in partial agenesis of the corpus callosum and hydrocephalus but midline glia are

maintained (Campbell et al., 2008; Driller et al., 2007). In addition, hyperproliferation of neural precursor cells is detected in the brains of *Nfix-/-* mice in stark contrast to *Nfia-/-* and *Nfib-/-* mice (Campbell et al., 2008). These mice also display skeletal and gastrointestinal defects (Driller et al., 2007).

Gene expression analysis of different NFI family members in knock-out mice reveals additional complexity through compensatory pathways. For example, a modest increase in *Nfib* expression (1.3-fold) is observed in the brains of *Nfia-/-* mice (Wong et al., 2007), whereas *Nfia* expression is increased 2.2 fold in the brains of *Nfib-/-* mice, with no change in expression of *Nfic* or *Nfix* (Steele-Perkins et al., 2005). In *Nfib-/-* lungs, expression of *Nfia* is up-regulated 5.1-fold, and *Nfic* and *Nfix* levels are increased by ~3 fold (Steele-Perkins et al., 2005). This suggests that there is tissue-specific crosstalk between the different members of the NFI family, and that the different family members are not interchangeable, as indicated by the severe phenotype observed in the lungs of *Nfib*-/- mice despite increases in *Nfia*, *Nfic*, and *Nfix* in this tissue (Steele-Perkins et al., 2005).

1.3.4 NFI in gliogenesis

Expression of *Nfia*, *Nfib*, and *Nfix* in the developing brain, combined with the major disruptions evident in brain development in the corresponding knockout mice indicates an important role for the NFI family in regulating development and differentiation in the CNS. The phenotypes observed in *Nfia-/-, Nfib-/-*, and *Nfix-/-* mice (das Neves et al., 1999a; Heng et al., 2014; Piper et al., 2014; Piper et al., 2010; Steele-Perkins et al., 2005), particularly the delayed differentiation of glial

cell populations and disruption of progenitor cells, suggest a role for NFI in the regulation of gliogenesis. This is further supported by the regulation of the glial specific gene *GFAP* by NFI in differentiating astrocytes *in vitro* (Cebolla and Vallejo, 2006) and *in vivo* (Deneen et al., 2006; Glasgow et al., 2014).

In the developing spinal cord, NFIA and NFIB expression is induced in the ventricular zone at the onset of gliogenesis (Deneen et al., 2006). In a chicken model, early expression of NFIA or NFIB induces expression of glial genes including *B-FABP, FGFR3*, and *GLAST*, while loss of NFIA results in loss of NFIB expression, along with a decrease of glial progenitor cells, both in the astrocytic and oligodendroglial lineages (Deneen et al., 2006). Following gliogenesis, NFIA and NFIB further promote astrocyte differentiation (Deneen et al., 2006). In the same model, NFIA was also shown to be necessary for maintenance of progenitor cells, such that knockdown of NFIA results in decreased expression of progenitor cell markers and ectopic neurogenesis (Deneen et al., 2006). Expression of the Notch effector *Hes5* is decreased when NFIA is knocked down (Deneen et al., 2006), and Hes genes are vital to the maintenance of neural precursor cells (Ohtsuka et al., 2001). Expression of Notch effectors can rescue the defect in progenitor cell maintenance upon NFIA knockdown, but is unable to restore normal glial cell differentiation (Deneen et al., 2006). In contrast to Hes5, NFIA represses expression of Hes1 in the telencephalic ventricular zone (Piper et al., 2010), suggesting that NFI regulation is tissue specific (Harris et al., 2015; Piper et al., 2010).

Expression of NFIA is induced by Notch signaling and Sox9 in neural precursor cells. As seen in Section 1.2.2, Notch signaling induces expression of NFIA, which is necessary for demethylation of astrocyte-specific genes by displacing DNMT1 from the promoter of *GFAP* (Figure 1-4) (Namihira et al., 2009). NFI also directly binds the *GFAP* promoter in differentiating precursor cells at NFI consensus binding sites (Cebolla and Vallejo, 2006), and regulates transcription of *GFAP* (Gopalan et al., 2006b). Sox9 is expressed in neural precursor cells, and expression begins prior to gliogenesis (Scott et al., 2010; Stolt et al., 2003). In the spinal cord, Sox9 directly activates transcription of NFIA during gliogenesis, and then interacts with NFIA to coordinate expression of genes that are important in gliogenesis and glial precursors (Figure 1-4) (Kang et al., 2012).

As seen in chick spinal cord, NFIA and NFIB promote astrocyte differentiation of glial progenitor cells (Deneen et al., 2006), and expression of NFI is increased in fetal astrocytes (Malik et al., 2014). Apart from activation of astrocyte-specific genes, NFIA also represses oligodendrocyte differentiation by antagonizing the action of Sox10 (Figure 1-4) (Fancy et al., 2012; Glasgow et al., 2014). Sox10 promotes differentiation of oligodendrocyte precursors into mature oligodendrocytes (Stolt et al., 2002). Interaction of Sox10 with NFIA represses promoter activity of NFIA target genes (*Gfap* and *Apcdd1*) expressed in astrocytes. Conversely, NFIA interaction with Sox10 represses expression of oligodendrocyte specific genes, including myelin binding protein (*MBP*), proteolipid protein 1 (*PLP1*), and myelin-associated glycoprotein (*MAG*) (Glasgow et al., 2014). In all of

these genes, Sox and NFI binding sites are located in close proximity (Glasgow et al., 2014).

In the adult brain, NFIA, NFIB and NFIX are detected in the subventricular zone, which contains neural stem cells (Heng et al., 2014; Plachez et al., 2012), and NFI binding elements are enriched in neural stem cells enhancers (Mateo et al., 2015). NFI binding is also enhanced in enhancers activated in a quiescent neural stem cell model, suggesting that NFIs may be important for maintenance of quiescence in these cells (Martynoga et al., 2013). Expression of NFIX, but not other NFIs, is increased in quiescent neural stem cells, and knockdown of NFIX in this model results in delayed quiescence (Martynoga et al., 2013). This suggests that during development, NFI promotes gliogenesis and astrocyte differentiation, but in the adult brain NFI may be important for the maintenance of neural stem cells (Harris et al., 2013; Martynoga et al., 2013).

1.3.5 NFI in neuronal development

While NFIA and NFIB promote glial specification and astrocyte differentiation, NFI may also play important roles in neuronal differentiation. In the developing murine olfactory bulb, NFIA and NFIB are expressed in distinct populations, with NFIA expressed in subventricular zone astrocytes, while NFIB is expressed in neuronal cells (Plachez et al., 2012). In the rostral migratory stream and adult subventricular zone, both NFIA and NFIB are expressed in astrocytes and neuroblasts, but expression is lost in interneurons, though expression of NFIB

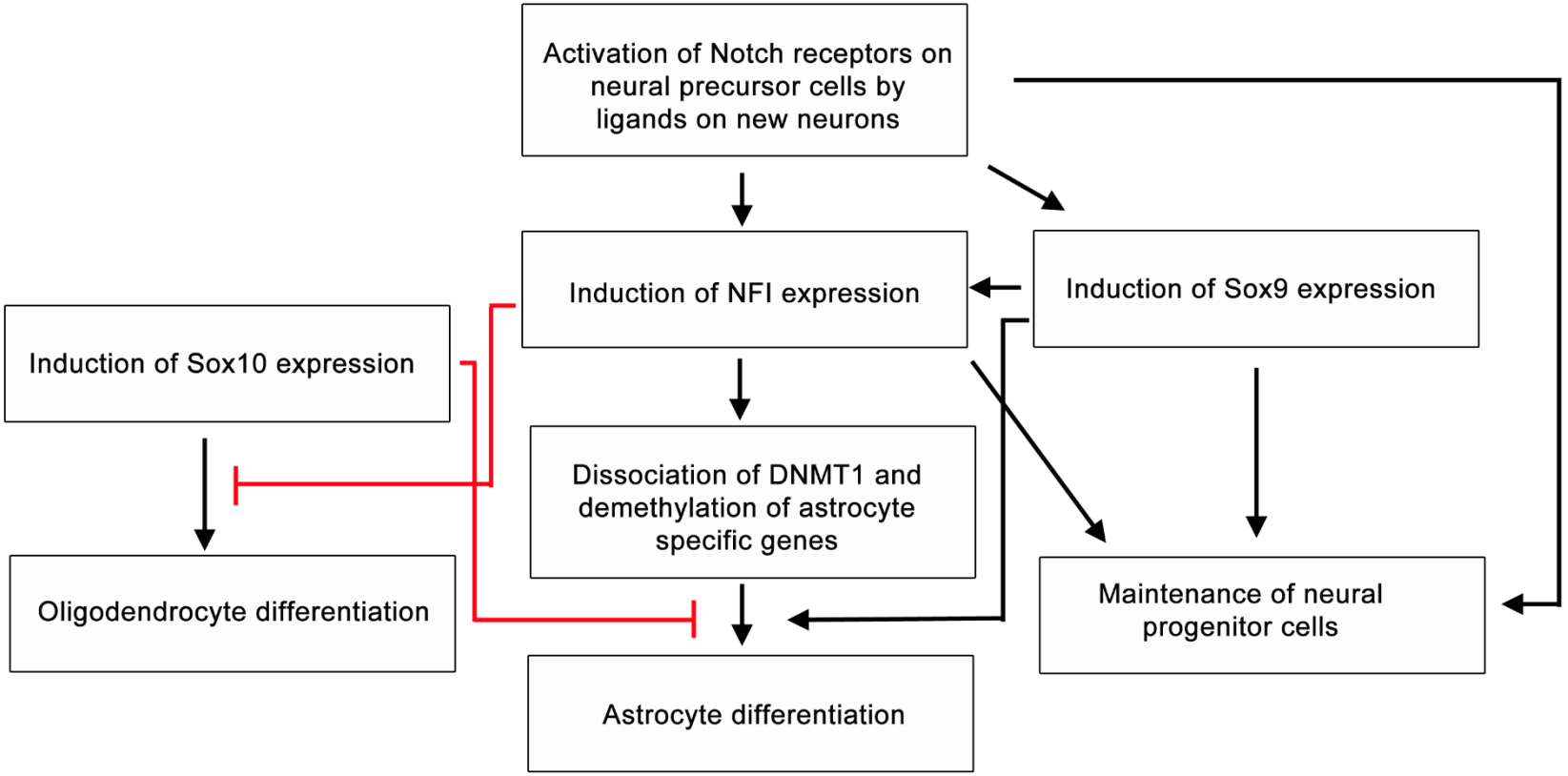
Activation of Notch receptors on neural precursor cells by ligands on new neurons
Induction of NFI expression
Induction of Sox9 expression
Induction of Sox10 expression
Dissociation of DNMT1 and demethylation of astrocyte specific genes
Oligodendrocyte differentiation
Maintenance of neural progenitor cells
Astrocyte differentiation

Figure 1-4: Schematic of NFI in glial cell differentiation. Activation of Notch signaling in neural precursor cells by ligands expressed on newborn neurons induces expression of NFIA and Sox9. NFIA binding at the promoters of astrocyte specific genes leads to dissociation of DNMT1 from these promoters, and subsequent demethylation of these promoters. This allows access of transcription factors, including NFIA and Sox9, which interact, to bind and activate transcription of astrocyte specific genes. NFIA, Sox9, and Notch signaling also contribute to maintenance of neural progenitor cells. NFIA antagonizes Sox10 to inhibit oligodendrocyte differentiation, and Sox10 antagonizes NFIA to suppress astrocyte differentiation.

is maintained in excitatory neurons (Plachez et al., 2012). This suggests that NFIs contribute not only to gliogenesis, but also to neuronal differentiation.

NFIs have also been implicated in neuronal differentiation within the cerebellum. Cerebellar granular neuron maturation occurs in defined steps, characterized by proliferation, followed by exit from the cell cycle, differentiation, migration, and finally extension of dendrites and synapse formation (Chedotal, 2010). NFIs are highly expressed in cerebellar granular neurons, and in these cells NFI regulates expression of the gamma-aminobutyric acid type a receptor 6 (GABRA6) subunit, which is specifically expressed as cerebellar granular neurons mature (Wang et al., 2004). Early in development, the RE1 silencing transcription factor (REST) occupies the GABRA6 promoter, preventing NFI binding and activation of GABRA6 transcription until cerebellar granular neurons mature (Wang et al., 2011).

Nuclear factor of activated T cells (NFAT) proteins also bind to the promoters of additional NFI regulated genes expressed in maturing cerebellar granular neurons. The close proximity of NFAT and NFI binding sites prevents NFI transactivation when these promoters are bound by NFAT (Ding et al., 2013). As cerebellar granular neurons mature, NFAT binding decreases and NFI is able to bind to these promoters and promote maturation of these cells (Ding et al., 2013). Expression of a dominant negative NFI revealed additional roles for NFI in axon extension, migration, dendritogenesis, and synapse formation in cerebellar granular neurons through regulation of cellular adhesion molecules including Ephrin B1, N-cadherin, and Tag-1, and signaling molecules including Wnt7a

(Kilpatrick et al., 2012; Wang et al., 2010; Wang et al., 2007). This suggests an important role for NFI in neuronal cells.

1.3.6 NFI in malignant glioma

NFIA RNA levels are significantly increased in GBM tumours compared to normal brain (Scrideli et al., 2008). At the protein level, NFIA expression is detected in all grades of astrocytoma: in grade II astrocytomas, NFIA was detected in ~80% of cells, compared to 48% of cells in grade III and 37% of cells in grade IV astrocytomas (Song et al., 2010). In contrast, NFIA was detected in ≤5% of cells in other brain tumours analyzed, including oligodendroglioma (Song et al., 2010). In an oligodendroglioma tumour model, where *RasV12* is specifically targeted to cells in the oligodendrocyte lineage in the developing mouse cortex, forced expression of NFIA resulted in tumours that resembled astrocytomas (Glasgow et al., 2014), suggesting that NFIA is important for the astrocytic phenotype of MG tumours.

In GBM tumours, NFIA expression is heterogeneous, with fewer positive cells in the main tumour mass, but more positive cells in perivascular infiltrating cells (Song et al., 2010). In MG (combined grades III and IV astrocytomas), expression of NFIA correlates with better survival in both adult and pediatric data sets (Song et al., 2010), but conversely, was shown to have a tumour promoting role in MG in both a cell culture and xenograft model of MG (Glasgow et al., 2013; Lee et al., 2014). Knockdown of NFIA in U87 MG cells orthotopically implanted in the brains of nude mice prevented tumour formation, whereas overexpression of

NFIA in the same model resulted in larger tumours, increased proliferation, and a dramatic increase in cells migrating away from the main tumour mass (Lee et al., 2014).

In MG cell lines, NFI regulates expression of numerous genes that may contribute to migratory activity and tumourigenesis. GFAP expression is a defining characteristic of astrocytomas (Louis et al., 2007). NFI regulates the expression of *GFAP* in MG cell lines (Gopalan et al., 2006b; Singh et al., 2011a). B-FABP is a marker of radial glial cells in the developing brain (Feng et al., 1994). B-FABP and GFAP are co-expressed in a subset of MG cell lines (Godbout et al., 1998), and NFI binding sites in the *B-FABP* promoter are critical for promoter activity (Bisgrove et al., 2000). B-FABP expression increases migration and invasion in MG cell lines (Mita et al., 2007), and expression of B-FABP in GBM tumours correlates with a worse prognosis (Kaloshi et al., 2007; Liang et al., 2006). In MG tumours, B-FABP-positive cells are primarily found in areas of infiltration, including perivascular cells, similar to expression of NFIA (Mita et al., 2007; Song et al., 2010).

Overexpression of NFIX isoform 3 and NFIA in MG cell lines increases their migratory activity. This increase in migration is linked to activation of the secreted glycoprotein YKL-40, and repression of the plasminogen activator inhibitor PAI1 (Lee et al., 2014; Singh et al., 2011a). NFI has previously been shown to activate transcription of the tumour suppressor gene *TP53* in HeLa cells and in the mammary gland (Furlong et al., 1996; Johansson et al., 2003), and repress transcription of the gene encoding p21 (Ouellet et al., 2006; Singh et al., 2011b).

In MG cells, NFIA represses expression of both p53 and p21 (Glasgow et al., 2013; Lee et al., 2014).

NFI has also been implicated in other tumour types. In breast cancer primary tumours, expression of NFIC represses epithelial-mesenchymal transition (EMT), and NFIC expression correlates with a better prognosis (Nilsson et al., 2010). In contrast, NFIB expression is increased in triple-negative and Her2 subtype breast cancers, and knockdown of NFIB in a breast cancer cell line reduces cell proliferation and activates apoptotic signaling (Moon et al., 2011). Increases in NFIB expression have also been detected in small cell lung cancer (SCLC), whereas, similar to breast cancer, knockdown of NFIB expression in cell lines results in decreased proliferation and increased apoptosis. Ectopic expression of NFIB in a mouse SCLC cell lines increase proliferation and anchorage independent growth, suggesting NFIB may be acting as an oncogene in these cells (Dooley et al., 2011).

1.4 HEY1

1.4.1 The Hey family of Notch effector genes

The Notch signaling pathway plays a fundamental role in development, regulating gene expression programs during cell specification and differentiation (Bray, 2006). Members of the Hey (hairy/E(spl)-related with YPRW motif) family are closely related to the Hes family and *Drosophila hairy* and *Enhancer of split* genes, all of which are class E bHLH transcriptional repressors induced by Notch signaling (Nakagawa et al., 2000; Weber et al., 2014). The Hey family contains a

basic domain that binds E-box DNA sequences CACGTG and CACGCG (Heisig et al., 2012), followed by a helix-loop-helix (HLH) domain and an orange domain. The latter domains mediate homo- and heterodimerization and additional protein interactions with other bHLH proteins, transcription factors and cofactors (Fischer and Gessler, 2007). Two conserved motifs are found at the C-terminus of Hey family members, a YPRW motif similar to the WRPW motif found in the Hes family, and a TE(I/V)GAF motif (Leimeister et al., 1999).

There is one Hey gene in *D. melanogaster*, and three mammalian genes: *HEY1*, *HEY2*, and *HEYL* [also known as Hes-related (Hesr) 1-3, hairy-related transcription factor (HRT) 1-3, and cardiovascular helix-loop-helix factor (CHF) 2,1,3] (Kokubo et al., 1999; Leimeister et al., 1999; Nakagawa et al., 2000; Nakagawa et al., 1999). Ligands, including Delta and Jagged (delta like (DLL) 1/3/4 and Jagged1/2 in mammals), expressed on neighboring cells bind to Notch receptors (1-4) on adjacent cells. Upon activation of Notch receptors, proteolysis releases Notch intracellular domain (NICD) from the membrane, which then translocates to the nucleus and, with mastermind-like protein (MAML), binds to its DNA binding partner RBP-Jκ (Ables et al., 2011; Bray, 2006). In the absence of NICD and MAML, RBP-Jκ interacts with co-repressors and represses transcription in a sequence-specific manner (Ables et al., 2011). Binding of NICD and MAML to RBP-Jκ recruits co-activators and displaces co-repressors, transforming the complex into a transcriptional activator (Ables et al., 2011). The promoters of mouse *Hey1*, *Hey2*, and *HeyL* all contain RBP-Jκ binding sites and are

upregulated in response to Notch signaling downstream of RBP-Jκ (Iso et al., 2002; Iso et al., 2001a; Maier and Gessler, 2000; Nakagawa et al., 2000).

In addition to regulation by Notch, HEY1 is also regulated by additional pathways. *HEY1* is direct target of TGFβ/Smad signaling (Sharff et al., 2009; Zavadil et al., 2004). Bone morphogenetic proteins (BMPs) 2, 7, and 9, which are members of the TGF-β super family, activate *HEY1* expression in mesenchymal progenitor cells during differentiation (Lavery et al., 2009; Liu et al., 2007; Sharff et al., 2009). In endothelial cells of the vascular system, CoupTF-II represses expression of *HEY1* and *HEY2* to inhibit arterial differentiation (Aranguren et al., 2013). *HEY1* expression is also induced by E2F transcription factors: E2F binding sites are present in the *HEY1* promoter, and E2F transcription factors bind the *HEY1* promoter (Hulleman et al., 2009).

Hey1, *Hey2*, and *HeyL* are expressed in distinct patterns during mouse development. *Hey1* is expressed in multiple developing tissues, including developing somites, heart, nervous system, limb buds, muscle precursors, and the craniofacial region (Leimeister et al., 1999). Similarly, *Hey2* is expressed in the developing somites, heart, nervous system, and craniofacial region (Leimeister et al., 1999). Of note, in the developing heart and nervous system, *Hey1* and *Hey2* are expressed in different subpopulations (Leimeister et al., 1999; Nakagawa et al., 1999). *HeyL* is also expressed in developing somites, the PNS, and in the vasculature (Leimeister et al., 2000). *Hey1-/-* and *HeyL-/-* mice are viable, but *Hey1-/-* mice exhibit behavioral defects (Fischer et al., 2004; Fuke et al., 2006). Double knockout of *Hey1* and *HeyL* in mice is postnatal lethal due to cardiac

defects (Fischer et al., 2007). Similarly, *Hey2-/-* mice have cardiac defects and high postnatal lethality (Donovan et al., 2002; Gessler et al., 2002; Sakata et al., 2002), whereas *Hey1/Hey2* deletion is embryonic lethal due to major vascular defects (Fischer et al., 2004).

Atrioventricular explants from *Hey1/HeyL-/-* and *Hey2-/-* embryos showed impaired epithelial-to-mesenchymal transition, similar to *Notch1-/-* explants, demonstrating an important role for the Hey family in transduction of Notch signaling in cardiac development (Fischer et al., 2007). Additionally, the Hey family plays important roles in muscle stem cell homeostasis and bone development (Fukada et al., 2011; Sharff et al., 2009; Zanotti and Canalis, 2013). *Hey1/Hey2* null nice exhibit decreased body and skeletal muscle weight, and satellite cells (muscle stem cells) from these mice express differentiation markers and fail to enter an undifferentiated quiescent state, demonstrating an important role in progenitor cell maintenance (Fukada et al., 2011).

Hey proteins transcriptionally repress target genes through interactions with transcriptional repressors including histone deacetylases and repressor complexes (Iso et al., 2001b; Takata and Ishikawa, 2003). In addition, Hey proteins can also bind transcriptional activators and repress transcription of the target genes of these transcriptional activators, including GATA transcription factors and MyoD (Fischer et al., 2005; Sun et al., 2001a; Weber et al., 2014). (Nakagawa et al., 2000). Multiple targets have been identified by microarray and chromatin immunoprecipitation, including Hey members themselves, suggesting a negative feedback loop (Heisig et al., 2012). Hey target genes are enriched for

transcriptional regulators, developmentally regulated genes and genes involved in differentiation (Heisig et al., 2012). This analysis also revealed that regulation by different Hey family members is highly redundant, despite different expression patterns, suggesting that the varied phenotypes of knockout mice are due mainly to the cells in which the Hey family members are expressed in (Heisig et al., 2012).

1.4.2 Hey1 in the brain

Notch signaling in neural development regulates maintenance of progenitor cells and promotes gliogenesis (Morrison et al., 2000; Namihira et al., 2009; Pierfelice et al., 2011; Taylor et al., 2007). Hes1 and Hes5 are necessary for maintenance of neural progenitor cells in the brain (Ohtsuka et al., 2001). Hes1, but not Hes5, further promotes astrocyte differentiation following the onset of gliogenesis (Wu et al., 2003), while both Hes1 and Hes5 promote gliogenesis in the retina (Furukawa et al., 2000; Scheer et al., 2001). Hey1 and Hey2 are both expressed in the ventricular zone of the developing brain and spinal cord, with Hey1 expression observed throughout the brain while Hey2 expression is more restricted (Sakamoto et al., 2003). HeyL is expressed in the telencephalon and olfactory bulb (Leimeister et al., 2000).

Similar to Hes1 and Hes5, Hey1 and Hey2 both promote maintenance of neural precursor cells in the developing brain (Sakamoto et al., 2003). Misexpression of these genes during neurogenesis in the mouse ventricular zone results in expansion of neural precursor cells and decreased neurogenesis, while misexpression later in development results in increased production of astrocytes

(Sakamoto et al., 2003). *HEY1* expression is increased in astrocytes compared to neural stem cells (Malik et al., 2014), and Hey1 and Hey2 both inhibit the transcriptional activity of the proneural bHLH genes *Ascl1* (*Mash1*) and *NeuroD4* (*Math3*) (Sakamoto et al., 2003). Oligodendrocyte differentiation is promoted by signaling through sonic hedgehog (Shh) (Nery et al., 2001), and inhibited by BMP4 signaling (Gomes et al., 2003). Treatment of oligodendrocyte precursors cells with BMP4 induces astrocyte differentiation and increased expression of Notch effectors, including *Hey1, Hey2, Hes1*, and *Hes5* (Wu et al., 2012). In contrast to Hey and Hey2, HeyL promotes neuronal differentiation and activates the promoter of the proneural bHLH gene *Neurog2*, whereas Hey1 represses *Neurog2* promoter activity (Jalali et al., 2011).

1.4.3 HEY1 in malignant glioma

Disruption of Notch signaling in MG through dysregulation of Notch ligands and receptors has previously been reported, although the role of Notch signaling in tumour development and growth remains unclear (Alqudah et al., 2013; El Hindy et al., 2013; Purow et al., 2005; Stockhausen et al., 2010; Xu et al., 2009). One study reported NOTCH1, 3, and 4, but not NOTCH2 expression in astrocytomas, with increased expression correlated to increasing grade (Xu et al., 2009). However, another study found higher expression of NOTCH1 in grade II and III astrocytomas compared to grade IV tumours (Dell'albani et al., 2014). Purow *et al.* (Purow et al., 2005) reported that expression of NOTCH1 in the cytoplasm did not vary between astrocytoma tumour grades; however, Notch1 in the nucleus was

higher in grade II and III tumours compared to grade IV tumours, and this finding was mirrored by expression of the Notch ligand DLL1 (Purow et al., 2005). In contrast, highest levels of the ligand Jagged-1 (JAG-1) were observed in grade IV tumours (Purow et al., 2005). Upon knockdown of *NOTCH1*, *DLL1*, and *JAG1* with siRNA, MG cell lines showed decreased proliferation. Knockdown of both *NOTCH1* or *DLL1,* but not *JAG-1,* further increased cell death in MG cell lines, and increased survival in an orthotopic tumour model, suggesting that Notch signaling may contribute to MG cell proliferation and survival (Purow et al., 2005). Upregulation of Notch pathway genes, including *HEY1*, in MG correlates with increased expression of hypoxia markers, and Notch signaling has been implicated in promoting angiogenesis in MG cell lines and tumours (El Hindy et al., 2013; Guichet et al., 2015; Irshad et al., 2015; Nandhu et al., 2014).

HEY1 is expressed in astrocytoma tumours, with an increase in cells expressing *HEY1* correlating with increasing tumour grade (Hulleman et al., 2009). Of note, expression of *HEY1* correlates significantly with decreased overall survival and disease free survival in GBM patients. In a small cohort of 62 GBM cases, patients with *HEY1*-negative GBM tumours survived twice as long as patients with *HEY1*-positive tumours (21.67 vs 10.87 months) (Gaetani et al., 2010; Hulleman et al., 2009). In MG cell lines, knockdown of *HEY1* decreases proliferation in *HEY*1-expressing cells, while ectopic expression of HEY1 in neural stem cells isolated from mice increases neurosphere size, suggesting that HEY1 contributes to cell growth (Hulleman et al., 2009).

1.5 Calcineurin

1.5.1 Calcineurin structure and function

Calcineurin, also referred to as protein phosphatase 2B (PP2B), and protein phosphatase 3 (PPP3), is a calcium/calmodulin-dependent serine/threonine phosphatase (Hogan and Li, 2005; Klee et al., 1979). Calcineurin is composed of two subunits, a catalytic subunit, calcineurin A (CNA), and a regulatory subunit, calcineurin B (CNB) (Hogan and Li, 2005). CNA is a 60 kDa subunit composed of an N-terminal catalytic domain, followed by a CNB binding domain, a calmodulin binding domain, and at the C-terminus, an auto-inhibitory domain (Figure 1-5A) (Li et al., 2011). The regulatory CNB subunit is 19 kDa, and consists of 4 EF-hand motifs that bind Ca^{2+} ions (Kakalis et al., 1995). Calmodulin (CaM) is a ubiquitous 17 kDa protein that acts as a calcium sensor, and also contains 4-EF-hand motifs to bind Ca^{2+} (Tidow and Nissen, 2013). CaM binding to calcineurin is calcium dependent, and is necessary for full activity (Li et al., 2011). Upon activation by calcium signaling, calcineurin dephosphorylates target substrates (Klee et al., 1998).

In humans, three isoforms of CNA have been identified, encoded by three separate genes, *PPP3A*, *PPP3B,* and *PPP3C*, encoding CNAα, CNAβ, and CNAγ (Eastwood et al., 2005; Rusnak and Mertz, 2000). The three isoforms have variable N and C-terminal tails, but are otherwise highly conserved. CNAα and CNAβ are ubiquitously expressed, with high expression in the brain (Kuno et al., 1992; Rusnak and Mertz, 2000). CNAγ was originally believed to be testis-specific (Muramatsu et al., 1992), but has also been detected in the brain (Eastwood et al.,

2005; Gerber et al., 2003). CNB is encoded by two separate genes, *PPP3R1*, which is widely expressed, and *PPP3RL*, which is testis-specific (Liu et al., 2005b; Rusnak and Mertz, 2000; Ueki et al., 1992). Inhibition of calcineurin activity by the immunosuppressive agents cyclosporin A (CsA) and FK506 (a.k.a tacrolimus) revealed an important role for calcineurin in regulating T cell activation through the NFAT family (Clipstone and Crabtree, 1992; Liu et al., 1992; Shaw et al., 1995). *CNAα-/-* mice have normal T-cell development, but show defective T-cell response to antigen (Zhang et al., 1996), impaired kidney development (Gooch et al., 2004), and defects in bone formation (Sun et al., 2005). In the brain, there is accumulation of hyperphosphorylated tau, a critical component of neurofibrillary tangles seen in Alzheimer's disease (Kayyali et al., 1997), and defects in synaptic depotentiation (Zhuo et al., 1999). *CNAβ-/-* mice have more severe defects in T-cell development and response than *CNAα-/-* mice (Bueno et al., 2002; Manicassamy et al., 2008), and show defects in cardiac hypertrophic response and hyperlipidemia (Suk et al., 2013). These phenotypes demonstrate isoform-specific functions.

Calcineurin substrate specificity remains poorly understood. A PxIxIT motif first identified in NFAT1 interacts with CNA (Aramburu et al., 1999; Garcia-Cozar et al., 1998). In addition, NFAT also interacts with CNA through a second, less conserved binding site LxVP (Liu et al., 1999; Park et al., 2000; Rodriguez et al., 2009). PxIxIT motifs have been identified in many calcineurin substrates and interacting proteins including the potassium channel substrate TRESK, and calcineurin targeting protein A-kinase anchoring protein AKAP-79 (Li et al., 2011). Kinase suppressor of Ras 2 (KSR2) interacts and is dephosphorylated by

calcineurin via an LxVP motif (Li et al., 2011). Interaction of an LxVP peptide with calcineurin requires both CNA and CNB subunits, Ca^{2+} and calmodulin, demonstrating that interaction at this docking site requires calcineurin to be in an active state (Li et al., 2011). This docking site is close to the active site of calcineurin and is essential for binding the immunosuppressant inhibitors CsA and FK506 (Rodriguez et al., 2009). In contrast, the PxIxIT binding site is accessible in both active and inactive calcineurin (Li et al., 2011). Additional calcineurin substrates contain neither LxVP or PxIxIT motifs, suggesting additional motifs may contribute to substrate binding and dephosphorylation (Li et al., 2011).

The NFAT family is the best characterized target of calcineurin (Jain et al., 1993; Li et al., 2011). In resting cells, NFAT is inactive, phosphorylated, and sequestered in the cytoplasm (Hogan et al., 2003; Shaw et al., 1995). Upon calcium signaling, calcineurin is activated and dephosphorylates multiple serines in the N-terminal regulatory domain of NFAT family members (Hogan et al., 2003). Following dephosphorylation, NFAT translocates to the nucleus, where it binds DNA and activates transcription of numerous genes (Beals et al., 1997; Hogan et al., 2003; Shaw et al., 1995; Shibasaki et al., 1996). In T cells, binding of the T-cell receptor results in release of calcium from intracellular stores, which activates sustained Ca^{2+} entry through Ca^{2+} release activated Ca^{2+} (CRAC) channels (Macian, 2005). Calcineurin is activated and NFAT is dephosphorylated and shuttles to the nucleus where it binds to the promoters of T cell activated proteins including interleukin 2 (IL-2) and interleukin 3 (IL-3), to induce transcription (Hogan et al., 2003; Serfling et al., 2000). The immunosuppressant actions of CsA and

FK506, specific inhibitors of calcineurin, are mediated by inhibiting dephosphorylation of NFAT by calcineurin in immune cells, especially T cells (Hogan et al., 2003; Liu et al., 1991; Matsuda et al., 2000; Shaw et al., 1995).

1.5.2 Regulation of calcineurin activity

As a calcium-dependent phosphatase, calcineurin is activated by calcium signaling. CNA and CNB interact tightly even in low calcium conditions (Stemmer and Klee, 1994). CNB has 4 EF hand domains that bind 4 Ca^{2+} ions. Two domains are high affinity sites, and stabilize interaction with CNA (Kakalis et al., 1995; Stemmer and Klee, 1994). The other two domains have lower affinity, and occupation of these sites causes a conformational change that makes the CaM binding domain of CNA accessible to CaM (Klee et al., 1998; Yang and Klee, 2000). CaM binding is necessary for the displacement of the CNA autoinhibitory domain from the catalytic site (Kissinger et al., 1995; Li et al., 2011).

Calcineurin is further regulated by interaction with additional proteins. Regulators of calcineurin (RCANs) include RCAN1 (a.k.a DSCR1, MCIP1, Adapt78, calcipressin1), RCAN2 (a.k.a ZAKI-4, DSCR1L1, calcipressin2), RCAN3 (a.k.a. DSCR1L2, MCIP2), and RCAN4 (Davies et al., 2007). These proteins can bind to and inhibit calcineurin activity (Fuentes et al., 2000; Kingsbury and Cunningham, 2000; Rothermel et al., 2000). In contrast, RCANs may also stimulate calcineurin activity, as disruption of RCAN genes in mouse and yeast results in decreased calcineurin activity (Kingsbury and Cunningham, 2000; Sanna et al., 2006; Vega et al., 2003). RCANs bind calcineurin at the same site as NFAT,

and one mechanism of action is via competition for binding (Martinez-Martinez et al., 2009). A second mechanism is through direct inhibition mediated by the extreme C-terminus of RCAN1 (Martinez-Martinez et al., 2009). RCANs are widely expressed, and expression of RCAN1 is upregulated in response to stress, suggesting RCANs may function in adaption to stress (Ermak et al., 2002; Li et al., 2011).

Subcellular localization of calcineurin is also an important regulator of calcineurin activity. Calcineurin is predominantly cytosolic in unstimulated cells (Hallhuber et al., 2006; Shibasaki and McKeon, 1995). However, in response to calcium signaling, calcineurin can translocate to the nucleus to interact with target substrates (Shibasaki et al., 1996). In the heart, nuclear accumulation is observed in response to myocardial infarction (Hallhuber et al., 2006). A nuclear localization signal (NLS) in the catalytic domain of CNA is necessary for nuclear import of activated calcineurin via importin β1, and a nuclear export signal (NES) is present in the C-terminus of CNA (Figure 1-5A) (Hallhuber et al., 2006). Interestingly, the auto-inhibitory domain of CNA regulates nuclear import and export by masking the NLS in inactive calcineurin, in addition to binding the catalytic site (Hallhuber et al., 2006; Li et al., 2011). Subcellular localization is also mediated by interaction with targeting proteins. The AKAP 79/150 scaffold anchors PKC, PKA, and calcineurin at distinct subcellular locations (Coghlan et al., 1995). This complex has been implicated in neuronal signaling (Coghlan et al., 1995; Dacher et al., 2013; Jurado et al., 2010; Oliveria et al., 2007).

The auto-inhibitory domain of calcineurin is located in the C-terminus of CNA (Hallhuber et al., 2006). In the myocardium, hypertrophy is characterized by increases in calcineurin activity (Ritter et al., 2002). Increased activity is due to proteolysis of calcineurin by the Ca^{2+}-dependent cysteine-protease calpain in the C-terminus of CNA, resulting in a cleaved 48 kDa form of CNA with the auto-inhibitory domain removed (Burkard et al., 2005; Hallhuber et al., 2006). This cleaved form is constitutively active, and localizes to the nucleus (Burkard et al., 2005). Cleaved forms of CNA have also been observed in the brains of Alzheimer disease patients, in response to neurotoxicity, and in a glaucoma model (Huang et al., 2005; Liu et al., 2005a; Wu et al., 2004). In Alzheimer disease brains, a 57 kDa cleaved form of CNA retains the auto-inhibitory domain, still requires Ca^{2+} and calmodulin, but has increased activity compared to the 60 kDa uncleaved form of CNA (Liu et al., 2005a). Inducing excitotoxicity in neurons induces cleavage of CNA by calpain resulting in multiple cleaved forms of CNA, including a 45 kDa fragment, a 48 kDa fragment and a 57 kDa fragment (Figure 1-5B) (Wu et al., 2004). The 45 kDa and 48 kDa forms do not contain the auto-inhibitory domain and are constitutively active, while in this study the 57 kDa appears to have activity similar to the full length 60 kDa form (Wu et al., 2004).

1.5.3 Calcineurin in the brain

Calcineurin is highly expressed in neurons, with highest expression detected in the hippocampus and moderate expression in the cerebellum and cerebral cortex in rat (Goto et al., 1986). In neurons, calcineurin associates with

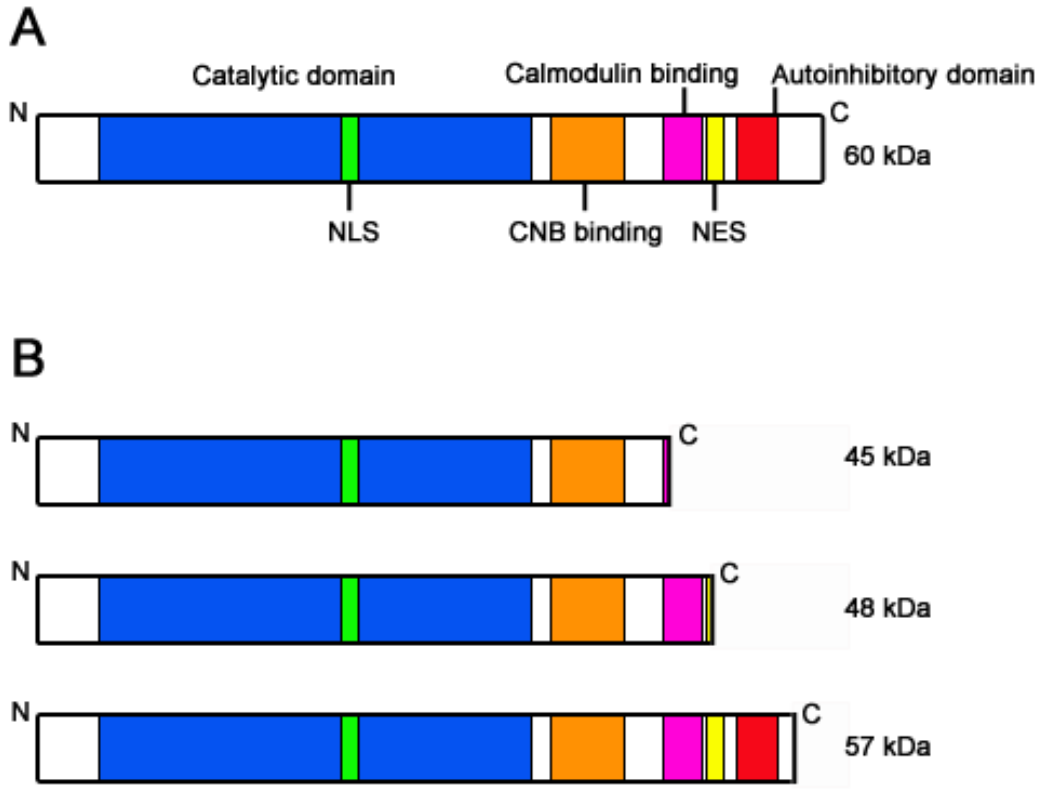

Figure 1-5: Calcineurin A domain structure. (A) Protein organization of calcineurin A with domains labeled. NLS-nuclear localization sequence, CNB-calcineurin B, NES-nuclear export sequence. (B) Cleaved forms of calcineurin. Size indicated on right. Adapted from *Wu et al* (Wu et al., 2004).

the cytoskeleton, and localizes to growth cones during neurite development (Ferreira et al., 1993). Calcineurin also localizes to post-synaptic densities, somata, axons and synaptic terminals in neurons (Goto et al., 1986). Calcineurin plays important roles in synaptic signaling, regulating plasticity at both inhibitory and excitatory synapses (Baumgartel and Mansuy, 2012). This occurs via regulation of multiple substrates and targeting mechanisms at both the presynaptic and post-synaptic terminals of neurons. Targets include potassium channels (Czirjak and Enyedi, 2006; Czirjak et al., 2004), membrane receptors (Alagarsamy et al., 2005; Lu et al., 2000; Sanderson et al., 2012) and associated proteins (Baumgartel and Mansuy, 2012). Calcineurin is critical for cyclic AMP response element binding protein (CREB)-dependent gene transcription in cortical neurons (Kingsbury et al., 2007), and activation of NFAT family members by calcineurin in neurons is necessary for axonal growth during neural development (Graef et al., 2003).

Normal astrocytes express low levels of calcineurin (Vinade et al., 1997), with expression increasing in reactive astrocytes (Hashimoto et al., 1998). In reactive astrocytes, calcineurin integrates pro-inflammatory and anti-inflammatory signals (Fernandez et al., 2007). In quiescent astrocytes, inflammatory challenge stimulates expression of calcineurin and downstream activation of NFκB/NFAT pro-inflammatory signaling. If calcineurin is already expressed, as in reactive astrocytes, calcineurin inhibits NFκB/NFAT pro-inflammatory signaling and decreases neuronal cell death (Fernandez et al., 2007). Expression of calcineurin

in activated astrocytes increases with age, and is also associated with Alzheimer's disease (Norris et al., 2005). This, combined with recent work demonstrating activation of calcineurin, the NFAT pathway and the neuroinflammatory response in astrocytes, suggests that calcineurin may play important roles in neurodegeneration in these cells (Abdul et al., 2009; Norris et al., 2005; Sama et al., 2008).

1.6 Research Objectives

1.6.1 Chapter 2

Glial fibrillary acidic protein (GFAP), an intermediate filament protein normally found in astrocytes, and the radial glial marker brain fatty acid-binding protein (B-FABP, FABP7), are co-expressed in malignant glioma cell lines and tumours. Nuclear Factor I (NFI) recognition sites have been identified in the *B-FABP* and *GFAP* promoters, and transcription of both genes is believed to be regulated by NFI. In Chapter 2, we study the role of the different members of the NFI family in regulating endogenous and ectopic *B-FABP* and *GFAP* gene transcription in human malignant glioma cells. We show by gel shifts that all four members of the NFI family (NFIA, NFIB, NFIC, NFIX) bind to *B-FABP* and *GFAP* NFI consensus sites. Over-expression of NFIs, in conjunction with mutation analysis of NFI consensus sites using a reporter gene assay, support a role for all four NFIs in the regulation of the *GFAP* and *B-FABP* genes. Knock-down of single or combined NFIs reveals promoter-dependent and promoter context-dependent interaction patterns, and suggests cross-talk between the different members of the

NFI family. Our data indicate that the NFI family of transcription factors plays a key role in the regulation of both the *B-FABP* and *GFAP* genes in malignant glioma cells.

1.6.2 Chapter 3

Grade III and IV astrocytomas, commonly referred to as malignant glioma (MG), are the most common adult human brain tumours. Despite aggressive treatment including surgery, radiation, and chemotherapy, median survival remains less than two years. The Nuclear Factor I (NFI) transcription factor family (NFIA, B, C, and X) is normally expressed in the developing brain and promotes glial cell differentiation. NFI is also expressed in MG, where it regulates expression of glial genes, and genes involved in proliferation and migration. In chapter 3 we use chromatin immunoprecipitation (ChIP)-on-chip with a promoter microarray to identify additional NFI target genes in MG cells. We identify 403 putative NFI target genes, including *HEY1*, a Notch effector gene that promotes maintenance of undifferentiated cells in the developing brain. Using electrophoretic mobility shift assays we show that NFI binds to NFI consensus binding sites in the *HEY1* promoter. Knockdown of NFIs in conjunction with reporter gene assays and quantitative PCR (qPCR) reveal that NFI represses expression of *HEY1* in MG cells. We also examined expression of glial genes, including NFIs following *HEY1* knockdown, as HEY1 promotes maintenance of undifferentiated cells. Knockdown of HEY1 in MG cells resulted in increased expression of *GFAP* and decreased expression of *NFIB*. Taken together, our data demonstrate that NFI represses

expression of *HEY1* in MG, and in turn HEY1 modulates expression of glial genes in these cells.

1.6.3 Chapter 4

Malignant gliomas (MG), comprising grades III and IV astrocytomas, are the most common adult brain tumours. These tumours are highly aggressive with a median survival of less than two years. Nuclear Factor I (NFI) is a family of transcription factors that regulates the expression of glial genes in the developing brain. We have previously shown that regulation of the brain fatty acid-binding protein (*B-FABP*) and glial fibrillary acidic protein (*GFAP*) genes in MG cells is dependent on the phosphorylation state of NFI, with hypophosphorylation of NFI correlating with GFAP and B-FABP expression. Importantly, NFI phosphorylation is dependent on phosphatase activity that is enriched in GFAP/B-FABP+ve cells. Using chromatin immunoprecipitation, we show that NFI occupies the *GFAP* and *B-FABP* promoters in NFI-hypophosphorylated GFAP/B-FABP+ve MG cells. NFI occupancy, NFI-dependent transcription activity and NFI phosphorylation are all modulated by the serine/threonine phosphatase calcineurin. Importantly, a cleaved form of calcineurin, associated with increased phosphatase activity, is specifically expressed in NFI-hypophosphorylated GFAP/B-FABP+ve MG cells. Calcineurin in GFAP/B-FABP+ve MG cells localizes to the nucleus. In contrast, calcineurin is primarily found in the cytoplasm of GFAP/B-FABP-ve cells, suggesting a dual mechanism for calcineurin activation in MG. Finally, our results demonstrate that calcineurin expression is upregulated in areas of high infiltration/migration in grade

IV astrocytoma tumour tissue. Our data suggest a critical role for calcineurin in NFI transcriptional regulation and in the determination of MG infiltrative properties.

Chapter 2

NUCLEAR FACTOR I REGULATES BRAIN FATTY ACID-BINDING PROTEIN AND GLIAL FIBRILLARY ACIDIC PROTEIN GENE EXPRESSION IN MALIGNANT GLIOMA CELL LINES

A version of this chapter has been published. Brun, M.[1], Coles, J.E.[1], Monckton, E.A., Glubrecht, D.D., Bisgrove, D., Godbout, R. (2009). Nuclear factor I regulates brain fatty acid-binding protein and glial fibrillary acidic protein gene expression in malignant glioma cell lines, Journal of Molecular Biology 391: 282-300. [1]co-first authors

2.1 Introduction

Malignant gliomas, comprising grades III and IV astrocytomas (also called anaplastic astrocytoma and glioblastoma, respectively), are the most common brain tumours in adults (Bohnen and Radhakrishnan, 1997). These highly invasive tumours are usually fatal within two years of diagnosis. Histopathological analysis of malignant gliomas has shown that increasing anaplasia correlates with reduced levels of the intermediate filament protein GFAP (Eng and Rubinstein, 1978; van der Meulen et al., 1978). Manipulation of GFAP levels in malignant glioma cells suggests an association between GFAP expression and a reduced transformed state (Chen and Liem, 1994; Engelhard et al., 1997; Langlois et al., 2002; Murphy et al., 1998; Rutka et al., 1994; Rutka and Smith, 1993).

Brain fatty acid-binding protein (B-FABP; also known as FABP7 or BLBP) is a marker of radial glial cells (Feng et al., 1994; Kurtz et al., 1994). B-FABP has been implicated in the establishment of the radial glial fiber system required for the migration of neurons to their correct location in the central nervous system and in glial cell differentiation (Feng et al., 1994; Kurtz et al., 1994). It is generally believed that neural stem cells give rise to radial glial cells which in turn become mature astrocytes once neuronal migration is complete (Culican et al., 1990; Schmechel and Rakic, 1979). However, radial glial cells can also give rise to neurons and have been proposed to function as neural stem cells (Anthony et al., 2004; Malatesta et al., 2003; Noctor et al., 2002). B-FABP expression has recently been shown to be associated with increased cell migration in malignant glioma cells and with a worse clinical prognosis in high grade astrocytomas (Kaloshi et al., 2007; Liang et al.,

2005; Mita et al., 2007). Of note, malignant glioma cell lines that express B-FABP also express GFAP, suggesting either a functional or regulatory link between these two proteins (Godbout et al., 1998).

Nuclear Factor I (NFI) has been implicated in the regulation of both the *B-FABP* and *GFAP* genes (Bisgrove et al., 2000; Cebolla and Vallejo, 2006; Gopalan et al., 2006b). NFI is a family of transcription factors that includes four genes: *NFIA*, *NFIB*, *NFIC*, *NFIX/NFID* (Qian et al., 1995). Additional diversity within this family comes from alternative splicing and post-translational modification (reviewed in (Gronostajski, 2000)). NFI proteins bind to the consensus sequence 5'-TTGGCN_5GCCAA-3' as homodimers or heterodimers with the same apparent affinity (Kruse and Sippel, 1994b; Roulet et al., 2000). NFIs are widely expressed in different tissues and cell types, although the distribution pattern of each NFI varies from tissue to tissue (Chaudhry et al., 1997). NFI consensus binding sites are found in many brain-specific gene promoters/enhancers and NFI transcription factors have been proposed to play a role in the determination of gene expression in glial cells (Amemiya et al., 1992; Deneen et al., 2006; Inoue et al., 1990; Kumar et al., 1993; Major et al., 1990; Shu et al., 2003).

The *B-FABP* promoter has at least two NFI recognition elements located within 500 bp of the *B-FABP* transcription start site. Using a combination of gel shift assays and potato acid phosphatase treatment, NFI was shown to be hyperphosphorylated in GFAP/B-FABP-negative malignant glioma cell lines compared to GFAP/B-FABP-positive lines (Bisgrove et al., 2000). Phosphorylation of NFI did not appear to affect DNA binding activity *in vitro*, in agreement with a

previous report (Yang et al., 1993). Similarly, transfection and DNase I footprinting analysis revealed three footprints in the promoter region of the *GFAP* gene in the B-FABP/GFAP-positive malignant glioma cell line U251 (Besnard et al., 1991; Masood et al., 1993). Putative NFI binding sites were identified in all three regulatory regions. Direct evidence demonstrating occupancy of the *GFAP* promoter by NFIs was obtained by chromatin immunoprecipitation using primary cortical neuroepithelial cells (Cebolla and Vallejo, 2006).

All four NFI genes have been disrupted in mice (das Neves et al., 1999b; Driller et al., 2007; Shu et al., 2003; Steele-Perkins et al., 2003; Steele-Perkins et al., 2005). Whereas *Nfic*-deficient animals have defects in tooth root formation, disruption of either *Nfia* or *Nfib* results in forebrain defects and loss of specific midline glial populations. In addition to having more severe forebrain defects than *Nfia*, *Nfib* knock-outs have abnormalities in lung maturation and development of the pons (Steele-Perkins et al., 2005). *Nfix-/-* mice show enlargement of the lateral and third brain ventricles, expansion of the entire brain along the dorsal ventral axis, aberrant formation of the hippocampus, deformation of the spine and impaired ossification of vertebra and femur (Campbell et al., 2008; Driller et al., 2007). *GFAP* mRNA levels are decreased 10-fold and 5-fold in *Nfia-/-* and *Nfib-/-* mice, respectively, suggesting involvement of these two NFIs in *GFAP* regulation (Steele-Perkins et al., 2005). Activation of Notch signaling in mid-gestational neural precursor cells has recently been shown to induce NFIA, resulting in demethylation and activation of astrocytic gene promoters including *GFAP* (Namihira et al., 2009).

Thus, NFIA appears to play a fundamental role in potentiating the differentiation of neural precursor cells along the astrocytic lineage.

Here, we investigate the role of NFI in the regulation of the *GFAP* and *B-FABP* genes in malignant glioma cells. We use chromatin immunoprecipitations (ChIP) to demonstrate the occupancy of NFIs at both the endogenous *GFAP* and *B-FABP* promoters. We study the expression patterns of all four *NFI* genes in B-FABP/GFAP-positive and B-FABP/GFAP-negative malignant glioma cell lines and use the gel shift assay to examine the binding of each NFI to three NFI recognition sites located at the 5' ends of each of the *B-FABP* and *GFAP* genes. We use a combination of RNA interference, ectopic NFI expression, reporter gene assay, and analysis of endogenous *GFAP* and *B-FABP* RNA to investigate the biological activity of NFIs *in vivo*. Our results suggest complex antagonistic and compensatory interactions between the four members of the NFI family which all appear to be involved in the regulation of *B-FABP* and *GFAP* transcription.

2.2 Materials and methods

2.2.1 Cell lines, constructs and transfections

The sources of the human malignant glioma cell lines included in this analysis have been previously described (Godbout et al., 1998) with the exception of M103 which was established by Dr. Rufus Day (Department of Oncology, University of Alberta) from a malignant glioma biopsy. Cells were cultured in Dulbecco's modification of Eagle's MEM supplemented with 10% fetal calf serum, 100 U/ml penicillin and 100 µg/ml streptomycin.

The pCH-NFI expression vectors (pCH, pCH-NFIA, pCH-NFIB, pCH-NFIC, pCH-NFIX) were obtained from Dr. R. Gronostajski (Case Western Reserve University). The following chloramphenicol acetyltransferase (CAT) reporter gene constructs were used for the *B-FABP* and *GFAP* promoter assays: (i) pCAT/B-FABP-1785 containing 5' *B-FABP* flanking DNA from -1785 to +20 bp, (ii) pCAT/GFAP-168 with 5' *GFAP* flanking DNA from -168 to +8 bp. and (iii) pCAT/GFAP-1708 with 5' *GFAP* flanking DNA from -1708 to +8 bp. Plasmids were introduced into the U251 malignant glioma cell line by polyethylenimine (PEI – Polysciences Inc.) -mediated DNA transfection. Cells were harvested 60 h after transfection and a fixed portion (75 or 80% depending on the experiment) used to prepare lysates for CAT activity. CAT activity was measured using 1/10 of the lysates following the protocol supplied by Promega. Acetylated ^{14}C-chloramphenicol was measured (in cpm) using a scintillation counter. To control for plate to plate variation in amount of transfected DNA, a fixed portion of the cells (20 or 25% depending on the experiment) was used to isolate non-integrated DNA

(Hirt, 1967). The DNA was restriction enzyme-digested, electrophoresed on a 1% agarose gel, transferred to nitrocellulose and probed with radioactively-labeled pCAT basic DNA.

Single, double and triple mutations of the three NFI binding sites (G-br1, G-br2 and G-br3) located upstream of the *GFAP* transcription start site were generated by sequential PCR (Cormack and Castano, 2002). For single mutations, complementary oligonucleotides carrying two base pair substitutions (GG $\rightarrow$ AA) for each of G-br1, G-br2 and G-br3 were used in conjunction with upstream and downstream pCAT-1708 primers to generate fragments corresponding to the 1708 bp *GFAP* promoter region. *GFAP* promoter fragments mutated at either G-br1 (G-br1*), G-br2 (G-br2*) or G-br3 (G-br3*) (Figure 2-2C) were inserted in the pCAT basic vector. The double mutant (G-br2*/G-br3*) was generated from the G-br2* mutant whereas the triple mutant (G-br1*/G-br2*/G-br3*) was generated from the G-br2*/G-br3* double mutant. Sequence analysis revealed that all mutated sites were as expected except for the G-br2 site in the triple mutant where GG was converted to AG instead of AA.

2.2.2 Northern blot analysis

Conditions for poly(A)$^+$ RNA isolation, probe hybridization, washing filters, and stripping filters have been described (Godbout et al., 1998). The following probes were used for hybridization: 1.8 kb *Eco*RI/*Nco*I cDNA insert from human *NFIA* EST clone #45182 (Genome Systems, Inc.); 600 bp human *NFIB* cDNA corresponding to sequences 934 to 1521 of U85193 (GenBank Accession

Number) generated by PCR amplification; 800 bp *Eco*RI/*Hin*dIII cDNA insert from human *NFIC* EST clone #129328; 700 bp *Pst*I/*Xho*I cDNA insert from human *NFIX* EST clone #154038; 500 bp *Eco*RI/*Eco*RV *GFAP* cDNA insert (GenBank M78090) (American Type Culture Collection, Rockville, MD); 700 bp *B-FABP* cDNA insert (Godbout et al., 1998); and 500 bp mouse actin cDNA (Minty et al., 1981).

2.2.3 Quantitative RT-PCR analysis

Total RNA was isolated using the RNeasy Plus Kit (QIAGEN) and first strand cDNA synthesized from 3.5 μg RNA using Superscript reverse transcriptase (Invitrogen). The cDNA was amplified using TaqMan Universal PCR Master Mix and gene-specific oligonucleotides (NFIA – Hs00325656_m1, NFIB – Hs00232149_m1, NFIC - Hs00907819_m1 , NFIX - Hs00958849_m1, GFAP – Hs00157674_m1, B-FABP – Hs00361426_m1, GAPDH – Hs99999905_m1) labeled at the 5' end with the fluorescent reporter dye FAM (Applied Biosystems) (ABI 7900HT Fast Real-Time PCR System). All cDNAs were run in triplicate and the data normalized using *GAPDH*.

2.2.4 Western blot analysis

Nuclear extracts were prepared as described (Dignam et al., 1983). Whole cell extracts were prepared by resuspending the cells in 50 mM Tris-HCl pH 7.5, 150 mM NaCl, 0.5% sodium deoxycholate, 1% Nonidet P-40, 25 mM sodium pyrophosphate, 50 mM sodium fluoride, 1X Complete protease inhibitor (Roche), 1 mM PMSF, and lysing cells on ice for 20 minutes. Protein extracts were

electrophoresed in polyacrylamide-SDS gels followed by electroblotting onto PVDF or nitrocellulose membranes. Blots were immunostained with mouse anti-hemagglutinin (HA) antibody (Sigma: Clone HA-7, Cat. No. H9658) (1:10000), mouse anti-proliferating cell nuclear antigen (PCNA) antibody (BD Biosciences: Clone 24, Cat No. 610664) (1:1000), rabbit anti-B-FABP (Godbout et al., 1998) (1:2000), mouse-GFAP antibody (BD Biosciences: Clone G-A-5, Cat. No. 814369) (1:10000), and mouse anti-actin antibody (Sigma: Clone AC-15, Cat. No. A5441) (1:50000). Primary antibodies were detected with horseradish peroxidase-conjugated secondary antibodies (Jackson ImmunoResearch Biotech) using the ECL detection system (Amersham Biosciences).

2.2.5 Gel shift assay

The gel shift assay was carried out as described (O'Brien et al., 1995). The sequences of the *B-FABP* (B-br1, B-br2, B-br3) and *GFAP* (G-br1, G-br2, G-br3) NFI binding regions are listed in Figure 2-2. Complementary oligonucleotides were annealed and radiolabeled by filling-in with Klenow polymerase in the presence of [α-^{32}P]dCTP. Site-directed mutagenesis of G-br1, G-br2 and G-br3 was carried out by substituting the conserved G-G residues at positions 3 and 4 of the NFI consensus binding site with A-A (Figure 2-2). NFI, Sp1 and AP-2 double-stranded oligonucleotides were generated by annealing: 5'-ATTTTGGCTTGAAGCCAATATG-3' and 5'-CATATTGGCTTCAAGCCAA AAT-3' (NFI consensus binding site is underlined); 5'-GATCGATCGGGGCGGGGCGATC-3' and 5'-

GATCGCCCCGCCCCGATCGATC-3' (Sp1); 5'-GATCGAACTGACCGCCCGCGGCCCGT-3' and 3'-ACGGGCCGCGGGCGGTCAGTTCGATC-3' (AP-2).

Nuclear extracts from T98, U251, as well as T98 cells transiently transfected with 10 μg pCH control vector or pCH HA-tagged NFIA, NFIB, NFIC and NFIX expression constructs were prepared as described earlier. Nuclear extracts (4 μg for T98 and U251 and 1 μg for transfected cells) were pre-incubated in the presence of 1.25 μg poly(dI-dC) in binding buffer (20 mM HEPES pH 7.9, 20 mM KCl, 1 mM spermidine, 10 mM dithiothreitol, 10% glycerol, 0.1% Nonidet P-40) for 10 min at room temperature. When included, a 100X molar excess of unlabeled competitor oligonucleotide was added during the pre-incubation stage. For supershift experiments, 1 μl anti-HA antibody (Sigma: Clone HA-7, Cat. No. H9658), 1 μl anti-NFI antibody, obtained from Dr. Naoko Tanese (NYU Medical Center NY), 1 μl anti-AP-2 antibody (negative control) (Santa Cruz Biotechnology Inc.: Clone C18, Cat No. sc-184) or 1 μl anti-Pax6 antibody (negative control) (Developmental Studies Hybridoma Bank maintained by the University of Iowa under contract NO1-HD-7-3263 from the NICHD) was included in the pre-incubation reaction. Labeled DNA was added and incubated for 20 min at room temperature. DNA-protein complexes were resolved on a 6% polyacrylamide gel in 0.5X TBE.

2.2.6 Knock-down of endogenous NFIs

The following Stealth siRNAs were used to transfect U251 cells: NM_005595_stealth_919 targeting 5'-GAAAGUUCUUCAUACUACAGCAUGA-3' of NFIA, NM_005596_stealth_1020 targeting 5'-AAGCCACAAUGAUCCUGCCAAGAAU- 3' of NFIB, NM_005597_stealth_1045 targeting 5'- CAGAGAUGGACAAGUCACCAUUCAA-3' of NFIC, NM_002501_stealth_752 targeting 5'-GAGAGUAUCACAGACUCCUGUUGCA-3' of NFIX, and control siRNA (Cat. No. 12935-200 and 12935-300) (Invitrogen). Cells were transfected with 10 nM Stealth siRNAs targeting individual NFI genes using the RNAi-MAX Lipofectamine reagent (Invitrogen). Where appropriate, cells were transfected the following day with either GFAP- or B-FABP-CAT constructs using the PEI reagent. Cells were harvested 60 h after the last transfection. When multiple rounds of siRNA transfections were carried out, 9/10 of cells were harvested at confluency and 1/10 of the cells re-plated and re-transfected.

2.2.7 Chromatin immunoprecipitation

Chromatin immunoprecipitation was carried out as per Pillai *et al.* (Pillai et al., 2009). U251 cells were cross-linked with 1% formaldehyde for 20 min at room temperature. The cross-linking reaction was terminated with the addition of glycine to a final concentration of 0.125 M. Cells were harvested by cell scraping in 1X PBS, washed, and resuspended in lysis buffer (44 mM Tris-HCl pH 8.0, 1% SDS, 10 mM EDTA, 1 mM PMSF, and 1X Complete protease inhibitor cocktail). Cells

were sonicated for 3 X 30 s at 30% output (Model 300VT, Ultrasonic Homogenizer, BioLogics Inc.). Following sonication, ChIP lysate was precleared by incubation with protein A Sepharose beads (GE Healthcare). The pre-cleared ChIP lysate was incubated with either 3 µg rabbit anti-NFI antibody (Santa Cruz: Clone N-20, Cat. No. sc-870) or 3 µg rabbit IgG (negative control) at 4ºC overnight. Protein A Sepharose beads were added to the ChIP lysate-antibody mixture and incubated for an additional 2 h at 4ºC. Beads were washed and protein-DNA complexes eluted in 0.1 M $NaHCO_3$, 1% SDS, 5 mM NaCl. Cross-links were reversed by incubation at 65ºC for 5 h. Proteins were digested with proteinase K and the DNA purified using a DNA purification kit (Marligen Rapid PCR purification system). Primers used to amplify specific regions of the GFAP, B-FABP, and GAPDH (negative control) promoters are listed in Table 2-1. PCR conditions were: 95ºC for 2 min, followed by 30 cycles at 95ºC for 30 s, 55ºC for 30 s, and 72ºC for 30 s, followed by an additional 7 min incubation at 72ºC. PCR products were resolved on a 1% agarose gel, and detected using ethidium bromide.

Table 2-1: Sequences of primers used for ChIP analysis

Fragment	Forward Sequence (5'-3')	Reverse Sequence (5'-3')
G-br1	GTCCTCTTGCTTCAGCGG	TGGGCTAGACTGGCGATG
G-br2	CAGGGCCTCCTCTTCATG	TAGAGCCTTGTTCTCCACC
G-br3	GGACGCTGCTCTGACAGA	CACTGGGCATGAAGAGGAG
G-br2/3	CAGACCTGGCAGCATTGG	CTGCTCAATGGGCTTCTCG
B-br1	GATTGGAGCCTCACTCGAG	CTGCAGCTCAGAAGACCC
B-br2	GCATAAGGGCTGTAGTGTG	CAGTGTCCCTCTTTCCAAG
B-br3	GTCTGAGATTGCCTTTGCC	GTTAGCGGAGTAGGTCGAG
B-br1/2/3	CGAACCTGAAAGCCCTTCT	GCTCCTGCCTTCTTATTTGG
GAPDH	GAACCAGCACCGATCACC	CCAGCCCAAGGTCTTGAG

2.3 Results

2.3.1 Expression of NFI mRNA in malignant glioma cell lines

The four *NFI* genes (*NFIA*, *NFIB, NFIC, NFIX*) are differentially expressed in various tissues and cell types. To identify which NFIs are expressed in malignant glioma cells, northern blot analysis was carried out using poly(A)$^+$ RNA isolated from five B-FABP/GFAP-negative malignant glioma lines (A172, CLA, M021, T98, U87) and five B-FABP/GFAP-positive malignant glioma lines (M016, M049, M103, U251, U373) (Figure 2-1). Highest levels of *NFIA* transcripts were detected in M049 and M103. *NFIB* mRNA was most abundant in B-FABP/GFAP-positive M049, M103, U251 and U373 lines. *NFIC* transcripts were found in all 10 lines. Highest levels of *NFIX* mRNA were observed in M103 and M021, with an easily detectable signal in every cell line except U87. Actin mRNA served as the loading control and was relatively uniform in the ten malignant glioma lines. Overall, B-FABP/GFAP-positive malignant glioma lines appear to express higher levels of NFI mRNAs than B-FABP/GFAP-negative lines, with the most dramatic differences observed with *NFIA* and *NFIB*.

2.3.2 *In vitro* binding of proteins to GFAP NFI recognition sites

Sequence analysis of the *GFAP* promoter region revealed three putative NFI binding sites in the upstream region of the *GFAP* gene, located at -120 to -106 bp, -1585 to -1571 bp and -1633 to -1619 bp. Each of these three sites is bound by protein based on DNase I footprinting analysis (Besnard et al., 1991; Masood et al., 1993) and gel shift assays (Gopalan et al., 2006b). We used gel shifts

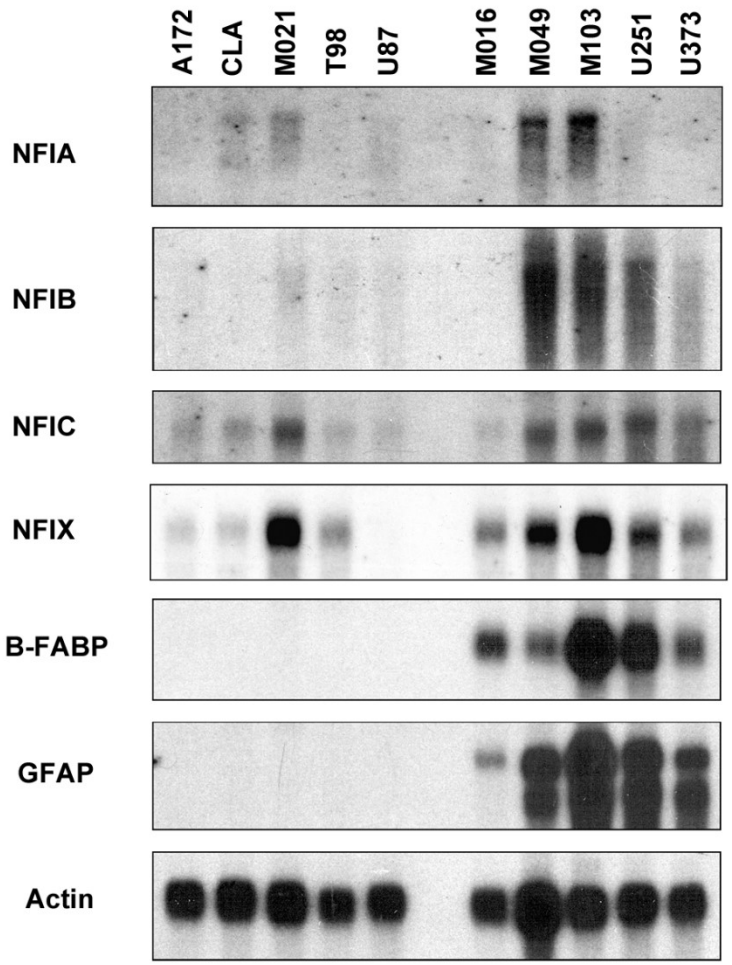

Figure 2-1: RNA analysis of malignant glioma cell lines. Northern blots were prepared using poly(A)$^+$ RNA (2 µg per lane) isolated from five human B-FABP/GFAP-negative lines (A172, CLA, M021, T98, and U87) and five human B-FABP/GFAP-positive lines (M016, M049, M103, U251, and U373). The filter was sequentially hybridized with ^{32}P-labeled cDNAs from *NFIA, NFIB, NFIC, NFIX, B-FABP, GFAP,* and actin.

to determine whether NFIs from T98 (B-FABP/GFAP-negative) and U251 (B-FABP/GFAP-positive) malignant glioma lines could bind to the three putative NFI binding sites located at the 5' end of the *GFAP* gene. Double-stranded oligonucleotides representing each of the three *GFAP* NFI binding regions: [G-br1 (-126 to -100 bp), G-br2 (-1591 to -1564 bp), G-br3 (-1639 to -1613 bp)] were generated. Radiolabeled oligonucleotides were incubated with nuclear extracts prepared from either T98 or U251 cells. A 100X molar excess of unlabeled competitor oligonucleotides was included in some of the lanes. Competitor oligonucleotides included G-br1, G-br2, G-br3 (wild-type and mutated at conserved residues 3 and 4), Sp1, NFI and AP-2 (Figure 2-2).

As shown in Figure 2-3A, a major DNA-protein complex was observed when G-br1, G-br2 or G-br3 was incubated with T98 nuclear extracts. Addition of excess mutated G-br1*, G-br2* or G-br3* oligonucleotides as competitors did not result in a significant reduction in the signal intensity of the complex, indicating that protein binding to these oligonucleotides requires an intact NFI binding site. All three unlabeled wild-type G-br oligonucleotides served as effective competitors for all three G-br probes. Furthermore, the intensity of the DNA-protein complex was significantly reduced in the presence of consensus NFI oligonucleotides, but not Sp1 or AP-2 oligonucleotides. These results indicate that the factor bound to G-br1, G-br2 and G-br3 is NFI or NFI-like.

Similar observations were made when G-br1 and G-br2 probes were incubated with U251 nuclear extracts, except that the migration rate of the DNA-protein complex was considerably faster than that observed with T98 extracts

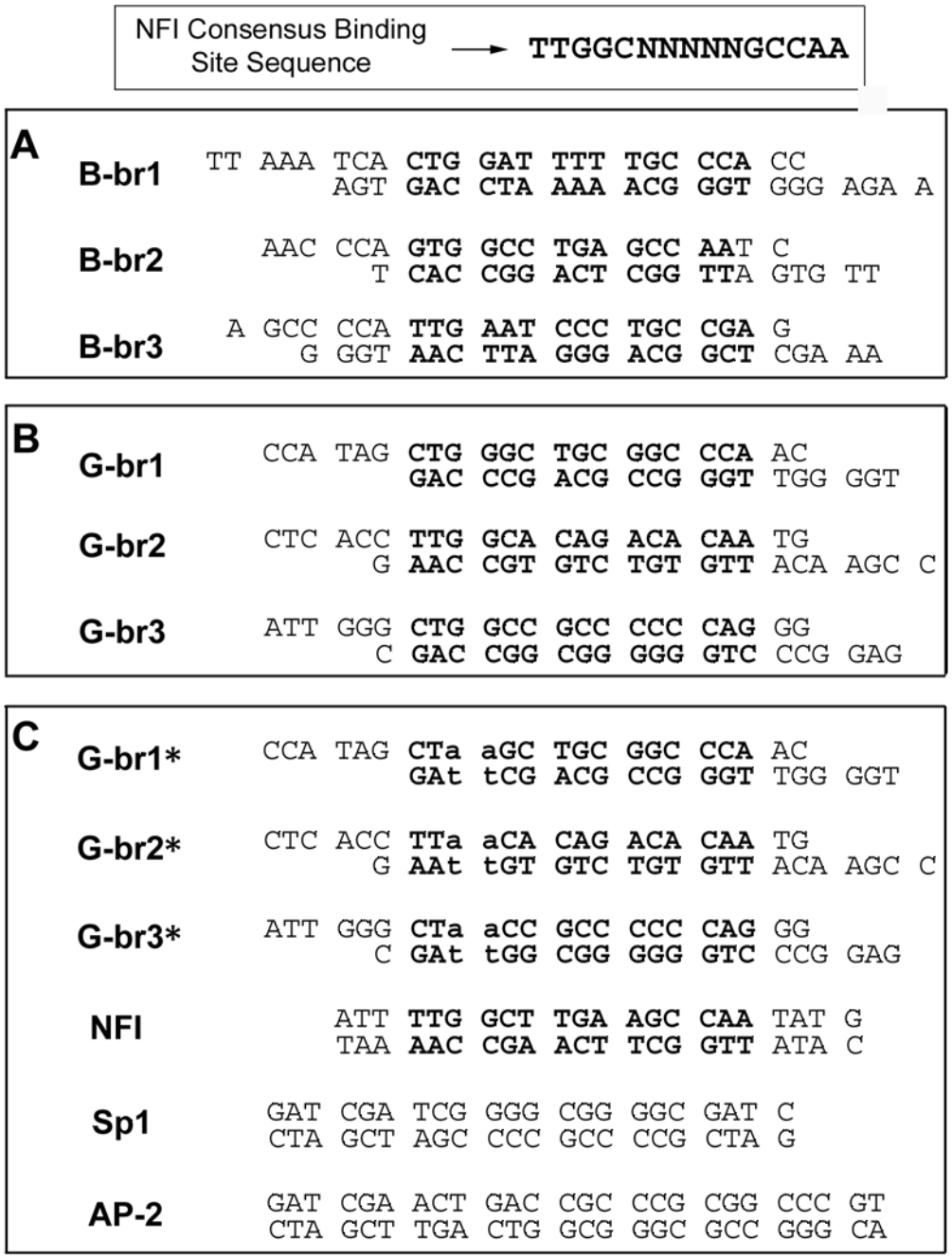
NFI Consensus Binding Site Sequence
TTGGCNNNNNGCCAA
A
B-br1
TT AAA TCA CTG GAT TTT TGC CCA CC
AGT GAC CTA AAA ACG GGT GGG AGA A
B-br2
AAC CCA GTG GCC TGA GCC AAT C
T CAC CGG ACT CGG TTA GTG TT
B-br3
A GCC CCA TTG AAT CCC TGC CGA G
G GGT AAC TTA GGG ACG GCT CGA AA
B
G-br1
CCA TAG CTG GGC TGC GGC CCA AC
GAC CCG ACG CCG GGT TGG GGT
G-br2
CTC ACC TTG GCA CAG ACA CAA TG
G AAC CGT GTC TGT GTT ACA AGC C
G-br3
ATT GGG CTG GCC GCC CCC CAG GG
C GAC CGG CGG GGG GTC CCG GAG
C
G-br1*
CCA TAG CTa aGC TGC GGC CCA AC
GAt tCG ACG CCG GGT TGG GGT
G-br2*
CTC ACC TTa aCA CAG ACA CAA TG
G AAt tGT GTC TGT GTT ACA AGC C
G-br3*
ATT GGG CTa aCC GCC CCC CAG GG
C GAt tGG CGG GGG GTC CCG GAG
NFI
ATT TTG GCT TGA AGC CAA TAT G
TAA AAC CGA ACT TCG GTT ATA C
Sp1
GAT CGA TCG GGG CGG GGC GAT C
CTA GCT AGC CCC GCC CCG CTA G
AP-2
GAT CGA ACT GAC CGC CCG CGG CCC GT
CTA GCT TGA CTG GCG GGC GCC GGG CA

Figure 2-2: **Oligonucleotides used for the gel shift experiments.** The NFI consensus binding site sequence is indicated on top. The primers used to generate (A) *B-FABP* NFI binding regions (B-br1, B-br2, B-br3) and (B) *GFAP* NFI binding regions (G-br1, G-br2, G-br3) are shown with the NFI consensus sites indicated in bold. (C) Site-directed mutagenesis was used to convert the third and fourth residues of the *GFAP* NFI binding regions from GG to AA (indicated in small letters). Both these residues have been shown to be critical for binding to NFI. The sequences of the NFI, Sp1 and AP2 oligonucleotides are based on consensus binding sites.

(Figure 2-3B). These results are in agreement with our previous work indicating that NFIs expressed in U251 and T98 migrate at different rates in gel shift assays because the T98 NFIs are hyperphosphorylated compared to U251 NFIs (Bisgrove et al., 2000). In contrast to G-br1 and G-br2 which generated one major protein-DNA complex, three DNA-protein complexes were observed when U251 nuclear extracts were incubated with G-br3. As the intensity of the middle band (indicated by arrow) was greatly decreased in the presence of excess wild-type G-br1, G-br2, G-br3 and NFI consensus oligonucleotides but not mutated G-br3 oligonucleotide, it is likely that this is the only band that contains NFI-DNA complexes. Interestingly, the faster migrating complex disappeared in the presence of AP-2 competitor suggesting the presence of both NFI and AP-2 binding sites within the G-br3 oligonucleotide. Examination of the G-br3 sequence reveals putative AP-2 binding sites (consensus GCCNNNGGC) spanning the NFI binding site.

2.3.3 *In vitro* binding of proteins to B-FABP NFI recognition sites

Previous work from our lab identified two NFI binding sites in the 5' flanking DNA of the *B-FABP* gene, located at -54 to -40 bp (B-br1) and -256 to -242 bp (B-br3) (Bisgrove et al., 2000). These sites were identified by DNase I footprinting and binding of NFI to these sites was confirmed by gel shift assays and methylation interference. A third putative NFI-like binding site, located at -176 to -163 bp (B-br2), was not analyzed because: (i) it was found at the 5' edge of a DNase I footprint and (ii) it had N-4 spacing between the NFI half-sites rather than the consensus N-5 spacing. Addition or subtraction of 1 bp from the 5 bp internal

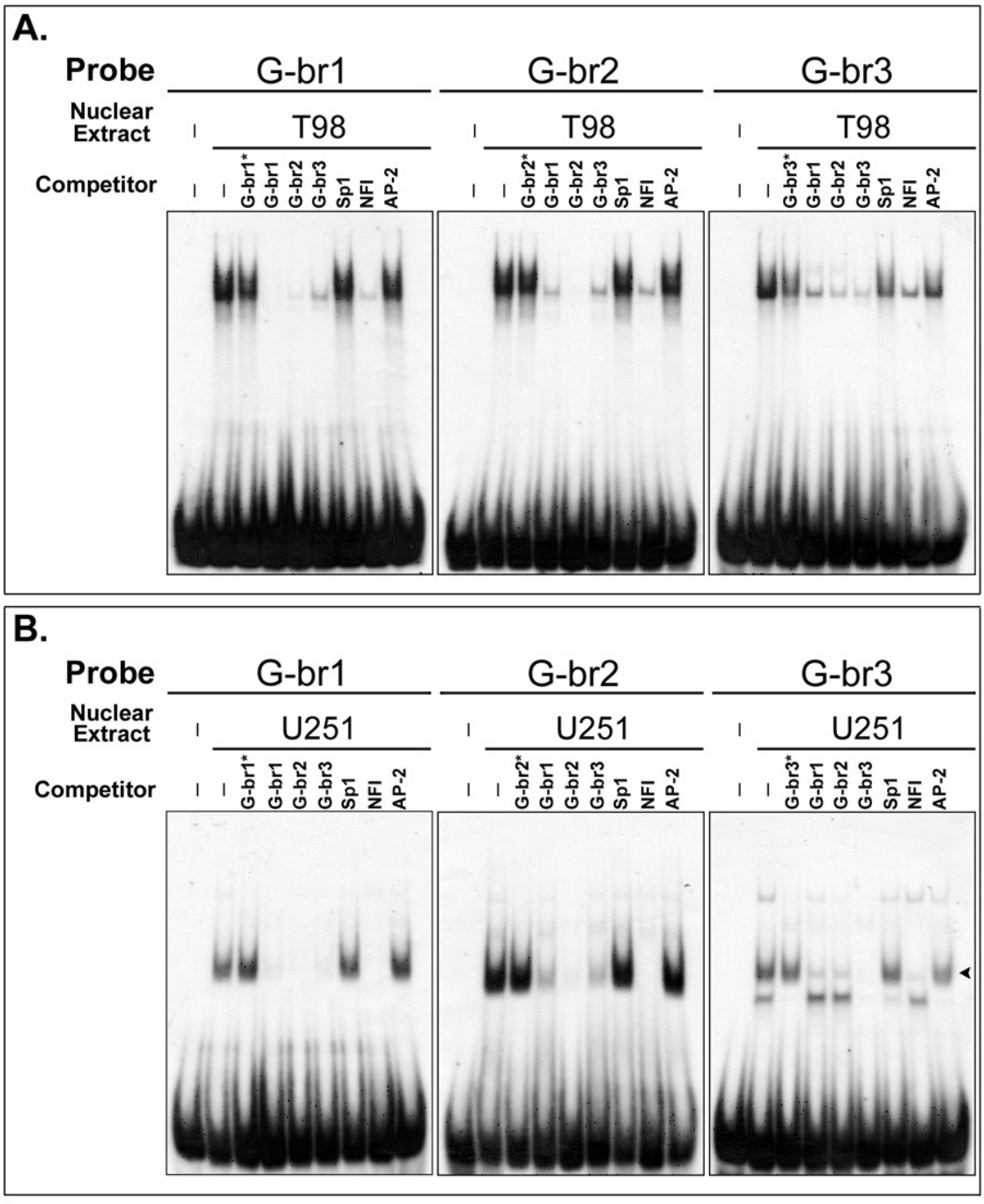
A.
Probe
G-br1
G-br2
G-br3
Nuclear Extract
–
T98
T98
T98
Competitor
–
–
G-br1*
G-br1
G-br2
G-br3
Sp1
NFI
AP-2
–
–
G-br2*
G-br1
G-br2
G-br3
Sp1
NFI
AP-2
–
–
G-br3*
G-br1
G-br2
G-br3
Sp1
NFI
AP-2
B.
Probe
G-br1
G-br2
G-br3
Nuclear Extract
–
U251
U251
U251
Competitor
–
–
G-br1*
G-br1
G-br2
G-br3
Sp1
NFI
AP-2
–
–
G-br2*
G-br1
G-br2
G-br3
Sp1
NFI
AP-2
–
–
G-br3*
G-br1
G-br2
G-br3
Sp1
NFI
AP-2

Figure 2-3: Binding of NFI to G-br1, G-br2 and G-br3. Gel shift experiments were carried out with radiolabeled G-br1, G-br2 or G-br3 double-stranded oligonucleotides and (A) T98 or (B) U251 nuclear extracts. DNA binding reactions were electrophoresed in a 6% polyacrylamide gel in 0.5X TBE buffer to separate unbound DNA and DNA-protein complexes. Where indicated, a 100-fold excess of unlabeled competitor oligonucleotides were added to the DNA binding reaction. The asterisks indicate that the NFI binding site was mutated.

spacer has been shown to drastically reduce NFI binding *in vitro* (Gronostajski, 1987). We used the gel shift assay to determine whether a radiolabeled double-stranded oligonucleotide corresponding to B-br2 could bind NFI or NFI-like proteins. As shown in Figure 2-4 (left panel), a DNA-protein complex was observed using U251 nuclear extracts, although the intensity of the complex in relation to free oligonucleotides appeared low when compared with B-br1 (Figure 2-4 - right panel). The protein complex formed with B-br2 was significantly reduced in the presence of excess cold competitors B-br1, B-br2 and B-br3, NFI consensus binding site, but not AP-2 and Sp1 consensus binding sites. Conversely, addition of excess B-br2 significantly reduced the intensity of the DNA-protein complex obtained with B-br1.

2.3.4 *In vivo* occupancy of NFIs at the endogenous *B-FABP* and *GFAP* promoters

We carried out ChIP analysis using U251 cells and a pan-specific NFI antibody to determine whether NFIs reside in close proximity to *GFAP* and *B-FABP* NFI binding sites *in vivo.* DNA cross-linked to NFIs was PCR-amplified using primer pairs flanking individual or combined *GFAP* and *B-FABP* NFI binding sites. Normal rabbit IgG served as the negative control for the ChIP experiments. Bands corresponding to each of the three *GFAP* NFI binding sites (G-br1, G-br2 and G-br3) were easily detected using this approach (Figure 2-5). Similarly, ChIP analysis revealed NFIs at all three *B-FABP* NFI binding sites, although the intensity of the

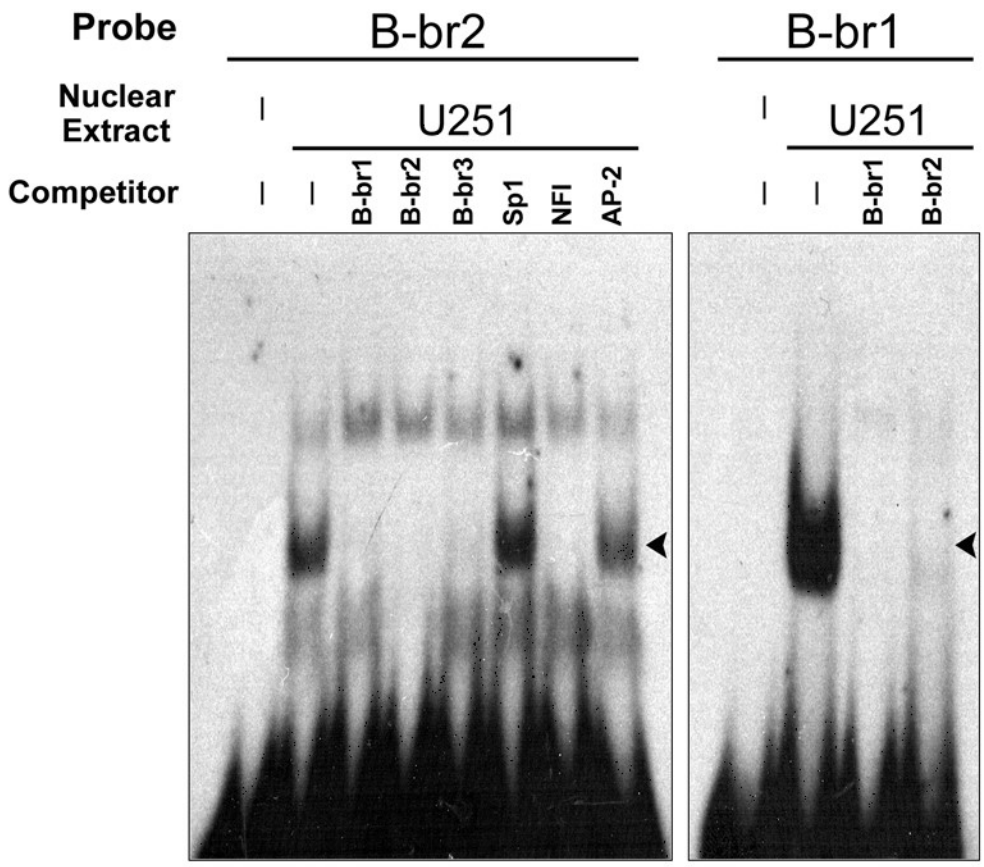

Figure 2-4: Binding of NFI to B-br2. Gel shift experiments were carried out with radiolabeled B-br2 double-stranded oligonucleotide. The arrow indicates the protein-DNA complex specific to B-br2 (left panel) and B-br1 (right panel).

band obtained with primers flanking B-br1 was weak. No DNA bands were detected in any of the IgG lanes. As well, no signal was detected in either the IgG or NFI lanes when primers to the *GAPDH* promoter were utilized. Together, these data indicate that NFIs occupy the regions of the *B-FABP* and *GFAP* promoters containing NFI binding sites.

2.3.5 Binding of specific NFIs to GFAP and B-FABP NFI recognition sites

Our gel shift data suggest that one or more NFI protein(s) can bind to each of the three NFI recognition sites located upstream of the *GFAP* gene (Figure 2-3) as well as to the three NFI recognition sites located upstream of the *B-FABP* gene (Figure 2-4) (Bisgrove et al., 2000). To address the specificity of the different NFI proteins for *GFAP* and *B-FABP* NFI recognition sites, we examined the binding of each of the four NFIs to G-br and B-br oligonucleotides. T98 cells were transfected with HA-tagged NFIA, NFIB, NFIC and NFIX expression constructs as well as empty vector. Nuclear extracts were prepared and analyzed for level of NFI protein. As shown in Figure 2-6A, each HA-tagged NFI protein was abundantly expressed in T98 transfectants, with NFIA present at ~2-fold lower levels and NFIC expressed at ~1.5-fold higher levels compared to NFIB and NFIX.

For the gel shift assays, an equal amount of each of these nuclear extracts (~1 μg of protein) was incubated with radiolabeled G-br1, G-br2 and G-br3 oligonucleotides (Figure 2-6B). Strong binding was observed when either NFIA or NFIX was incubated with G-br1, whereas NFIB and NFIC generated weaker

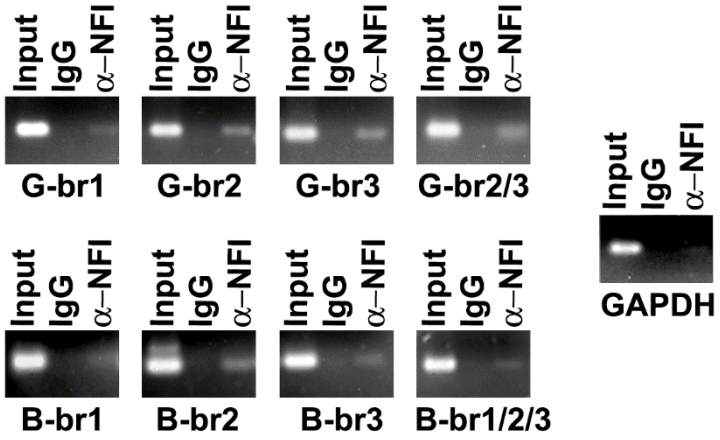

Figure 2-5: Chromatin immunoprecipitation analysis indicating that NFIs occupy the endogenous GFAP and B-FABP promoters. Chromatin immunoprecipitations were carried out using either a pan-specific anti-NFI antibody or normal rabbit IgG and U251 cell lysates. Primers flanking the NFI recognition sites identified in the *GFAP* and *B-FABP* promoters (G-br1, G-br2, G-br3, G-br2/3, B-br1, B-br2, B-br3, B-br1/2/3) were used for PCR amplification. Primers corresponding to the proximal GAPDH promoter (200 bp upstream region) were used as a negative control. Input DNA represents DNA isolated from U251 cell lysates after sonication but prior to immunoprecipitation. Input DNA reveals PCR-amplified products of the expected sizes for all primer combinations analyzed.

signals. Similarly, a strong signal was observed when NFIX was incubated with G-br3, with a weaker signal observed with NFIA. There was no apparent change in signal intensity in lanes containing NFIB and NFIC compared to pCH control. In contrast to G-br1 and G-br3, all four NFIs generated a strong signal when incubated with G-br2. Addition of anti-HA antibody to NFIX-enriched nuclear extracts resulted in a supershifted band (arrowhead) indicating that HA-NFIX binds to G-Br2. The residual band in this lane is of the same intensity as that seen in pCH control and likely represents endogenous NFIs binding to G-br2.

To address whether the shifted band observed in the pCH (control) lanes represents endogenous NFI bound to G-br oligonucleotides, we carried out supershift experiments with an anti-NFI antibody previously used to supershift the endogenous NFI/B-br1 complex (Bisgrove et al., 2000). This antibody preferentially recognizes NFIC, although it can also bind to NFIX (data not shown). Addition of anti-NFI antibody to G-br2 oligonucleotides in the presence of nuclear extracts derived from pCH-transfected T98 cells produced a supershifted band (shown by arrow), indicating the presence of an anti-NFI antibody/NFI protein/G-br2 oligonucleotide tri-complex (Figure 2-6C). The weak intensity of the supershifted band combined with the decrease in intensity of the shifted band indicates that the anti-NFI antibody used in these experiments interferes with the binding of the transcription factor to G-br2. As expected, neither anti-AP-2 antibody nor anti-Pax6 antibody produced a supershifted band or affected NFI binding to G-br2.

Next, we examined binding of the four NFIs to labeled oligonucleotides corresponding to the three NFI-like binding sites in the upstream region of the *B-FABP* gene. Gel shift assays indicated that all four NFI proteins could effectively bind B-br1 and B-br2 (Figure 2-6D), although NFIC and NFIX generated a stronger signal than NFIA and NFIB when incubated with B-br1. The most striking differential binding was observed using B-br3 oligonucleotide as the probe, with NFIX producing the strongest signal, followed by NFIC, then NFIA. Incubation of B-br3 with nuclear extracts from NFIB-transfected cells produced only background signal. Combined, our results suggest that specific NFIs (alone or in combination with other proteins found in the nuclear extracts) preferentially bind to specific NFI recognition sites.

2.3.6 Transcriptional regulation of GFAP and B-FABP by NFI proteins

To study the role of the different members of the NFI family in the regulation of *B-FABP* and *GFAP* promoter activity *in vivo*, U251 cells were co-transfected with: (i) plasmids containing the chloramphenicol acetyltransferase (CAT) reporter gene under the control of either the *GFAP* (pCAT/GFAP-1708) or *B-FABP* (pCAT/B-FABP-1785) upstream region, and (ii) NFI expression constructs. Ectopic expression of NFIA had the strongest effect on the *GFAP* promoter, increasing CAT activity by 5.4-fold compared to cells transfected with pCH control vector (Figure 2-7A). In comparison, NFIB, NFIC and NFIX expression constructs increased GFAP-driven CAT activity by 2.9-fold, 2.1-fold and 2.7-fold, respectively.

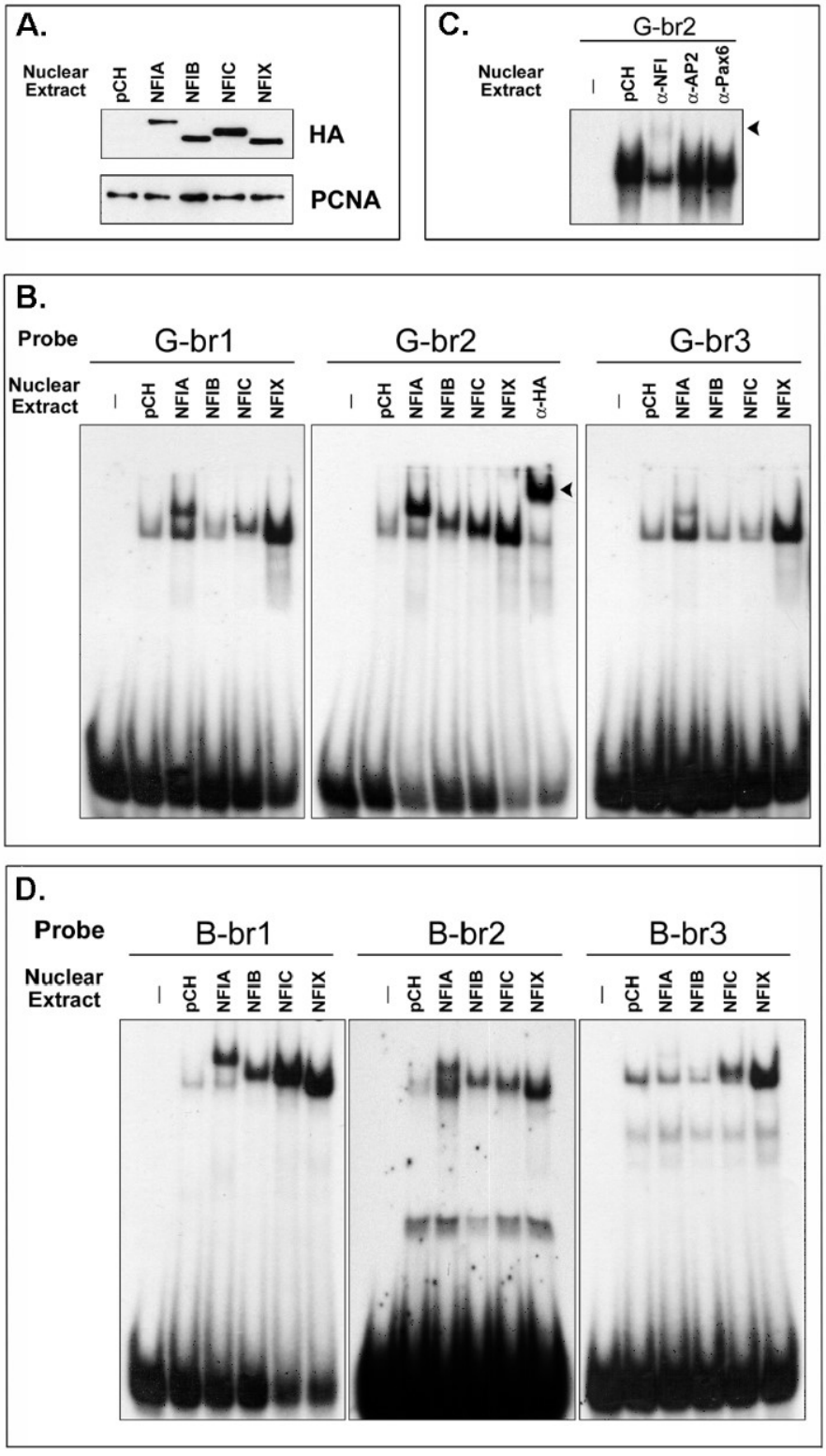
A.
Nuclear Extract
pCH
NFIA
NFIB
NFIC
NFIX
HA
PCNA
C.
G-br2
Nuclear Extract
–
pCH
α-NFI
α-AP2
α-Pax6
B.
Probe
G-br1
G-br2
G-br3
Nuclear Extract
–
pCH
NFIA
NFIB
NFIC
NFIX
α-HA
D.
Probe
B-br1
B-br2
B-br3
Nuclear Extract
–
pCH
NFIA
NFIB
NFIC
NFIX

Figure 2-6: Binding of NFIA, NFIB, NFIC and NFIX to *GFAP* and *B-FABP* NFI recognition sites. Nuclear extracts were prepared from T98 cells transfected with control (pCH), pCH-NFIA, pCH-NFIB, pCH-NFIC or pCH-NFIX expression constructs. (A) Western blot analysis of transfected cells. Nuclear extracts (10 µg per lane) were electrophoresed through a 10% polyacrylamide-SDS gel and electroblotted to a nitrocellulose filter. The filter was incubated with mouse anti-HA antibody or mouse anti-PCNA antibody and the signal detected using the ECL system. (B) Gel shift experiments were carried out using radiolabeled G-br1, G-br2 or G-br3 and 1 µg nuclear extract. A supershift experiment (labeled α-HA in the middle panel) was performed by incubating anti-HA antibody with nuclear extracts prepared from T98 cells transfected with NFIX. The arrowhead shows the supershifted band. (C) Supershift experiment using radiolabled G-br2, 1 µg nuclear extract from T98 transfected with pCH vector and anti-NFI, anti-AP2 or anti-Pax6 antibody. The arrowhead indicates the position of the supershifted band. (D) Gel shift experiments were carried out using radiolabeled B-br1, B-br2 or B-br3 and 1 µg nuclear extract.

In contrast, ectopic expression of either NFIC or NFIX resulted in a 2.2 and 1.9-fold reduction in *B-FABP* promoter activity, respectively (Figure 2-7B). No differences in CAT activity were observed in cells co-transfected with pCAT/B-FABP-1785 and either the NFIA or NFIB expression constructs.

The β-galactosidase expression construct under the control of the SV40 promoter was initially used to control for plate-to-plate variation in transfection efficiency. However, the SV40 promoter was found to be highly responsive to NFIC. To preclude any modifying effect of NFIs on control reporter genes, we used southern blotting of non-integrated (Hirt) DNA to control for transfection efficiency (Hirt, 1967). As shown in Figure 2-7C, there was little variation in the level of non-integrated plasmid DNA within each set of transfected cells. Thus, the CAT activity shown in Figures 2-7A and 2-7B is a direct measurement (in counts per minute - cpm) of acetylated ^{14}C-chloramphenicol, with cpm values obtained for each of the pCH-NFI expression constructs compared to pCH control.

To determine whether over-expression of NFIs affects endogenous GFAP and B-FABP protein levels, we carried out western blot analysis of U251 cells transfected with individual NFI expression constructs. Although high levels of HA-tagged NFI proteins were observed in transfected cells, there was no significant differences in GFAP and B-FABP levels compared to controls (Figure 2-7D). These results indicate that factors in addition to NFI are required for regulation of endogenous B-FABP and GFAP expression.

The role of NFIs in the regulation of *GFAP* and *B-FABP* transcription was further investigated using an RNA interference approach to reduce endogenous

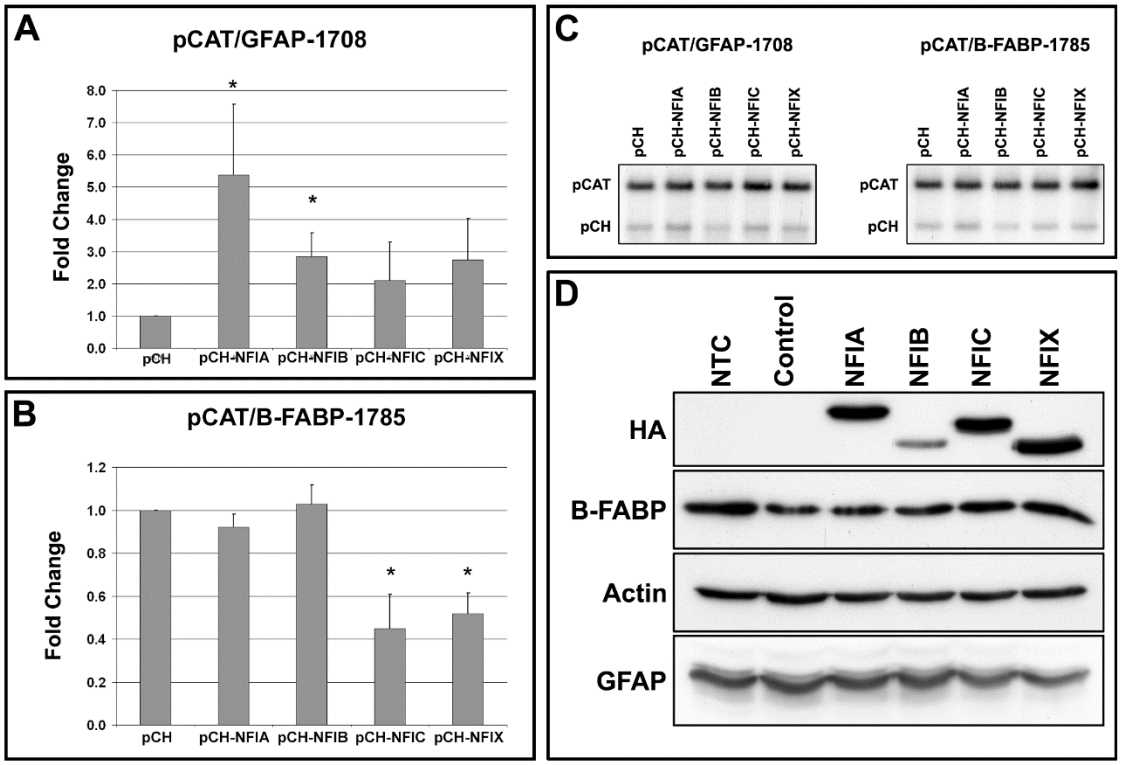
A
pCAT/GFAP-1708
Fold Change
8.0
7.0
6.0
5.0
4.0
3.0
2.0
1.0
0.0
*
*
pCH
pCH-NFIA
pCH-NFIB
pCH-NFIC
pCH-NFIX
B
pCAT/B-FABP-1785
Fold Change
1.2
1.0
0.8
0.6
0.4
0.2
0.0
*
*
pCH
pCH-NFIA
pCH-NFIB
pCH-NFIC
pCH-NFIX
C
pCAT/GFAP-1708
pCAT/B-FABP-1785
pCH
pCH-NFIA
pCH-NFIB
pCH-NFIC
pCH-NFIX
pCAT
pCH
D
NTC
Control
NFIA
NFIB
NFIC
NFIX
HA
B-FABP
Actin
GFAP

Figure 2-7: Co-transfection of NFI expression constructs with pCAT/GFAP or pCAT/B-FABP reporter genes. U251 cells were co-transfected with pCAT/GFAP-1708 (A) or pCAT/B-FABP-1785 (B) and pCH-NFI expression constructs. Acetylated ^{14}C-chloramphenicol (cpm) was measured from equal aliquots of transfected cell lysates using a scintillation counter. The fold increases in CAT activity are relative to the pCH (empty vector) co-transfectants. The ratio of pCAT plasmid DNA to pCH-NFI expression construct was 10:1 (i.e. 3.6 µg pCAT plasmid DNA and 0.4 µg pCH-NFI expression construct per 60 mm plate). The results shown are an average of three to five independent experiments with S.E.M. indicated by the error bars. Statistical significance was determined using the unpaired t-test. The asterisk indicates that the data are significantly different from the pCH control (P <0.05). (C) Southern blot analysis of non-integrated (Hirt) DNA from two representative experiments. Hirt DNA was extracted from the same fraction (typically 1/5 or 1/4) of cells from each plate. Equal aliquots of DNA were digested with *BamH*1, electrophoresed on a 1% agarose gel, transferred to nitrocellulose and probed with ^{32}P-labeled pCAT-basic vector DNA. The top band represents the pCAT/GFAP-1708 DNA (left) and pCAT/GFAP-1785 DNA (right). The lower migrating band represents the co-transfected pCH-NFI DNA. As shown here, there was little variation in amount of transfected DNA from plate-to-plate. (D) Western blot analysis of B-FABP and GFAP in U251 cells over-expressing NFIs. U251 cells were transfected with individual pCH/NFI expression constructs (4-8 µg per 100 mm plate) and cells harvested 60 h later. Cell lysates (50 µg/lane) were electrophoresed in a 13.5% acrylamide-SDS gel (HA, B-FABP, actin), or 10% acrylamide-SDS gel (GFAP), transferred to PVDF membranes, and immunostained with mouse anti-HA antibody, rabbit anti-B-FABP antibody, and mouse anti-actin antibody (13.5% gel) and mouse anti-GFAP antibody (10%). Primary antibodies were detected with horseradish peroxidase-conjugated secondary antibodies and the signal detected using the ECL reagent. Because levels of HA-tagged NFIB were consistently lower than that of the other NFIs, we transfected cells with a range of pCH-NFIB DNA (0.8 – 16 µg per 100 mm plate). HA-NFIB levels increased up to 8 µg of transfected DNA, and remained constant from 8 to 16 µg of transfected DNA, suggesting post-translational regulation of NFIB protein levels in U251 cells.

levels of specific NFIs in U251. Cells were first transfected with control (scrambled) siRNA, or siRNAs targeting *NFIA*, *NFIB*, *NFIC* or *NFIX*, under conditions that resulted in ~90% transfection efficiency. The same cultures were transfected 24 h later with either pCAT/GFAP-1708 or pCAT-B-FABP-1785. Cells were harvested 60 h after the second transfection and analyzed for: (i) endogenous *NFIA*, *NFIB*, *NFIC, NFIX* RNA levels (Figure 2-8A), (ii) endogenous *GFAP* and *B-FABP* RNA levels (Figure 2-8B) and (iii) pCAT activity (Figure 2-8C). Real-time quantitative RT-PCR analysis revealed 79% or greater reduction in *NFIA, NFIB*, *NFIC* and *NFIX* RNA levels in NFI siRNA-transfected cells compared to control siRNA-transfected cells. Two separate experiments are represented in Figure 2-8A with pCAT/GFAP-1708 co-transfectants shown on the left and pCAT/B-FABP-1785 co-transfectants shown on the right. Interestingly, reduction of one NFI often resulted in up-regulation of a second NFI suggesting cross-talk between the different members of the NFI family. For example, NFIA knock-down resulted in increased *NFIX* RNA levels, NFIB knock-down increased *NFIA* RNA levels, NFIC knock-down decreased *NFIB* RNA levels, whereas NFIX knock-down cells showed increased levels of *NFIA* RNA.

Next, we examined endogenous *GFAP* and *B-FABP* RNA levels in NFI knock-down cells by real-time RT-PCR. The most consistent and dramatic decreases in endogenous *GFAP* RNA levels were observed in cells transfected with *NFIB* and *NFIC* siRNAs, followed by *NFIX* and *NFIA* siRNAs (Figure 2-8B – top panels). There was a slight (10-40% depending on the experiment) reduction in endogenous *B-FABP* RNA levels in cells transfected with *NFIA* siRNA, indicating

that NFIA may play a positive role in *B-FABP* transcription. A 1.6 - 2-fold increase in *B-FABP* RNA was consistently observed in NFIB knock-down cells (Figure 2-8B – bottom panel). These data suggest that either NFIB functions as a repressor of endogenous *B-FABP* promoter activity, or more likely in light of the elevated endogenous *NFIB* RNA levels observed in B-FABP-positive glioma cells, the increase in *NFIA* RNA levels associated with NFIB knock-down activates the *B-FABP* promoter.

As promoter analyses are classically carried out using reporter genes, we also used the CAT reporter gene under the control of the 1.7 or 1.8 kb *GFAP* or *B-FABP* promoter, respectively, to investigate the effect of NFI knock-down on transcriptional activity. Analysis of CAT activity in U251 cells co-transfected with pCAT/GFAP-1708 and NFI siRNAs revealed decreased transcriptional activity in NFIA (37% of control), NFIB (50%) and NFIX (48%) knock-downs (Figure 2-8C), suggesting a positive role for these three NFIs in *GFAP* regulation. Surprisingly, CAT activity was increased 2.3-fold in NFIC knock-downs even though endogenous *GFAP* RNA levels were significantly reduced in these cells. Similar to pCAT/GFAP transfectants, decreases in CAT activity were observed in cells co-transfected with pCAT/B-FABP-1785 and either *NFIA* or *NFIB* siRNAs (Figure 2-8C), in support of a positive role for these two NFIs in *B-FABP* regulation. NFIC appears to play a major repressor role in *B-FABP* transcription as cells co-transfected with *NFIC* siRNA showed a 15-fold increase in *B-FABP* promoter activity. As mentioned earlier, endogenous *B-FABP* RNA levels were not altered

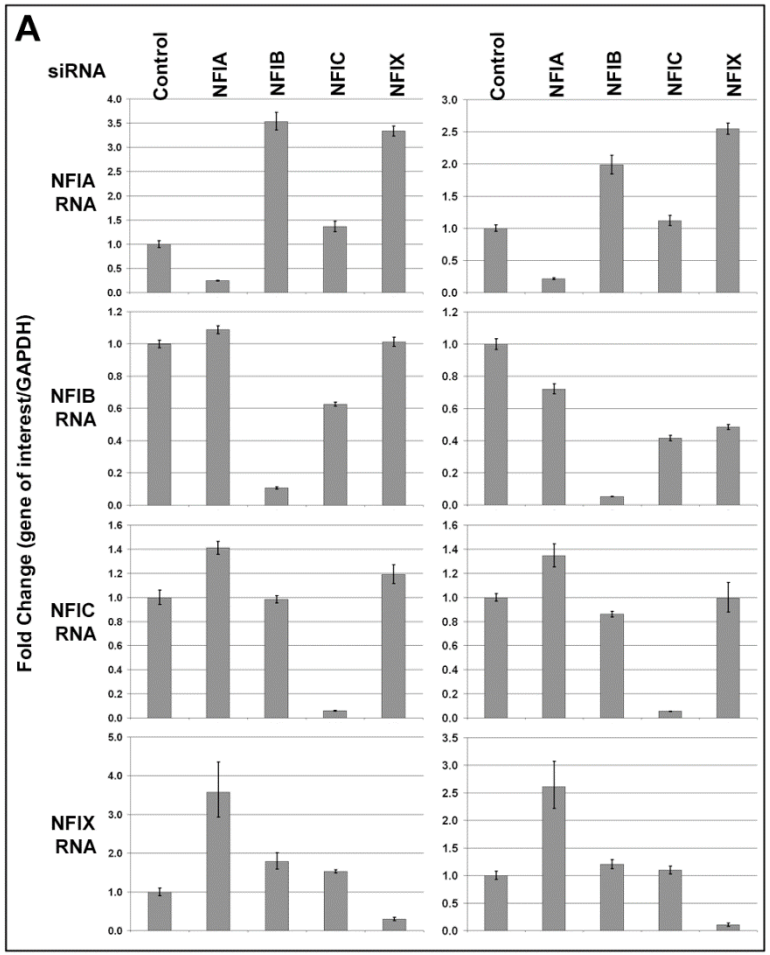
A
siRNA
Control
NFIA
NFIB
NFIC
NFIX
Fold Change (gene of interest/GAPDH)
NFIA RNA
NFIB RNA
NFIC RNA
NFIX RNA

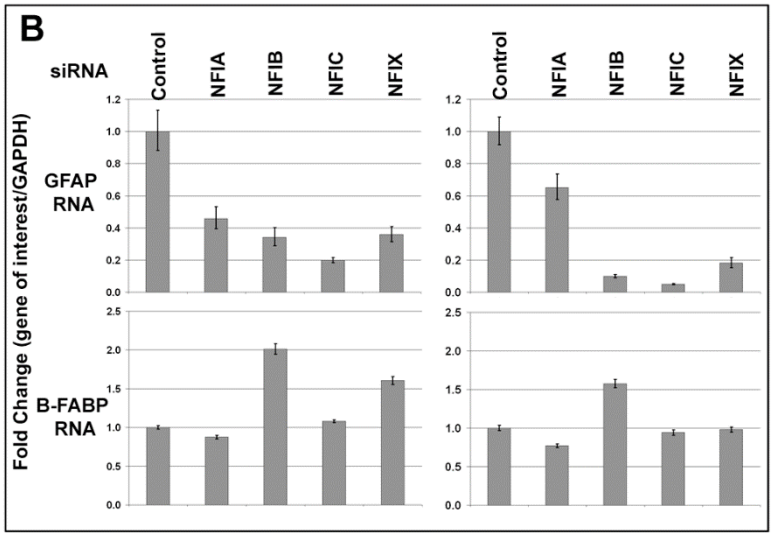
B
siRNA
Control
NFIA
NFIB
NFIC
NFIX
Fold Change (gene of interest/GAPDH)
GFAP RNA
B-FABP RNA

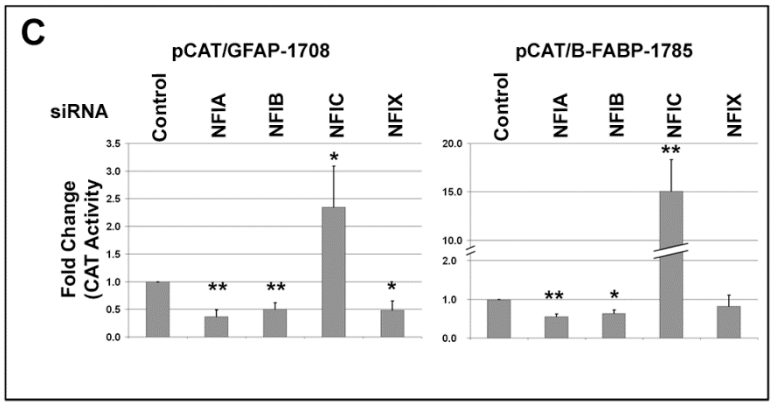
C
pCAT/GFAP-1708
pCAT/B-FABP-1785
siRNA
Control
NFIA
NFIB
NFIC
NFIX
Fold Change (CAT Activity

Figure 2-8: Regulation of *B-FABP* and *GFAP* promoter activity by NFIs. U251 cells were transfected with 10 nM control (scrambled), *NFIA, NFIB, NFIC,* or *NFIX* Stealth siRNAs, followed by pCAT/GFAP-1708 or pCAT/B-FABP-1785 (4 µg per 60 mm plates) 24 h later**.** Cells were harvested after an additional 60 h. (A) Quantitative RT-PCR analysis of *NFIA*, *NFIB*, *NFIC* and *NFIX* in two representative experiments, with pCAT/GFAP-1708 co-transfectants shown on the left and pCAT/B-FABP-1785 co-transfectants shown on the right. The fold changes in endogenous *NFIA, NFIB*, *NFIC* and *NFIX* RNA levels (Y axis) are shown for each of the control, *NFIA*, *NFIB*, *NFIC* and *NFIX* siRNA transfectants (indicated on the X axis). (B) Quantitative RT-PCR analysis of endogenous *GFAP* and *B-FABP* RNA levels in the two sets of transfectants described in (A). *GAPDH* served as the standard for the quantitative RT-PCR analysis. Similar data were obtained in 4 separate experiments. (C) CAT activity in U251 cells transiently transfected with siRNAs and pCAT vectors, as described in (A). Changes in CAT activity are relative to the CAT activity obtained in cells co-transfected with control siRNA and either pCAT/GFAP-1708 or pCAT/B-FABP-1785. The data are from three independent experiments, each carried out in duplicate. S.E.M. is indicated by the error bars. Statistical significance, determined using the unpaired t-test, is indicated by one asterisk (P <0.05) or two asterisks (P <0.001).

upon *NFIC* knock-down (Figure 2-8B). These results suggest a fundamental difference in the way that the NFIC transcription factor interacts with chromosomal versus episomal *B-FABP* and *GFAP* NFI binding sites.

To investigate whether decreases in endogenous *GFAP* RNA were accompanied by decreases in GFAP protein levels, we transfected U251 cells with control siRNA or individual siRNAs targeting each of the four NFIs. No decreases in GFAP protein levels were observed 60 h after the initial transfection. However, significant decreases in GFAP were observed after a second round of transfection with *NFIB*, *NFIC* or *NFIX*, but not *NFIA*, siRNAs (Figure 2-9A). After a total of three consecutive transfections, GFAP was barely detectable in *NFIB*, *NFIC* and *NFIX* siRNA transfectants, and dramatically reduced in *NFIA* siRNA transfectants. No alterations in B-FABP protein levels were observed in U251 cells transfected once with NFI siRNAs. After two rounds of transfections, a slight increase in B-FABP was observed in the NFIB knock-down cells, in agreement with the RNA data (Figures 2-9B and 2-8B). A ~2 – 4-fold decrease in B-FABP levels was observed in all four NFI knock-downs after three consecutive rounds of transfections, with the greatest reduction observed in cells transfected with *NFIX* siRNA. Because of the lag time, it's not clear whether the reduction in B-FABP levels observed after three rounds of transfection is a direct or indirect consequence of NFI knock-down.

Overall, there was general agreement between the NFI over-expression and knock-down data with regards to GFAP. Over-expression of all four NFIs increased ectopic *GFAP* promoter activity, whereas reduction in the levels of all four NFIs decreased endogenous *GFAP* RNA (and eventually protein) levels.

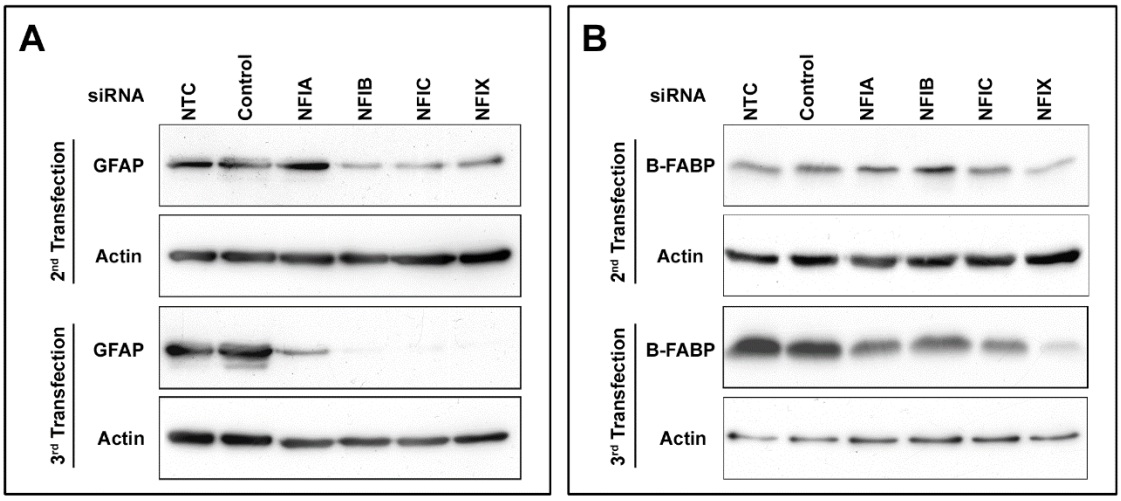

Figure 2-9: Western blot analysis of B-FABP and GFAP in U251 cells transiently transfected with NFI siRNAs. U251 cells were sequentially transfected three times with 10 nM control, *NFIA, NFIB, NFIC,* and *NFIX* Stealth siRNAs over a period of 12 - 15 days. Cells were harvested after each transfection and whole cell lysates prepared. For the second and third rounds of transfection, 1/10 of the cells were re-plated and re-transfected and allowed to reach confluence prior to harvest (and re-plating). Cell lysates (40 µg/lane) were electrophoresed, transferred to PVDF membranes, and immunostained with (A) mouse anti-GFAP and (B) rabbit anti-B-FABP antibodies. Membranes were then stripped and probed with mouse anti-actin antibody. Primary antibodies were detected with horseradish peroxidase-conjugated secondary antibodies and the signal detected using the ECL reagent. No changes in GFAP and B-FABP levels were observed after the first transfection (data not shown). NTC: non-transfected control.

Furthermore, ectopic *GFAP* promoter activity was decreased upon NFIA, NFIB and NFIX knock-down. The situation with B-FABP appears considerably more complex as NFI over-expression either had no effect (NFIA, NFIB) or resulted in decreased ectopic *B-FABP* promoter activity (NFIC, NFIX). Reduction in NFI levels was accompanied by increased endogenous *B-FABP* mRNA in the case of NFIB, decreased B-FABP protein levels after multiple rounds of transfection, and either decreased (NFIA, NFIB) or dramatically increased (NFIC) ectopic *B-FABP* promoter activity.

2.3.7 Mutational analysis of NFI binding sites in the GFAP promoter

We have previously shown that mutation of NFI binding sites in the *B-FABP* promoter reduces its transcriptional activity (Bisgrove et al., 2000). Here, we extend the analysis to *GFAP* by mutating the NFI recognition sites in the *GFAP* upstream region (Figure 2-10A), first in the context of the pCAT/GFAP-168 construct which contains the G-br1 binding site, and second in the context of pCAT/GFAP-1705 which contains all three NFI binding sites.

As shown in Figure 2-10B, a 3.2-fold increase in CAT activity was observed with wild-type pCAT/GFAP-168 compared to pCAT basic vector. To investigate which of the four NFIs target G-br1, pCAT/GFAP-168 was co-transfected into U251 cells along with control or NFI siRNAs. Decreased CAT activity was observed in the presence of *NFIB* siRNA and increased CAT activity in the presence of *NFIC* siRNA, indicating that at least these two NFIs bind to G-br1 (Figure 2-10C). In this regard it is interesting to note that NFIB and NFIC showed the weakest binding to

G-br1 based on the gel shift assay (Figure 2-6B). Mutation of G-br1 in pCAT/GFAP-168 completely abolished its transcriptional activity, with no further decreases observed upon co-transfection of NFI siRNAs (Figures 2-10B, C).

CAT activity was induced 7.6-fold in pCAT/GFAP-1708-transfected cells compared to pCAT basic vector (Figure 2-10B). Mutation in G-br1* resulted in a 5.1-fold decrease in CAT activity (1.5-fold increase compared to pCAT basic), mutation in combined G-br2*/G-br3* resulted in a 2.2-fold decrease in CAT activity (3.4-fold increase compared to pCAT basic), whereas combined mutation of G-br1*/G-br2*/G-br3* reduced CAT activity 6-fold (1.3-fold increase compared to pCAT basic), thus demonstrating the importance of the NFI binding sites, particularly G-br1, in the *GFAP* promoter. Although overall CAT activity was barely above background in pCAT/GFAP-1708 G-br1*- transfected cells, knock-down experiments revealed a 2.9-fold increase in CAT activity in the presence of *NFIC* siRNA, suggesting that NFIC can still interact with G-br2 and G-br3 in the absence of G-br1. Knock-down of NFIA in pCAT/GFAP-1708 G-br2*/G-br3*-transfected cells produced the most dramatic decrease in CAT activity. As expected, only minor variations compared to basal CAT activity were observed in cells transfected with the triple mutant construct. These results indicate that G-br1 plays a major role in *GFAP* regulation although it is clear that G-br2 and G-br3 are also involved in this process. Mutation analysis in the context of the *GFAP-1708* promoter suggests a positive regulatory role for NFIA primarily through G-br1, and an inhibitory role for NFIC primarily through G-br2 and G-br3.

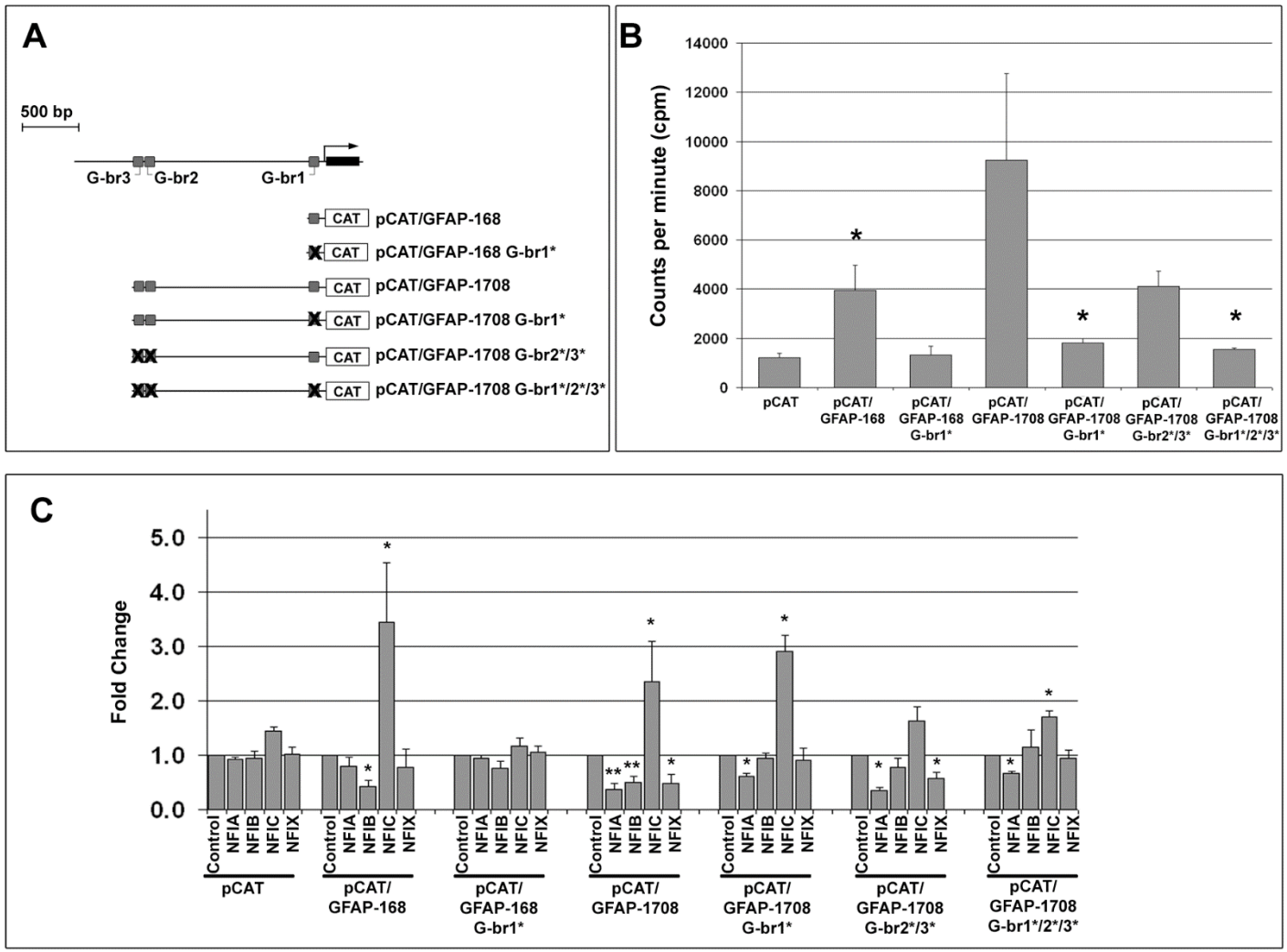
A
500 bp
G-br3
G-br2
G-br1
CAT
pCAT/GFAP-168
pCAT/GFAP-168 G-br1*
pCAT/GFAP-1708
pCAT/GFAP-1708 G-br1*
pCAT/GFAP-1708 G-br2*/3*
pCAT/GFAP-1708 G-br1*/2*/3*
B
Counts per minute (cpm)
14000
12000
10000
8000
6000
4000
2000
0
pCAT
pCAT/ GFAP-168
pCAT/ GFAP-168 G-br1*
pCAT/ GFAP-1708
pCAT/ GFAP-1708 G-br1*
pCAT/ GFAP-1708 G-br2*/3*
pCAT/ GFAP-1708 G-br1*/2*/3*
C
Fold Change
5.0
4.0
3.0
2.0
1.0
0.0
Control
NFIA
NFIB
NFIC
NFIX
pCAT
pCAT/ GFAP-168
pCAT/ GFAP-168 G-br1*
pCAT/ GFAP-1708
pCAT/ GFAP-1708 G-br1*
pCAT/ GFAP-1708 G-br2*/3*
pCAT/ GFAP-1708 G-br1*/2*/3*

Figure 2-10: Mutational Analysis of NFI binding sites in the *GFAP* promoter. (A) Schematic diagram of the *GFAP* promoter region showing the relative location of the three NFI binding sites and the names of the wild-type (pCAT/GFAP-168 and pCAT/GFAP-1708 carrying 168 and 1708 of 5' flanking DNA, respectively) and mutant (pCAT/GFAP-168 G-br1* with mutated G-br1, pCAT/GFAP-1708 G-br1*, pCAT/GFAP-1708 G-br2*/3* with mutated G-br2 and G-br3, and pCAT/GFAP-1708 G-br1*/2*/3* mutated at all three NFI recognition sites) constructs. The transcription start site is indicated by the arrow. (B) CAT activity (in cpm) obtained upon transfecting U251 cells with each of the wild-type and mutant constructs indicated in (A) as well as pCAT basic (containing neither promoter nor enhancer). Four μg of DNA were used to transfect each 60 mm plate. (C) Relative CAT activity obtained from U251 cells transfected with 10 nM control, *NFIA, NFIB, NFIC,* or *NFIX* siRNA, followed 24 h later by transfection with the indicated CAT reporter constructs (4 μg per 60 mm plate)**.** Changes in CAT activity are relative to the CAT activity obtained in cells co-transfected with the indicated pCAT construct and control siRNA. The data are from three independent experiments, each carried out in duplicate. S.E.M. is indicated by the error bars. Statistical significance, determined using the paired t-test (B) and unpaired t-test (C), is indicated by one asterisk (P <0.05) or two asterisks (P <0.001).

2.3.8 Combined NFI knock-downs reveal cross-talk between all four members of the NFI family

As shown earlier, knock-down of one NFI can affect the levels of other NFIs, suggesting cross-talk between different members of the NFI family. To further investigate the possibility of cross-talk or compensatory feedback loops within the NFI family, we transfected U251 cells with the following combinations of NFI siRNAs: NFIA/NFIB, NFIC/NFIX, NFIA/NFIB/NFIC, NFIA/NFB/NFIX, and NFIA/NFIB/NFIC/NFIX (Figure 2-11). For these experiments, the total concentration of siRNA used per plate ranged from 10 nM for single transfectants (NFIA) to 40 nM for quadruple siRNA transfectants (NFIA/NFIB/NFIC/NFIX). As shown in Figure 2-12, similar results were obtained for the quadruple knock-downs when the total amount of siRNA transfected per plate was 10 nM.

Transfection of combined *NFIA/NFIB* siRNAs resulted in increased *GFAP* promoter activity compared with *NFIA* siRNA alone (Figure 2-11A). There was a 1.5-fold increase in CAT activity in cells transfected with combined *NFIC/NFIX* siRNAs, whereas combined *NFIA/NFIB/NFIC* siRNAs generated close to control levels of CAT activity. Knock-down of all four NFIs resulted in a 60% decrease in CAT activity compared to control transfectants. These data support a role for all four NFIs in episomal *GFAP* regulation, and also indicate that the ratio of the four NFIs may be an important determinant of *GFAP* transcriptional activity, thus explaining the "normalization" of *GFAP* promoter activity observed upon transfection of multiple NFI siRNAs.

In contrast to the *GFAP* promoter, knock-down of combined NFIA/NFIB in pCAT/B-FABP-1785 transfectants resulted in a cumulative decrease in *B-FABP* promoter activity [to background levels (or 27% of the levels observed with scrambled siRNA) and 48% of levels observed with *NFIA* siRNA] (Figure 2-11B). These results suggest an important role for both NFIA and NFIB in *B-FABP* transcription. It is noteworthy that in spite of targeting all three positive-acting NFIs while retaining the inhibitory NFIC, the *NFIA/NFIB/NFIX* siRNA combination did not result in a further decrease in CAT activity compared to the NFIA knock-down. Inclusion of *NFIC* siRNA in any combination of NFI siRNAs (*NFIC/NFIX*, *NFIA/NFIB/NFIC*, *NFIA/NFIB/NFIC/NFIX*) increased *B-FABP* promoter activity, although the fold increase in CAT activity was lower than that obtained with *NFIC* siRNA alone (Figure 2-8) and a significant increase was only observed with the *NFIC/NFIX* siRNA combination (Figure 2-11B). The quenching effect observed upon transfection of *NFIX* siRNA along with *NFIC* siRNA (compared to *NFIC* siRNA alone) suggest a positive role for NFIX on *B-FABP* promoter activity, even though single NFIX knock-down has little effect on this promoter. Cultures transfected with all four NFI siRNAs still showed a 2-fold increase in CAT activity compared to control transfectants, demonstrating the complex interplay between the positive-acting and negative-acting NFIs.

We then investigated how knock-down of combined NFIs might affect endogenous *GFAP* and *B-FABP* RNA levels. In agreement with the single NFI knock-down data indicating roles for all four NFIs in endogenous *GFAP* regulation (Figures 2-8 and 2-9), all combinations of NFI siRNAs tested generated significant

decreases in endogenous *GFAP* levels (Figure 2-11C). The most significant reductions in *GFAP* RNA were observed when *NFIC* siRNA was included in the siRNA mixes, as predicted by the single *NFIC* siRNA knock-down data. Although decreases in endogenous *B-FABP* RNA levels were also observed with all combinations of NFI siRNAs tested, fold-changes were of considerably lower magnitude than those obtained for endogenous *GFAP* (2-11D).

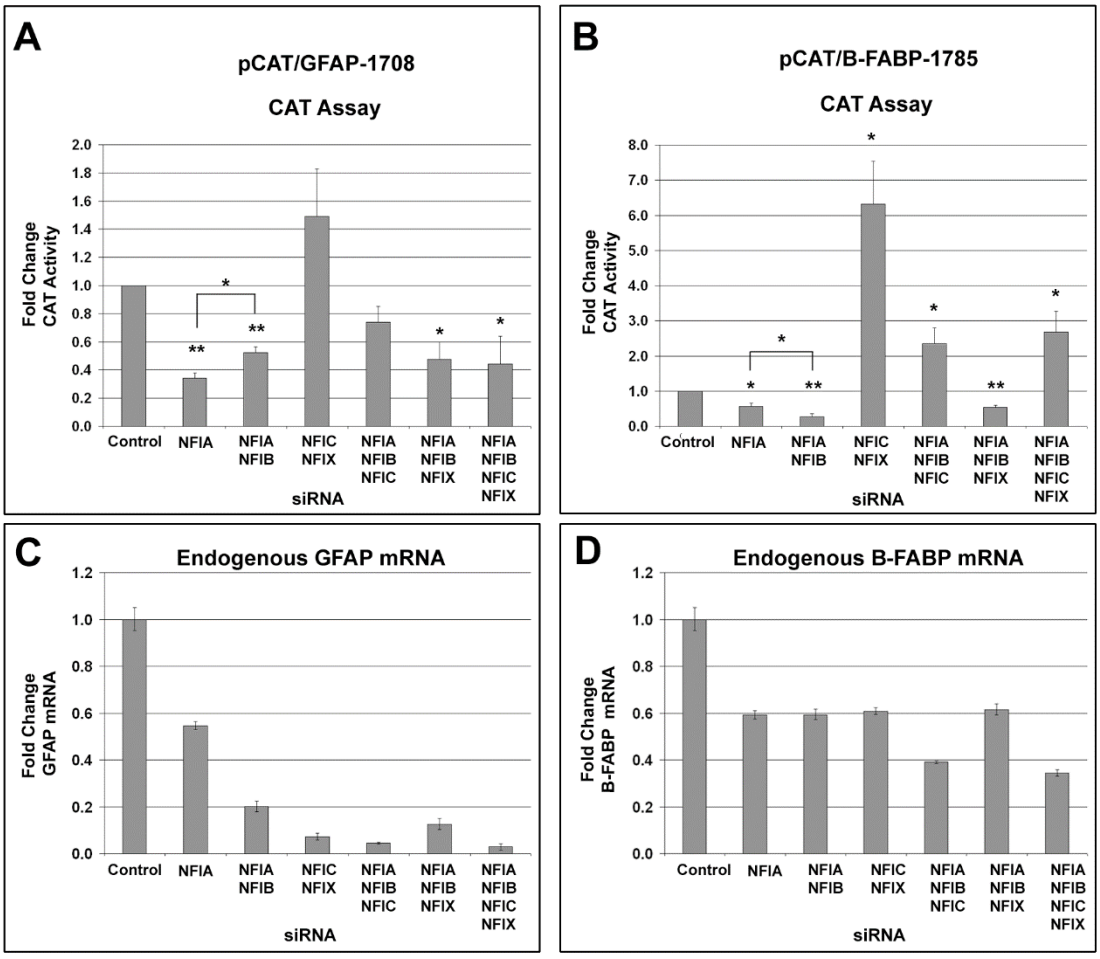
A
pCAT/GFAP-1708
CAT Assay
Fold Change CAT Activity
2.0
1.8
1.6
1.4
1.2
1.0
0.8
0.6
0.4
0.2
0.0
Control
NFIA
NFIA NFIB
NFIC NFIX
NFIA NFIB NFIC
NFIA NFIB NFIX
NFIA NFIB NFIC NFIX
siRNA
B
pCAT/B-FABP-1785
CAT Assay
Fold Change CAT Activity
8.0
7.0
6.0
5.0
4.0
3.0
2.0
1.0
0.0
Control
NFIA
NFIA NFIB
NFIC NFIX
NFIA NFIB NFIC
NFIA NFIB NFIX
NFIA NFIB NFIC NFIX
siRNA
C
Endogenous GFAP mRNA
Fold Change GFAP mRNA
1.2
1.0
0.8
0.6
0.4
0.2
0.0
Control
NFIA
NFIA NFIB
NFIC NFIX
NFIA NFIB NFIC
NFIA NFIB NFIX
NFIA NFIB NFIC NFIX
siRNA
D
Endogenous B-FABP mRNA
Fold Change B-FABP mRNA
1.2
1.0
0.8
0.6
0.4
0.2
0.0
Control
NFIA
NFIA NFIB
NFIC NFIX
NFIA NFIB NFIC
NFIA NFIB NFIX
NFIA NFIB NFIC NFIX
siRNA

Figure 2-11: Regulation of episomal and endogenous *GFAP* and *B-FABP* promoter activity by combined NFI knock-downs. U251 cells were transfected with control (scrambled), *NFIA, NFIA/NFIB, NFIC/NFIX, NFIA/NFIB/NFIC, NFIA/NFIB/NFIX* or *NFIA/NFIB/NFIC/NFIX* Stealth siRNAs (10 nM for each siRNA). (A, B) Following siRNA transfection, cells were transfected with pCAT/GFAP-1708 (A) or pCAT/B-FABP-1785 (B) (4 µg per 60 mm plate) 24 h later**.** Cells were harvested after an additional 60 h, lysed and assayed for CAT activity. Changes in CAT activity are relative to the CAT activity obtained in cells co-transfected with control siRNA and either pCAT/GFAP-1708 or pCAT/B-FABP-1785. The data are from three independent experiments. S.E.M. is indicated by the error bars. Statistical significance, determined by the unpaired t-test, is indicated by one asterisk (P <0.05) or two asterisks (P <0.001). (C, D) Quantitative RT-PCR analysis of endogenous *GFAP* (C) and *B-FABP* (D) RNA in U251 cells transfected with NFI siRNAs. Cells were harvested 60 h after transfection. *GAPDH* served as the standard. S.E.M is indicated by the error bars.

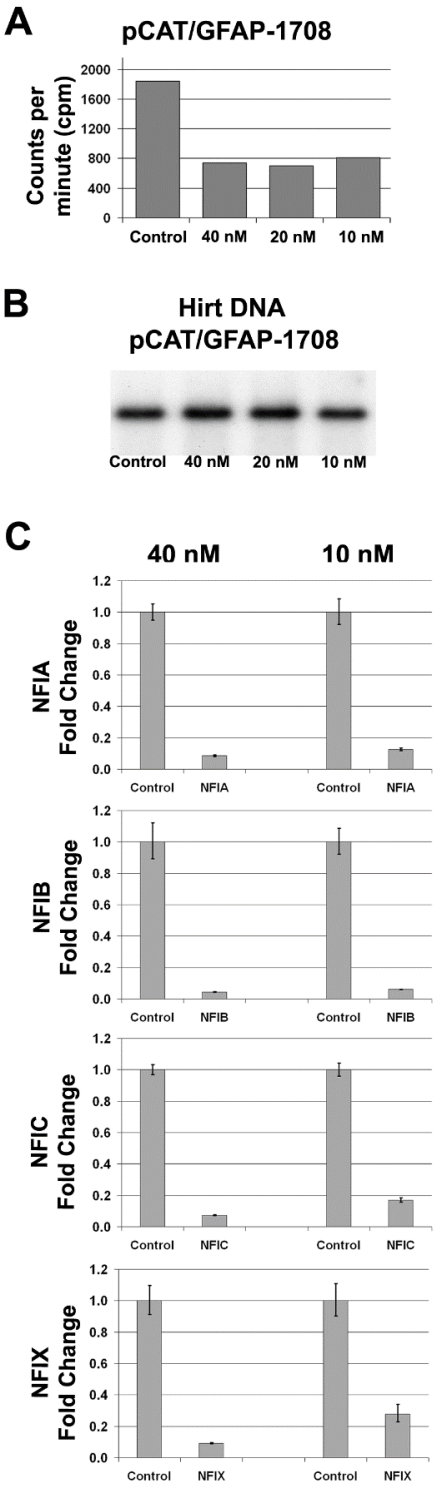
A
pCAT/GFAP-1708
Counts per minute (cpm)
2000
1600
1200
800
400
0
Control
40 nM
20 nM
10 nM
B
Hirt DNA
pCAT/GFAP-1708
Control
40 nM
20 nM
10 nM
C
40 nM
10 nM
NFIA Fold Change
NFIB Fold Change
NFIC Fold Change
NFIX Fold Change
1.2
1.0
0.8
0.6
0.4
0.2
0.0
Control
NFIA
NFIB
NFIC
NFIX

Figure 2-12: Comparison of CAT activity and NFI RNA levels in cells transfected with 10 nM versus 40 nM NFI siRNAs. (A) U251 cells were transfected with the following combinations of siRNAs: mix A – 10 nM each of *NFIA*, *NFIB*, *NFIC* and *NFIX* siRNAs for a total concentration of 40 nM; mix B – 5 nM each of *NFIA*, *NFIB*, *NFIC* and *NFIX* siRNAs for a total concentration of 20 nM; and mix C – 2.5 nM each of *NFIA*, *NFIB*, *NFIC* and *NFIX* siRNAs for a total concentration of 10 nM. Cells were transfected one day later with pCAT/GFAP-1705 (4 µg per 60 mm plate) and CAT activity measured (in cpm). There was no significant difference in the CAT activity obtained with the three siRNA mixes. (B) Hirt DNA is included to demonstrate that there was little variation in the amount of transfected pCAT/GFAP-1705 DNA from plate-to-plate. (C) Quantitative RT-PCR analysis of *NFIA*, *NFIB*, *NFIC*, and *NFIX* in cells transfected with NFI siRNA mix A (40 nM) and NFI siRNA mix C (10 nM). All four NFIs were effectively reduced using both 40 nM and 10 nM total NFI siRNA.

2.4 Discussion

B-FABP and GFAP are normally found in radial glial cells and astrocytes, respectively, and are co-expressed in malignant glioma tumours and in a subset of malignant glioma cell lines (Godbout et al., 1998). Previous experiments by us and by others have demonstrated that NFIs are involved in the regulation of the *B-FABP* and *GFAP* genes (Besnard et al., 1991; Bisgrove et al., 2000; Cebolla and Vallejo, 2006; Gopalan et al., 2006a; Masood et al., 1993). Tissue-specific expression patterns support a role for NFIs, particularly NFIA, NFIB and NFIX, in the regulation of genes expressed in glial cells. For example, in postnatal mice, NFIA and NFIB localize primarily to the white matter of the cerebral cortex, suggesting a glial cell-specific distribution (Chaudhry et al., 1997). In humans, NFIA and NFIX are expressed in glial cells where they appear to have greater transactivation capacity than NFIC (Krebs et al., 1996; Sumner et al., 1996). A role for NFIA and NFIB in glia is supported by the observation that both *Nfia-/-* and *Nfib-/-* mice show losses of midline glial structures, which are accompanied by significant reductions in GFAP levels (das Neves et al., 1999b; Steele-Perkins et al., 2005). While brain defects have been reported in *Nfix-/-* mice, there is no indication of glial defects in these mice and *GFAP* RNA levels are not altered (Driller et al., 2007).

We show here that all four NFIs are expressed in malignant glioma cell lines, with a trend towards higher levels of *NFIB* RNA in B-FABP/GFAP-positive versus B-FABP/GFAP-negative lines. Both ectopic over-expression and RNA interference were used to investigate the consequence of modulating levels of NFIs on *GFAP*- and *B-FABP*-driven CAT reporter activity. There was general agreement between

the two approaches in that NFIA had the strongest positive effect on *GFAP* promoter activity, followed by NFIB and NFIX. The NFI knock-down data further suggested that NFIC plays a negative role in the regulation of *GFAP*. In the case of *B-FABP*, the NFI over-expression and knock-down data both supported a role for NFIC in the down-regulation of *B-FABP* transcription. Knock-down experiments also demonstrated a role for NFIA and NFIB in the up-regulation of *B-FABP* promoter activity, with the most dramatic effect observed when both NFIA and NFIB were targeted by siRNAs. These results suggest that NFIA/NFIB heterodimers may be particularly effective in the activation of *B-FABP* transcription. A summary of the combined data obtained with the NFI knock-down/CAT reporter gene assay is schematically represented in Figure 2-13A.

In contrast to ectopic promoter activity, NFI over-expression had no effect on either endogenous GFAP or B-FABP levels, indicating that: (i) factors in addition to NFI are required for the expression of these two genes, and (ii) at least some of these factors are in limiting amounts. RNA interference experiments revealed an important role for each NFI in the up-regulation of *GFAP*, with knock-down of each NFI accompanied by dramatic decreases in endogenous *GFAP* RNA (and subsequently protein) levels. These results indicate that although knock-down of one NFI can affect the levels of a different NFI (e.g. up-regulation of NFIA upon NFIB knock-down), members of the NFI family cannot fully compensate for one another in the case of *GFAP*. Thus, all four NFIs, or the ratio of the four NFIs, may play critical roles in *GFAP* regulation.

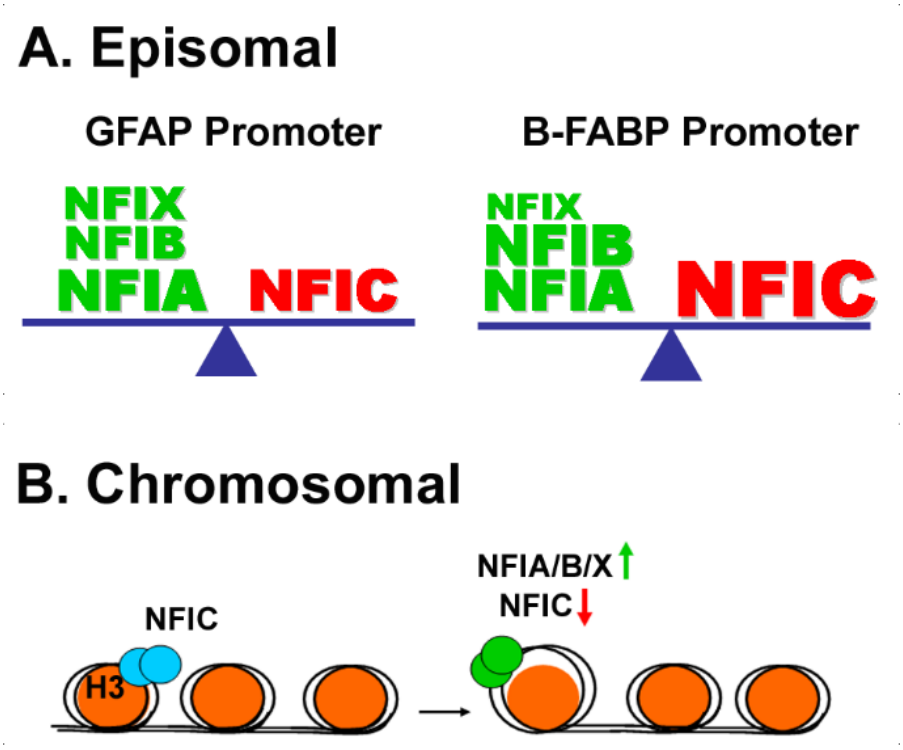

Figure 2-13: Model of NFI transcriptional activity. (A) Schematic representation of the relative importance (indicated by font size) of the different NFIs in the up-regulation (green color) and down-regulation (red color) of *GFAP* and *B-FABP* promoter activity in an episomal context. (B) Roles of NFIs in a chromosomal promoter context using *GFAP* as our model. By binding to histone H3, NFIC (and possibly other NFIs) relaxes the nucleosome structure, thus facilitating binding of NFIs and other transcription factors to *GFAP* upstream sequences.

Although results obtained with the ectopic versus endogenous *GFAP* promoter are mostly in agreement, the reduction in endogenous *GFAP* RNA (and protein) levels observed upon NFIC knock-down is inconsistent with the proposed inhibitory role for NFIC in the context of episomal pCAT/GFAP-1708 DNA. Differing results have been reported by others upon comparing promoter activity in an episomal versus chromosomal context (Archer et al., 1992; Gerber et al., 1997). A likely explanation for this discrepancy is the nucleosomal organization of chromosomal versus episomal promoters. While core histones in episomal DNA display similar stoichiometry to that found in chromosomal DNA, episomal templates have fewer H1 linker histones resulting in a lower level of nucleosome assembly (thus facilitating access to transcription factors) compared to chromosomal DNA (Hebbar and Archer, 2008). In this regard, it is important to note that NFIC has been shown to play a chromatin restructuring role at target promoter sites by specifically binding histone H3 through its proline-rich transcriptional activation domain (Alevizopoulos et al., 1995). A consequence of NFIC knock-down may therefore be reconfiguration of the core nucleosome structure and reduced accessibility of the endogenous *GFAP* promoter to transcription factors (Figure 2-13B). We propose that NFIC functions as a transcriptional activator in the context of the endogenous *GFAP* promoter through its chromatin restructuring role and as a transcriptional repressor in the context of the episomal *GFAP* promoter through its classic DNA-binding transcription factor role. In contrast, NFIA, NFIB and NFIX appear to serve as classic promoter-binding transcriptional activators regardless of *GFAP* promoter context.

Single and combined NFI knock-downs had limited effects on endogenous *B-FABP* RNA levels, with a maximum reduction of ~60% observed in the NFIA/B/C/X quadruple knock-down. The increase in *B-FABP* RNA levels observed upon single NFIB knock-down is likely the consequence of a compensatory increase in NFIA. Furthermore, significant decreases in endogenous B-FABP protein levels were only observed after three rounds of NFI siRNA transfections and may be an indirect consequence of long-term reduction in NFI transcription activity as NFIs have numerous target genes. The different effects observed at the endogenous *GFAP* and *B-FABP* promoters upon NFI knock-down could be explained by: (i) the *B-FABP* transcript being more stable than the *GFAP* transcript, (i) NFIC not playing a role in chromatin remodeling at the *B-FABP* promoter, and/or (iii) different members of the NFI family being able to compensate for one another at the *B-FABP* but not the *GFAP* promoter.

An important outcome of the NFI knock-down experiments was the discovery that there is cross-talk between different members of the NFI family. The consequence of NFIA knock-down was up-regulation of *NFIX* and vice versa, whereas knock-downs of NFIC and NFIB resulted in reduced *NFIB* and increased *NFIA*, respectively. These compensatory effects are in keeping with the 2.2-fold increase in *Nfia* observed in *Nfib-/-* mice (Steele-Perkins et al., 2005) and the 1.3-fold increase in *Nfib* observed in *Nfia-/-* mice (Wong et al., 2007). Thus, the increase in *B-FABP* RNA levels observed in the brains of *Nfia-/-* mice based on microarray analysis (Wong et al., 2007) may be explained by the compensatory increase in *Nfib* levels.

Chromatin immunoprecipitation assays have previously demonstrated occupancy of the endogenous *GFAP* promoter by NFIs in primary cortical neuroepithelial cells (Cebolla and Vallejo, 2006). Here, we demonstrate that NFIs also occupy the promoter regions of the endogenous *GFAP* and *B-FABP* genes in U251 malignant glioma cells. *In vitro* gel shift experiments using nuclear extracts from B-FABP/GFAP-negative T98 and B-FABP/GFAP-positive U251 cell lines revealed binding of NFIs to NFI recognition sites in the *GFAP* and *B-FABP* promoters. Retarded bands of similar intensities were observed with both extracts, in spite of the fact that T98 has lower levels of *NFI* RNA compared to U251. Possible explanations for this apparent discrepancy include: (i) *NFI* RNA levels may not reflect NFI protein levels in T98 and U251 cells, (ii) hyperphosphorylation of NFIs in T98 may stabilize the protein, or (iii) hyperphosphorylated NFIs may bind more tightly to NFI recognition sites *in vitro* (although the literature would suggest otherwise) (Yang et al., 1993).

To investigate whether different members of the NFI family can preferentially bind to the NFI recognition sites found upstream of the *GFAP* and *B-FABP* promoters, we carried out gel shifts with nuclear extracts prepared from T98 cells over-expressing individual NFIs. NFIX showed the least discrimination for NFI recognition sites, effectively binding to the three G-br binding sites in the *GFAP* promoter and the three B-br binding sites in the *B-FABP* promoter *in vitro*. NFIA could also bind to all six NFI recognition sites, although only weakly to B-br3. NFIC appeared to recognize B-br binding sites much more efficiently than G-br sites, with

strong binding to all three B-br sites. NFIB showed the highest degree of discrimination, binding to G-br2, B-br1 and B-br2, and to a lesser extent G-br1.

We examined the sequences of the *B-FABP* and *GFAP* NFI binding sites in an attempt to link DNA binding by the more discriminatory NFIs to one or more specific target sequences. We found that none of the six NFI binding sites (B-br1, B-br2, B-br3, G-br1, G-br2, G-br3) were identical to one another and none were identical to the 15-bp NFI consensus binding site TTGGCN$_5$GCCAA. The six NFI binding sites each had one to three bp deviations from the consensus sequence. With the exception of B-br2 (4 bp internal spacer), all had a 5 bp internal spacer. Interestingly, NFI binding sites most closely resembling the consensus sequence (e.g B-br2, with a single bp substitution at position 1; G-br2, with two bp substitutions at positions 11 and 12) were bound equally well by all four NFIs. With the exception of B-br1, NFI binding sites with three bp substitutions (e.g. G-br3, B-br3) demonstrated the highest degree of differential binding.

There was little correlation between the ability of NFIs to bind to G-br and B-br sites and NFI transcription activity. For example, even though NFIX and NFIA both formed complexes with all six G-br/B-br oligonucleotides, NFIX knock-down had little effect on *B-FABP*-driven CAT activity whereas NFIA knock-down decreased the activity of both the *GFAP* and *B-FABP* promoters. These results are in agreement with other reports indicating that transcription factor binding affinity is a poor predictor of transcription activity (Bachurski et al., 2003; Osada et al., 1999). Furthermore, mutation of individual or combined G-br recognition sites suggests context-dependent binding by NFIs, with NFIB knock-down having the strongest

effect on G-br1 in the context of the -168 bp upstream region, and NFIA knock-down resulting in a significant decrease in CAT activity when in the context of the -1708 bp upstream region mutated at G-br2* and G-br3* (leaving only the G-br1 intact). It is clear that factors other than ability to bind NFI consensus sites *in vitro* are important for NFI transactivation, including recruitment of transcriptional co-factors and/or cooperative interactions with different members of the NFI family or factors that bind to neighboring elements.

A number of transcription factors and pathways have been implicated in *B-FABP* and *GFAP* regulation. For example, *B-FABP* has recently been shown to be a downstream target of the Notch effector CBF1 in radial glial cells and of Pax6 in the neuroepithelial cells of the developing rat cortex (Anthony et al., 2005; Arai et al., 2005). Previous work has identified a radial glial element located within 800 bp of the *B-FABP* transcription start site (Feng and Heintz, 1995) and a hybrid Pbx/POU binding site at -370 bp (Josephson et al., 1998). Similarly, AP-1 (Gopalan et al., 2006a) and the TGF-β, MAP kinase, PI-3-kinase and Smad pathways (Romao et al., 2008) are believed to be involved in the regulation of *GFAP* in astrocytes. Our data indicate that NFIs, in conjunction with other transcription factors, should be added to the list of important transcription factors involved in the control of *B-FABP* and *GFAP* expression.

In conclusion, our data demonstrate the importance of all four NFIs, in conjunction with NFI phosphorylation, in the regulation of *GFAP* and *B-FABP* promoter activity in malignant glioma cells. We show that there is cross-talk between the different members of the NFI family and that particular NFIs or combinations of

NFIs (either in the form of homodimers or heterodimers) are more effective at up-regulating or down-regulating *GFAP* and *B-FABP* promoter activity. Of note, significant differences in NFI transcriptional activity were observed depending on whether the promoter was in a chromosomal or episomal configuration, likely reflecting a dual role for NFIs in chromatin remodeling and as classic transcription factors. Future work will involve chromatin immunoprecipitation to study the *in vivo* occupancy of individual NFIs at the endogenous *GFAP* and *B-FABP* promoters and to identify additional NFI target genes in malignant glioma.

Chapter 3

NUCLEAR FACTOR I REGULATES EXPRESSION OF *HEY1* IN MALIGNANT GLIOMA

3.1 Introduction

Grade III (or anaplastic astrocytoma) and IV (or glioblastoma) astrocytomas, collectively referred to as malignant glioma (MG), are the most common adult brain tumours (Ohgaki and Kleihues, 2005b). Despite aggressive treatment including surgical resection, radiotherapy, and adjuvant chemotherapy with temozolomide, the median survival is less than 2 years (Mason et al., 2007; Stupp et al., 2005). These tumours are highly infiltrative, resulting in high recurrence and treatment failure. MGs express brain fatty acid-binding protein (B-FABP, FABP7 or BLBP), and the intermediate filament protein glial fibrillary acidic protein (GFAP), two proteins expressed in the glial cell lineage (Doetsch, 2003a; Godbout et al., 1998). B-FABP is expressed in radial glial cells, which act as neural precursors in the brain (Anthony et al., 2004; Feng et al., 1994), whereas GFAP is expressed in astrocytes, including subventricular zone astrocytes (Doetsch et al., 1999a). B-FABP expression is associated with increased migration in MG cell lines and sites of infiltration in grade IV astrocytoma tumours (Mita et al., 2007). Elevated levels of B-FABP have been shown to correlate with a worse prognosis in grade IV astrocytomas (De Rosa et al., 2012; Kaloshi et al., 2007; Liang et al., 2005).

The Nuclear Factor I (NFI) family of transcription factors regulates expression of the *B-FABP* and *GFAP* genes in MG (Chapter 2) (Bisgrove et al., 2000). The four members of the NFI family (NFIA, B, C and X) bind to the consensus binding site 5'-TTGGCA(N_5)GCCAA-3' as homo- and heterodimers (Gronostajski, 1986; Kruse et al., 1991; Kruse and Sippel, 1994b). While the N-terminal DNA binding and dimerization domain is highly conserved among NFI family members, the C-terminal

domain is more divergent, resulting in variation in transactivation potential (Chaudhry et al., 1998). NFIs can activate or repress the expression of genes with NFI-dependent promoters, and regulation of transcription is dependent on promoter context and is tissue-specific (Chapter 2) (Gronostajski, 2000).

NFI binding sites are enriched in brain-specific promoters (Amemiya et al., 1992) and NFIs are important regulators of gliogenesis and astrocyte differentiation in the developing central nervous system (Deneen et al., 2006; Namihira et al., 2009). NFIA is necessary for the onset of gliogenesis downstream of Notch signaling (Namihira et al., 2009). Following glial fate specification, NFIA further promotes astrocyte differentiation and antagonizes oligodendrocyte differentiation (Deneen et al., 2006; Glasgow et al., 2014; Kang et al., 2012). *Nfia-/-, Nfib-/-* and *Nfix-/-* mice all display delayed neuronal and glial cell differentiation in the brain (Betancourt et al., 2014; das Neves et al., 1999a; Driller et al., 2007; Heng et al., 2014; Shu et al., 2003; Steele-Perkins et al., 2005; Wong et al., 2007).

NFIA expression is increased in MG compared to normal brain, with expression detected in 48% of cells in grade III, and 37% of cells in grade IV astrocytomas (Lee et al., 2014; Song et al., 2010). NFIA is enriched in astrocytoma compared to other tumours, with fewer than 5% of cells expressing NFIA in oligodendrogliomas and other brain tumours. Furthermore, expression of NFIA in an oligodendroglioma model promotes conversion to an astrocytoma-like phenotype (Glasgow et al., 2014). NFIA expression increases proliferation and migration in both MG cell lines and in orthotopic xenografts through repression of p53, p21, and plasminogen activator inhibitor 1 (PAI1) (Glasgow et al., 2013; Lee et al., 2014).

In order to identify additional NFI target genes in MG, we performed chromatin immunoprecipitation (ChIP)-on-chip using a pan-specific NFI antibody. We identified over 400 putative target genes, including *HEY1*, a Notch effector gene. *HEY1* is expressed in the brain, and is important for maintenance of neural precursor cells (Sakamoto et al., 2003). In astrocytoma, expression of *HEY1* correlates with increasing tumour grade, and with shorter survival based on a cohort of 62 GBM patients (Hulleman et al., 2009). Here, we show that NFI represses expression of *HEY1* in MG cell lines, and conversely, HEY1 modulates expression glial genes including NFI.

3.2 Methods

3.2.1 Cell lines, constructs, siRNAs, and transfections

The human MG cell lines used in this study have been previously described (Chapter 2) (Godbout et al., 1998). Cells were cultured in Dulbecco's modification of Eagle's minimum essential medium (DMEM) supplemented with 10% fetal calf serum, penicillin (100 U/mL) and streptomycin (100 µg/mL).

The pCH-NFI expression vectors pCH, pCH-NFIA, pCH-NFIB, pCH-NFIC and pCH-NFIX were obtained from Dr. R. Gronostajski (State University of New York at Buffalo). The luciferase reporter gene construct was prepared by inserting the 5' *HEY1* flanking DNA from -913 bp to +15 bp into the pGL3-Basic vector (Promega). Mutations of the -332 bp [Hey1-binding region 1 (H-br1)] and -794 bp (H-br3) NFI binding sites located upstream of the *HEY1* transcription start site were generated using QuikChange site-directed mutagenesis (Agilent Technologies) using oligonucleotides with GG→AA mutations in the NFI binding sites. The double mutant (H-br1*/3*) was generated from the single H-br1* construct. Mutations were verified by sequence analysis.

Stealth siRNAs (Life Technologies) were used to knockdown NFIA, NFIB, NFIC, NFIX, and HEY1: NM_005595_stealth_919 targeting 5′-GAAAGUUCUUCAUACUACAGCAUGA-3′ (NFIA); NM_005596_stealth_1020 targeting 5′-AAGCCACAAUGAUCCUGCCAAGAAU-3′ (NFIB); NM_005597_stealth_1045 targeting 5′-CAGAGAUGGACAAGUCACCAUUCAA-3′ (NFIC); NM_002501_stealth_752 targeting 5′-GAGAGUAUCACAGACUCCUGUUGCA-3′ (NFIX); NM_ 012258.3_stealth_284

targeting 5'-UAGAGCCGAACUCAAGUUUCCAUUC-3' and NM_012258.3_stealth_652 targeting 5'-UUGAGAUGCGAAACCAGUCGAACUC-3' (HEY1). Scrambled siRNAs (cat. nos. 12935-200 and 12935-300) were used as negative controls. The siRNAs targeting NFI family members have been previously validated (Chapter 2).

U251 MG cells were transfected using polyethylenimine (PEI) (Polysciences Inc.), and U87 MG cells were transfected using calcium phosphate-mediated DNA precipitation. Cells were transfected with 10 nM siRNAs using RNAiMAX-Lipofectamine (Life Techonologies). Where indicated, cells were transfected first with siRNA, followed by plasmid transfection 24 h later. Cells were harvested 60 h after the last transfection. For 2X transfections with siRNAs, cells were transfected, grown to confluency, replated at 1/7 dilution, and transfected again.

3.2.2 Chromatin immunoprecipitation-on-chip

ChIP to isolate NFI-bound DNA was carried out following Agilent's mammalian ChIP-on-chip protocol version 10.0 (May 2008). Briefly, ~ 8 x 10^8 U251 MG cells were crosslinked with 1% formaldehyde for 12 min at room temperature, followed by addition of glycine to 0.125 M to terminate the crosslinking reaction. Cells were scraped in cold 1X phosphate buffered saline (PBS), and the cell pellet was frozen in liquid nitrogen. Cells were lysed in lysis buffer 1 [50 mM Hepes-NaOH pH 7.5, 140 mM NaCl, 1 mM EDTA (ethylene diamine tetraacetic acid), 10% glycerol, 0.5% Nonidet-P40, 0.25% Triton X-100, 1X Complete protease inhibitor (Roche)], and centrifuged at 1350 x g for 5 min at 4°C. The pellet was resuspended

in lysis buffer 2 [10 mM Tris-HCl pH 8.0, 200 mM NaCl, 1 mM EDTA, 0.5 mM EGTA (ethylene glycol tetraacetic acid), 1X Complete protease inhibitor], and centrifuged at 1350 x g for 5 min at 4°C to precipitate the nuclei. Nuclei were resuspended in 3 mL lysis buffer 3 (10 mM Tris-HCl pH 8.0, 100 mM NaCl, 1 mM EDTA, 0.5 mM EGTA, 0.1% sodium deoxycholate, 0.5% N-laurylsarcosine, 1X Complete protease inhibitor). Nuclei were sonicated 30 x 30 s at 30% output (model 300VT, Ultrasonic Homogenizer, BioLogics, Inc), and Triton X-100 added to a final concentration of 1%. Cellular debris was removed by centrifugation and 50 µL of the ChIP lysate frozen at -20°C for input DNA (non-enriched control). The remaining ChIP lysate was precleared with Protein-A Sepharose beads (GE Healthcare). The precleared lysate was incubated with 3 µg anti-NFI antibody (Santa Cruz Biotechnology: Clone N-20, Cat. No. sc-870) and incubated at 4°C for 16 h. Protein-A Sepharose beads were added and incubated for 2 h at 4°C. Beads were washed 7X in wash buffer (50 mM Hepes-KOH, 500 mM LiCl, 1 mM EDTA, 1% Nonidet-P40, 0.7% sodium deoxycholate), and 1X in TE with 50 mM NaCl at 4°C. Protein-DNA complexes were eluted in elution buffer (50 mM Tris-HCl pH 8.0, 10 mM EDTA, 1% SDS) at 65°C for 15 min. Elution buffer (3 volumes) was also added to input DNA. ChIP sample and input DNA were incubated at 65°C for 16 h to reverse crosslinks. RNA was digested with RNase A (0.2 mg/mL) for 2 h at 37°C, followed by protein digestion with proteinase K (0.2 mg/mL) in the presence of 0.2 mM $CaCl_2$ at 55°C for 30 min. ChIP and input DNAs were purified by phenol:chloroform:isoamyl alcohol extraction and ethanol precipitation, and blunt-ended by addition of 1.5 U T4 DNA polymerase (New England Biolabs (NEB)) in the presence of 1X NEB Buffer 2, 5 µg BSA, and 100 µM

dNTPs and incubated at 12°C for 20 minutes. Phenol:chloroform:isoamyl alcohol extraction and ethanol precipitation were repeated, and linkers for ligation mediated-PCR (LM-PCR) were ligated to blunt-end DNA with T4 DNA ligase (NEB) in 1X ligase buffer (Life Technologies) at 16°C for 16 h, followed by ethanol precipitation.

Linkers (5'-GCGGTGACCCGGGAGATCTGAATTC-3', and 5'-GAATTCAGATC-3') were prepared by annealing at 70°C for 1 min, and cooling slowly to 4°C. Input and ChIP DNAs were amplified by LM-PCR. PCR reactions containing input or ChIP DNAs, 1X Thermopol buffer (NEB), 250 μM dNTPs, 1 μM LM-PCR primer 5'-GCGGTGACCCGGGAGATCTGAATTC-3', and 0.25 U Taq polymerase were carried out as follows: 55°C/4 min, 72°C/3 min, 95°C/2 min, (95°C/30 s, 60°C/30 s, 72°C/1 min) X 15, 72°C/5 min. One hundredth of the resulting PCR products were used in a second round of PCR amplification as described above for 25 cycles. The PCR products were precipitated with ethanol, resuspended in sterile H_20, and diluted to 100 ng/μL.

Input and ChIP DNAs were fluorescently labeled with Agilent Genomic DNA Labeling Kit PLUS (Agilent Technologies). For each reaction, 2 μg input or ChIP DNA were incubated with 5 μL Random Primers, 1X buffer, 1X dNTPs, 3 μL 1.0 mM Cyanine 3-dUTP (Cy3) (input DNA) or 3 μL 1.0 mM Cyanine 5-dUTP (Cy5) (ChIP DNA), and 1 μL Exo-Klenow DNA polymerase fragment in a final volume of 50 μL, and incubated at 37°C for 2 h, followed by 10 min incubation at 65°C to inactivate the enzyme. For hybridization, 5 μg Cy3-labeled DNA, 5 μg Cy5-labeled DNA, 50 μg Human Cot1, 1X Agilent blocking agent, and 1X Agilent hybridization buffer per slide were heated for 3 min at 95°C, followed by incubation at 37°C for 30 min, then

applied to the Agilent Human Promoter 1 ChIP-on-chip 244K 014706 and 014797 (Agilent Technologies) in duplicate (4 slides total). Slides were hybridized with shaking (20 RPM) in a hybridization oven at 65°C for 40 h. The slides were then washed 1X with Oligo aCGH/ChIP-on-chip wash buffer (Agilent Technologies) at room temperature and 1X with Oligo aCGH/ChIP-on-chip wash buffer at 31°C. Slides were scanned on a GenePix 4000B scanner, and data extracted using Agilent Feature Extraction Software (Agilent Technologies. Data was analyzed using Agilent Genomic Workbench (Agilent Technologies).

3.2.3 Electrophoretic mobility shift assays (EMSAs)

EMSAs were carried out as previously described (O'Brien et al., 1995). Putative NFI binding sequences in the *HEY1* promoter are listed in Figure 3-1A. Complementary oligonucleotides (Figure 3-1B) were annealed and radiolabeled by Klenow polymerase in the presence of α-^{32}P-deoxycytidine triphosphate. Oligonucleotides containing mutated NFI binding sites were generated by substituting AA for the conserved GG at positions 3 and 4 of the NFI consensus binding site (Figure 3-1B). Nuclear extracts were prepared from untransfected U251 MG cells as described previously (Roy et al., 1991), and nuclear extracts from U251 MG cells transfected with pCH, pCH-NFIA, pCH-NFIB, pCH-NFIC, and pCH-NFIX were prepared using the Thermo Scientific NE-PER Nuclear and Cytoplasmic Extraction Kit (Life Technologies). Nuclear extracts (3 µg for untransfected U251 MG cells, 2 µg for pCH-transfected cells, 3 µg for pCH-NFIA-transfected cells, 4 µg for pCH-NFIB-transfected cells, 1 µg for pCH-NFIC-transfected cells, and 2 µg for pCH-

NFIX-transfected cells) were preincubated in binding buffer (20 mM Hepes pH 7.9, 20 mM KCl, 1 mM spermidine, 10 mM dithiothreitol, 10% glycerol, 0.1% Nonidet P-40) in the presence of 1.25 µg poly(dI-dC) for 10 min at room temperature. Where indicated, a 100X molar excess of competitor oligonucleotide was included during preincubation. Radiolabeled oligonucleotides were added to the reaction mixture and incubated 20 min at room temperature. For supershift experiments, 1 µL anti-NFI antibody (a gift from Dr. N. Tanese, New York University Medical Center), 1 µL anti-AP2 antibody (negative control) (Santa Cruz Biotechnology Inc.: Clone C18, Cat No. sc-184) or 1 µL anti-Pax6 (negative control) (Developmental Studies Hybridoma Bank maintained by the University of Iowa under contract NO1-HD-7-3263 from the NICHD) was added with the radiolabeled oligonucleotides. DNA-protein complexes were electrophoresed in 6% native polyacrylamide gels in 0.5X TBE buffer, and exposed to film.

3.2.4 Western blot analysis

Nuclear extracts were prepared using Thermo-Scientific NE-PER Nuclear and Cytoplasmic Extraction Kit (Life Technologies). Protein extracts were electrophoresed in 8% polyacrylamide-SDS gel and transferred to PVDF (polyvinylidene fluoride) membrane. The membrane was immunostained with mouse anti-HA antibody (Sigma: Clone HA-7, Cat. No. H9658) (1:10 000) and rabbit anti-DDX1 antibody (Bleoo et al., 2001) (1:5000). Primary antibodies were detected with horseradish-peroxidase-conjugated secondary antibodies (Jackson ImmunoResearch Biotech) using Immobilon (EMD Millipore).

3.2.5 Quantitative real time-PCR (qPCR)

Total RNA was isolated from MG cells with the RNeasy Plus Kit (Qiagen), and cDNA synthesized with Superscript II reverse transcriptase (Life Technologies). qPCR was carried out using an ABI 7900HT Fast Real-Time PCR System, with gene-specific oligonucleotides labeled at the 5' end with the fluorescent reporter dye FAM (NFIA, Hs00325656_m1; NFIB, Hs00232149_m1; NFIC, Hs00907819_m1; NFIX, Hs00958849_m1; GFAP, Hs00157674_m1; B-FABP, Hs00361426_m1; NES, Hs04187831_g1: HEY1, Hs01114113_m1; GAPDH, Hs99999905_m1) and Taqman Fast Master Mix (Life Technologies). All samples were tested in triplicate, and gene expression normalized to *GAPDH.*

3.2.6 Reporter gene assay

U251 MG cells were cultured in 12-well cell culture plates. Following transfection (see Section 3.2.1), cells were harvested in 250 µL of 1X Luciferase Cell Culture Lysis Buffer (Promega), and stored at -80°C. Luciferase activity was measured in 20 µL aliquots of lysate following automatic injection of 100 µL of Luciferase Assay Reagent (Promega) using a FLUOstar Optima microplate reader (BMG Labtech).

3.3 Results

3.3.1 Chromatin immunoprecipitation (ChIP)-on-chip of NFI binding regions

To identify NFI target genes in MG, we hybridized NFI-bound immunoprecipitated DNA in duplicate to Agilent Human Promoter 1 arrays (Agilent Technologies). These arrays contain probes from -5.5 kb upstream to +2.5 kb downstream from the transcription start site of ~17 000 RefSeq genes. Arrays were analyzed with ChIP Analytics software (Agilent Technologies) resulting in the identification of 403 genes with enriched binding based on a cutoff of log (2) ratio >0.85 (enrichment of >1.8 fold) ($p<0.01$) (Table 3-1). The list includes previously identified NFI target genes including *GFAP* (Chapter 2) (Cebolla and Vallejo, 2006; Gopalan et al., 2006b), p21 (CDKN1A) (Lee et al., 2014; Ouellet et al., 2006), and neurofilament (NEFL) (Amemiya et al., 1992).

Gene ontology (GO) enrichment analysis (GO biological process complete annotation data set, 27 378 terms) of NFI putative target genes revealed enrichment in several developmental processes, including system development, organ morphogenesis, differentiation, and specifically cardiovascular, skeletal, and neuronal development (Table 3-2) (2015; Ashburner et al., 2000). NFI target genes also demonstrated enrichment for genes involved in regulation of gene expression, both positive and negative, and transcription from RNA pol II promoters (Table 3-2), suggesting NFI is upstream of additional factors involved in regulating gene expression. In addition, GO enrichment analysis using the PANTHER GO Slim Biological Process annotation data set, which contains 257 biological process

Table 3-1: Putative NFI target genes identified by ChIP-on-chip.
Continued next page.

Gene	Chr	Start[1]	Location[2]	Log Ratio 1[3]	Log Ratio 2[4]
A2M	12	9113245	Inside	2.3449	2.13
ABCD3	1	94655702	Promoter	0.8391	0.8578
ABL1	9	132699679	Promoter	1.9824	2.8428
ABLIM1	10	116434625	Promoter		1.2935
ACTA2	10	90700226	Inside	1.2636	1.5899
ADAM12	10	128065860	Inside	1.3293	1.0154
ADIPOR2	12	1669620	Promoter	1.6344	1.0305
AKAP12	6	151604981	Inside	1.0677	0.5923
AP3S2	15	88238623	Promoter	2.3766	4.452
AP4S1	14	30605761	Inside	4.1749	2.6825
ARAP2	4	35922189	Inside	0.883	0.9511
ARFGEF2	20	46973980	Inside	1.0145	1.6826
ARID3A	19	873094	Promoter	1.3973	2.8587
ARID5A	2	96561634	Promoter	1.3574	1.4605
ARNTL2	12	27378226	Inside	2.9563	1.4642
ASPH	8	62788839	Inside	1.3963	0.9914
ASXL1	20	30408852	Promoter	1.8043	1.819
AZI2	3	28365132	Inside	0.8752	0.9516
B3GAT2	6	71723193	Inside	0.5558	1.0723
BARD1	2	215383130	Promoter	0.8541	0.8832
BARX1	9	95757258	Inside	0.9012	0.9674
BBS4	15	70766186	Inside	0.9716	0.883
BCOR	X	39844258	Promoter	1.123	0.9873
BHLHE40	3	4997058	Inside	1.9107	1.9376
BIVM	13	102250488	Inside	1.5475	1.7952
BMPR1A	10	88623573	Inside	2.0163	1.427
BOK	2	242146996	Inside	2.8644	
C12orf50	12	86945053	Inside		1.3029
C14orf93	14	22548858	Inside	2.1231	0.6826
C4orf46	4	159811801	Inside	0.8529	0.795
C6orf226	6	42966730	Promoter	0.9194	0.8339
C6orf48	6	31902882	Promoter	2.9354	1.9704
CAB39L	13	48871772	Inside		2.7623
CALD1	7	134221728	Promoter	1.043	0.8438
CALU	7	128168470	Inside	1.0949	1.0157
CAMK1	3	9787282	Promoter	0.7474	1.2159
CAPS2	12	74070664	Inside	1.5286	0.6155
CASD1	7	93978527	Inside	0.9683	0.7883
CAST	5	96080515	Inside	0.7114	0.86

Gene	Chr	Start[1]	Location[2]	Log Ratio 1[3]	Log Ratio 2[4]
CBLN3	14	23964730	Downstream	2.1749	1.75
CCBE1	18	55519524	Promoter	1.0248	1.228
CCDC150	2	197212889	Inside	1.0609	0.7303
CCDC18	1	93417823	Promoter	1.6742	2.8547
CCDC63	12	109767259	Promoter	1.3922	2.3241
CCDC89	11	85075244	Promoter	0.7093	0.9903
CCL2	17	29605928	Promoter	1.4862	1.5466
CCM2	7	45005877	Promoter	0.8848	0.8779
CCNA1	13	35900528	Promoter	2.7599	5.2676
CCNL1	3	158360010	Inside	0.9441	0.8409
CCNT2	2	135393397	Inside	0.931	0.7432
CCNYL1	2	208284923	Inside	0.9386	0.7282
CCRN4L	4	140156163	Promoter	0.9815	1.0638
CCT4	2	61968894	Inside	1.0762	1.4236
CD274	9	5440826	Inside	1.3285	2.3594
CD55	1	205561713	Inside	0.8691	0.8141
CDH26	20	58001523	Promoter	1.9592	0.7257
CDK1	10	62209644	Promoter	1.8754	0.6561
CDKL1	14	49936425	Promoter	1.1446	1.6956
CDKN1A	6	36756502	Inside	0.881	0.6717
CDR2	16	22291327	Inside	2.3448	2.1586
CEP170-SDCCAG8	1	241485512	Divergent promoter	1.941	2.2168
CEP85	1	26474887	Inside	0.8501	0.6725
CHL1	3	215054	Inside	0.9341	0.9227
CHST12	7	2406240	Promoter	1.479	1.446
CLEC18C	17	3238495	Inside	0.7295	1.1596
CLEC2D	12	9714034	Inside	3.1749	
CNNM3	2	96845754	Inside	0.8178	0.8617
COL12A1	6	75970048	Inside	0.7777	1.3099
COQ4	9	130124836	Inside	5.9865	
CORO1C	12	107647973	Inside	1.3954	0.9799
CSF1R	5	149472454	Inside	1.5463	1.2047
CSRP3	11	19178852	Inside	1.6173	1.7579
CTGF	6	132317596	Promoter	1.1817	0.9029
CTHRC1	8	104453722	Inside	1.5791	1.3662
CTNNA1	5	138118093	Inside	1.1389	1.0538
CTNND2	5	11957555	Promoter	1.0407	0.9424
CTR9	11	10728883	Promoter		2.6155
CUL1	7	148026670	Promoter	0.8901	0.9048
CXCL9	4	77152060	Promoter	0.9205	0.9392

Gene	Chr	Start[1]	Location[2]	Log Ratio 1[3]	Log Ratio 2[4]
CXXC5	5	139008561	Promoter	0.9512	0.9865
CYBRD1	2	172087903	Inside	0.8191	0.9964
DALRD3	3	49030738	Inside	0.7058	0.8781
DCAF6	1	166173189	Inside	1.3486	0.5098
DCBLD2	3	100107833	Promoter	1.4793	1.5552
DDB2	11	47194632	Inside	0.9606	1.1489
DEFB118	20	29420503	Inside		2.867
DEPTOR	8	120955481	Inside	1.1023	0.8643
DLAT	11	111398703	Promoter	1.7599	3.5086
DNAH5	5	13998104	Promoter	1.0857	0.9746
DNAJB6	7	156824418	Inside	1.5893	1.8169
DNMBP	10	101727078	Promoter		1.9456
DTWD1	15	47700817	Inside		1.9236
DUSP14	17	32922698	Promoter	1.0192	1.0282
DUSP22	6	236964	Promoter	1.0673	1.414
DYRK3	1	204876002	Inside	1.046	1.1218
E2F5	8	86320350	Downstream	1.5241	1.2968
EFCAB2	1	243201339	Inside	1.4662	1.2058
EIF4A2	3	187983486	Promoter	1.0448	1.5373
ELL3	15	41856955	Promoter	4.2047	1.9385
EMP1	12	13237614	Promoter	1.2064	1.9012
ENAH	1	223910311	Promoter	1.1427	1.0571
ENO1	1	8862939	Promoter		3.1611
EPAS1	2	46380123	Inside	0.6408	0.9732
EPB41L3	18	5538249	Promoter		2.1301
ERLIN2	8	37713231	Promoter	4.0235	1.1796
ERRFI1	1	8008978	Promoter	0.7638	0.883
ETV1	7	13998960	Promoter	2.4876	2.8207
F12	5	176763982	Inside	1.4547	1.3798
FAM133A	X	92820651	Inside	2.1749	1.3386
FAM150B	2	278156	Inside	1.0176	1.0877
FAM160A2	11	6210731	Inside	1.3302	2.3487
FAM184A	6	119442219	Promoter	2.467	
FAM198B	4	159310123	Inside	1.6559	0.8468
FAM212B	1	112084649	Promoter	1.2915	1.2984
FAM26D	6	116986039	Inside	0.9273	1.1093
FAM43B	1	20752757	Inside	0.7069	0.903
FAM46A	6	82518382	Inside	0.7327	0.9501
FAM5C	1	188714347	Promoter	1.1799	1.1724
FAM63B	15	56850025	Promoter	1.4249	1.9441

Gene	Chr	Start[1]	Location[2]	Log Ratio 1[3]	Log Ratio 2[4]
FAM76B	11	95160902	Inside		3.3524
FAM83D	20	36989268	Inside	2.068	1.3931
FAS	10	90738240	Promoter	1.4337	0.8922
FBXL5	4	15265780	Inside	0.8179	0.8869
FGF9	13	21143410	Promoter	0.6079	1.0686
FLJ38984	1	35956513	Inside	1.2656	1.0383
FNTA	8	43030356	Promoter	0.9929	0.9401
FOXJ2	12	8073435	Promoter	1.6774	2.2678
FZD7	2	202605768	Promoter	1.1294	1.2073
GABPB2	15	48434824	Promoter	0.8781	1.1448
GALNT7	4	174327101	Inside	1.2428	1.0712
GBE1	3	81892929	Inside	0.9443	0.7074
GBP5	1	89509960	Inside	0.8174	0.9367
GCLM	1	94146101	Inside	1.7484	1.9013
GFAP	17	40348396	Promoter	1.471	1.6689
GGNBP2	17	31972190	Promoter		2.1301
GIN1	5	102483328	Inside	1.096	1.3189
GLI3	7	42232735	Inside	2.2832	
GLIPR1	12	74158401	Promoter		1.1139
GLIPR2	9	36122089	Promoter	1.08	1.0909
GNAI3	1	109892505	Promoter	0.9276	1.1387
GORAB	1	168768031	Inside	0.9291	0.6116
GPCPD1	20	5541103	Promoter	1.4644	1.9307
GSX2	4	54660676	Promoter	2.0596	2.6342
GUK1	1	226394685	Inside	0.9175	0.8924
HBP1	7	106596263	Promoter	1.3612	1.1513
HDGF	1	154987886	Inside	0.9429	0.9364
HELZ	17	62669404	Inside	0.9055	0.6826
HEXIM1	17	40581111	Inside	1.853	1.046
HEY1	8	80843258	Promoter	0.9866	0.9256
HIST1H2BJ	6	27207844	Downstream	2.6994	3.298
HMG20A	15	75499939	Promoter	0.7708	1.1065
HNRPDL	4	83569798	Inside	0.5667	0.9533
HSF2BP	21	43901045	Inside	1.512	1.3931
ICMT-HES3	1	6224841	Divergent promoter	1.006	1.0496
ID3	1	23757574	Inside	1.883	
IER5L	9	130979866	Inside	0.8672	0.7791
IFIT1	10	91140690	Promoter	1.8876	3.3931
IFRD2	3	50304903	Promoter	0.9265	
IFT88	13	20039819	Inside	6.0329	4.6661

Gene	Chr	Start[1]	Location[2]	Log Ratio 1[3]	Log Ratio 2[4]
IL1RAPL2	X	103790321	Inside		2.8081
INA	10	105023095	Promoter	0.847	0.8954
ING2	4	184663304	Inside	1.0897	1.0266
INTS12-GSTCD	4	106849357	Divergent promoter	1.1416	
IRF2BP2	1	232814979	Promoter	1.7022	1.6503
IRS2	13	109242223	Promoter	0.7599	1.1618
ITGBL1	13	100900982	Promoter	0.9854	0.6561
JAG1	20	10600976	Inside	1.465	1.4926
KANK1	9	494998	Inside	1.0107	0.9323
KCNH2	7	150286133	Promoter	1.0967	1.0681
KCNK10	14	87863177	Promoter	2.2983	1.3151
KCTD13	16	29843124	Inside		3.5086
KDM3A	2	86521682	Promoter	2.1711	
KIF18A	11	28085526	Inside	1.8057	2.6826
KLF9	9	72217435	Inside	0.9515	0.7306
KLRF1	12	9873240	Inside	2.6344	
KRT10	17	36236502	Promoter	1.0267	0.9381
KRT13	17	36914588	Inside	0.9703	1.1909
KRT37	17	36838500	Promoter	0.9259	1.04876
KRTAP19-5	21	30797152	Promoter		1.7821
KRTAP23-1	21	30643668	Promoter	1.2097	5.5985
KRTAP4-2	17	36591407	Promoter	1.3448	
KTN1	14	55115205	Promoter	0.7037	0.9873
L3MBTL4	18	6299434	Inside	1.9317	2.5895
LARP6	15	68931809	Inside	0.9787	0.9348
LEMD3	12	63849245	Promoter	1.1687	1.2232
LHX1	17	32363515	Promoter	1.2987	1.4615
LIN7B	19	54305925	Promoter	1.3844	1.0712
LINC00173	12	115456450	Inside		3.715
LIX1L	1	144189562	Inside	3.1479	1.7586
LMBR1	7	156378711	Promoter	1.1167	0.8903
LNX2	13	27091478	Inside	0.863	1.0914
LOXL2	8	23321325	Promoter	1.6795	1.5987
LPGAT1	1	210070651	Inside	0.9113	0.6642
LRIG3	12	57601195	Promoter	3.0818	0.6312
LRP11	6	150226326	Inside	0.844	0.9151
LUC7L3	17	46153029	Inside	0.7599	2.0008
LYST	1	234113659	Promoter	1.0678	1.0687
MAB21L1	13	34949195	Promoter	2.0246	1.4995
MAGEB3	X	30165456	Inside	Infinity	1.2676

Gene	Chr	Start[1]	Location[2]	Log Ratio 1[3]	Log Ratio 2[4]
MARCKS	6	114287069	Inside	0.8813	1.4392
MBNL1	3	153499615	Promoter	1.281	0.8607
MCU	10	74123406	Inside	1.7932	1.8959
MED20	6	41996698	Inside	2.6175	0.8524
MEF2C	5	88213383	Inside	1.1965	1.7183
MEIS2	15	35179607	Promoter		1.4909
METAP2	12	94393160	Inside	0.9339	1.5737
METTL23	17	72234989	Inside	1.3492	1.2214
METTL7A	12	49604807	Inside	3.6344	4.9723
MGP	12	14930159	Promoter	1.2727	1.3211
MGST1	12	16393324	Promoter	1.3499	1.657
MIR125B2	21	16880927	Promoter	1.0955	2.452
MIR149	2	241040806	Promoter	0.8737	0.8394
MIR181A1	1	197094961	Promoter	0.8738	1.2512
MIR205	1	207673444	Downstream	1.1632	0.8121
MIR216A	2	56073153	Promoter	1.0836	0.9672
MIR548B	6	119441594	Promoter	1.1045	1.6763
MIR99A	21	16828801	Promoter	1.0363	1.1253
MIRLET7I	12	61287764	Downstream		1.13
MPPED2	11	30558664	Promoter	2.5534	1.408
MPZL3	11	117628311	Promoter	1.0034	1.0256
MRPL1	4	78999542	Promoter	1.094	0.9655
MTFMT	15	63113497	Promoter		2.0176
MTPN	7	135312739	Promoter	0.7316	1.1827
MUTYH	1	45578374	Promoter	0.7639	1.1403
NAA50	3	114947510	Inside	1.187	0.9951
NARG2	15	58556607	Inside	1.7599	
NCAM2	21	21287395	Promoter	2.5672	1.6706
NCAPH	2	96360052	Promoter	0.9675	0.9379
NDUFA4	7	10946379	Promoter	1.1701	1.2548
NEDD4	15	53997292	Promoter	1.1285	1.9057
NEFL	8	24875334	Promoter	1.1197	1.0298
NEK6	9	126061540	Inside	1.0058	2.3111
NFIA	1	61318395	Promoter	1.7578	1.5734
NHS	X	17662326	Inside		3.666
NPR3	5	32821654	Inside	0.8681	0.7434
NR2F1	5	92944603	Promoter	1.724	1.6766
NRXN3	14	78185282	Inside		3.8956
NSUN4	1	46578948	Promoter	0.3593	2.1549
NUP153	6	17815540	Promoter	1.3413	1.339

Gene	Chr	Start[1]	Location[2]	Log Ratio 1[3]	Log Ratio 2[4]
NUSAP1	15	39412952	Inside	0.7062	0.9863
OR4K5	14	19457562	Promoter	1.1584	0.5645
OR5B2	11	57949404	Promoter		2.2411
OR8K1	11	55867174	Promoter	4.2624	0.7744
OSGIN2	8	90983730	Inside	0.9755	0.8275
OSMR	5	38881767	Promoter	2.2867	3.6053
OSTM1	6	108502607	Inside	0.8983	0.7542
OTOF	2	26639471	Promoter	1.4405	1.4627
PAICS	4	56996755	Promoter	1.4424	1.3502
PAK3	X	110253345	Inside		2.5086
PAN2-IL23A	12	55014286	Divergent Promoter	1.1135	2.978
PAPSS2	10	89407139	Promoter	1.3973	
PARPBP	12	101114267	Inside	0.8564	0.7389
PCDH11Y	Y	4982161	Promoter	1.4969	3.5086
PCDH20	13	60887639	Promoter	2.0018	2.5372
PCDHGC3	5	140835207	Promoter	0.5412	1.0438
PCYOX1L	5	148717764	Promoter	0.806	0.8943
PDCD5	19	37764645	Inside	1.5551	0.984
PDE1C	7	32075349	Inside	0.9477	1.213
PHEX	X	21961908	Inside	1.3092	0.8861
PHIP	6	79844705	Promoter	0.8298	0.9198
PHKB	16	46056443	Inside	Infinity	3.7467
PHKG2	16	30662879	Promoter	1.9475	0.5451
PIGW	17	31968591	Inside	2.4229	1.6237
PLA2G6	22	36907952	Promoter	0.8237	1.0237
PLAG1-CHCHD7	8	57286601	Divergent promoter	1.0339	1.0007
PLEKHA1	10	124125339	Inside		3.2676
PLEKHF2	8	96215015	Promoter	0.8497	0.8805
PLEKHG7	12	91650086	Promoter	1.4745	2.1036
PLSCR4	3	147451761	Promoter	1.4499	1.3556
PLXND1	3	130807793	Inside	1.2362	1.2639
PMCH	12	101114699	Inside	1.8754	1.9236
POLR2M	15	55786150	Promoter	1.376	1.4702
POP7	7	100142485	Inside	1.163	1.2064
PPIB	15	62247347	Promoter	0.7599	1.2588
PPM1D	17	56033871	Inside	0.9405	0.957
PPRC1	10	103882474	Promoter	1.5316	1.893
PREP	6	105957405	Inside	0.8652	0.9023
PRKCZ	1	1971786	Inside	1.0996	1.2305

Gene	Chr	Start[1]	Location[2]	Log Ratio 1[3]	Log Ratio 2[4]
PRR11	17	54598116	Inside	1.1638	1.1606
PSMD5	9	122645227	Promoter		1.752
PTCH1	9	97309577	Promoter	4.667	2.5832
PTHLH	12	28012193	Inside	1.916	4.3931
PVRL3	3	112273071	Promoter	1.1668	0.8705
QKI	6	163755950	Inside	0.8161	0.9088
QSOX1	1	178387365	Promoter	1.3136	1.2724
RAB13	1	152225381	Inside	0.8856	0.5711
RAB27A	15	53369884	Promoter	1.8754	1.7257
RAB32	6	146906540	Inside	0.9266	0.9193
RAB3GAP2	1	218512608	Promoter	1.6686	2.1385
RAB4A	1	227472130	Promoter	1.5611	1.1593
RARB	3	25444505	Promoter	1.5131	1.1602
RASL10B	17	31077950	Promoter	1.4961	1.5103
RBM8A	1	144219300	Inside	0.8511	0.6152
RCBTB1	13	49058882	Promoter	2.005	1.715
RGS12	4	3341510	Inside	1.1184	0.9916
RNF219	13	78131510	Promoter	2.0182	1.1107
RNF43	17	53850241	Promoter	1.3202	1.1636
RPA3	7	7725436	Promoter	0.9336	1.1595
RPL35-ARPC5L	9	126671430	Inside	0.8536	0.7386
RPL7-RDH10	8	74368863	Divergent promoter	2.142	
RPS14	5	149809356	Inside	0.9447	0.7391
RPS26P25	12	54722045	Promoter	2.0229	1.2747
RPS6KA5	14	90594136	Inside	0.8299	1.1171
RUNX1	21	35187762	Promoter		1.8081
RXRA	9	136466823	Inside	1.4666	1.1116
S100A10	1	150234089	Promoter	1.7226	1.3661
S100A2	1	151805208	Promoter	0.7175	0.8918
SAAL1	11	18084458	Promoter	0.9111	0.8292
SALL1	16	49742667	Promoter	0.8851	0.9548
SAP30BP	17	71176036	Inside	0.7296	0.9472
SATB2	2	200028516	Inside	1.4823	1.1501
SEC22B	1	143804069	Promoter	1.8402	1.6841
SEC63	6	108386153	Promoter	1.2092	0.8009
SEMA3C	7	80384831	Inside	2.0581	2.2209
SENP2	3	186784484	Promoter	0.8401	0.8536
SERPINA12	14	94054227	Promoter	0.9043	1.0203
SERPINE1	7	100556642	Promoter	1.281	1.0997

Gene	Chr	Start[1]	Location[2]	Log Ratio 1[3]	Log Ratio 2[4]
SERPINE2	2	224615283	Promoter	1.7994	1.8375
SFR1	10	105867828	Promoter	1.5961	1.5375
SGPP2	2	222997476	Promoter	0.832	0.8975
SH3GLB1	1	86942572	Promoter	1.0742	0.7759
SLC1A3	5	36641944	Promoter	1.9592	1.9216
SLC25A24	1	108544889	Promoter	1.2235	1.0073
SLC25A38	3	39400641	Inside	0.9268	0.6487
SLC2A8	9	129199290	Inside	0.8095	0.9206
SLC34A2	4	25266397	Promoter	0.6397	0.9394
SLC35A1	6	88234292	Promoter	0.9993	0.9899
SLC39A1	1	152202903	Inside	1.2398	1.2455
SLC4A2	7	150388856	Inside	1.2223	1.12
SNAP91	6	84475571	Promoter	0.6865	0.8948
SNORD61	X	135789798	Promoter	0.9994	0.923
SNX18	5	53847891	Promoter	1.4868	1.8669
SOS2	14	49766863	Inside	1.2745	1.2881
SOX21	13	94164394	Promoter	1.4906	1.6101
SPATA31E1	9	89683959	Promoter	3.3902	1.7178
SPATA7	14	87918342	Promoter	0.9405	1.5419
SREBF2	22	40558801	Promoter	1.0166	1.0877
SRRT	7	100310524	Promoter	1.2548	1.0389
ST5	11	8884780	Inside		2.8081
STAMBP	2	73911856	Inside	1.2324	1.2124
STC1	8	23767712	Inside	1.7308	1.8818
SWAP70	11	9643126	Inside	1.2258	1.3621
SYTL2	11	85114675	Promoter	2.3124	0.5451
TANK	2	161700020	Promoter	1.8117	1.5764
TBC1D4	13	74958764	Promoter	2.1749	1.1077
TBC1D9	4	141897691	Promoter	1.3521	1.2753
TCF12	15	55295998	Promoter	Infinity	2.0305
TEKT2	1	36322390	Inside	1.2207	0.8003
TGFB1	5	135392598	Inside	0.9168	0.7522
TGFB2	1	216585830	Promoter	0.8472	0.8786
TIA1	2	70328493	Inside	1.2478	1.2808
TIPARP	3	157875103	Inside	0.9606	0.9971
TLE3	15	68180782	Promoter	1.4118	1.5755
TLN2	15	60727365	Inside		3.5086
TMEM106B	7	12218056	Inside	1.4318	1.2735
TMEM117	12	42517112	Inside	2.4969	0.8081
TMEM165	4	55957822	Inside	0.8309	1.5276

Gene	Chr	Start[1]	Location[2]	Log Ratio 1[3]	Log Ratio 2[4]
TMEM18	2	667475	Promoter	0.8736	1.0234
TMEM5	12	62458480	Promoter	1.0193	1.5086
TMEM68	8	56848373	Inside	1.4128	1.0885
TNC	9	116920425	Promoter	1.0671	1.1067
TNK2	3	197108216	Promoter	1.424	1.4345
TNRC6B	22	38769059	Promoter	Infinity	1.8849
TOP2B	3	25681044	Promoter	1.091	1.1184
TPM1	15	61130006	Inside	1.3379	1.0357
TRAPPC6B	14	38706756	Inside	3.8188	
TRIM24	7	137796161	Inside	0.9419	0.8926
TRIM27	6	28999877	Promoter	0.4587	1.0425
TRIM39	6	30401356	Promoter	0.9795	0.7046
TRIM68	11	4588395	Promoter	0.8437	1.978
TRIM7	5	180566074	Promoter	1.2226	1.5655
TRMT13	1	100371465	Inside	1.2459	0.872
TRMT5	14	60514612	Inside	2.1618	
TSC22D1	13	43908581	Inside	1.3124	1.8273
TSHZ1	18	71054967	Inside	1.1078	1.7696
TSPAN1	1	46421794	Inside	1.6963	0.4872
UBP1	3	33456791	Promoter		0.9941
UBQLNL	11	5494712	Promoter	3.8188	
UBTF	17	39656567	Promoter	2.232	2.261
UGT1A6	2	234263596	Promoter	1.0837	0.68
UPP1	7	48091159	Promoter	1.8999	1.868
UTRN	6	144650122	Promoter	1.6635	1.4185
UTS2D	3	192483245	Promoter	0.7589	1.1478
VWCE	11	60821797	Promoter	1.0582	1.1159
WAC	10	28862027	Promoter	0.9559	0.9373
WBSCR17	7	70232063	Promoter	1.4624	1.4046
WHSC1	4	1842782	Promoter	1.0058	0.7851
WNT2B	1	112810639	Promoter	1.2258	0.6594
WNT5A	3	55500570	Promoter	0.9735	0.7655
WNT9A	1	226202113	Inside	1.1542	1.2018
ZBTB8OS-RBBP4	1	32889059	Divergent promoter	1.1693	0.9177
ZFAND3	6	37894564	Promoter	1.2631	1.2166
ZIM2	19	62044765	Promoter		1.37
ZKSCAN8	6	28212586	Promoter	1.8771	1.3735
ZMYND11	10	171940	Inside	0.8085	0.8826
ZMYND8	20	45422915	Promoter	0.9489	1.1383
ZNF24	18	31179965	Promoter	1.3257	0.7557

Gene	Chr	Start[1]	Location[2]	Log Ratio 1[3]	Log Ratio 2[4]
ZNF426	19	9510687	Promoter	0.7344	0.9575
ZNF615	19	57201227	Inside	1.3593	0.8723
ZNF703	8	37668165	Promoter	1.2573	1.3695
ZNF706	8	102287188	Promoter	0.8385	0.8897
ZNF76	6	35335395	Promoter	2.258	2.4167

DNA crosslinked to NFI was isolated and hybridized to Human Promoter 1 microarray (Agilent) in duplicate. Arrays were analyzed using ChIP analytics software (Agilent). Genes with a log (2) ratio >0.85 (enrichment of >1.8 fold) ($p<0.01$) are listed.
[1]chromosomal location of bound probe on NCBI36/hg18 assembly
[2]location of bound probe relative to gene
[3,4]replicate 1[3] and replicate 2[4]

terms, clearly highlights enrichment in development, specifically nervous system development (Table 3-3) (Mi et al., 2013). *HEY1*, a Notch effector gene, was identified as a putative NFI target gene. HEY1 is important for maintenance of neural precursor cells and is highly expressed in MG compared to normal brain. Here, we examine NFI regulation of *HEY1* expression in MG.

3.3.2 NFI binds to NFI binding sequences in the *HEY1* promoter

ChIP analysis identified enriched binding of NFI to a ChIP probe corresponding to the region from -705 to -645 bp upstream of the *HEY1* transcription start site. NFI binding to the *HEY1* promoter has been validated with ChIP (data not shown). Sequence analysis of the *HEY1* promoter from -1100 bp upstream to the transcription start site revealed four putative NFI binding sites, located at -32 to -17 bp, -332 to -317 bp, -411 to -396 bp and 794 to -779 bp. Previously, the region spanning -30 to -247 bp upstream of the mouse *Hey1* transcription start site was reported to be essential for basal *Hey1* transcription, with additional regulatory sequences between -247 to -647 bp in mouse (-680 bp in human) (Maier and Gessler, 2000).

We used electrophoretic mobility shift assays (EMSAs) to examine if NFIs are able to bind to these putative NFI binding sites. Double-stranded oligonucleotides (Figure 3-1) corresponding to each putative binding site were radiolabeled and incubated with nuclear extracts prepared from U251 MG cells. To address specificity of binding, a 100X fold molar excess of unlabeled oligonucleotides was used as a

Table 3-2: Gene ontology enrichment analysis of putative NFI target genes identified by ChIP-on-chip. Continued next page.

Gene Ontology Term	Sample Frequency[1]	Expected Frequency[2]	Fold Enrichment[3]	P value
positive regulation of biological process	158	85.68	1.84	8.12E-13
biological process	344	280.17	1.23	1.41E-12
positive regulation of cellular process	135	72.87	1.85	4.37E-10
cellular process	304	237.63	1.28	1.03E-09
system development	124	65.15	1.9	1.24E-09
biological regulation	257	186.86	1.38	2.05E-09
regulation of metabolic process	177	110.62	1.6	3.68E-09
single-organism process	282	215.41	1.31	7.59E-09
multicellular organismal development	134	75.13	1.78	1.03E-08
organ development	97	46.67	2.08	1.17E-08
single-organism cellular process	260	192.89	1.35	1.70E-08
anatomical structure morphogenesis	83	37.07	2.24	1.85E-08
anatomical structure development	135	76.67	1.76	2.07E-08
regulation of cellular process	239	171.65	1.39	2.17E-08
positive regulation of metabolic process	107	55.42	1.93	5.26E-08
organ morphogenesis	47	15.18	3.1	8.76E-08
regulation of primary metabolic process	150	91.29	1.64	1.36E-07
regulation of biological process	243	178.39	1.36	1.47E-07
single-organism developmental process	143	85.48	1.67	1.54E-07
regulation of gene expression	124	69.87	1.77	1.63E-07
cell differentiation	104	54.67	1.9	2.83E-07
regulation of cellular metabolic process	155	96.53	1.61	3.01E-07
regulation of macromolecule metabolic process	149	91.71	1.62	4.02E-07
multicellular organismal process	166	106.73	1.56	4.63E-07
single-multicellular organism process	161	102.37	1.57	4.87E-07
developmental process	143	86.83	1.65	4.93E-07
negative regulation of biological process	126	72.67	1.73	4.97E-07
negative regulation of cellular process	118	66.8	1.77	8.78E-07

Gene Ontology Term	Sample Frequency[1]	Expected Frequency[2]	Fold Enrichment[3]	P value
circulatory system development	41	13.21	3.1	1.88E-06
cardiovascular system development	41	13.21	3.1	1.88E-06
cellular developmental process	104	57.09	1.82	3.40E-06
cellular response to chemical stimulus	78	37.85	2.06	4.93E-06
negative regulation of metabolic process	81	40.03	2.02	4.95E-06
positive regulation of gene expression	60	25.76	2.33	8.36E-06
regulation of biosynthetic process	118	69.29	1.7	8.49E-06
cellular response to organic substance	67	30.55	2.19	8.86E-06
positive regulation of macromolecule metabolic process	83	42.25	1.96	1.15E-05
negative regulation of gene expression	54	22.06	2.45	1.19E-05
negative regulation of macromolecule metabolic process	72	34.32	2.1	1.23E-05
cellular component organization	134	83.36	1.61	1.54E-05
regulation of nucleobase-containing compound metabolic process	113	66.23	1.71	2.05E-05
regulation of response to stimulus	104	59.05	1.76	2.18E-05
regulation of nitrogen compound metabolic process	115	67.97	1.69	2.26E-05
regulation of macromolecule biosynthetic process	112	65.53	1.71	2.27E-05
regulation of transcription from RNA polymerase II promoter	62	28.34	2.19	4.52E-05
response to organic substance	79	40.8	1.94	6.05E-05
response to stimulus	180	126.37	1.42	6.44E-05
regulation of cellular macromolecule biosynthetic process	108	63.49	1.7	6.49E-05
regulation of cellular biosynthetic process	114	68.4	1.67	6.54E-05
cellular component organization or biogenesis	134	85.4	1.57	7.41E-05
cellular macromolecule metabolic process	162	110.09	1.47	7.44E-05
positive regulation of biosynthetic process	60	27.41	2.19	8.18E-05

Gene Ontology Term	Sample Frequency[1]	Expected Frequency[2]	Fold Enrichment[3]	P value
regulation of RNA metabolic process	104	60.58	1.72	8.59E-05
positive regulation of macromolecule biosynthetic process	56	24.92	2.25	1.12E-04
generation of neurons	53	23	2.3	1.29E-04
neurogenesis	55	24.35	2.26	1.29E-04
positive regulation of nitrogen compound metabolic process	59	27.1	2.18	1.33E-04
macromolecule metabolic process	174	122.03	1.43	1.41E-04
heart development	27	7.53	3.59	1.43E-04
positive regulation of cellular metabolic process	83	44.65	1.86	1.43E-04
negative regulation of cellular metabolic process	71	35.73	1.99	1.50E-04
positive regulation of nucleobase-containing compound metabolic process	58	26.58	2.18	1.65E-04
regulation of multicellular organismal process	75	38.92	1.93	1.94E-04
tissue development	59	27.4	2.15	1.95E-04
skeletal system development	28	8.21	3.41	2.20E-04
regulation of cell communication	90	50.73	1.77	2.70E-04
cellular response to endogenous stimulus	42	16.4	2.56	2.75E-04
regulation of developmental process	68	34.42	1.98	3.98E-04
cellular response to stimulus	150	102.55	1.46	6.44E-04
response to endogenous stimulus	51	23	2.22	8.13E-04
neuron differentiation	42	17.08	2.46	8.22E-04
regulation of nucleic acid-templated transcription	98	58.49	1.68	8.84E-04
regulation of signaling	88	50.52	1.74	9.19E-04
cellular response to lipid	22	5.73	3.84	9.83E-04

Gene ontology enrichment analysis of putative NFI target genes identified by ChIP-on-chip. Genes listed in Table 1 were analyzed using PANTHER overrepresentation test using GO biological process complete annotation data set (27 378 terms). Enriched biological process terms with a p value < 1.0E-4 are included.

[1] number of genes from NFI chIP-on-chip gene list (403 genes, Table 3-1) annotated to Gene Ontology term

[2]number of genes in pathway expected in a random sample of non-enriched genes with same sample size as [1]

[3]ratio between NFI ChIP-on-chip and expected frequency

Table 3-3: PANTHER enrichment analysis of putative NFI target genes identified by ChIP-on-chip.

Gene Ontology Term	Sample Frequency[1]	Expected Frequency[2]	Fold Enrichment[3]	P value
developmental process	85	49.6	1.71	9.02E-05
cellular process	144	103.73	1.39	9.56E-04
regulation of biological process	65	37.91	1.71	2.75E-03
system development	51	28.67	1.78	1.07E-02
biological regulation	84	56.68	1.48	2.55E-02
nervous system development	34	17.57	1.94	4.70E-02

[1]number of genes from NFI ChIP-on-chip gene list (403 genes, Table 3-1) annotated to Gene Ontology term
[2]number of genes in pathway expected in a random sample of non-enriched genes with same sample size as [1]
[3]ratio between NFI ChIP-on-chip and expected frequency

competitor. Competitor oligonucleotides included the -32 bp, -332 bp, -411 bp and -794 bp NFI binding sites, as well as the mutated -32* bp, -332* bp, -411* bp, -794* bp binding sites, and the NFI consensus binding site (Figure 3-1).

Two intense and one weak DNA-protein complexes were observed when the -32 bp probe was incubated with nuclear extracts from U251 MG cells, and one major DNA-protein complex was observed upon incubation of these nuclear extracts with the -332 bp, -411 bp, and -794 bp probes (Figure 3-2). Incubation with excess mutated -32* bp oligonucleotide with two key NFI binding residues mutated, resulted in complete loss of shifted bands, indicating that the DNA-protein complexes observed with the -32 bp probe does not involve NFI binding. These data are further supported by the inability of excess oligonucleotide to the NFI consensus binding site to compete with the -32 bp probe.

In contrast to the -32 bp probe, addition of the appropriate wild-type competitor oligonucleotides fully abolished binding to the -332 bp, -411 bp and -794 bp probes, while addition of excess NFI consensus oligonucleotide significantly reducing signal intensity of DNA-protein complexes (Figure 3-2). Addition of excess -332* bp oligonucleotode did not significantly alter binding to the radiolabeled -332 bp probe, whereas addition of excess -411* bp and -794* bp oligonucleotides resulted in significant and slight reductions in binding, respectively.

To determine if the observed DNA-protein complexes contain NFI, we incubated the radiolabeled probes with nuclear extracts from U251 MG cells and an anti-NFI antibody that has previously been shown to supershift NFI-DNA complexes (Chapter 2) (Bisgrove et al., 2000). Addition of the anti-NFI antibody resulted in a

A

NFI consensus binding site: TTGGC(NNNNN)GCCAA

-32 to -17 bp	5'-TTGCC(GCCCC)GCCTC-3'
-332 to -317 bp	5'-CTGGC(GCGCG)GCCAG-3'
-411 to -396 bp	5'-TTGGC(TGGCG)GCCGC-3'
-794 to -779 bp	5'-TGGGC(TGGTG)GCCAC-3'

B

Probes

-32	5'	CTG GAG **TTG CCG CCC CGC CTC** TC	3'
	3'	C **AAC GGC GGG GCG GAG** AGG C	5'
-332	5'	CGG CC**C TGG CGC GCG GCC AG**G C	3'
	3'	G**G ACC GCG CGC CGG TC**C G GTT A	5'
-411	5'	CCG GA**T TGG CTG GCG GCC GC**G	3'
	3'	CT**A ACC GAC CGC CGG CG**C CGC G	5'
-794	5'	GCC CC**T GGG CTG GTG GCC A**	3'
	3'	GG**A CCC GAC CAC CGG TG**A CAC	5'

Competitors

-32*	5'	CTG GAG **Taa CCG CCC CGC CTC** TC	3'
	3'	C **Att GGC GGG GCG GAG** AGG C	5'
-332*	5'	CGG CC**C Taa CGC GCG GCC AG**G C	3'
	3'	G**G Att GCG CGC CGG TC**C G GTT A	5'
-411*	5'	CCG GA**T Taa CTG GCG GCC GC**G	3'
	3'	CT**A Att GAC CGC CGG CG**C CGC G	5'
-794*	5'	GCC CC**T aaG CTG GTG GCC A**	3'
	3'	GG**A ttC GAC CAC CGG TG**A CAC	5'
NFI	5'	ATT **TTG GCT TGA AGC CAA** TAT G	3'
	3'	TAA **AAC CGA ACT TCG GTT** ATA C	5'

Figure 3-1: NFI binding sequences upstream of the *HEY1* transcription start site. (A) Consensus NFI binding site, and putative NFI binding sequences identified upstream of the *HEY1* transcription start site (+1). (B) Primers used to generate oligonucleotides for the electrophoretic mobility shift assays, with putative NFI binding sequences in bold. The third and fourth residues in the NFI binding sequences were mutated from GG→AA (* denotes mutated NFI binding site). These residues are critical for NFI binding.

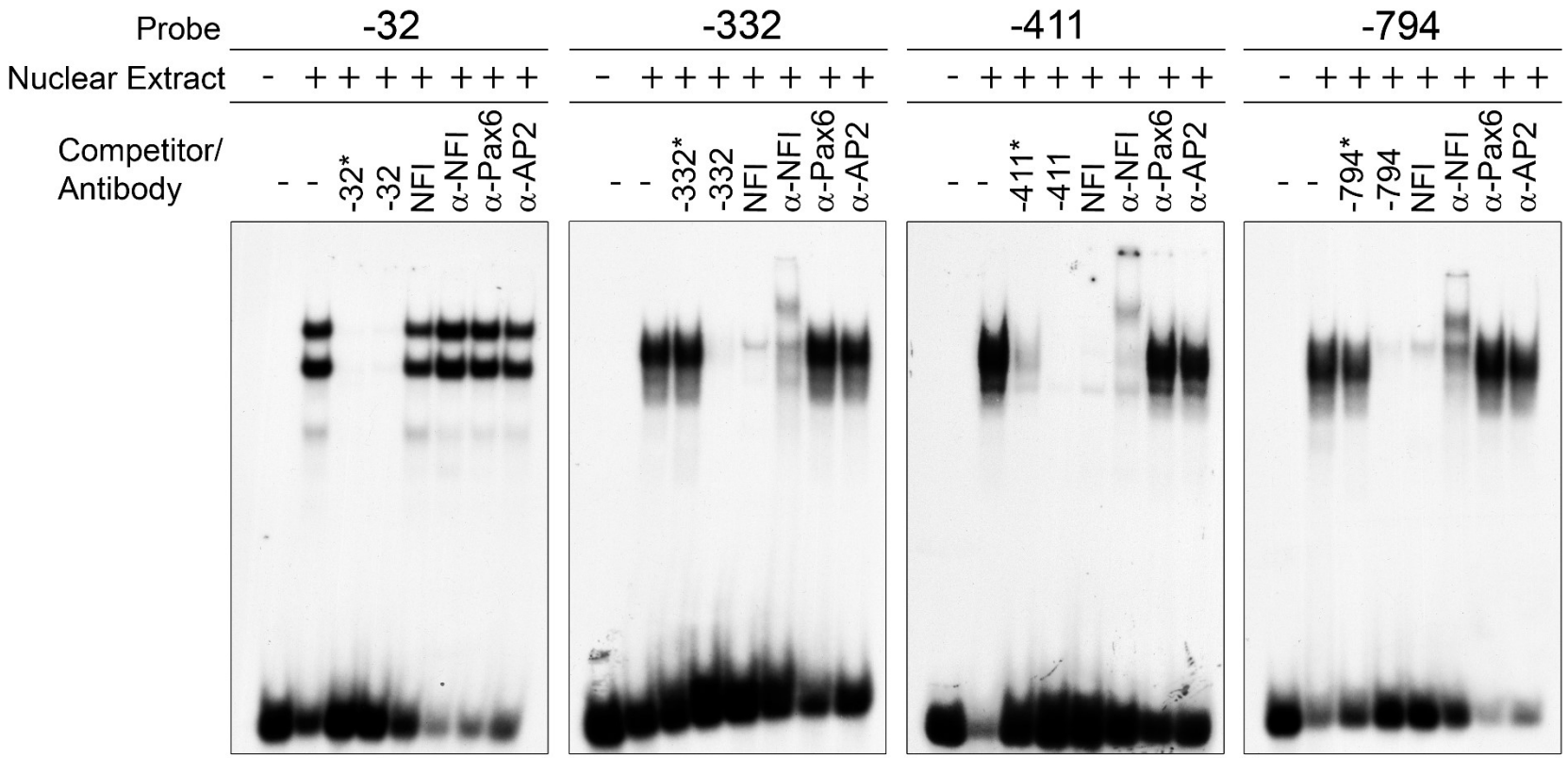
Probe
-32
-332
-411
-794
Nuclear Extract
- + + + + + + +
Competitor/
Antibody
- - -32* -32 NFI α-NFI α-Pax6 α-AP2
- - -332* -332 NFI α-NFI α-Pax6 α-AP2
- - -411* -411 NFI α-NFI α-Pax6 α-AP2
- - -794* -794 NFI α-NFI α-Pax6 α-AP2

Figure 3-2: Binding of NFI to putative NFI binding sequences in the *HEY1* promoter. Electrophoretic mobility shift assays were carried out by incubating radiolabeled probes -32 bp, -332 bp, -411 bp, and -794 bp, with 2 µg U251 MG nuclear extracts. DNA-protein complexes were electrophoresed through a 6% polyacrylamide gel buffered in 0.5 X TBE. Where indicated, a 100X molar excess of competitors (* denotes mutated NFI binding site) were added to the binding reaction. Where indicated, antibodies (1 µL) to NFI (α-NFI), Pax6 (α-Pax6), and AP2 (α-AP2) were added immediately before the radiolabeled probes.

supershifted band for the -332 bp, -411 bp and -794 bp probes, but not the -32 bp probe. Addition of anti-Pax6 or anti-AP2 antibodies did not produce supershifted bands for any of the probes, or decreased intensity of DNA-protein complexes. The relatively weak intensity of the supershifted bands observed with the anti-NFI antibody, combined with the significant decrease in intensity of the DNA-protein complexes, suggests that the anti-NFI antibody impedes binding of NFI to these probes.

To identify which NFIs are able to bind to NFI recognition motifs upstream of the *HEY1* transcription start site, we examined binding of NFIA, NFIB, NFIC, and NFIX to the -32 bp, -332 bp, -411 bp and -794 bp oligonucleotides. U251 MG cells were transfected with pCH (empty vector), HA-NFIA, HA-NFIB, HA-NFIC, or HA-NFIX expression constructs. Nuclear extracts were prepared, and expression of NFIs analyzed by western blot. HA-NFIs are highly overexpressed (>5-fold higher than endogenous levels, data not shown), with expression of NFIC was the highest, followed by NFIX, NFIA, and NFIB (Figure 3-3A). To account for differences in exogenous NFI expression levels, we incubated 1 μg of NFIC nuclear extract, 2 μg NFIX nuclear extract, 3 μg NFIA nuclear extract, and 4 μg of NFIB nuclear extract with radiolabeled -32 bp, -332 bp, -411 bp, and -794 bp oligonucleotides. No DNA-protein complexes were observed with the -32 bp oligonucleotide with nuclear extracts from pCH or HA-NFI transfected cells. This is in contrast to Figure 3-2, and is due to the different methods used for preparing nuclear extracts from cells expressing endogenous versus ectopic NFI. The absence of DNA-complex formation upon NFI overexpression indicates that NFIs

are not binding to this region. However, NFIA, NFIB, NFIC, and NFIX all formed complexes with the -332 bp, -411 bp, and -794 bp oligonucleotides (Figure 3-3B).

One strong band and at least three weaker bands were observed when nuclear extracts prepared from HA-NFIA-transfected cells were incubated with either the -332 bp or -794 bp probe. Only weak bands were observed when these same extracts were incubated with the -411 bp probe. Nuclear extracts prepared from HA-NFIB-transfected cells generated two bands of varying intensities, with strong, moderate and weak signal intensities for the -332 bp, -794 bp and -411 bp probes, respectively. Interestingly, bands of similar intensities were observed when nuclear extracts prepared from HA-NFIX-transfected cells were incubated with the probes. Results with HA-NFIC nuclear extracts were similar to those described for HA-NFIA and HA-NFIB except that somewhat stronger relative signals were observed for the -794 bp and -411 bp probes. Taken together, these results indicate that all four NFIs can bind, albeit with different affinities, to the -332 bp, -411 bp and -794 bp probes, with NFIA and NFIB showing preference for the -332 bp probe, NFIX showing no preference for any of the three probes and NFIC showing preference for the -332 bp and -794 bp probes.

3.3.3 Expression of *HEY1* in MG cell lines

HEY1 is expressed in the developing CNS and in MG tumours (Hulleman et al., 2009; Sakamoto et al., 2003). We used qPCR to examine levels of *HEY1* mRNA in a panel of 10 MG cell lines using U251 MG as our reference cell line (Figure 3-4). mRNA levels were lowest in A172, CLA, U87 and T98 MG cells, with

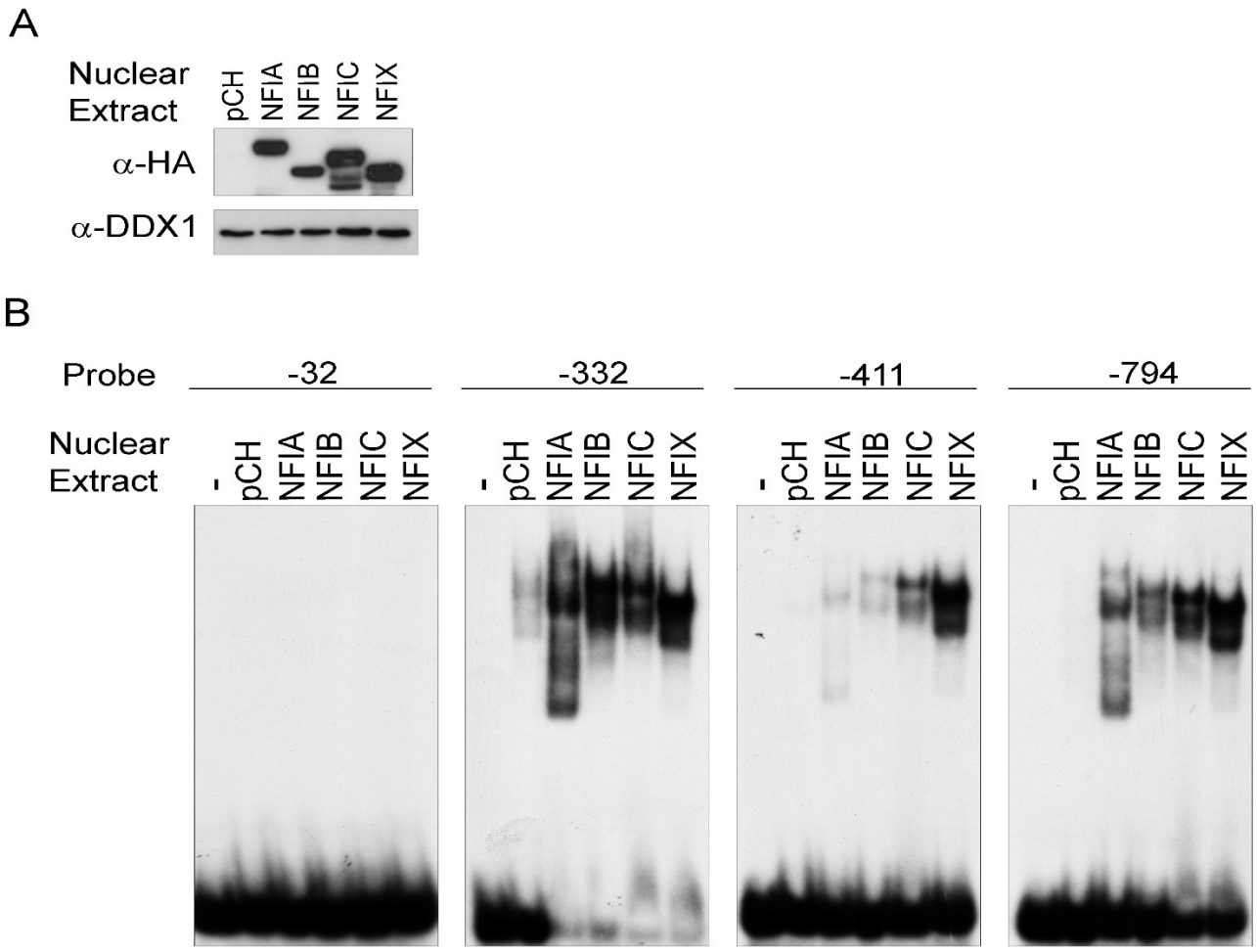
A
Nuclear Extract
pCH
NFIA
NFIB
NFIC
NFIX
α-HA
α-DDX1
B
Probe
-32
-332
-411
-794
Nuclear Extract
-
pCH
NFIA
NFIB
NFIC
NFIX

Figure 3-3: Binding of NFIA, NFIB, NFIC, and NFIX to NFI binding sites in the *HEY1* promoter. Nuclear extracts were prepared from U251 MG cells transfected with control (pCH), NFIA (pCH-NFIA), NFIB (pCH-NFIB), NFIC (pCH-NFIC), or NFIX (pCH-NFIX) expression constructs. (A) Western blot analysis of transfected cells. Nuclear extracts (20 µg) were electrophoresed through an 8% polyacrylamide-SDS gel, electroblotted onto PVDF (polyvinylidene fluoride) membranes, and immunostained with α-HA antibody or α-DDX1 antibody. (B) Electrophoretic mobility shift assays were performed with the indicated radiolabeled probes: -32 bp, -332 bp, -411 bp and -794 bp. Probes were incubated with the indicated nuclear extracts (2 µg pCH, 3 µg NFIA, 4 µg NFIB, 1 µg NFIC, and 2 µg NFIX). Amounts of protein were adjusted to compensate for differences in expression of transfected HA-NFIs. DNA-protein complexes were electrophoresed through a 6% polyacrylamide gel buffered in 0.5X TBE.

highest levels observed in M016, M049 and M103 MG cells (6.2 to 8.4-fold higher than U251 MG cells). *HEY1* mRNA levels in U373 MG cells were 3.4-fold higher than U251 cells.

3.3.4 NFI regulates endogenous *HEY1* expression in MG cells

To investigate a possible relationship between NFI and HEY1, we examined changes in *HEY1* mRNA levels in U251 MG cells following transfection with control (scrambled) siRNA, or siRNAs targeting specific NFIs, alone or in combination. Where noted, cells were transfected a second time before analysis. The NFI siRNAs used in this analysis have been previously validated (Chapter 2), with *NFIA, NFIB, NFIC,* and *NFIX* mRNA levels decreased by 75-93% after one round of siRNA transfection (Figure 3-5A). As previously reported, we see compensation between NFIs (Chapter 2), with knockdown of NFIA resulting in a 1.7-fold increase in *NFIX* mRNA, and knockdown of NFIX increasing levels of *NFIC* mRNA by 1.4-fold. After two rounds of combined NFIA and NFIB siRNA transfection, there was a 2.4 fold increase in *NFIC* mRNA and a 1.8 fold increase in *NFIX* mRNA.

Endogenous levels of *HEY1* mRNA were decreased slightly upon knockdown of single NFIs; however, upon knockdown of combinations of NFIs, a dramatic increase in *HEY1* expression was observed, with knockdown of NFIC and NFIX increasing *HEY1* expression 1.7-fold, and knockdown of all four NFIs resulting in 2.4-fold increase in *HEY1* (Figure 3-5B). *HEY1* expression increased to an even greater extent with a second round of transfection, with 2.8-fold, 4.1-fold, and 4.6-fold increases upon knockdown of NFIA/NFIB, NFIC/NFIX, and all four NFIs, respectively. These data suggest that the NFI family in concert

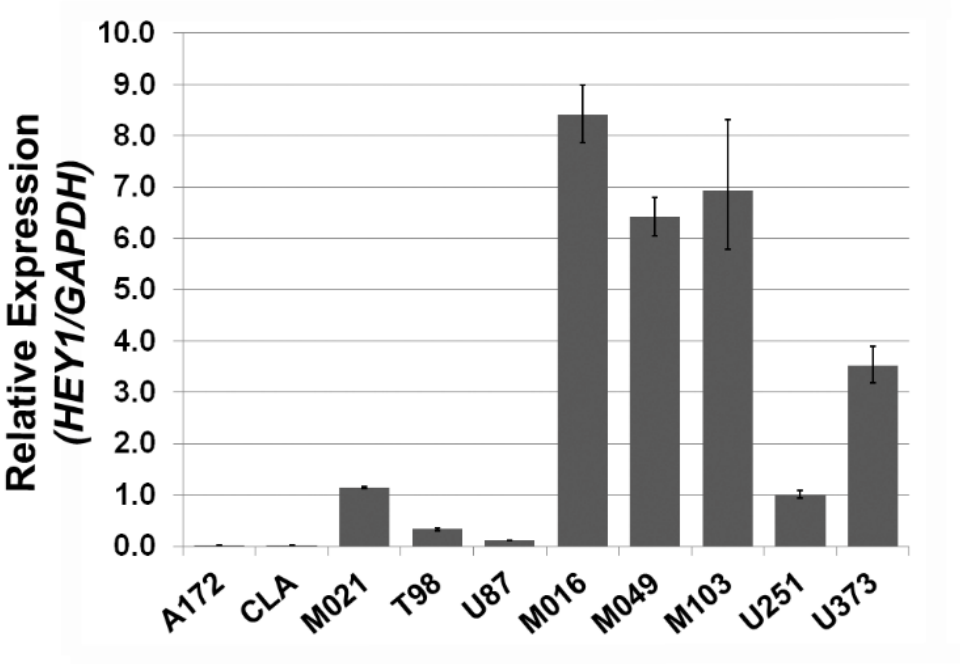

Figure 3-4: Expression of *HEY1* in MG cell lines. *HEY1* expression in a panel of 10 MG cell lines was analyzed by qPCR. *GAPDH* was used as the endogenous control. All values shown are in relation to U251 (set to 1). Standard deviation is indicated by error bars.

represses *HEY1* transcription. We were unable to examine whether HEY1 protein levels were increased concomitant with *HEY1* mRNA levels as we were unable to find an antibody suitable for western blotting.

3.3.5 NFI regulates *HEY1* promoter activity

We used the luciferase reporter gene under the control of the *HEY1* promoter to investigate the effect of NFI on transcriptional activity. U251 MG cells were transfected with siRNA to knockdown single and combined NFIs, followed by transfection with pGL3/HEY1, containing -915 to +15 bp of the *HEY1* promoter upstream of the firefly luciferase reporter gene. Knockdown of NFIA did not affect *HEY1* transcriptional activity based on the luciferase assay (Figure 3-5C). However, transcriptional activity was significantly increased following knockdown of NFIB (3.1-fold), NFIC (6.1-fold) and NFIX (1.6-fold), suggesting that these three NFIs repress transcription from the *HEY1* promoter. Unexpectedly, when NFIA and NFIB were depleted in combination, transcriptional activity decreased 1.6-fold. Knockdown of combined NFIC and NFIX together resulted in a modest 1.5-fold increase in transcriptional activity, less than either NFIC or NFIX alone. Knockdown of all four NFIs increased transcriptional activity 5.6-fold compared to control (scrambled) siRNA.

As mentioned previously, knockdown of combined NFIA and NFIB increases *NFIC* and *NFIX* mRNA levels. This observation may explain why *HEY1* transcriptional activity is decreased upon NFIA and NFIB depletion. Furthermore, the biggest increase in *HEY1* transcriptional activity was observed upon NFIC

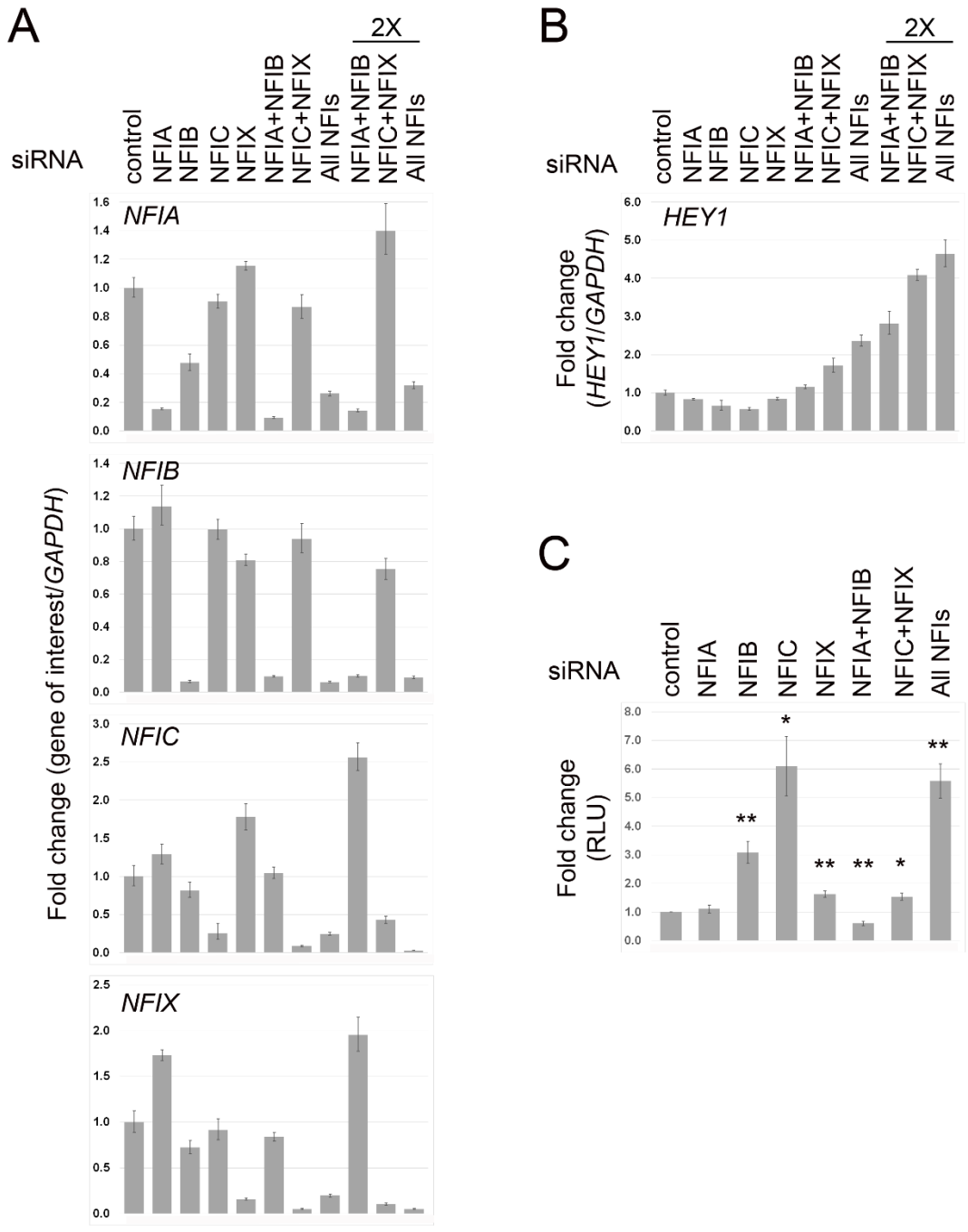
A
2X
siRNA
control
NFIA
NFIB
NFIC
NFIX
NFIA+NFIB
NFIC+NFIX
All NFIs
NFIA+NFIB
NFIC+NFIX
All NFIs
Fold change (gene of interest/GAPDH)
NFIA
NFIB
NFIC
NFIX
B
2X
siRNA
control
NFIA
NFIB
NFIC
NFIX
NFIA+NFIB
NFIC+NFIX
All NFIs
NFIA+NFIB
NFIC+NFIX
All NFIs
Fold change (HEY1/GAPDH)
HEY1
C
siRNA
control
NFIA
NFIB
NFIC
NFIX
NFIA+NFIB
NFIC+NFIX
All NFIs
Fold change (RLU)

Figure 3-5: Regulation of *HEY1* promoter activity by NFI. U251 MG cells were transfected with 10 nM siRNAs, including control (scrambled), *NFIA, NFIB, NFIC, NFIX*, or combinations of NFI siRNAs. Where indicated, cells underwent two rounds of siRNA transfection. (A) *NFIA, NFIB, NFIC, NFIX* and (B) *HEY1* mRNA expression was analyzed by qPCR. *GAPDH* was used as an endogenous control. Similar data were obtained in two separate experiments. (C) U251 MG cells were transfected with 10 nM siRNAs, including control (scrambled), *NFIA, NFIB, NFIC, NFIX*, or combinations of NFI siRNAs, followed 24 h later by transfection with pGL3/HEY1. Cells were harvested 60 h later, and luciferase activity quantified. Changes in RLU (relative light units) are relative to RLU obtained in U251 MG cells transfected with control (scrambled) siRNA and pGL3/HEY1. The data are from three experiments. S.E.M. is indicated by error bars. Statistical significance, determined using the unpaired *t* test, is indicated by * $p<0.05$ and ** $p<0.01$.

knockdown, with a similar effect seen upon knockdown of all four NFIs, these results suggest that NFIC may be a key player in the repression of *HEY1* promoter activity. Although the activity from the *HEY1* promoter upon NFI knockdown does not appear to mirror the changes in endogenous *HEY1* expression observed upon NFI knockdown (Figure 3-5B), there are some similarities. For example, both endogenous *HEY1* expression and *HEY1* promoter (luciferase) activity were increased upon knockdown of combined NFIC/NFIX and combined NFIA/NFIB/NFIC/NFIX.

We further analyzed the role of NFI in regulating the activity of the *HEY1* promoter by mutating NFI binding sites in the *HEY1* promoter (Figure 3-6A). When the *HEY1* upstream region was cloned upstream of the luciferase gene (pGL3/HEY1), transcriptional activity increases 4.3-fold compared to pGL3-Basic (Figure 3-6B). Mutation of H-br3 (-794) (pGL3/HEY1 H-br3*) did not significantly alter transcriptional activity compared to the wild-type construct (pGL3/HEY1); however, mutation of H-br1 (-332) (pGL3/HEY1 H-br1*) decreased transcriptional activity 2.5-fold. Combined mutation of H-br1* and H-br3* (pGL3/HEY1 Hbr1*/3*) reduced transcriptional activity to background (pGL3-Basic), suggesting that these NFI binding sites, especially H-br1* are important for *HEY1* transcriptional regulation. Mutation of H-br2 is currently underway.

To investigate which NFIs target H-br1 and H-br3, we transfected the mutated pGL3/HEY1 constructs into U251 MG cells following NFI siRNA transfection. The changes in transcriptional activity of these mutated constructs upon knowdown of NFI was remarkably similar to that of the wild-type construct

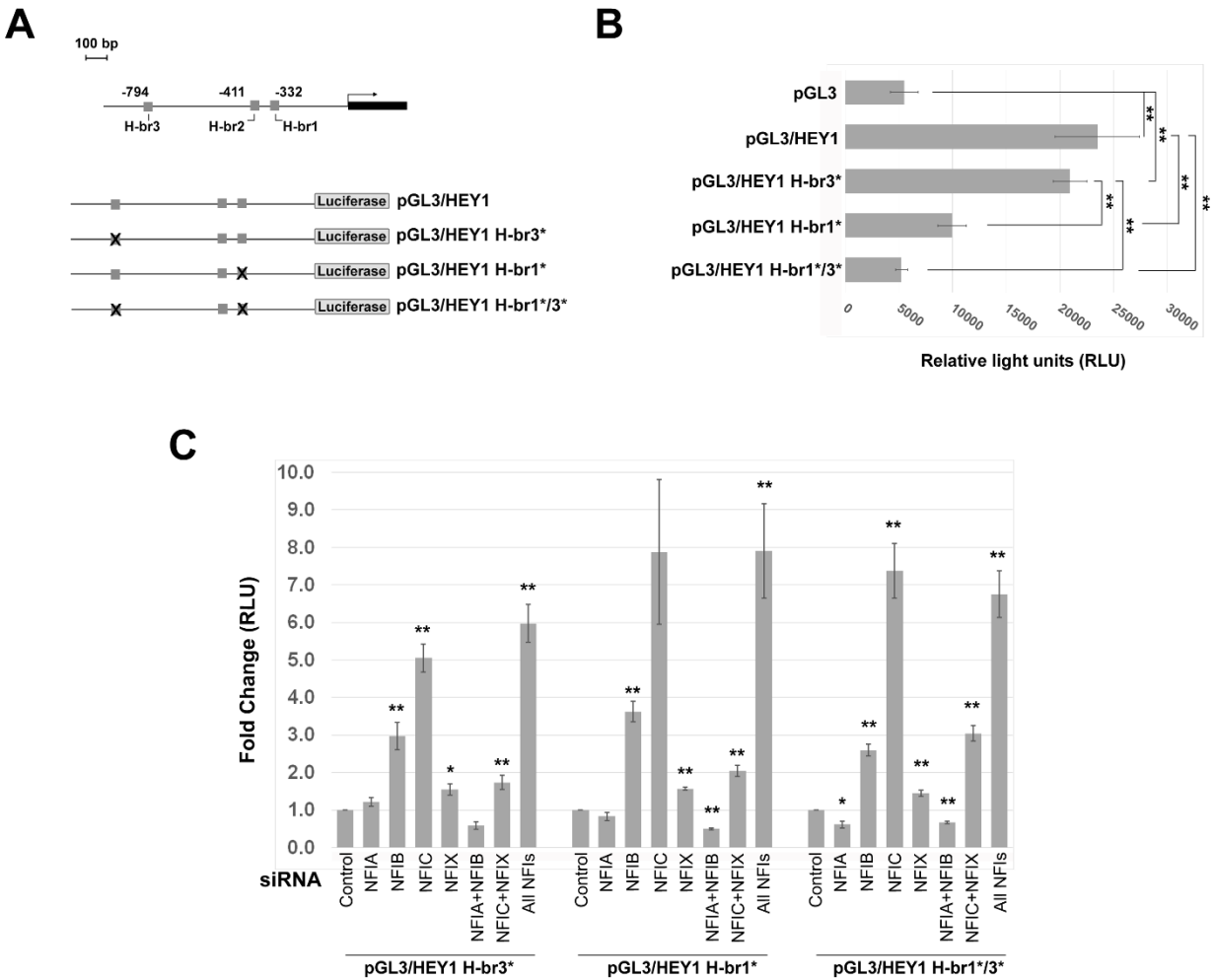
A
100 bp
-794
-411
-332
H-br3
H-br2
H-br1
Luciferase pGL3/HEY1
Luciferase pGL3/HEY1 H-br3*
Luciferase pGL3/HEY1 H-br1*
Luciferase pGL3/HEY1 H-br1*/3*
B
pGL3
pGL3/HEY1
pGL3/HEY1 H-br3*
pGL3/HEY1 H-br1*
pGL3/HEY1 H-br1*/3*
0
5000
10000
15000
20000
25000
30000
Relative light units (RLU)
C
Fold Change (RLU)
siRNA
Control
NFIA
NFIB
NFIC
NFIX
NFIA+NFIB
NFIC+NFIX
All NFIs
pGL3/HEY1 H-br3*
pGL3/HEY1 H-br1*
pGL3/HEY1 H-br1*/3*

Figure 3-6: Mutational analysis of NFI binding sites in the *HEY1* promoter. (A) Schematic representation of the region upstream of the *HEY1* transcription start site (+1) (shown by arrow) with locations of NFI binding sites denoted. Constructs containing NFI binding sites with conserved GG residues mutated to AA to abolish NFI binding sites are shown. (B) Luciferase activity in RLU (relative light units) in U251 MG cells transfected with constructs shown in (A), or pGL3-Basic (no enhancer or promoter). (C) U251 MG cells were transfected with 10 nM control (scrambled), *NFIA, NFIB, NFIC, NFIX*, or combinations of NFI siRNAs, followed 24 h later by transfection with the indicated pGL3 constructs. Cells were harvested 60 h later, and luciferase activity quantified. Changes in RLU are relative to RLU obtained in U251 MG cells transfected with control (scrambled) siRNA and the indicated pGL3 constructs. The data are from three experiments. SEM is indicated by error bars. Statistical significance for (B) was determined by ANOVA analysis; * $p<0.05$ and ** $p<0.01$. Statistical significance for (C) was determined using the unpaired *t* test; * $p<0.05$ and ** $p<0.01$.

(compare Figures 3-5C and 3-6C). In fact, the changes in luciferase activity of the H-br1 mutant and H-br1/H-br3 double mutant constructs were as high if not higher than the wild-type constructs upon knockdown of combined NFIC and NFIX. Thus, binding of NFIC and NFIX to H-br1 may promote rather than repress *HEY1* expression, suggesting that the increase in *HEY1* promoter activity observed upon knockdown of NFIC and NFIX may be mediated through H-br2 or require H-br2.

3.3.6 HEY1 modulates expression of glial genes

In the developing brain, HEY1 is required for the maintenance of neural precursor cells (Sakamoto et al., 2003). Furthermore, Notch signaling has previously been shown to activate expression of NFIA during gliogenesis (Namihira et al., 2009). Here, we investigate the effect of modulating HEY1 levels on the expression of genes associated with glial cell differentiation. We transfected U87, U251 and M049 MG cells with siRNAs targeting *HEY1* and used qPCR to examine levels of *HEY1*, *B-FABP*, *GFAP*, *NES* (nestin), *NFIA*, *NFIB*, *NFIC*, *NFIX* mRNA. U87, U251, and M049 MG cell lines were used for these analyses as they express low, medium, and high levels of *HEY1*, respectively (Figure 3-4). *HEY1* expression was decreased by 88-94% in cells transfected with *HEY1* siRNA compared to control (scrambled) siRNA (Figure 3-7).

The levels of *B-FABP* and *GFAP* mRNA, which are barely detectable in U87 cells, were relatively unchanged in these cells. Although *B-FABP* mRNA levels did not change in U251 MG cells, there was a 2.1 fold increase in M049 MG cells. *GFAP* mRNA levels increased 1.8- and 2.0-fold in U251 and M049 MG cells,

respectively. Slight changes in *NES* expression were observed in U87, U251 and M049 MG cells. Of the four NFIs, *NFIB* mRNA levels were the most consistently altered, decreasing between 2.5 to 3.3-fold in all three MG cell lines. *NFIC* mRNA levels were also reduced in U87 (decreased 2-fold) and M049 (decreased 2.9 fold) MG cells. There was considerable variation in *NFIX* mRNA levels.

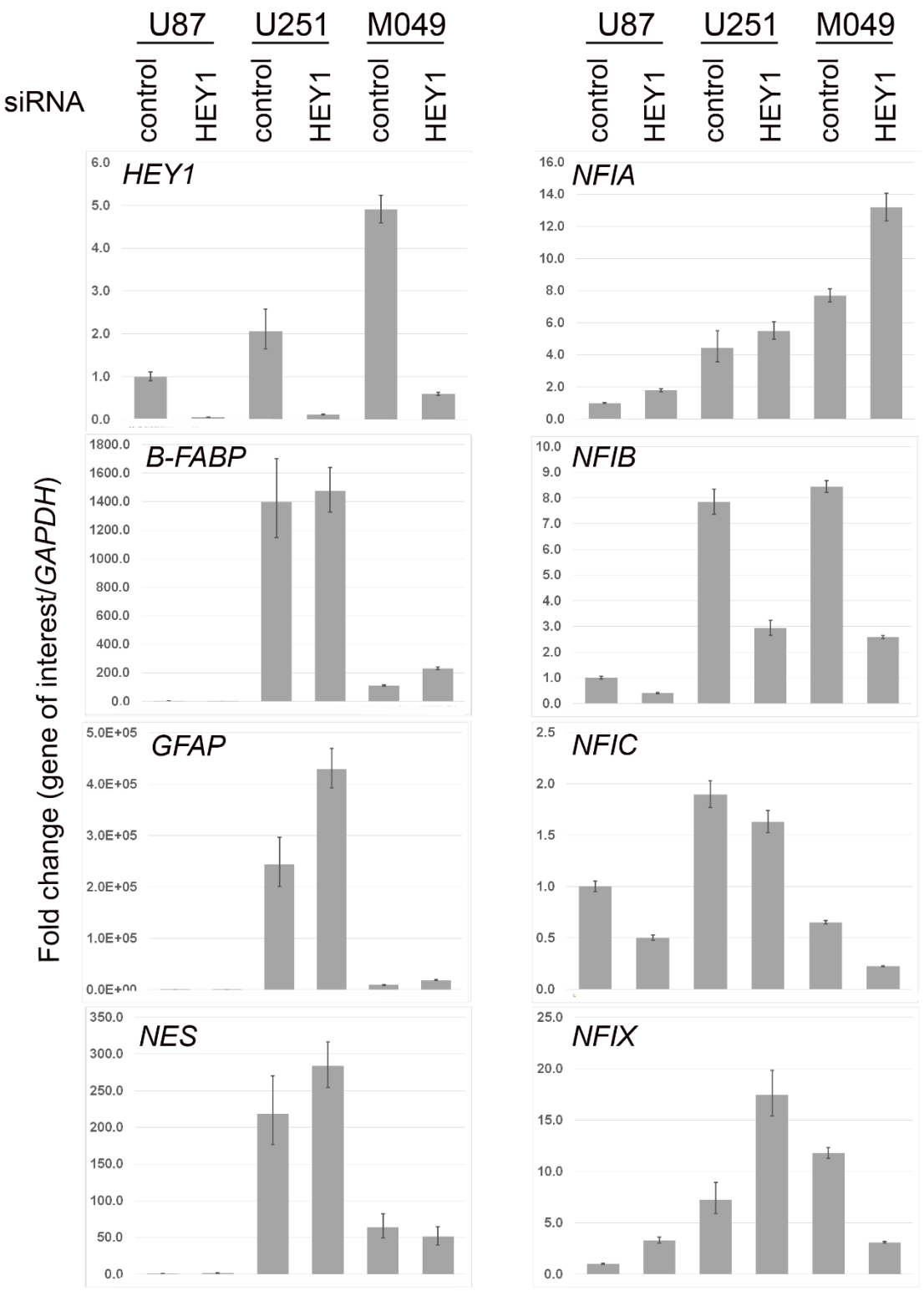
U87
U251
M049
U87
U251
M049
siRNA
control
HEY1
control
HEY1
control
HEY1
control
HEY1
control
HEY1
control
HEY1
Fold change (gene of interest/GAPDH)
HEY1
NFIA
B-FABP
NFIB
GFAP
NFIC
NES
NFIX

Figure 3-7: Knockdown of *HEY1* alters mRNA expression of glial genes. U87, U251, and M049 MG cells were transfected with 10 nM control (scrambled) siRNA, or two different siRNAs targeting *HEY1,* and harvested 60 h later. qPCR was used to analyze *HEY1, B-FABP, GFAP, NES, NFIA, NFIB, NFIC* and *NFIX* mRNA levels. *GAPDH* served as an endogenous control. RNA levels are expressed as fold-change compared to U87 control (scrambled). Error bars denote standard deviation of samples run in triplicate. Similar data were obtained in a duplicate experiment.

3.4. Discussion

The NFI family is an important regulator of glial cell differentiation during development (Deneen et al., 2006), as well as a regulator of the glial genes *B-FABP* and *GFAP* in MG cell lines (Chapter 2) (Bisgrove et al., 2000). B-FABP is normally expressed in radial glial cells and immature astrocytes in the developing brain (Feng et al., 1994; Kurtz et al., 1994), whereas GFAP is expressed in astrocytes (Eng, 1985). Radial glial cells act as neural stem cells during development, giving rise to both neurons and glial cells in the developing brain (Anthony et al., 2004). Radial glial cells also give rise to GFAP-expressing astrocytes in the subventricular zone, and these astrocytes act as adult neural stem cells (Merkle et al., 2004). Here, we identify additional NFI target genes in MG using ChIP-on-chip analysis of a human promoter array containing the promoters regions of 17 000 genes, with 403 genes found to be enriched following chromatin immunoprecipitation with a pan-specific α-NFI antibody. Gene ontology analysis of putative NFI target genes identified enrichment of genes involved in multiple biological processes including gene expression, development and differentiation, and, of particular interest, genes involved in nervous system development.

One of the 403 genes identified by Chip-on-chip was the Notch effector gene *HEY1*. The HEY family consists of three basic helix-loop-helix (bHLH) proteins (HEY1, HEY2, and HEYL) closely related to the HES family of transcriptional repressors (Nakagawa et al., 1999). Hey1 is expressed in the developing mouse brain in undifferentiated cells (Sakamoto et al., 2003).

Misexpression of Hey1 in the developing mouse brain inhibits neurogenesis and promotes maintenance of undifferentiated cells, resulting in increased production of astrocytes following the onset of gliogenesis (Sakamoto et al., 2003). Promoter assays indicate that Hey1 acts by inhibiting the neuronal bHLH genes *Ascl1* (also known as *Mash1*) and *Neurod4* (also known as *Math3*) (Sakamoto et al., 2003).

We identified four putative NFI binding sites within a 1000 bp region immediately upstream of the *HEY1* transcription start site. Electrophoretic mobility shift assays revealed NFI binding to three of these four putative sites, at -794 bp, -411 bp, and -332 bp. Although multiple protein-DNA complexes were obtained with the putative NFI binding site at -32 bp, these complexes were competed out with excess mutated cold oligonucleotide that should no longer bind NFIs. Furthermore, the consensus NFI binding site was unable to compete for binding, and anti-NFI antibody failed to supershift any of the DNA-protein complexes, providing strong evidence for interaction with transcription factor(s) other than NFI. Using nuclear extracts enriched for each of the four NFIs, we observed differential binding to the three NFI binding sites, at -332 bp, -411 bp and -794 bp. Of note, the NFI binding site at -332 bp (H-br1) was bound strongly by all four NFIs based on the gel shift assay. NFIC and NFIX bound with greater relative affinity than NFIA and NFIB to the NFI binding sites at -411 bp (H-br2) and -794 bp (H-br3). Differential binding by different NFI family members *in vitro* has been previously reported (Chapter 2) (Mukhopadhyay et al., 2001; Osada et al., 1999).

Changes in *HEY1* promoter activity upon single or combined knockdown of NFIs suggest complex regulation and cross-talk between NFI family members.

While knockdown of NFIA had little effect on *HEY1* promoter activity, NFIB knockdown increased *HEY1* promoter activity, and knockdown of combined NFIA and NFIB decreased promoter activity. Similarly, whereas knockdown of either NFIC or NFIX increased promoter activity by 6.1-fold and 1.6-fold, respectively, combined knockdown of NFIC and NFIX only increased promoter activity by 1.5-fold. There is considerable variability in the transactivation domain of NFI family members, and NFIs can bind DNA as both heterodimers and homodimers (Gronostajski, 2000; Kruse and Sippel, 1994b). The transactivation potential of heterodimers has previously been reported to be the intermediate of NFIs as homodimers (Chaudhry et al., 1998). Thus, knockdown of single and combinations of NFIs may alter the dynamics of NFI dimerization in the cell.

As knockdown of NFIA doesn't alter *HEY1* promoter activity, this suggests that NFIA/NFIA, NFIA/NFIB, NFIA/NFIC, and NFIA/NFIX dimers are not important in activation or repression of transcriptional activity. In contrast, as loss of NFIB represses promoter activity, NFIB/NFIB, NFIB/NFIC, and NFIB/NFIX combinations may all repress promoter activity. The fact that knockdown of NFIC increases *HEY1* promoter activity to the greatest extent suggests that at least one dimer containing NFIC (NFIB/NFIC, NFIC/NFIC and/or NFIC/NFIX) strongly contributes to transcriptional repression. Our data indicate that knockdown of both NFIA and NFIB in U251 MG cells results in increased *NFIC* expression. Increased NFIC may in turn increase the relative population of dimers containing NFIC, leading to the decrease in promoter activity seen under these conditions. Knockdown of NFIX slightly increases promoter activity, suggesting that dimers containing NFIX

(NFIB/NFIX, NFIC/NFIX, and NFIX/NFIX) weakly repress transcription from the *HEY1* promoter. Thus, the modest increase in promoter activity observed upon combined knockdown of NFIC and NFIX may be due to the fact that NFIA/NFIA, NFIA/NFIB and NFIB/NFIB dimers are preferentially formed under these conditions, with concomitant decrease in the relative levels of repressive NFIB/NFIC and NFIC/NFIC dimers.

We also examined changes in endogenous *HEY1* mRNA expression upon NFI modulation. Upon knockdown of all four NFIs, both *HEY1* promoter activity and endogenous expression were markedly increased, demonstrating negative regulation of *HEY1* expression by NFI. This agrees with previous studies reporting upregulation of *Hey1*, along with other members of the Notch signaling pathway in the brains of *Nfib-/-* mice (Betancourt et al., 2014). In contrast to knockdown of all four NFIs, knockdown of single NFIs resulted in a decrease in endogenous *HEY1* expression, but promoter activity was unchanged upon NFIA knockdown, and increased upon knockdown of NFIB, NFIC and NFIX. Combined NFIA and NFIB depletion increased endogenous *HEY1* expression, but decreased *HEY1* promoter activity, even though knockdown of NFIA alone did not alter promoter activity, and NFIB alone increased. These results suggest compensatory mechanisms perhaps by other members of the NFI family in the context of the endogenous promoter. Differences in regulation of NFI-dependent promoter activity in an endogenous or chromosomal context versus ectopic context have previously been reported. This has been observed for regulation of *B-FABP* and *GFAP* expression, as well as regulation of the MMTV promoter (Chapter 2) (Archer et al., 1992).

Based on our results, it appears that the multiple NFI binding sites in the *HEY1* promoter may act in opposing manners to fine tune expression. Mutation of H-br3 does not alter promoter activity compared to the wild-type promoter, while mutation of H-br1 significantly decreases *HEY1* promoter activity (Figure 3-6A). This contrasts to the repressive role of NFIs on *HEY1* expression revealed both endogenously and by reporter gene assay. The decrease in promoter activity upon abolishing the H-br1 binding site demonstrates that this site positively regulates *HEY1* expression. Also, even when both H-br1 and H-br3 NFI binding sites are mutated (pGL3/HEY1 Hbr1*/3*), and promoter activity is the same as pGL3-basic, this construct is still responsive to modulation of NFI, and responds to NFI knockdown in a very similar manner to the wild-type HEY1 promoter (Figure 3-5C and Figure 3-6C). This suggests that the H-br2 NFI binding site mediates NFI repression.

The opposing actions of these NFI binding sites may be facilitated by additional transactivating factors. It is unclear whether NFI binding to the *HEY1* promoter directly represses transcriptional activity, or whether NFI binding precludes binding and activation by additional transcription factors. For example, the H-br2 site at -411 to -396 bp is located 12 bp upstream of an RBP-Jκ binding site that mediates activation by Notch1 (Maier and Gessler, 2000), and 12 bp downstream of a putative SMAD binding site (Figure 3-8) (Woltje et al., 2015). Similar binding sites are not located in close vicinity to H-br1 (-332 bp) and H-br3 (-794 bp) NFI binding sites. SMADs mediate bone morphogenetic protein (BMP) signaling, and signaling through the BMP-SMAD axis shapes neuronal and glial

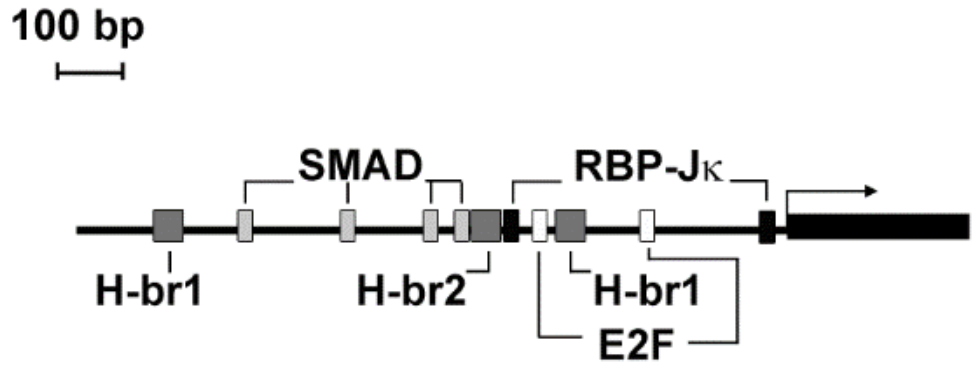

Figure 3-8: Schematic representation of the *HEY1* promoter.

differentiation (Hegarty et al., 2013). Notch and BMP-SMAD signaling cooperate to induce expression of HEY1 in endothelial cells, and myogenic progenitor cells (Dahlqvist et al., 2003; Larrivee et al., 2012). In myogenic progenitor cells, HEY1 binds to myogenic genes to repress expression and maintain cells in an undifferentiated state (Buas et al., 2010; Fukada et al., 2011). Thus, binding by NFI to H-br2 may repress HEY1 expression indirectly by blocking access to either the RBP-Jκ transcriptional activator complex, Smads, or both.

HEY1 expression in MG correlates with increased tumour grade and decreased survival, and knockdown of HEY1 in MG cell lines decreases proliferation (Hulleman et al., 2009). Here, we found that *HEY1* is differentially expressed in MG cells lines. siRNA targeting *HEY1* increased expression of the astrocyte marker GFAP in U251 and M049 MG cells, but not in U87 MG cells, which do not normally express GFAP. Combined with the role of HEY1 in the maintenance neural progenitor cells (Sakamoto et al., 2003), this suggests that expression of *HEY1* contributes to maintaining MG cells in a less differentiated state. Differentiation of tumour initiating cells in glioblastoma models has previously been reported to decrease tumourigenicity, and has been suggested as promising treatment strategy (Piccirillo et al., 2006; Zheng et al., 2008). To determine if HEY1 contributes to a less differentiated phenotype in MG cells, it will be useful to examine the expression of markers of neural progenitor cells, including nestin, Sox2, and CD133, within cells upon modulation of HEY. In the same cells, it will also be important to monitor changes in expression of markers of neural cell differentiation, and cellular proliferation. It has previously been shown that Notch

activation through inhibitor of differentiation 4 (Id4) results in hyperproliferation of Ink4a/Arf$^{-/-}$ astrocytes, and conversion of these astrocytes to a neural stem cell like state, including upregulation of *Hey1* expression (Jeon et al., 2008). These studies will clarify the contribution of HEY1 to maintaining an undifferentiated phenotype, and its role in regulating proliferation in MG cells. Within tumour tissue, it will also be valuable to examine if HEY1 expressing cells correlate with markers of neural progenitor cells and/or proliferation.

Expression of *NFIB* is markedly decreased at the mRNA level following *HEY1* knockdown. Downregulation of *NFIB* upon knockdown of *HEY1* has been observed previously in HEK293 cells, but as HEY1 acts as a transcriptional repressor this effect on NFI expression is likely not direct, but downstream of HEY1 target genes (Heisig et al., 2012). Little is known of the direct regulation of NFIB expression. In the developing CNS, *Nfia* expression, but not *Nfib,* is induced directly by Notch signaling (Namihira et al., 2009). NFIA expression in MG promotes tumour growth (Glasgow et al., 2013; Lee et al., 2014), however, the role of NFIB in MG has not been examined, although *Nfib-/-* mice have similar defects as *Nfia-/- mice* in gliogenesis (Steele-Perkins et al., 2005). Significantly, *Nfib-/-* mice have an increase in neural progenitor cells, and Nfib represses *Ezh2*, which contributes to preserving the undifferentiated state of neural progenitor cells, elucidating the role of NFIB in promoting differentiation. (Piper et al., 2014). This is in contrast to the role of HEY1 in promoting maintenance of progenitor cells (Sakamoto et al., 2003). It will be important to examine the expression of NFIB in

MG, to see if NFIB and HEY1 expression correlate, and to determine if NFIB, similar to NFIA, promotes tumour growth.

In summary, we show that the NFI transcription factor binds to the promoters of multiple genes, involved in many biological processes, in MG cells. We identify three NFI binding sites in the *HEY1* promoter, and show that NFI represses *HEY1* promoter activity and expression in MG cells. We demonstrate differential binding of the four members of the NFI family to the different NFI binding sites in the *HEY1* promoter. Our results indicate complex interactions between the different members of the NFI family and suggest that NFI dimerization, along with additional transcription factors, are involved in the regulation of the *HEY1* gene in MG.

Chapter 4

CALCINEURIN REGULATES NUCLEAR FACTOR I DEPHOSPHORYLATION AND ACTIVITY IN MALIGNANT GLIOMA CELL LINES

A version of this chapter has been published. Brun, M., Glubrecht, D.D., Baksh, S., Godbout, R. (2013). Calcineurin regulates nuclear factor I dephosphorylation and activity in malignant glioma cell lines, Journal of Biological Chemistry 288(33):24104-24115.

4.1 Introduction

Malignant gliomas (MG), comprising grades III and IV astrocytomas, are the most common adult brain tumours. These tumours have a dismal prognosis with a median survival of less than two years (Ohgaki and Kleihues, 2005a). MGs are highly infiltrative, resulting in recurrence despite aggressive treatment including surgical resection, radiotherapy, and chemotherapy (Mason et al., 2007). MGs have traditionally been hypothesized to arise from astrocytes as tumour cells express glial fibrillary acidic protein (GFAP), an intermediate filament protein expressed in differentiated astrocytes (Eng and Rubinstein, 1978). More recent findings suggest that these tumours may arise from less differentiated glial cell types (Mita et al., 2007; Sanai et al., 2005). MG tumours express brain fatty acid-binding protein (B-FABP) (Godbout et al., 1998), a marker of radial glial cells. Radial glial cells have been shown to have neural precursor cell properties as defined by the ability to self-renew and differentiate into glial and neuronal cells (Feng et al., 1994; Hansen et al., 2010; Kriegstein and Alvarez-Buylla, 2009; Kurtz et al., 1994; Merkle et al., 2004). B-FABP expression correlates with decreased survival in grade IV astrocytomas (De Rosa et al., 2012; Kaloshi et al., 2007; Liang et al., 2005) and B-FABP expression increases MG cell migration and is associated with sites of infiltration in MG tumours (Mita et al., 2010; Mita et al., 2007).

Expression of B-FABP and GFAP in MG cells is regulated by Nuclear Factor I (NFI) (Chapter 2) (Bisgrove et al., 2000). The NFI family of transcription factors consists of four genes: NFIA, NFIB, NFIC, NFIX, all of which can bind to the

consensus binding site 5'TTGGCN$_5$GCCAA 3' as a homodimer or heterodimer, to regulate target gene expression (Kruse and Sippel, 1994b; Roulet et al., 2000). While the N-terminal DNA-binding domain is highly conserved in all four NFIs, the C-terminal domain shows divergence among family members (Gronostajski, 2000). Our lab has demonstrated that specific NFIs have distinct effects on NFI-dependent promoter activity (Chapter 2). Furthermore, NFIs can either activate or repress transcription from NFI-dependent promoters, and regulation by NFI is both tissue- and promoter context-dependent (Chapter 2) (Gronostajski, 2000).

In addition to B-FABP and GFAP, NFI consensus binding sites have been identified in many brain-specific promoters (Amemiya et al., 1992), and NFIs have been shown to be regulators of glial cell differentiation (Deneen et al., 2006; Kang et al., 2012; Namihira et al., 2009). *Nfia-/-* and *Nfib-/-* mice exhibit agenesis of the corpus callosum, enlargement of lateral ventricles, and reduction of specific glial cell populations (das Neves et al., 1999a; Shu et al., 2003; Steele-Perkins et al., 2005). In addition, *Nfib-/-* mice have defects in lung maturation (Grunder et al., 2002; Steele-Perkins et al., 2005). *Nfix-/-* mice show enlargement of lateral ventricles and a host of skeletal defects (Driller et al., 2007). Unlike *Nfia, Nfib,* and *Nfix* knock-out mice*, Nfic-/-* mice have defects in tooth root development, but no apparent brain defects (Lee et al., 2009; Steele-Perkins et al., 2003). In the developing spinal cord, NFIA and NFIB control glial fate specification (Deneen et al., 2006). At early stages of development, both NFIA and NFIB are necessary for the maintenance of neural progenitor cells including radial glial cells. At later stages of development, NFIA regulates the migration and differentiation of these

precursor cells into astrocytes (Deneen et al., 2006). NFIA has also been shown to be critical for astrocyte differentiation of neural precursor cells in the developing brain (Namihira et al., 2009).

The *B-FABP* and *GFAP* promoters each contain three NFI consensus binding sites (Chapter 2) (Bisgrove et al., 2000; Cebolla and Vallejo, 2006). Based on chromatin immunoprecipitation (ChIP) and electrophoretic mobility shift assays, NFI binds to all three NFI consensus sites in both genes. In addition, we have shown that modulation of NFI expression alters *B-FABP* and *GFAP* promoter activity, as well as endogenous expression of B-FABP and GFAP in MG cell lines. Our data indicate that NFI is differentially phosphorylated in different MG cell lines and that NFI phosphorylation state correlates with expression of B-FABP and GFAP; i.e., NFI is hyperphosphorylated in MG cell lines that do not express B-FABP or GFAP and is hypophosphorylated in MG cell lines that express B-FABP and GFAP (Bisgrove et al., 2000). Intriguingly, this differential phosphorylation appears to be due to a phosphatase activity that is specifically present in MG cell lines with hypophosphorylated NFI (Bisgrove et al., 2000). Thus, regulation of NFI dephosphorylation may be vital to the control of neural/glial gene expression in MG.

Calcineurin is a calcium-dependent serine/threonine phosphatase (Klee et al., 1979) composed of two subunits: calcineurin A (CNA; PP2B), the catalytic subunit (Klee et al., 1979), and calcineurin B (CNB), a regulatory calcium binding subunit (Klee et al., 1988). Calcineurin plays a wide variety of biological functions, linking calcium signaling to multiple outputs ranging from immediate cellular

responses to long term alterations in gene expression (Aramburu et al., 2000; Shibasaki et al., 2002). In the brain, calcineurin is highly expressed, and plays important roles in synaptic plasticity (Baumgartel and Mansuy, 2012; Schwartz et al., 2009; Yakel, 1997). In developing cerebellar granule neurons, calcineurin signaling activates NFAT binding to NFI target genes, blocking NFI occupancy. As these neurons mature, binding of NFAT is temporally downregulated resulting in an increase in NFI binding to target genes (Ding et al., 2013). A more direct link between calcineurin and NFI comes from the observation that calcineurin is able to activate the transactivation domain of NFIC in fibroblasts (Alevizopoulos et al., 1997).

Here, we investigate the regulation of NFI dephosphorylation and activity in MG cell lines. We show that calcineurin regulates NFI dephosphorylation and activity in MG cell lines. In addition, we identify a cleaved form of CNA that is specific to MG cell lines with hypophosphorylated NFI. A similar truncated form of CNA has previously been shown to have increased phosphatase activity, suggesting that NFI dephosphorylation and activation is regulated by activated calcineurin in MG. The discovery of a novel regulatory mechanism for controlling the expression of neural and glial genes in MG opens up new avenues for controlling the growth properties of MG.

4.2 Experimental Procedures

4.2.1 Cell lines, constructs, chemicals, and transfections

The human MG cell lines have been previously described (Chapter 2) (Godbout et al., 1998). All cell lines were cultured in Dulbecco's modification of Eagle's minimum essential medium supplemented with 10% fetal calf serum, penicillin (100 U/mL), and streptomycin (100 µg/mL). Cyclosporin A (CsA) was obtained from Sigma-Aldrich, and ionomycin from Fisher Scientific. The pCAT/GFAP reporter construct contains -1708 to +8 bp of the *GFAP* promoter cloned into the pCAT basic vector. The pCAT/GFAP G-br1*, pCAT/GFAP G-br2*, pCAT/GFAP G-br3* and pCAT/GFAP G-br1*/G-br2*/G-br3* reporter constructs contain mutations disrupting one or all three NFI binding sites (Chapter 2). The HA-tagged constitutively active CNA expression construct (CNA-CA) and catalytically inactive construct (CNA-IN) in pcDNA3 were obtained from Dr. R. Chen (School of Life Sciences, Xiamen University, China) and have previously been described (Chen et al., 2008). HA-DDX1 cloned into pcDNA3 (Invitrogen) was used as a transfection control. The calpastatin expression vector was obtained from Dr. D. Jay (Cross Cancer Institute, Edmonton, Canada) (Garcia et al., 2006). U251 MG cells were transfected using polyethylenimine (PEI) (Polysciences Inc). U87 MG cells were transfected by calcium phosphate-mediated DNA precipitation. Cells were harvested 60 h post-transfection. Where indicated, cells were treated 24 h post-transfection with drugs, and harvested 24 h later. Chloramphenicol acetyltransferase (CAT) activity from pCAT (Promega) in lysates was measured

following the manufacturer's protocol. Acetylated [^{14}C]chloramphenicol was quantified in cpm using a scintillation counter.

4.2.2 Chromatin immunoprecipitation

ChIP was carried out as previously described (Chapter 2) (Pillai et al., 2009). Primers (Table 4-1) were designed to amplify regions of the *GFAP* and *B-FABP* promoters containing NFI binding sites. The *GAPDH* promoter was used as a negative control. A pan-specific anti-NFI antibody (Santa Cruz Biotechnology: Clone N-20, Cat. No. sc-870) and purified rabbit IgG (negative control) were used for immunoprecipitations.

4.2.3 Western blot analysis and phosphatase treatment

Whole cell extracts were prepared by lysing cells on ice for 20 min in 50 mM Tris-HCl pH 7.5, 150 mM NaCl, 0.5% sodium deoxycholate, 1% Nonidet P-40, 1X Complete protease inhibitor (Roche), 1 mM PMSF. Nuclear extracts were prepared by lysing purified nuclei. Briefly, 3 X 10^6 cells were resuspended in 200 µL nuclei isolation buffer (20 mM Tris-HCl pH 8.0, 150 mM NaCl, 1.5 mM $MgCl_2$, 0.2 mM $CaCl_2$, 250 mM sucrose, 0.1% Nonidet P-40, 1X Complete protease inhibitor, 1XZ PhoSTOP phosphatase inhibitor cocktail (Roche) and incubated on ice for 10 min. Nuclei were pelleted by centrifugation at 3200 x g for 10 min at 4ºC, washed once in nuclei isolation buffer (Andrin et al., 2012) and lysed in 200 µL RIPA buffer [50 mM Tris-HCl pH 8.0, 150 mM NaCl, 0.1% (w/v) SDS, 0.5% (w/v) sodium deoxycholate, 1% (v/v) Triton X-100] containing 1X Complete protease inhibitor

and 1X PhoSTOP. Chromatin was digested by addition of microccocal nuclease (New England Biolabs) and 1 µL 1 M $CaCl_2$. Protein extracts were electrophoresed in 10% polyacrylamide-SDS gels, and transferred to polyvinylidene fluoride (PVDF) membranes. Membranes were immunostained with mouse anti-CNA (BD Pharmigen: Cat. No. G182-1847) (1:10 000), rabbit anti-CNAα (Millipore: Cat. No 07-1492) (1:1000), rabbit anti-CNAβ (Millipore: Cat. No. 07-1493) (1:1000), rabbit anti-NFI (a gift from Dr. N Tanese, NYU Medical Center, NY) (1:1000), rabbit anti-DDX1 (Bleoo et al., 2001) (1:5000) and mouse anti-α-tubulin (12G10; Developmental Studies Hybridoma Bank) (1:100 000) antibodies. Primary antibodies were detected with horseradish-peroxidase-conjugated secondary antibodies (Jackson ImmunoResearch Biotech) using Immobilon (Millipore). For phosphatase treatment, nuclear extracts were prepared in the absence of 1x PhoSTOP, and incubated for 1 h at 37ºC in λ-phosphatase buffer (50 mM Tris-HCl pH 7.5, 100 mM NaCl, 0.1 mM EGTA, 2 mM dithiothreitol, 0.01% Brij 35, 2 mM $MnCl_2$) with or without 400 U λ-phosphatase (New England Biolabs).

4.2.4 Co-immunoprecipitations

Whole cell extracts were prepared as described above. For co-immunoprecipitations, 500 µg of U251 whole cell extracts were diluted in wash buffer [50 mM Tris-HCl pH 7.5, 150 mM NaCl, 0.25% sodium deoxycholate, 0.5% Nonidet P-40, 1X Complete protease inhibitor (Roche)], incubated with 2 µL anti-CNA antibody (BD Pharmigen: Cat. No. G182-1847) or 2 µg purified mouse IgG (negative control) for 3 h at 4ºC, and immunoprecipitated with protein G Sepharose

beads (GE healthcare). Immunoprecipitates were washed three times, and subjected to western blot analysis.

4.2.5 Calcineurin activity assay

Whole cell lysates were prepared by lysing cells in hypotonic lysis buffer (50 mM Tris-HCl pH 7.5, 0.1 mM EGTA, 1 mM EDTA, 0.5 mM DTT, 50 µg/mL PMSF, 50 µg/mL trypsin inhibitor, 10 µg/mL leupeptin, 10 µg/mL aprotinin) (Fruman et al., 1992). Calcineurin activity in extracts was measured using [γ-^{32}P]RII peptide substrate as previously described (Fruman et al., 1992).

4.2.6 Immunofluorescence analysis

Cells growing on coverslips were treated for 1 h with 10 µM ionomycin or DMSO (control), and fixed with 1% (U251 cells) or 2% (U87 cells) paraformaldehyde in phosphate-buffered saline for 10 min, followed by permeabilization in 0.5% Triton X-100 for 5 min. Cells were immunostained with mouse anti-CNA antibody (BD Pharmigen: Cat. No. G182-1847) (1:50-1:200), followed by Alexa 488-conjugated goat anti-mouse secondary antibody (1:200). Coverslips were mounted onto slides with polyvinylalcohol containing 1 µg/mL 4'6-diamidino-2-phenylindole (DAPI). Images were acquired with a 40X/1.3 oil immersion lens on a Zeiss LSM 710 confocal microscope.

4.2.7 Immunohistochemical analysis

Paraffin-embedded grade IV astrocytomas were obtained from the Brain Tumour Tissue Bank, London Health Sciences Centre, London (Canada). Tissues were de-waxed in xylene, and rehydrated in 100% ethanol. Slides were microwaved for 10 min in citraconic anhydride epitope retrieval buffer (pH 7.4), and blocked with 0.5% fish gelatin in Tris-buffered saline with 0.1% Tween 20. Slides were incubated in anti-CNA antibody (BD Pharmigen: Cat. No. G182-1847) (1:500) overnight at 4ºC, then washed and incubated with anti-mouse DakoCytomation Envision+System labelled polymer HRP (DakoCytomation, Denmark) for 1 h. CNA immunoreactivity was detected with Dako Liquid DAB+ Substrate Chromagen System, and counterstained with hematoxylin.

4.3 Results

4.3.1 In vivo occupancy of NFIs at endogenous promoters

B-FABP and GFAP expression correlates with NFI phosphorylation in MG cell lines. B-FABP and GFAP are expressed in MG cell lines that have hypophosphorylated NFIs, but not in cell lines that have hyperphosphorylated NFIs (Bisgrove et al., 2000). To compare NFI occupancy of the *GFAP* and *B-FABP* promoters in MG cells with hyperphosphorylated vs hypophosphorylated NFIs, we performed ChIP experiments using a pan-specific NFI antibody in B-FABP/GFAP+ve U251 (hypophosphorylated NFI) and B-FABP/GFAP-ve U87 (hyperphosphorylated NFI) MG cell lines (Bisgrove et al., 2000). DNA crosslinked to NFI was PCR amplified using primers flanking NFI binding sites in the *GFAP* and *B-FABP* promoters (Table 4-1 and Figure 4-1A). Bands corresponding to the NFI binding sites in the *GFAP* (G-br1, and G-br2/3) and *B-FABP* (B-br1/2/3) promoters were detected in samples from U251 cells, but not U87 cells (Figure 4-1B). No bands were detected using primers to the *GAPDH* promoter, or in the rabbit IgG lanes which served as the negative controls for the ChIP experiments. Input represents sonicated genomic DNA and thus serves as a positive control for the PCR reactions. These results indicate that NFI occupies NFI binding sites in U251 cells, but not in U87 cells.

4.3.2 CsA regulates NFI promoter binding and dephosphorylation

Our lab has previously shown by gel shifts and phosphatase inhibition experiments that there is a phosphatase activity in NFI-hypophosphorylated MG

Table 4-1: Sequences of primers used for ChIP analysis

Fragment	Forward Sequence (5'-3')	Reverse Sequence (5'-3')
G-br1	GTC CTC TTG CTT CAG CGG	TGG GCT AGA CTG GCG ATG
G-br2/3	CAG ACC TGG CAG CAT TGG	CTG CTC AAT GGG CTT CTC G
B-br1/2/3	CGA ACC TGA AAG CCC TTC T	GCT CCT GCC TTC TTA TTT GG
GAPDH	GAA CCA GCA CCG ATC ACC	CCA GCC CAA GGT CTT GAG

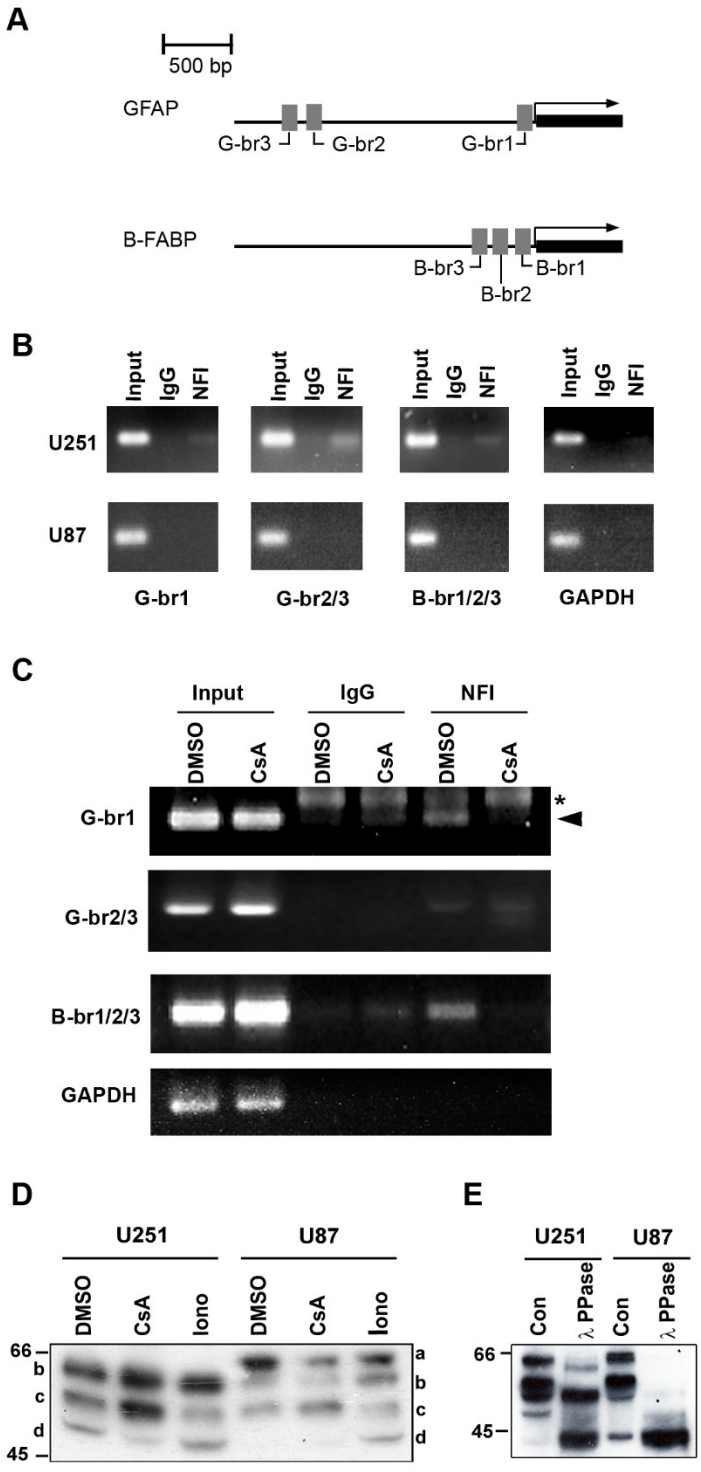
A
500 bp
GFAP
G-br3
G-br2
G-br1
B-FABP
B-br3
B-br2
B-br1
B
Input
IgG
NFI
U251
U87
G-br1
G-br2/3
B-br1/2/3
GAPDH
C
Input
IgG
NFI
DMSO
CsA
G-br1
G-br2/3
B-br1/2/3
GAPDH
D
U251
U87
DMSO
CsA
Iono
66
45
a
b
c
d
E
U251
U87
Con
λ PPase
66
45

Figure 4-1: NFI-dependent promoter binding and activity. (A) Schematic diagram of the *GFAP* and *B-FABP* promoter regions showing the relative location of the three NFI binding sites located in each promoter. (B) ChIP analysis was carried out in U251 and U87 cells using either a pan-specific anti-NFI antibody or rabbit IgG as a negative control. Primers flanking the NFI binding sites identified in the *GFAP* (G-br1 and G-br2/3) and *B-FABP* promoters (B-br1/2/3) were used for PCR amplification (Table 4-1). Primers flanking the proximal *GAPDH* promoter were used as a negative control. Input DNA represents DNA isolated from U251 or U87 cell lysates following sonication but prior to immunoprecipitation. Input DNA serves as the positive control for the PCR reactions, and reveals products of the expected sizes. (C) U251 cells were treated for 1 h with 10 μM CsA or DMSO (CON, control), followed by ChIP analysis as described in (B) Asterisk (*) denotes non-specific band, arrowhead denotes specific band. (D) Western blot analysis of NFI in U251 and U87 cells treated with CsA and ionomycin (Iono). U251 and U87 cells were treated for 1 h with DMSO, 10 μM CsA, or 10 μM ionomycin, and harvested using trypsin to dissociate the cells. Nuclear extracts were electrophoresed in a 10% SDS-polyacrylamide gel, transferred to a PVDF membrane, and immunostained with rabbit anti-NFI antibody. The primary antibody was detected with horseradish-peroxidase conjugated antibody and the signal was detected with Immobilon reagent. (E) Lambda phosphatase treatment of U251 and U87 nuclear extracts. U251 and U87 nuclear extracts were prepared in the absence of phosphatase inhibitors, and treated with or without λ-phosphatase (PPase) for 1 h at 30ºC. Following treatment, extracts were subjected to western blot analysis as in (D).

cells that is absent in NFI-hyperphosphorylated MG cells (Bisgrove et al., 2000). The serine/threonine phosphatase calcineurin is expressed in neurons and reactive astrocytes (Goto et al., 1986; Pyrzynska et al., 2001), and has previously been associated with NFIC transactivation in NIH3T3 cells (Alevizopoulos et al., 1997). We performed ChIP on U251 MG cells treated with the calcineurin inhibitor CsA to determine if there was any effect on NFI occupancy of endogenous promoters. U251 cells were incubated with 10 μM CsA, or DMSO (control) for 1 h followed by ChIP analysis as described above. Band intensity was markedly decreased in the presence of CsA compared to the DMSO control in the NFI IP lanes using primers flanking G-br1, and B-br1/2/3 (Figure 4-1C) indicating a decrease in immunoprecipitated DNA. No change was observed using primers flanking G-br2/3 (compare IgG and CsA lanes), and no signal was detected using primers to the GAPDH promoter. These results indicate that inhibition of calcineurin in U251 cells decreases NFI binding at endogenous consensus binding sites.

To determine if the decrease in *B-FABP* and *GFAP* promoter binding is due to changes in NFI phosphorylation, we treated U251 and U87 MG cells with 10 μM CsA, isolated nuclear extracts, and analyzed NFI phosphorylation by western blotting. The banding patterns of NFI were distinctly different in U251 and U87 cells (Figure 4-1D), with a slower migrating band (band a) specific to U87 cells observed in the DMSO lane. Furthermore, the fastest migrating band (band d) in the U251 control (DMSO) lane was absent in the U87 control (DMSO) lane. This recapitulates the increased phosphorylation of NFI reported in U87 compared to

U251 MG cells (Bisgrove et al., 2000). Upon inhibition of calcineurin with CsA, there was a shift up towards the slower migrating bands (bands b and c) in U251 cells (CsA lane) with a decrease in the intensity of the fastest migrating band (band d). CsA treatment did not alter the intensity of the slower migrating bands (bands b and c) in U87 cells.

Calcineurin is a calcium-dependent phosphatase. We therefore used the calcium ionophore ionomycin to increase the level of intracellular calcium in MG cells to determine if NFI phosphorylation is calcium sensitive. Western blot analysis of NFI following exposure of U87 cells to 10 μM ionomycin for 1 h revealed a change in NFI phosphorylation. In particular, we observed a faster migrating band in U87 cells which corresponds in size to the fastest migrating band in U251 (Figure 4-1C, lane 6, band d). There was no significant change in the NFI phosphorylation status of U251 cells treated with ionomycin.

To verify that changes in NFI mobility was due to phosphorylation, U251 and U87 nuclear extracts were prepared in the absence of phosphatase inhibitors, and treated with λ-phosphatase (Figure 4-1E). A shift to faster migrating bands was observed in the presence of λ-phosphatase in U251 cells. In comparison, all bands were shifted to the fastest migrating form when U87 cell lysates were incubated with λ-phosphatase. The persistence of slower migrating bands in phosphatase-treated U251 cell lysates suggests the presence of a different population of NFI family members.

4.3.3 Calcineurin regulates NFI activity

To study the effect of calcineurin modulation on NFI-dependent transcriptional activity, U251 cells were transfected with a CAT reporter gene under the control of the *GFAP* promoter (pCAT/GFAP) containing three well-characterized NFI binding sites, and treated with CsA or DMSO (control). Following treatment with CsA, CAT activity decreased to 74% of control levels ($p<0.001$) (Figure 4-2A). U251 cells were also transfected with the CAT reporter gene under the control of the *GFAP* promoter with each of the three NFI binding site mutated singly (pCAT/GFAP G-br1*, pCAT/GFAP G-br2*, pCAT/GFAP G-br3*) and in combination (pCAT/GFAP G-br1*/2*/3*). As previously reported, mutation of G-br1 had the most striking effect on promoter activity, with no further decreases observed upon mutation of all three NFI binding sites (Chapter 2). These results are consistent with our ChIP results showing strongest binding of NFI to G-br1. CsA treatment had no effect on the CAT activity of the mutated constructs.

To determine if increasing calcineurin activity modifies NFI-dependent promoter activity, U251 and U87 cells were co-transfected with: (i) pCAT/GFAP or pCAT/GFAP G-br1*/2*/3* and (ii) control (HA-tagged DDX1; used as transfection control), HA-tagged CNA-IN (catalytically inactive CNA) or HA-tagged CNA-CA (constitutively active CNA) construct. Expression of constitutively active CNA resulted in a 1.41-fold increase in CAT activity in U251 with pCAT/GFAP ($p<0.01$) (Figure 4-2B), and a 1.45-fold increase in CAT activity in U87 cells compared to expression of catalytically inactive CNA ($p<0.01$) (Figure 4-2C). There was no difference in CAT activity between control and CNA-IN, or upon co-transfection of

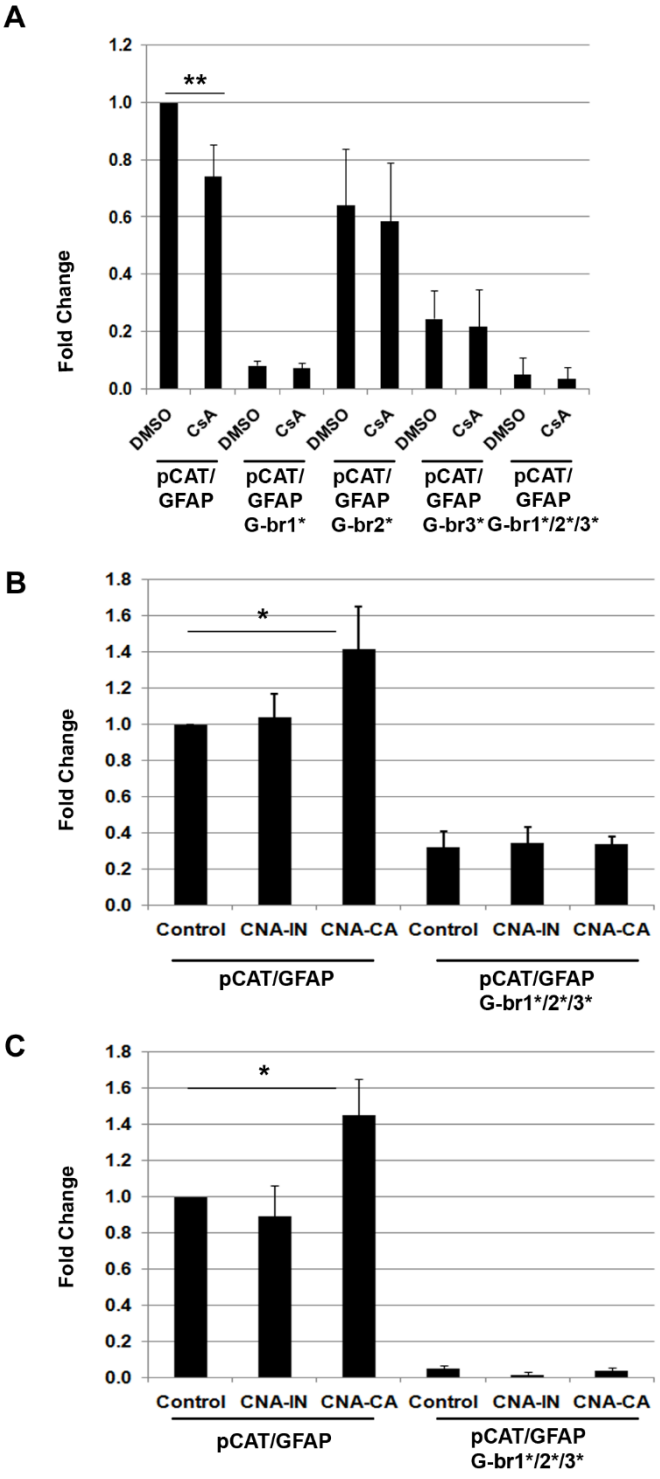
A
Fold Change
1.2
1.0
0.8
0.6
0.4
0.2
0.0
**
DMSO
CsA
pCAT/ GFAP
pCAT/ GFAP G-br1*
pCAT/ GFAP G-br2*
pCAT/ GFAP G-br3*
pCAT/ GFAP G-br1*/2*/3*
B
Fold Change
1.8
1.6
1.4
1.2
1.0
0.8
0.6
0.4
0.2
0.0
*
Control
CNA-IN
CNA-CA
pCAT/GFAP
pCAT/GFAP G-br1*/2*/3*
C
Fold Change
1.8
1.6
1.4
1.2
1.0
0.8
0.6
0.4
0.2
0.0
*
Control
CNA-IN
CNA-CA
pCAT/GFAP
pCAT/GFAP G-br1*/2*/3*

Figure 4-2: Calcineurin modulates NFI-dependent promoter activity. (A) U251 cells were transfected with pCAT/GFAP, pCAT/GFAP G-br1*, pCAT/GFAP G-br2*, pCAT/GFAP G-br3*, or pCAT/GFAP G-br1*/2*/3* (NFI sites mutated) and treated with 10 μM CsA, or DMSO (control) for 24 h. Acetylated [^{14}C]chloramphenicol was measured in cpm from equal aliquots of cell lysates using a scintillation counter. The fold increases in CAT activity are relative to U251 cells treated with DMSO and transfected with pCAT/GFAP. The results are an average of 4 (pCAT/GFAP G-br1*, pCAT/GFAP G-br2*, pCAT/GFAP G-br3*, pCAT/GFAP G-br1*/2*/3* constructs) to 6 (pCAT/GFAP construct) independent experiments with standard deviation indicated by error bars. (B, C) U251 (B) and U87 (C) cells were co-transfected with pCAT/GFAP or pCAT/GFAP G-br1*/2*/3* and HA-DDXI (control), catalytically inactive (CNA-IN) or constitutively active (CNA-CA) HA-tagged calcineurin. The fold increases in CAT activity are relative to U251 pCAT/GFAP: HA-DDXI (control) (B) or U87 pCAT/GFAP HA-DDX1 (control) (C). The results are an average of 4 independent experiments with standard deviation indicated by error bars. Statistical significance was determined using unpaired t test. * denotes $p<0.01$, ** denotes $p<0.001$.

control, CNA-IN or CNA-CA along with pCAT/GFAP G-br1*/2*/3* in either U251 or U87 cells (Figures 4-2B,C).

The alteration in NFI phosphorylation resulting from inhibition of calcineurin suggests that calcineurin is at least one of the phosphatases responsible for regulating the phosphorylation state of NFI. To address whether calcineurin exists in the same complex as NFI, we carried out co-immunoprecipitations. Using an anti-CNA antibody, we were able to immunoprecipitate a very large fraction of CNA, completely depleting CNA from the supernatant (Figure 4-3). A small amount of NFI was co-immunoprecipitated with CNA. No NFI was detected in the IgG control lane. We were unable to co-immunoprecipitate CNA with anti-NFI antibody. These results suggest that there may be a weak interaction between CNA and NFI and/or a small subset of NFI resides in the same cellular complex as calcineurin.

4.3.4 CNA expression in MG cell lines

Our results indicate a role for CNA in regulating NFI dephosphorylation. We therefore examined CNA expression in a panel of 10 MG cell lines, five that express B-FABP/GFAP and have hypophosphorylated NFI (M016, M049, M103, U251, and U373) and five that do not express B-FABP/GFAP and have hyperphosphorylated NFI (A172, CLA, M021, T98, and U87) (Bisgrove et al., 2000). Western blot analysis of whole cell extracts revealed significant variation in expression of CNA (60 kDa) with highest levels in A172, CLA, M021, and T98, and lowest levels in M103, U251, and U373 (Figure 4-4A). Intriguingly, we also observed a faster migrating band of approximately 57 kDa present exclusively in

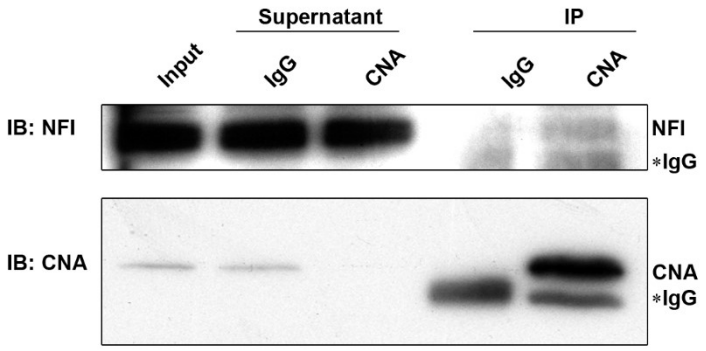

Figure 4-3: Co-immunoprecipitation of CNA and NFI. Whole cell extracts from U251 cells were incubated with either anti-CNA antibody or purified mouse IgG. The immunocomplexes were subjected to gel electrophoresis, transferred to a PVDF membrane and immunostained with anti-NFI antibody (Tanese) and anti-CNA antibody. Five percent of the supernatant from each immunoprecipitation was loaded in indicated lanes. IP, immunoprecipitation; IB, immunoblotting.

the five B-FABP/GFAP+ve cell lines with hypophosphorylated NFIs. This 57 kDa form of CNA has previously been reported to be a cleaved form of CNA with approximately 2-fold increased activity compared to uncleaved CNA (Liu et al., 2005a). The observed correlation between the 57 kDa form of CNA and NFI hypophosphorylation suggests that the cleaved form of CNA may regulate NFI dephosphorylation in MG cells.

Our antibody to CNA recognizes both the alpha and beta CNA isoforms. A third CNA isoform is testis-specific (Muramatsu et al., 1992; Muramatsu and Kincaid, 1992). To identify the CNA isoform(s) cleaved in B-FABP/GFAP+ve MG cells, we immunostained our panel of 10 MG cell lines with antibodies specific to CNAα and CNAβ. Overall, CNAα was expressed at higher levels in B-FABP/GFAP-ve cell lines, with only the higher-migrating band observed (Figure 4A). Immunostaining with anti-CNAβ antibody revealed two bands in B-FABP/GFAP+ve MG cell lines (Figure 4-4A). These results suggest that CNAβ, but not CNAα, is being cleaved and activated in B-FABP/GFAP+ve cells.

Specific calcineurin activity in whole cell lysates was measured by dephosphorylation of [^{32}P]RII peptide, a peptide selectively and efficiently dephosphorylated by calcineurin *in vitro* (Donella-Deana et al., 1994; Enz et al., 1994). As with CNA expression, calcineurin activity varied widely among MG cell lines (Figure 4-4B). Highest activity was detected in A172 and T98 cells, releasing 23.9 and 24.5 pmol/min/mg protein of [^{32}P] from the RII peptide. U87 cells had the lowest level of calcineurin activity, 5.7 pmol/min/mg protein. The remaining MG cell lines tested had activities ranging from 7.9 pmol/min/mg protein (M021) to 16.0

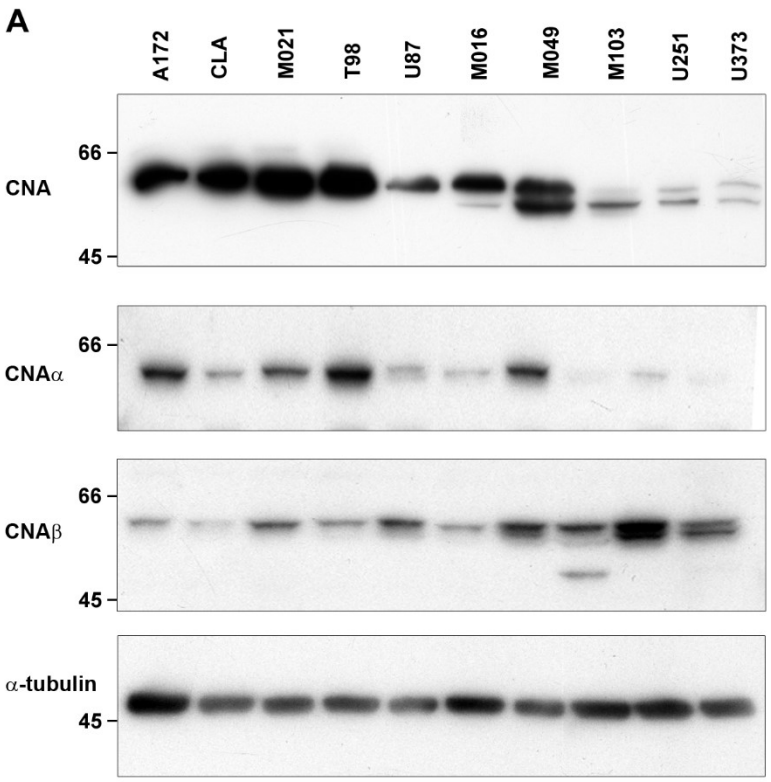
A
A172
CLA
M021
T98
U87
M016
M049
M103
U251
U373
66
CNA
45
66
CNAα
66
CNAβ
45
α-tubulin
45

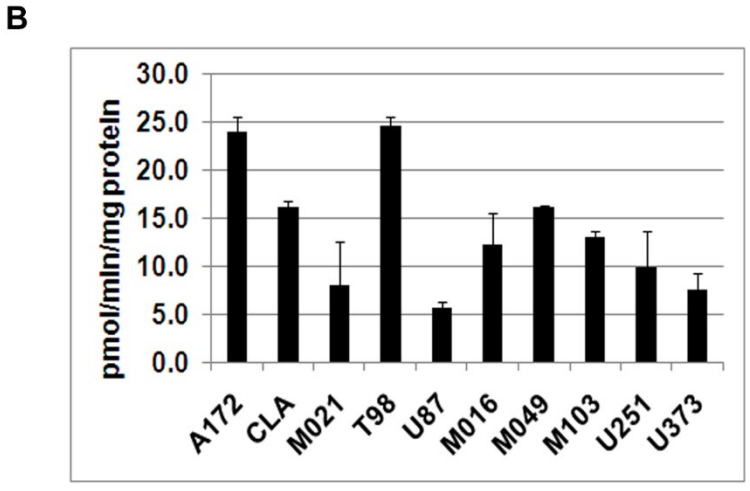
B
pmol/mln/mg proteln
30.0
25.0
20.0
15.0
10.0
5.0
0.0
A172
CLA
M021
T98
U87
M016
M049
M103
U251
U373

Figure 4-4: CNA expression in MG cell lines. (A) Whole cell extracts from MG cell lines were electrophoresed, transferred to PVDF membranes, and immunostained with anti-CNA, anti-CNAα, anti-CNAβ, and anti-α-tubulin antibodies. (B) Calcineurin activity (pmol/min/mg protein) in whole cell lysates was measured using [γ-^{32}P]RII peptide substrate. The results are an average of 3 replicates with standard deviation indicated by error bars.

pmol/min/mg (CLA). Interestingly, though expression of CNA was lowest in M103, U251, and U373, calcineurin activity in these cell lines using this assay was comparable to CLA and M021 which had very high levels of CNA.

4.3.5 Calpastatin modulates NFI-dependent promoter activity

CNA has been reported to be cleaved to a 57 kDa form by the protease calpain (Liu et al., 2005a; Wang et al., 1996). As calpastatin is an endogenous inhibitor of calpain activity (Goll et al., 2003), we co-transfected U251 and U87 cells with a calpastatin expression construct along with pCAT/GFAP to determine whether inhibition of calpain could alter NFI-dependent promoter activity. In U251 cells, calpastatin significantly decreased CAT activity, to 67% of the control levels obtained with empty vector ($p<0.05$) (Figure 4-5A). U87 cells, which do not have the 57 kDa cleaved form of CNA, showed no change in CAT activity. We also prepared nuclear and cytoplasmic extracts from U251 and U87 cells transfected with calpastatin. Expression of calpastatin did not alter CNAβ expression or cleavage in the cytoplasm of U251 or U87 cells; however, there was a clear decrease in the amount of cleaved CNAβ in the nucleus of U251 cells treated with calpastatin (Figure 4-5B). No CNAβ was detected in the nucleus of U87 cells.

4.3.6 Ionomycin alters NFI phosphorylation and NFI-dependent promoter activity

As previously shown in Figure 4-1D, treatment of U87 cells with the calcium ionophore ionomycin resulted in increased dephosphorylation of NFI. We therefore

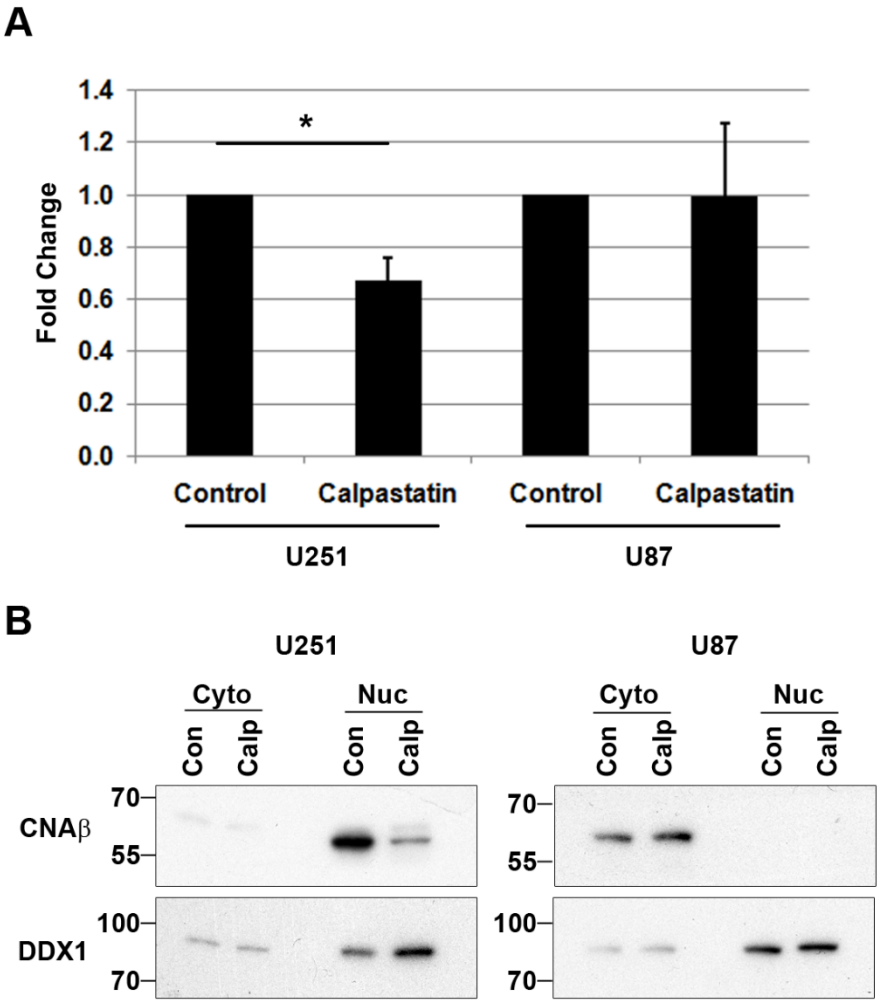
A
1.4
1.2
1.0
0.8
0.6
0.4
0.2
0.0
Fold Change
*
Control
Calpastatin
Control
Calpastatin
U251
U87
B
U251
U87
Cyto
Nuc
Cyto
Nuc
Con
Calp
Con
Calp
Con
Calp
Con
Calp
CNAβ
DDX1
70
55
100
70
70
55
100
70

Figure 4-5: Calpastatin alters NFI-dependent promoter activity. (A) U251 and U87 cells were co-transfected with pCAT/GFAP and control (empty vector) or calpastatin expression construct. Acetylated [^{14}C]chloramphenicol was measured from equal aliquots of cell lysates using a scintillation counter. The fold increases in CAT activity are relative to control (empty vector). The results are an average of 4 independent experiments with standard deviation indicated by error bars. Statistical significance was determined using unpaired t test. * denotes $p<0.01$. (B) U251 and U87 cells were transfected with control (Con; empty vector) or calpastatin (Calp), and cytoplasmic (Cyto) and nuclear (Nuc) fractions were prepared. Extracts were electrophoresed, transferred to PVDF membranes and immunostained with anti-CNAβ and anti-DDX1 (loading control) antibodies.

examined NFI-dependent promoter activity in U251 and U87 cells following treatment with ionomycin to see if changes in NFI phosphorylation might result in altered NFI activity. U251 and U87 cells were transfected with pCAT/GFAP, followed by treatment with ionomycin or DMSO (control) for 24 h. CAT activity was not altered in U251 cells where ionomycin had little effect on NFI phosphorylation (Figures 4-1C - lane 3 and 4-6A). However, in U87 cells, treatment with ionomycin increased CAT activity 1.8-fold ($p<0.001$) (Figure 4-6A).

4.3.7 CNA localization in MG cell lines and astrocytoma tumours

The differences in CNA expression and activity observed in U251 and U87 cells led us to examine CNA subcellular localization in these cells. In U251 control (DMSO-treated) cells, CNA was concentrated in the nucleus, with dense areas of perinuclear staining. CNA staining in the cytoplasm was much weaker than in the nucleus (Figure 4-6B). Interestingly, this pattern was reversed in U87 cells, with CNA primarily found in the cytoplasm. Upon addition of 10 μM ionomycin for 1 h, CNA translocated to the nucleus in U87 cells but had no effect on U251 cells. We then quantitated the subcellular localization of CNA in the cytoplasm and nucleus of U87 cells. As indicated in Figure 4-6C, CNA was primarily found in the cytoplasm of 99% of U87 control cells, with only 1% of untreated cells showing a predominantly nuclear pattern. Upon exposure to ionomycin, localization of CNA to the nucleus was observed in 88% of U87 cells. We verified these changes in subcellular localization by nuclear and cytoplasmic fractionation. Cleaved CNAβ was detected in the nucleus of U251 cells treated with DMSO and ionomycin, with

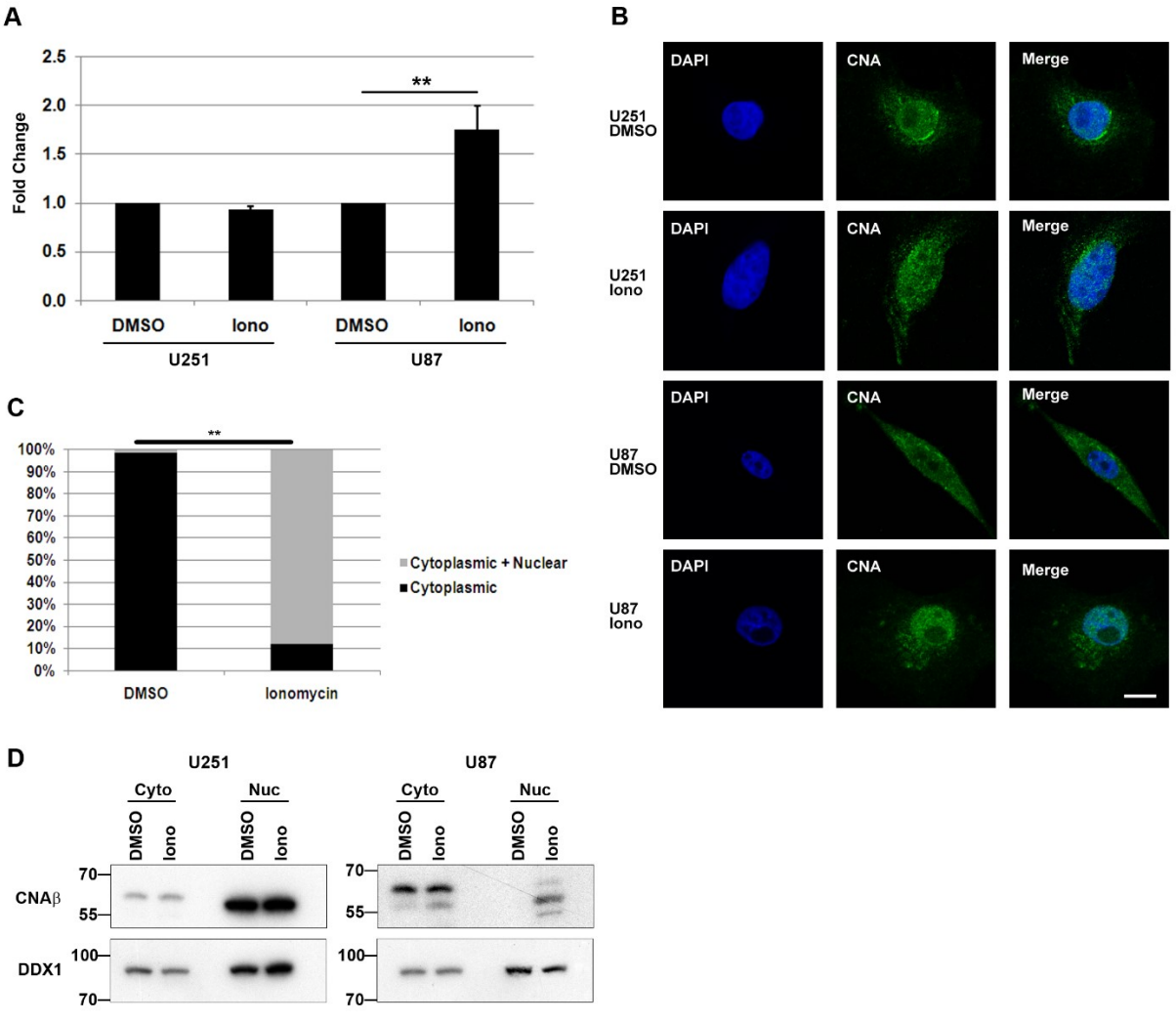
A
Fold Change
2.5
2.0
1.5
1.0
0.5
0.0
**
DMSO
Iono
DMSO
Iono
U251
U87
B
DAPI
CNA
Merge
U251 DMSO
U251 Iono
U87 DMSO
U87 Iono
C
**
100%
90%
80%
70%
60%
50%
40%
30%
20%
10%
0%
Cytoplasmic + Nuclear
Cytoplasmic
DMSO
Ionomycin
D
U251
U87
Cyto
Nuc
DMSO
Iono
CNAβ
DDX1
70
55
100

Figure 4-6: Ionomycin alters NFI-dependent promoter activity and calcineurin localization. (A) U251 and U87 cells were transfected with pCAT/GFAP and treated with 10 μM ionomycin (Iono), or DMSO (control) for 24 h. Acetylated [^{14}C]chloramphenicol was measured in cpm from equal aliquots of cell lysates using a scintillation counter. The fold increases in CAT activity are relative to the DMSO control. The results are an average of 4 independent experiments with standard deviation indicated by error bars. (B) Subcellular localization of calcineurin in U251 and U87 cells treated with DMSO (control) or 10 μM ionomycin (Iono) was analyzed by immunofluorescence using anti-CNA primary antibody followed by Alexa 488-conjugated secondary antibody. DNA was stained with 4'6-diamidino-2-phenylindole (DAPI). Bar = 10 μm. (C) Percentage of cells with predominantly cytoplasmic staining versus cells with nuclear and cytoplasmic staining for CNA in U87 cells treated with DMSO (control) or 10 μM ionomycin for 1 h. This analysis was carried out >100 cells for each parameter. Briefly, 10 separate fields with approximately 10 – 15 cells per field were randomly selected for each parameter. Line scans through the cytoplasm and nucleus of each cell were used to assess relative signal in the nucleus and cytoplasm. Statistical significance was determined using unpaired t test. ** denotes $p<0.001$. (D) U251 and U87 cells were treated with DMSO (control) or 10 μM ionomycin (Iono) for 1 h, harvested, and cytoplasmic and nuclear extracts were prepared. Extracts were electrophoresed, transferred to PVDF membranes and immunostained with anti-CNAβ and anti-DDX1 (loading control) antibodies.

uncleaved CNAβ detected only in the cytoplasm (Figure 4-6D). In U87 cells, CNAβ was not detected in the nucleus of DMSO-treated cells; however, following treatment with ionomycin, cleaved CNAβ was clearly detected in the nucleus.

Next, we examined CNA expression in brain and MG tumour tissue. CNA was not detected in normal human brain (frontal lobe) based on immunohistochemical analysis (Figure 4-7A). Immunostaining of grades I, II and IV astrocytoma tumour tissues revealed increased expression of CNA in high grade (grade IV) astrocytomas (Figures 4-7E-H) compared to grade I and II tumours (Figures 4-7B, C). Expression of CNA was primarily restricted to the cytoplasm of a small subset of cells in grade I tumours (Figure 4-7B). The immunostaining pattern in grade II astrocytomas was similar to that of grade I astrocytomas with CNA expression primarily found in the cytoplasm of a small number of cells. In grade IV tumours, we observed increased expression of CNA in areas of tumour infiltration. Figures 4-7D to F show progressively higher levels of CNA immunostaining in regions of low infiltration to high infiltration. In some areas (Figure 4-7E), CNA immunostaining was primarily diffuse and cytoplasmic, whereas in other areas (Figure 4-7F), CNA immunostaining was primarily perinuclear, with a small subset of cells showing nuclear immunostaining (indicated in inset). Of note, strong immunostaining was detected in pseudopalisading cells surrounding necrotic areas (Figures 4-7G, H). Hypercellular pseudopalisades are commonly observed in high grade astrocytomas and are formed by actively migrating cells (Brat et al., 2004).

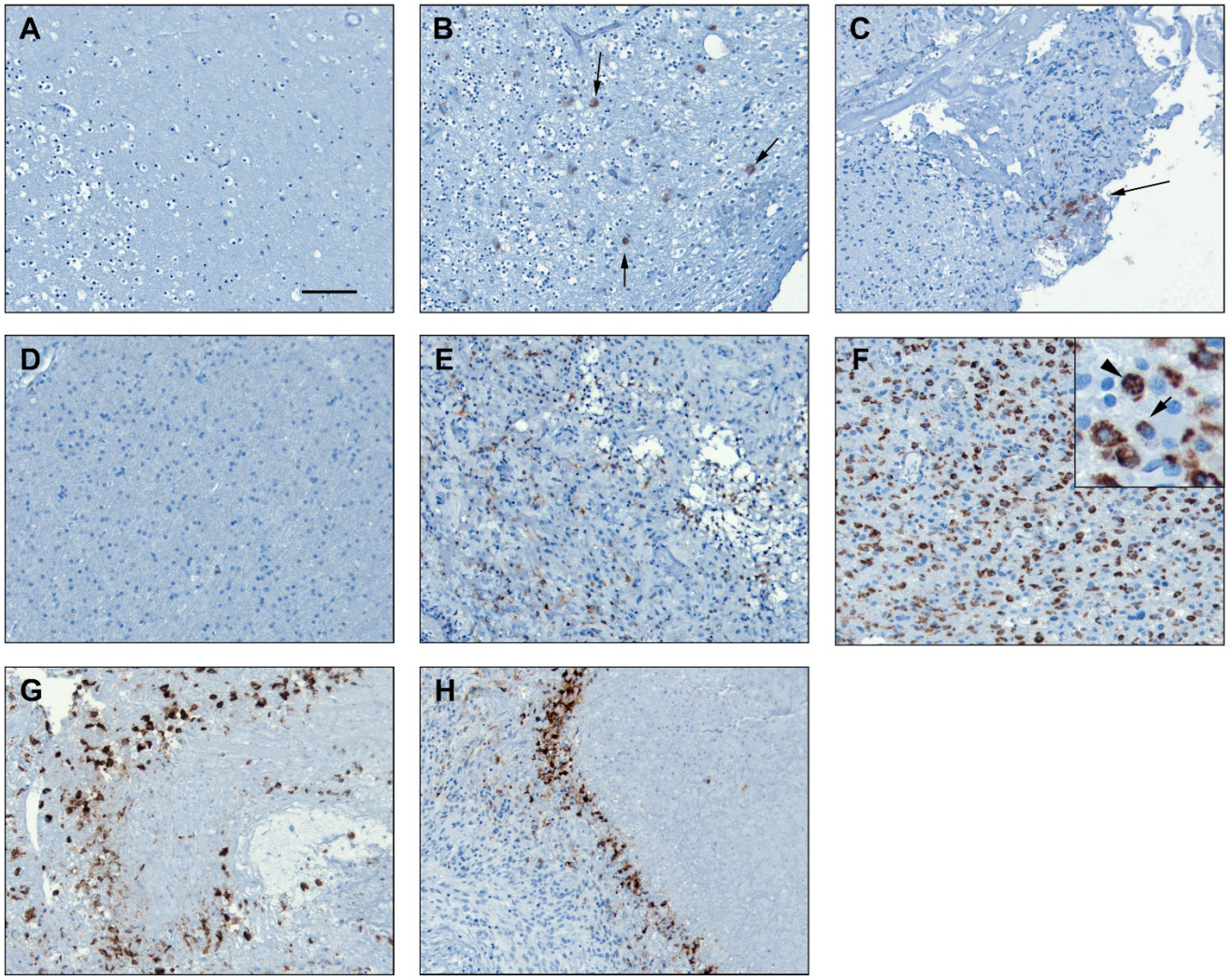
A
B
C
D
E
F
G
H

Figure 4-7: Immunohistochemical analysis of CNA in human astrocytoma tumours. Tissue sections were immunostained with anti-CNA antibody and counterstained with hematoxylin. (A) Normal human brain. (B) Grade I astrocytoma. Arrows indicate positive cells (patient 983). (C) Grade II astrocytoma (patient 470). Arrow indicates area of positive staining. (D) Grade IV astrocytoma, no visible tumour cells (patient 1046). (E) Grade IV astrocytoma, tumour centre (patient 1046). (F) Grade IV astrocytoma, heavy tumour infiltration. Inset: arrow indicates perinuclear staining; arrowhead indicates nuclear staining (patient 335). (G, H) Grade IV astrocytoma, heavy tumour infiltration (patient 1046).

4.4 Discussion

The NFI family of transcription factors is a key regulator of neural cell differentiation, playing an essential role in gliogenesis in the brain and spinal cord (Deneen et al., 2006; Namihira et al., 2009). In the spinal cord, induction of NFIA and NFIB expression coincides with the start of gliogenesis, and knockdown of NFIA results in loss of glial cell progenitors in the chick embryo (Deneen et al., 2006). Following gliogenesis, NFIA and NFIB promote astrocyte differentiation. In the brain, NFIA expression confers astrocytic potential on neural precursor cells downstream of Notch-induced signaling and Sox9 (Kang et al., 2012; Namihira et al., 2009). In MG, NFI regulates expression of *B-FABP* and *GFAP*, normally expressed in radial glial cells and in differentiated astrocytes, respectively (Chapter 2). Importantly, NFI is differentially phosphorylated in MG cells, with hypophosphorylated NFI found in B-FABP/GFAP+ve MG cell lines and hyperphosphorylated NFI found in B-FABP/GFAP-ve MG cell lines (Bisgrove et al., 2000). These observations agree with previous experiments demonstrating that increased phosphorylation of NFIs results in decreased transactivation of NFI-dependent promoters (Yang et al., 1993). Importantly, NFI activity appears to be regulated by a phosphatase activity that is specific to B-FABP/GFAP+ve (NFI hypophosphorylated) MG cells rather than a kinase activity that is specific to B-FABP/GFAP-ve (NFI hyperphosphorylated) MG cells (Bisgrove et al., 2000).

Here, we identify the phosphatase calcineurin as an important regulator of NFI dephosphorylation and activity in MG cells. Our combined approaches, including CNA overexpression and inhibition, co-immunoprecipitation with NFI,

ChIP analysis of NFI-dependent *B-FABP* and *GFAP* promoters, western blot analysis of CNA, and reporter gene assays, point to a direct link between calcineurin and dephosphorylation of NFI in MG cells. Calcineurin is a serine/threonine phosphatase that is highly expressed in neurons (Goto et al., 1986; Steiner et al., 1992). Calcineurin has also been detected in C6 glioma cells and cultured astrocytes (Farber et al., 1987; Matsuda et al., 1998). In astrocytes, calcineurin plays an important role in regulating the inflammatory response (Fernandez et al., 2007), and calcineurin expression increases in astrocytes but not neurons in a mouse aging model (Norris et al., 2005). Calcineurin has also been shown to increase NFIC transactivation (Alevizopoulos et al., 1997), providing a direct link between calcineurin and the NFI family.

The distinguishing characteristics of calcineurin in NFI-hypophosphorylated versus NFI-hyperphosphorylated MG cell lines are neither its expression levels nor its activity as measured using the RII peptide *in vitro* assay, but rather: (i) the presence of a cleaved 57 kDa CNA fragment specifically associated with NFI-hypophosphorylated MG cells, and (ii) the nuclear localization of CNA in NFI-hypophosphorylated MG cells. A 57 kDa cleaved product of CNA has been previously reported in cortical neurons following glutamate exposure and in the brains of Alzheimer's disease patients (Liu et al., 2005a; Wu et al., 2004). Of note, the 57 kDa form of calcineurin identified in the brains of Alzheimer's disease patients shows a 2-fold increase in phosphatase activity compared to full-length CNA (Liu et al., 2005a). There are two CNA isoforms expressed in brain, CNAα and CNAβ (Jiang et al., 1997). In this study, we demonstrate that the CNA isoform

that is cleaved in NFI-hypophosphorylated MG cells is CNAβ. Although both CNA isoforms have been shown to dephosphorylate the same substrates *in vitro*, each isoform has different substrate preference, and differs in substrate binding affinity and turnover (Kilka et al., 2009). The differential expression of CNAα and CNAβ in different MG cell lines, combined with specific cleavage of CNAβ in NFI-hypophosphorylated MG cell lines, suggest unique roles for these two CNA isoforms in these tumour cells.

It is unclear why the 57 kDa form of CNAβ is more active, as the cleavage site is C-terminal to the CNB binding domain, the calmodulin binding domain, and the autoinhibitory domain (Grundke-iqbal 2005). Furthermore, despite the cleavage site being located downstream of identified NLS and NES sequences (Hallhuber et al., 2006), we found that cleaved CNAβ preferentially localizes to the nucleus whereas the uncleaved form preferentially localizes to the cytoplasm. We postulate that removal of the C-terminal 20 amino acids of CNAβ increases both its phosphatase activity as the result of an altered protein structure and its ability to localize to the nucleus.

CNA is cleaved by the Ca^{2+}-dependent cysteine protease calpain, and inhibition of calpain inhibits this cleavage. Our results indicate that inhibition of calpain by calpastatin, a specific endogenous inhibitor of calpain (Goll et al., 2003), decreases NFI-dependent promoter activity in U251 cells, but not in U87 cells. These observations are in agreement with CNA cleavage being calpain-dependent in MG cell lines that express the hypophosphorylated form of NFI. It will be interesting to examine expression and activity of calpain, and calpain regulators

including calpastatin, in MG cell lines and tumours, as they may be important upstream regulators of calcineurin, and consequently NFI activity.

An intriguing finding is the different subcellular distribution of CNA in MG cell lines. In U251 cells, CNA localizes almost exclusively to the nucleus, whereas CNA is primarily found in the cytoplasm of U87 cells. When U87 cells are treated with ionomycin, a calcium ionophore that causes an influx of calcium in the cells, CNAβ is cleaved and translocates to the nucleus. CNA has been detected in the nucleus of a variety of cell types (Bosser et al., 1993; Pujol et al., 1993; Santella and Carafoli, 1997), and has been reported to translocate to the nucleus following addition of a calcium ionophore (Shibasaki et al., 1996). Translocation of CNA to the nucleus of MG cells may be an important regulatory step in NFI dephosphorylation as NFI is normally found in the nucleus (Bosher et al., 1992). In keeping with this idea, suppression of CNA translocation to the nucleus in cardiomyocytes obtained from cases of myocardial hypertrophy has been shown to inhibit CNA signaling (Cyert, 2001; Hallhuber et al., 2006). Thus, we propose that in B-FABP/GFAP+ve, NFI-hypophosphorylated MG cells, where CNA is truncated and nuclear, CNA is active and able to dephosphorylate NFI, whereas in B-FABP/GFAP-ve, NFI-hyperphosphorylated MG cells, CNA localization to the cytoplasm prevents interaction with and dephosphorylation of NFI.

Differential cleavage and localization of CNA suggests that there may be differences in calcium signaling in MG cell lines. In glial cells, calcium signaling regulates cell function by controlling cellular homeostasis and releasing gliotransmitters (Nedergaard et al., 2010). Interestingly, overexpression of

calcium-permeable AMPA receptors has been reported in brain tumour initiating cells (Oh et al., 2012). As AMPA receptors allow calcium influx upon stimulation, increased levels of these receptors in MG cells may contribute to the cleavage and activation of calcineurin. In turn, increased activity of calcineurin may have wide-ranging effects beyond NFI phosphorylation since calcineurin has many targets. Further examination of MG cell lines and tumour tissues for changes in calcium signaling including expression of calcium channels and receptors may elucidate how both calpain and calcineurin are activated in these cells.

In normal brain, CNA is highly expressed in neurons, with little or no expression in astrocytes (Dawson et al., 1994; Goto et al., 1986). Calcineurin is activated in astrocytes by inflammatory signals in a cell context-dependent manner, with activation of calcineurin in resting astrocytes resulting in progression of the inflammatory cascade, and resolution of the inflammatory cascade in activated astrocytes (Fernandez et al., 2007). In low grade astrocytomas, CNA expression is weak and limited to a small percentage of cells. However, CNA levels are considerably higher in grade IV astrocytomas, especially at sites of tumour infiltration and in pseudopalisading cells surrounding necrotic zones. Pseudopalisades, associated with aggressive tumours and a hallmark of grade IV astrocytomas, are regions of hypercellularity formed by tumour cells actively migrating away from hypoxic areas (Brat et al., 2004). Our results suggest that CNA is preferentially expressed in the most aggressively growing regions of the tumours. B-FABP, a target of NFI, has also been shown to be associated with sites of tumour infiltration and migration in MG tumours and cell lines (De Rosa et al.,

2012; Kaloshi et al., 2007; Liang et al., 2005; Mita et al., 2007). Thus, calcineurin may reside at the apex of a regulatory cascade centered on the activation of genes associated with migration/infiltration. As such, calcineurin may represent a key target for the treatment of high grade astrocytomas.

There are a number of NFI phosphorylation states in MG cells, suggesting that NFIs are phosphorylated at multiple sites (Bisgrove et al., 2000). In fact, even the most hypophosphorylated form of NFI in U251 can be further dephosphorylated by addition of potato acid phosphatase (Bisgrove et al., 2000). Thus, we propose that NFI phosphorylation effectively serves as a rheostat to control function, with increasing phosphorylation resulting in increased negative charge. The outcome is a gradual disruption of molecular interactions and decreased activity. A graded response to multisite phosphorylation has been characterized previously as a way of finely regulating DNA binding by the transcription factor Ets-1 (Pufall et al., 2005) and p53 binding to CREB-binding protein (Lee et al., 2010). Alternatively, there may be a threshold of phosphorylation/dephosphorylation that acts analogously to an on/off switch. Such a mechanism has been demonstrated for NFAT1 which requires dephosphorylation of thirteen phosphoserines by CNA for its activation (Okamura et al., 2000). A third possibility is that phosphorylation/dephosphorylation of one or a small number of specific residues regulates activity. This is the case for Fox03 in which phosphorylation of S207 by MST1, independent of other phosphorylation events, triggers nuclear localization (Lehtinen et al., 2006). It remains to be seen which of these mechanisms underlies the control of NFI activity.

Taken together, our data support an important role for calcineurin in the dephosphorylation and activation of NFI dependent promoter activity in MG cells. A complex regulatory picture emerges, consisting of at least four principal steps: (i) cleavage of full length calcineurin to the more active 57 kDa form, (ii) translocation of calcineurin to the nucleus, (iii) interaction of calcineurin with NFI resulting in NFI dephosphorylation, and (iv) binding of NFI to (and regulation of) NFI target gene promoters (Figure 4-8). Based on CNA's position at the top of this regulatory cascade, it should be possible to regulate the expression of NFI target genes in MG through modulation of CNA activity. One NFI target gene, B-FABP, has already been shown to correlate with poor prognosis and reduced survival in MG tumours (Kaloshi et al., 2007; Liang et al., 2006), as well as increased migration in MG cell lines and infiltration in grade IV astrocytomas (Mita et al., 2007). Thus, we may be able to alter the migratory properties of MG cells through modulation of NFI phosphorylation by inhibiting CNA activation and/or translocation. Future work will involve examining MG tumours to determine if the CNA detected in these tissues is activated through calpain and how NFI phosphorylation and expression of NFI target genes are affected by CNA expression in MG tumours.

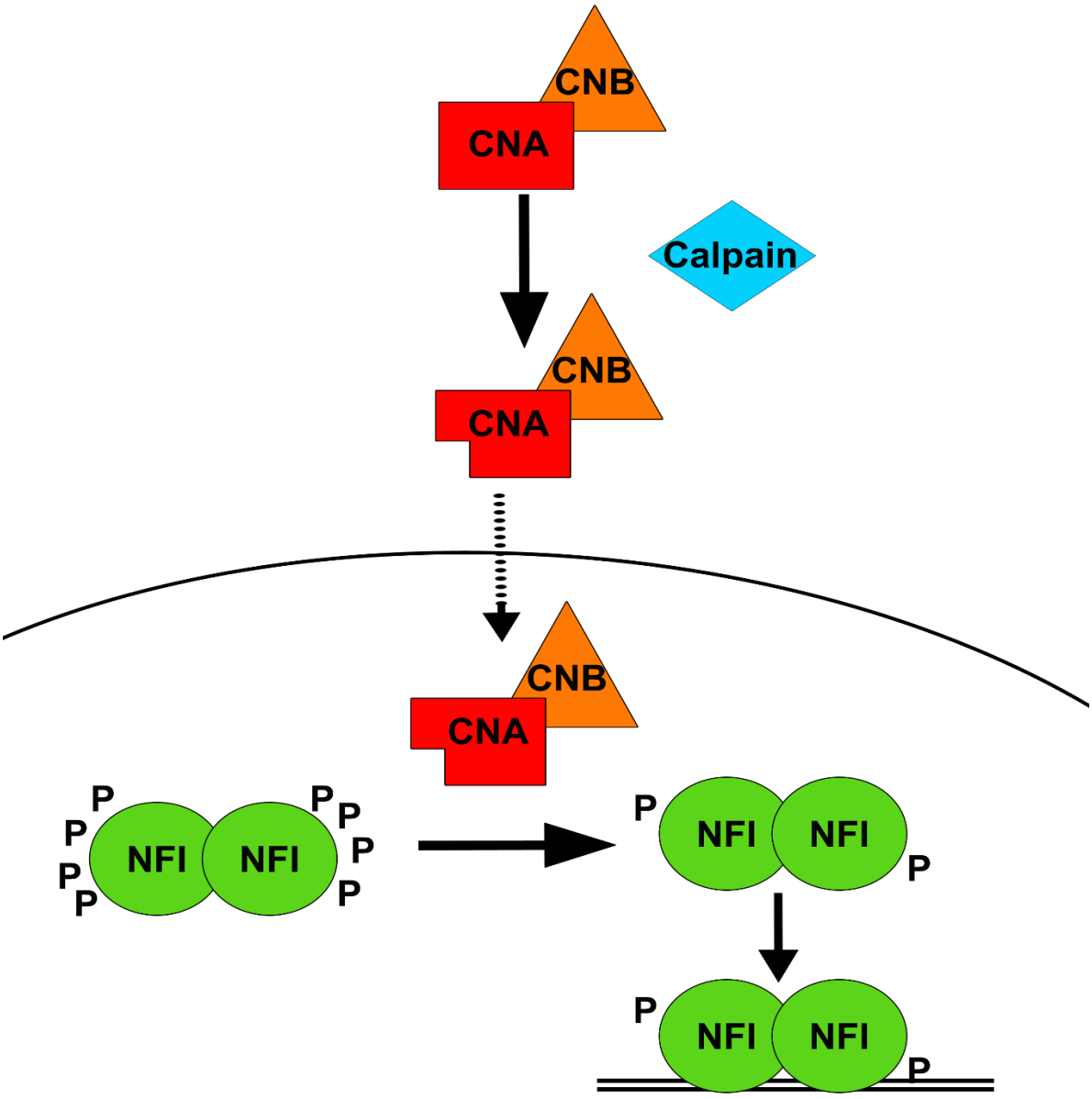

Figure 4-8: Model of regulation of calcineurin and NFI activity in MG cells. In the cytoplasm, calpain cleaves CNA (bound by regulatory subunit CNB). Cleaved CNA bound to CNB translocates to the nucleus and dephosphorylates NFI. Hypophosphorylated NFI can now interact with NFI consensus binding sites in target gene promoters.

Chapter 5

DISCUSSION

5.1 Discussion

5.1.1 Malignant glioma: co-opting development

Malignant gliomas (MGs) are notoriously difficult to treat and despite advances in surgical resection, radiation therapy, and the introduction of the chemotherapy drug temozolomide (TMZ), median survival is only 14.6 months for grade IV (glioblastoma (GBM)) and 31 months for grade III tumours (anaplastic astrocytoma) (Barker et al., 2014; Stupp et al., 2005). The cell-of-origin of MG remains unclear, and from recent studies, it appears possible that the cell-of-origin may be highly variable, ranging from adult neural stem cells to terminally differentiated cells (discussed in Section 1.1.4).

Previous work in our lab demonstrated co-expression of brain fatty acid-binding protein (B-FABP) with glial fibrillary acidic protein (GFAP) in a subset of MG cell lines (Godbout et al., 1998). In the developing brain, B-FABP is expressed in radial glial cells. Radial glial cells act as neural stem cells within the brain, first dividing to produce neurons, and following the onset of gliogenesis, giving rise to glial progenitor cells that further divide and differentiate to produce astrocytes and oligodendrocytes (Anthony et al., 2004; Casper and McCarthy, 2006; Malatesta et al., 2003; Malatesta et al., 2000). During neurogenesis, radial glial cells also form a scaffold that guides migrating neurons (Rakic, 1972). B-FABP expression is retained in adult neural stem cells located in the subventricular zone (Giachino et al., 2014). Expression of GFAP is activated during the onset of gliogenesis (Takizawa et al., 2001), and is also expressed in subventricular zone astrocytes which act as adult neural stem cells. (Doetsch et al., 1999a; Giachino et al., 2014).

Co-expression of B-FABP and GFAP in MG suggests that these cells may arise from subventricular astrocytes that retain neural stem cell properties, or cells within this lineage that retain expression of B-FABP and GFAP.

We demonstrate that NFI activates expression of GFAP and B-FABP in MG cell lines (Chapter 2). During development, NFI regulates the onset of gliogenesis downstream of Notch signaling (Deneen et al., 2006; Namihira et al., 2009). Specifically, NFIA is necessary for the demethylation of the *GFAP* promoter, and NFI binding to the *GFAP* promoter promotes its expression in neural precursor cells (Cebolla and Vallejo, 2006; Namihira et al., 2009). The onset of NFI expression correlates with onset of GFAP expression and gliogenesis in the developing brain (Cebolla and Vallejo, 2006; Chaudhry et al., 1997). In the adult brain, NFIA expression is principally detected in GFAP-positive cells, and is enriched in the subventricular zone (Song et al., 2010). This suggests that NFI expression may be preserved in astrocytes that retain neural stem cell characteristics in the adult brain. *Nfia-/-* murine neural stem cells display impaired neurosphere formation. Following transduction with oncogenes, these neural stem cells are unable to form tumours, in contrast to transduced *Nfia+/-* neural stem cells (Glasgow et al., 2013). This further suggests that NFIA, and possibly additional NFI family members, play a role in gene regulation of stem cell characteristics, and are necessary for MG tumour formation.

NFI also contributes to the migratory activity of MG cells. In radial glial cells, B-FABP is necessary for neuronal cell migration, and blocking of B-FABP with antibodies targeted to B-FABP prevents radial glial fibre formation (Feng et al.,

1994). In MG cells, B-FABP expression increases migration, and expression of B-FABP in GBM tumours correlates with a poorer prognosis (De Rosa et al., 2012; Kaloshi et al., 2007; Liang et al., 2006; Mita et al., 2010; Mita et al., 2007). NFI binds to the *B-FABP* promoter and activates expression of B-FABP in MG (Chapter 2), and NFI, specifically NFIA, increases migration in MG cell lines, and in orthotopic xenografts (Lee et al., 2014).

Different cell populations with the ability to generate tumours in mice have been identified in GBM tumours. These populations represent the glial cell lineage spectrum from less differentiated to more differentiated (Chen et al., 2010). Adding to the complexity, different oncogenic mutations can result in different tumour phenotypes even within the same cell type: astrocytomas and oligodendrogliomas can both arise from oligodendrocyte precursor cells, with the tumour phenotype dependent on oncogenic signaling (Lindberg et al., 2014). Conversely, the same oncogenic disruptions generate different tumour phenotypes when introduced into different glial progenitor cells (Wang et al., 2013). This suggests that complex interplay between oncogenic drivers, cell types, and cellular environment shapes gliomagenesis. Notably, NFIA expression has been shown to play a central role in shaping tumour phenotype; expression of NFIA in a mouse oligodendroglioma tumour model results in formation of tumours that express GFAP, and upon examination, look like astrocytomas (Glasgow et al., 2014). This suggests that the NFI family plays a seminal role in shaping MG phenotype.

During neurogenesis in the developing brain, glial-specific genes are hypermethylated and inactive (Takizawa et al., 2001). Many grade III astrocytomas

and secondary GBM are characterized by glioma CpG island methylator phenotype (G-CIMP) which is closely associated with isocitrate dehydrogenase (IDH) mutations (Noushmehr et al., 2010; Turcan et al., 2012). Microarray analysis of CpG methylation in GBM revealed widespread differential methylation, and also identified 25 hypermethylated and 7 hypomethylated genes in more than 20% of samples (Martinez et al., 2009). Of particular note, hypermethylated genes in GBM were enriched for targets of the polycomb repressive complex 2 (PRC2) in embryonic stem cells.

NFIs have been shown to contribute to demethylation. Following induction of *Nfia* in the developing mouse brain, DNA methyltransferase 1 (DNMT1) dissociates from hypermethylated promoters, resulting in demethylation and activation of glial genes, including *GFAP* (Namihira et al., 2009). In addition, NFIB represses expression of the murine histone methyltransferase gene *Ezh2* (Piper et al., 2014). EZH2 is a component of PRC2 that is expressed in neural stem cells, and is downregulated as these cells differentiate (Hirabayashi et al., 2009; Pereira et al., 2010). As part of PRC2, EZH2 also inhibits neurogenesis, and promotes the switch to astrocyte differentiation (Hirabayashi et al., 2009). Thus, NFIs contribute to the regulation of the epigenetic landscape during development. As the methylation profiles of GBM tumours suggest similarities to neural stem cells, NFIs may contribute to the epigenetic landscape in MG as well.

5.1.2 Notch and NFI in communication

Notch activates expression of both *NFIA* and *HEY1* (Nakagawa et al., 2000; Namihira et al., 2009). Conversely, we show that NFI represses expression of *HEY1* in MG cells (Chapter 3). Notch signaling suppresses neuronal differentiation, and promotes neural precursor cell maintenance as well as glial cell specification in the developing brain (Hitoshi et al., 2002; Morrison et al., 2000; Namihira et al., 2009; Ramasamy and Lenka, 2010; Taylor et al., 2007). These multiple, seemingly conflicting roles of Notch signaling are mediated by multiple ligands and receptors, as well as temporal stage-specific responses (Ramasamy and Lenka, 2010).

HEY1 overexpression in the developing mouse brain results in an increased population of neural precursor cells by inhibiting neurogenesis, and this leads to increased astrocyte production following the onset of gliogenesis (Sakamoto et al., 2003). Similarly, the related Notch effector HES1 promotes maintenance of neural precursor cells, and in addition promotes astrocyte differentiation (Ohtsuka et al., 2001; Wu et al., 2003). However, HES1 can only stimulate astrocyte differentiation following glial specification, and not in earlier precursor cells, demonstrating lineage restricted roles for Notch effectors (Wu et al., 2003). NFIA also represses expression of *Hes1*, and microarray analysis of hippocampal tissue from *Nfia-/-* mouse brain reveals upregulation of multiple Notch family members including *Hey1, Hes1, Hes5, Hey2,* and *Dll4* (Piper et al., 2010). This suggests that NFI may be an important regulator of Notch signaling during neural cell differentiation, and may be part of a negative feedback loop regulating Notch activity during neural cell differentiation.

In neural precursor cells, and other cell types, HES1 expression oscillates, and oscillation is necessary for normal development and cell fate choice (Baek et al., 2006; Hirata et al., 2002; Imayoshi and Kageyama, 2014; Shimojo et al., 2008). HES1 binds directly to its own promoter, and represses its own transcription (Takebayashi et al., 1994). Similarly, HEY2 also demonstrates negative autoregulation, and expression of HEY2 downregulates Notch stimulation of *Hey2* promoter activity, as well as *Hey1* promoter activity in mouse embryonic fibroblasts (Nakagawa et al., 2000). NFI repression of *HEY1* following induction of NFIA expression by Notch signaling may function as an additional regulator of Notch activity to ensure proper cell specification during development. NFIA expression promotes gliogenic differentiation, and even transient Notch activation is sufficient to instruct gliogenesis (Deneen et al., 2006; Morrison et al., 2000). Interestingly, the *B-FABP* promoter contains an RBP-Jκ binding site, and is directly activated by Notch signaling in radial glial cells (Anthony et al., 2004). Notch and NFI may thus coordinate expression of genes during neural differentiation. Following induction of NFIs at the onset of gliogenesis, NFI may become essential for expression of *B-FABP* and additional glial genes.

In MG, the number of cells expressing *HEY1* RNA correlates with increasing tumour grade and decreased survival compared to *HEY1*-negative tumours (Hulleman et al., 2009). Furthermore, knockdown of *HEY1* in MG cell lines results in decreased proliferation (Hulleman et al., 2009). In addition to repression of pro-neurogenic genes, HEY1 and HEY2 directly repress expression of the transcription factor genes *GATA4* and *GATA6* (Fischer et al., 2005). GATA4 and GATA6 are

normally expressed in astrocytes, and expression is lost in MG cell lines and tumours (Agnihotri et al., 2011; Agnihotri et al., 2009; Kamnasaran et al., 2007). Expression of GATA4 and GATA6 in MG cells decreases cell proliferation, with both transcription factors acting as tumour suppressors in these cells (Agnihotri et al., 2011; Kamnasaran et al., 2007). In MG cells, GATA4 directly activates expression of p21 to inhibit proliferation (Agnihotri et al., 2011). Conversely, NFIA represses expression of p21 in MG (Glasgow et al., 2013). This suggests multiple levels of control for cell proliferation, through both NFI and HEY1.

While expression of *HEY1* correlates with decreased survival in MG compared to patients with *HEY1*-negative tumours, the role of Notch signaling remains unclear (see Section 1.4.3). The importance of Notch signaling in maintaining neural progenitor cells suggests that Notch signaling may contribute to maintenance of a less differentiated phenotype in MG cells. In agreement with this idea, overexpression of the Notch intracellular domain (NICD) in a MG cell line enhances neurosphere growth (Zhang et al., 2008). In orthotopic xenografts of MG, activation of Notch signaling through overexpression of NICD increases tumour vascularization, but decreases cell migration (Guichet et al., 2015). Hypoxia activates Notch signaling, including upregulation of *HEY1* expression, in MG through HIF-1α, and increases expression of neural stem cell markers (Bar et al., 2010; Qiang et al., 2012). In MG tumours, B-FABP is expressed in pseudopalisading cells (Mita et al., 2007), and we have also observed expression of NFIA, NFIB (our unpublished data), and calcineurin in these cells (Chapter 4). Pseudopalisading cells are hypoxic and actively migrating away from areas of

necrosis (Brat et al., 2004). We propose that activation of Notch signaling in hypoxic cells may induce expression of both NFIA and HEY1. In turn, NFIs activate expression of B-FABP which increases MG cell migration, and repress HEY1 (Chapters 2 and 3) (Mita et al., 2007). As expression of Notch effectors has previously been shown to correlate with decreased migration and increased expression of pro-angiogenic factors (Guichet et al., 2015), the balance between NFIs and HEY1 and additional Notch effectors may control whether cells migrate or induce vascularization in response to hypoxia.

5.1.3 Calcineurin in malignant glioma

We observed expression of calcineurin in MG tumours and cell lines, with increased calcineurin expression in grade IV compared to grade II astrocytoma tumours (Chapter 4). In astrocytes, calcineurin expression is normally very low (Dawson et al., 1994; Goto et al., 1986). However, expression of calcineurin in astrocytes has been shown to increase during normal aging and in reactive astrocytes in a mouse model of Alzheimer's disease (Hashimoto et al., 1998; Norris et al., 2005). Reactive astrocytes share many characteristics with neural stem cells and radial glial cells including expression of B-FABP, nestin, and Sox2, as well as the ability to proliferate, self-renew and give rise to additional cell types (Buffo et al., 2008; Gotz et al., 2015). Expression of calcineurin in astrocytes replicates the hypertrophic phenotype seen in reactive astrocytes, and calcineurin expression in astrocytes can protect neurons against damage from inflammation following brain injury (Fernandez et al., 2007; Norris et al., 2005). MG incidence

increases with age, and expression of calcineurin in these tumours may be linked with increased age, or, alternatively, may be linked to significant disruption of the normal environment in MG tumours. Ischemia is a common characteristic of MG tumours (Jain et al., 2007), and calcineurin expression in MG tumours may mirror calcineurin expression in reactive astrocytes in response to ischemia. This possible scenario would also explain the presence of calcineurin in hypoxic pseudopalisading cells surrounding areas of necrosis in MG tumours (Chapter 4).

During development, calcineurin activity is required for specification of neural precursor cells from embryonic stem cells (Cho et al., 2014). In these cells, calcineurin targets the bone morphogenetic pathway (BMP) through dephosphorylation and inactivation of SMAD1/5, to modulate BMP signaling to allow neural induction. Following neural induction, BMP signaling in neural precursor cells promotes gliogenesis and astrocyte differentiation (Nakashima et al., 2001; Nakashima et al., 1999). In astrocyte cultures, BMP signaling through Smads inhibits proliferation and decreases expression of EGFR (Scholze et al., 2014). Calcineurin dephosphorylation of SMADs in MG may contribute to increased proliferation. NFI dephosphorylation and activation by calcineurin in MG may play a similar role, as NFIA expression increases proliferation in MG cell lines and tumours (Glasgow et al., 2013; Lee et al., 2014).

Cleavage of CNA, the catalytic subunit of calcineurin, by the serine protease calpain results in multiple cleaved forms of CNA that all demonstrate increased activity compared to full length CNA (Liu et al., 2005a; Wu et al., 2004). In MG cells, we detect a 57 kDa cleaved form of CNA that localizes to the nucleus, and

correlates with hypophosphorylated NFI (Chapter 4). Cleaved CNA is also detected in excitotoxic neurodegeneration, Alzheimer's disease brains, and in response to intraocular pressure in a glaucoma model (Huang et al., 2005; Liu et al., 2005a; Wu et al., 2004). This suggests that cleavage of CNA may be part of a response to pathological states within the central nervous system. We detect CNA in the nucleus of pseudopalisading cells in MG (Chapter 4) suggesting that CNA may also be cleaved in these tumour cells. As MG cells have been exposed to hypoxic conditions, cleavage of CNA in these cells may echo cleavage seen in other pathological states. The calcium dependent protease calpain cleaves CNA in Alzheimer's disease and in excitotoxic neurodegeneration (Liu et al., 2005a; Wu et al., 2004). Calpain is activated by hypoxia, and activation of calpain is associated with brain degeneration with age, trauma, stroke, and Alzheimer's disease (Vanderklish and Bahr, 2000). Calpain activation may also play an important role in MG.

5.1.4 Calcium signaling in malignant glioma

Calcium signaling promotes neural fate in embryonic stem cells, and then further promotes neurogenesis (Cho et al., 2014; Leclerc et al., 2011; Shin et al., 2010). Integration of calcium signaling is vital for neuronal function, including neuronal specification, synaptic plasticity, long term memory, survival and death (Burgoyne and Haynes, 2014; Leclerc et al., 2011). Calcium signaling also plays important roles in neural precursor cells, glial cell differentiation, and in astrocytes. These functions may be conserved in MG cells. In fact, calcium signaling has

previously been implicated in increased cell motility and proliferation in MG, in part through disassembly of focal adhesions, and activation of Akt (Giannone et al., 2002; Ishiuchi et al., 2007; Lyons et al., 2007).

Calcium mobilization in neural precursor cells is regulated by store-operated calcium channels (Somasundaram et al., 2014). Ca^{2+} release-activated Ca^{2+} (CRAC) channels are store-operated calcium channels that account for a large proportion of calcium release in neural precursor cells (Prakriya, 2009; Somasundaram et al., 2014). Subventricular zone astrocytes, which act as neural stem cells in the adult brain, also have CRAC channels, whereas protein components of CRAC channels are downregulated in neuroblasts. Calcium entry through these channels can be activated by exposure to epidermal growth factor (EGF), and promotes proliferation in neural precursor cells. Inhibition of these channels through knockdown of channel components decreases proliferation of adult neural stem cells (Somasundaram et al., 2014).

Calcium signaling can also promote astrocyte differentiation. Cyclic AMP (cAMP) promotes astrocyte differentiation via a cAMP-dependent increase in intracellular calcium (Cebolla et al., 2008; McManus et al., 1999). This increase in intracellular calcium activates the calcium binding protein downstream regulatory element antagonist modulator (DREAM), which then binds to the *GFAP* promoter and activates transcription (Carrion et al., 1999; Cebolla et al., 2008).

In astrocytes, intracellular calcium is modulated by release of neurotransmitters and growth factors. Rises in intracellular astrocytic calcium can be propagated in waves to adjacent astrocytes (Cornell-Bell et al., 1990; Volterra

et al., 2014). Similar to subventricular astrocytes/neural stem cells, EGF can increase intracellular calcium in astrocytes. This results in increased calcium oscillations in astrocytes, similar to oscillations observed in reactive astrocytes (Ding et al., 2007; Morita et al., 2005). Intracellular calcium is also increased in response to injury, including hypoxia (Duffy and MacVicar, 1996). Hypoxia and activation of EGF receptor (EGFR) signaling are frequent occurrences in MG (Chen et al., 2012). Increases in intracellular calcium in these cells may then result in calpain activation, cleavage and increased activation of calcineurin, and activation of NFI as well as numerous other calcium-dependent effectors. Taken together, the role of calcium signaling in neural precursor cells, glial differentiation, and astrocytes all support important roles for calcium signaling in MG tumourigenesis, growth and survival.

5.2 Future Directions

5.2.1 Validating novel NFI target genes

ChIP-on-chip analysis revealed NFI binding to promoter regions of 403 genes. In Chapter 3, we validated one identified gene, *HEY1*, as an NFI target gene in MG cells. Gene ontology analysis revealed enrichment of genes involved in a variety of biological processes. As predicted from the phenotypes observed in NFI knockout mice, NFI expression profiles, and developmental studies, NFI target genes were enriched in processes related to development of the of the nervous system, skeletal system and cardiovascular system (Table 3-2) (Chaudhry et al., 1997; Chaudhry et al., 1999; Driller et al., 2007; Holmfeldt et al., 2013; Steele-

Perkins et al., 2005). Also enriched were processes connected with regulation of gene expression, supporting a role for NFI in regulating transcriptional programs. Microarray analysis comparing expression of putative target genes in control MG cells compared to MG cells depleted of all four NFIs should identify those genes that are regulated by NFI in MG cells. These genes could then be validated as *bona fide* NFI target genes using gene reporter assays, electrophoretic mobility shift assays and qPCR.

Unexpectedly, gene ontology analysis revealed enrichment of genes in a large number of processes related to metabolism. This suggests that NFIs may play an important role in regulating metabolism in MG tumours. Grade IV astrocytomas show increased anabolic metabolism compared to grade II astrocytomas (Chinnaiyan et al., 2012), and altered metabolism with conversion to aerobic glycolysis is a hallmark of cancer (Hanahan and Weinberg, 2011; Warburg, 1956a; Warburg, 1956b). Recently, elevated expression of two mitochondrial genes, mitochondrial serine hydroxymethyltransferase (*SHMT2*) and glycine decarboxylase (*GLDC*), in pseudopalisading cells of GBM tumours was found to promote survival, with expression of SHMT2 also promoting cell survival in response to ischemia (Kim et al., 2015). As mentioned earlier, NFIA and NFIB are also expressed in pseudopalisading cells (our unpublished data). NFI regulation of metabolism in MG tumours may be an additional tumour-promoting role for NFIs. Investigating putative NFI target genes involved in metabolic processes may reveal additional alterations in cellular metabolism in MG.

5.2.2 NFI expression in malignant glioma

Expression of NFIA in MG tumours has been previously examined. In contrast to the tumour-promoting role of NFIA in MG cells, expression of NFIA correlates with increased survival in GBM tumours (Lee et al., 2014; Song et al., 2010). We show that all four NFIs contribute to the regulation of target genes *GFAP*, *B-FABP* and *HEY1* (Chapters 2 and 3). Comparing the levels of NFIB, NFIC, and NFIX in normal brain and grades II, III and IV astrocytoma tumours using tissue microarray (TMA) in conjunction with analysis of clinical data would reveal if there is any correlation between NFIB, NFIC and NFIX and tumour grade or changes in survival. It would also be valuable to look at large tumour sections to determine if expression of NFI family members is associated with different tumour microenvironments as we have previously observed expression of NFIA and NFIB in pseudopalisading cells. MG tumours are highly heterogeneous, and NFIs may be expressed in specific areas of the tumour, as previously seen with B-FABP (Mita et al., 2007).

NFI is differentially phosphorylated in MG cells, and NFI-dependent promoter activity is increased in cells with hypophosphorylated NFI (Chapter 4) (Bisgrove et al., 2000). Currently, there are no antibodies to distinguish between phosphorylated and hypophosphorylated forms of NFI, and changes in NFI phosphorylation are identified by changes in migration in SDS-PAGE or native gels (Chapter 4) (Bisgrove et al., 2000). While we have observed hypophosphorylated NFI in a subset of MG cell lines, long term culture of MG cells may result in widespread molecular changes (Li et al., 2008). Short term primary cultures

derived from MG tumours have been shown to retain molecular characteristics of tumours (Potter et al., 2009). Thus, analysis of NFI phosphorylation in short term primary MG cultures could be used to determine the extent to which NFI is hypophosphorylated in MG. One possibility is that NFI is hypophosphorylated in only a small subset of MG cells located in specific tumour microenvironments, such as areas of hypoxia. Generating antibodies that specifically recognize different phosphorylation states of NFI would facilitate analysis of NFI phosphorylation state in specific tumour regions.

NFIs can form both heterodimers and homodimers, and activity of heterodimers falls between the activity of NFI homodimers (Chaudhry et al., 1998; Kruse and Sippel, 1994b). To identify the population of dimers present in MG cells, co-immunoprecipitation of specific NFIs followed by western blot analysis using antibodies specific to the different members of the NFI family would reveal whether specific dimers are preferentially formed in MG cells. While this approach would identify the population of dimers within cells, it is highly probable that not all dimers can interact equally with target promoters, as NFIs have different affinities for NFI binding sites (Chapters 2 and 3) (Chaudhry et al., 1998). In order to identify the NFI dimers binding to the promoters of NFI target genes, sequential ChIP, or ChIP-Re-ChIP could be undertaken (Truax and Greer, 2012). This technique is similar to ChIP except that following isolation and elution of protein-DNA complexes with an antibody to a specific NFI, complexes would be immunoprecipitated a second time with an antibody to a second NFI. Assessing binding to multiple NFI target genes, including *B-FABP, GFAP, HEY1, p21*, and *p53* (Chapters 2 and 3) (Lee et

al., 2014) would further reveal if NFI dimers binding and repressing promoter activity are different than NFI dimers binding and activating promoter activity in MG cells.

5.2.3 Uncovering the off switch: the kinase that phosphorylates NFI

Hyperphosphorylation of NFI correlates with loss of expression of NFI target genes *B-FABP* and *GFAP* in MG cell lines, and inhibition of phosphatase activity results in NFI hyperphosphorylation (Bisgrove et al., 2000). This suggests that the kinase that phosphorylates NFI is constitutively active in these cells. Immunoprecipitation of NFI followed by immunoblotting with the α-phosphotyrosine antibody 4G10 suggests that NFI is not tyrosine phosphorylated. PhosphoSite Plus reveals multiple serine/threonine phosphorylation sites in all four NFIs by proteomic discovery-mode mass spectrometry. Phosphorylation sites identified thus far are concentrated in the C-terminus, with 30 sites in NFIA, 23 in NFIB, 39 in NFIC, and 21 in NFIX (Hornbeck et al., 2004). We have mutated 12 serine/threonine phosphorylation sites to alanine in an NFIA expression construct (HA-NFIA Δ12). Transfection of this plasmid in MG cells, followed by western blot analysis shows that this mutated NFIA has the same migration in SDS-polyacrylamide gels as wild-type NFIA (HA-NFIA) treated with λ-phosphatase (unpublished data), suggesting that one or more of these 12 sites is necessary for NFI phosphorylation in MG cells. Treatment of cells with either purvalanol A or roscovitine, two cyclin-dependent kinase (CDK) inhibitors, results in faster migration of HA-NFIA in a SDS-polyacrylamide gel. Within the 12 previously

mutated sites is a putative CDK5 phosphorylation motif. Mutation of this specific serine to alanine (HA-NFIA S300A) results in a migration pattern in a SDS-polyacrylamide gel that is identical to that of HA-NFIA Δ12, suggesting that this site is necessary for NFIA phosphorylation. Thus, Cdk5 may phosphorylate NFIA, and possibly other NFIs, in MG cells.

CDK5, unlike other CDKs, is not involved in cell cycle regulation in proliferating cells (Dhavan and Tsai, 2001). CDK5 is expressed in post-mitotic neurons and is necessary for proper neuronal function. The loss of Cdk5 results in defects in neuronal migration and in disruption of cortical lamination (Gilmore et al., 1998; Ohshima et al., 1996). Cdk5 also regulates differentiation of oligodendrocyte precursors (Miyamoto et al., 2007; Yang et al., 2013). Recently, a decrease in astrocyte and oligodendrocyte numbers was observed following Cdk5 knock-out in nestin-expressing cells during development, suggesting that Cdk5 may contribute to gliogenesis (Petrik et al., 2013). Interestingly, NFI has previously been shown to be rapidly phosphorylated in 3T3-L1 adipocytes in response to insulin, and Cdk5 is rapidly activated in the same cells following insulin treatment (Cooke and Lane, 1999b; Lalioti et al., 2009).

CDK5 is expressed in MG tumours and cell lines, and CDK5 activity in MG cells is much higher than in peripheral blood mononuclear cells (control) (Catania et al., 2001). *In vitro* phosphorylation assays with activated CDK5 and NFI family members could be used to determine whether NFI is phosphorylated by CDK5. This approach could also be used to determine if S300 in NFIA is a genuine CDK5 phosphorylation site, using HA-NFIA S300A as a substrate. To determine if CDK5

phosphorylates NFI in MG cells, changes in NFI phosphorylation following knockdown or specific inhibition of CDK5 could be examined. If CDK5 does phosphorylate NFI, this would provide an additional mechanism for regulating NFI-dependent promoter activity.

5.2.4 Investigating how phosphorylation attenuates NFI activity

NFI plays important roles in regulating development, especially in gliogenesis (see Section 1.3.5). NFI phosphorylation in development has not been examined, but may be an important regulatory mechanism during gliogenesis and astrocyte differentiation. Examining NFI phosphorylation in neural precursor cells, and as cells differentiate into neurons, astrocytes and oligodendrocytes, would reveal the role of NFI phosphorylation in regulating NFI activity and gliogenesis during development. These proposed experiments would also demonstrate whether NFI phosphorylation in MG is a conserved regulatory mechanism, or whether NFI phosphorylation is a tumour-specific event resulting from malignant transformation and disruption of normal signaling events.

Our preliminary work suggests that mutation of a single phosphorylation site, S300, abrogates NFIA phosphorylation. While multiple phosphorylation sites exist in NFI [e.g. 30 in NFIA (see Section 5.2.3)], our results indicate that S300 may be necessary for the phosphorylation of additional sites. Examples of hierarchical phosphorylation has been demonstrated in certain proteins and kinases. For example, phosphorylation of glycogen synthase by glycogen synthase kinase 3 (GSK3) requires a priming phosphorylation, and

phosphorylation at a specific site is part of GSK3's recognition motif (Fiol et al., 1987). Similarly, phosphorylation of NFATc4 by extracellular signal-regulated kinase 5 (ERK5) increases subsequent phosphorylation by casein kinase I (CK1) (Yang et al., 2008).

Our results show that HA-NFIA S300A is not phosphorylated in MG cells. It is currently unknown how phosphorylation affects NFI activity. ChIP experiments in MG cells treated with CsA reveal disruption of NFI binding to the promoters of target genes *in vivo*; however, phosphorylation does not affect DNA-binding *in vitro* (Chapter 4). This suggests that phosphorylation may alter protein-protein interactions resulting in changes in subnuclear localization or protein interaction with chromatin. To address this, changes in protein-protein interactions following co-immunoprecipitation of HA-NFIA and HA-NFIA S300A in MG cells where NFI is hyperphosphorylated could be examined by mass spectrometry. Fluorescence microscopy could be used to identify changes in subnuclear localization depending on NFI phosphorylation by co-immunostaining for NFI and markers of heterochromatin and active chromatin in MG cell lines with different NFI phosphorylation profiles. Similar experiments could also be carried out in cells transfected with HA-NFIA and HA-NFIA S300A. In addition, changes in protein dynamics could be measured by fluorescence recovery after photobleaching (FRAP), as phosphorylation may alter NFI complex formation. These experiments would give insight into how NFI phosphorylation alters NFI-dependent promoter activity in MG cells.

5.2.5 Expression and role of calcineurin in malignant glioma

In Chapter 4 we show increased expression and nuclear localization of the catalytic subunit of calcineurin, CNA, in grade IV astrocytoma compared to low grade astrocytoma and normal brain. We also observe CNA in pseudopalisading cells, similar to the expression pattern seen for the protein encoded by the NFI target gene *B-FABP* (Chapter 2) (Bisgrove et al., 2000). Pseudopalisading cells are actively migrating, and B-FABP increases migration in MG cells (Brat et al., 2004; Mita et al., 2007). To address the significance of CNA expression in MG, tissue microarray (TMA) analysis of CNA in MG tumours could be carried out to determine if increased expression and nuclear localization of CNA is a common event in MG, and if expression or nuclear localization correlates with survival in MG patients. In addition, co-immunostaining TMAs with antibodies to CNA and either markers of proliferation (Ki67, PCNA) or migration (B-FABP) would reveal if CNA expression and localization correlates with increased migratory or proliferative potential. We would predict that calcineurin expression may be a negative prognostic indicator in MG based on activation of NFI, and previously identified NFI target genes.

In Chapter 4, we observe a correlation between the cleaved 57 kDa form of CNA and hypophosphorylated NFI in a subset of MG cell lines. In Alzheimer's disease brains with the 57 kDA cleaved form, calcineurin activity is 2-fold greater than uncleaved CNA from control brains, but still requires the presence of Ca^{2+} and calmodulin for activity (Liu et al., 2005a). We found that the cleaved form of CNA preferentially localizes to the nucleus in MG cells that express the

hypophosphorylated form of NFI. Furthermore, U87 cells contain the uncleaved form of CNA, but following treatment with the calcium ionophore ionomycin, we observed the appearance of the 57 kDa form in the nucleus of these cells (Chapter 4). The cleavage site of CNA is located downstream of the nuclear export sequence (NES) and autoinhibitory domain. Thus, it is unclear how this cleavage alters localization and activity. It is possible that the 20 amino acids at the extreme C-terminus of CNA that are cleaved have a previously unidentified regulatory function. One way to investigate the function of the cleaved and uncleaved forms of CNA would be to carry out co-immunoprecipitations with full-length versus cleaved CNA and identify co-immunoprecipitated proteins by mass spectrometry. This approach would indicate whether the 20 amino acids that are removed in the cleaved form facilitate interaction with proteins that alter or constrict activity or subcellular localization. In conjunction, FRAP would reveal changes in dynamics due to changes in complex formation, and nucleocytoplasmic shuttling differences between the 57 kDa form and uncleaved 60 kDa form (Koster et al., 2005). This cleavage may also alter the structure of calcineurin. Crystallization of the calcineurin protein complex with the 57 kDa cleaved form of CNA compared to the 60 kDa uncleaved form would reveal changes in structure resulting from CNA cleavage (Griffith et al., 1995; Kissinger et al., 1995). It is possible that removal of 20 aa from the C-terminus alters protein folding, which may result in changes in binding to CNB or calmodulin through alteration of tertiary structure.

In addition to identifying how the cleavage of CNA alters calcineurin activity, it would also be useful to determine how this cleavage alters cell properties

including proliferation, migration, response to stress, and tumourigenicity. Calcineurin has many targets in addition to NFI, including NFATs, which are also expressed in MG and have been implicated in increased migratory activity (Tie et al., 2013; Wang et al., 2015). Increased activity and altered localization of calcineurin has the potential to have wide ranging effects. Comparison of migration and proliferation in MG cells transfected with the 57 kDa form, compared to full length CNA, would reveal if the cleaved form alters these properties. In addition, orthotopic xenografts with MG cells expressing either the cleaved 57 kDa form or the full length CNA would reveal if this cleaved form can enhance tumourigenicity *in vivo*.

Calcineurin is inhibited by cyclosporin A (CsA), an immunosuppressive drug widely used in transplant medicine (Azzi et al., 2013; Matsuda et al., 2000; Shaw et al., 1995). While little data exist regarding the incidence of MG in transplant patients treated with CsA, it has been shown that CsA plays a neuroprotective role following seizure, brain injury, and stroke (Albensi et al., 2000; Borlongan et al., 2005; Jung et al., 2012; Xie et al., 2012). Conversely, CsA reduces proliferation and migration in neural precursor cells, and decreases brain size during zebrafish development (Clift et al., 2015; Skardelly et al., 2013). Treatment with 30 μM CsA induces autophagic and apoptotic cell death in MG cells (Ciechomska et al., 2013), and reduces cell migration at lower concentrations (1-10 μM) in multiple cancer cell lines including MG, prostate, and liver (Kawahara et al., 2015a; Kawahara et al., 2015b; Tie et al., 2013). Inhibition of calcineurin with

CsA or other inhibitors in MG may be a potential therapy to decrease migration in MG, as these tumours are highly invasive, making them difficult to treat.

5.3 Significance

NFI is an important regulator of gliogenesis in the developing central nervous system. Here, we show that NFI promotes expression of the glial genes *GFAP* and *B-FABP*, and represses expression of *HEY1* in MG cells. GFAP and B-FABP are normally expressed in the glial cell lineage and in adult neural stem cells, whereas HEY1 is a Notch effector that promotes maintenance of neural precursor cells. Our data support a conserved role for NFI in glial cell differentiation in development and gliomagenesis. We also identify the calcium-dependent phosphatase calcineurin as an important activator of NFI activity in MG cells. Importantly, we describe a cleaved, activated form of calcineurin that localizes to the nucleus of MG cells, and find a link between nuclear localization of calcineurin and MG cell migration. The cleaved form of CNA reported in this thesis has been previously observed in pathological contexts including excitotoxic neurodegeneration and in Alzheimer's disease. Our findings reveal a novel signaling paradigm through calcineurin-NFI that regulates gene expression in MG cells, and may alter the migratory properties of these cells. We postulate that activated calcineurin may contribute to widespread effects in MG cells through dephosphorylation of additional substrates. The potential pathological activation of calcineurin observed in MG suggests a promising therapeutic avenue for the treatment of MG patients through reduction of cell migration and infiltration.

References

2008. Comprehensive genomic characterization defines human glioblastoma genes and core pathways. *Nature*. 455:1061-1068.

2015. Gene Ontology Consortium: going forward. *Nucleic acids research*. 43:D1049-1056.

Abdul, H.M., M.A. Sama, J.L. Furman, D.M. Mathis, T.L. Beckett, A.M. Weidner, E.S. Patel, I. Baig, M.P. Murphy, H. LeVine, 3rd, S.D. Kraner, and C.M. Norris. 2009. Cognitive decline in Alzheimer's disease is associated with selective changes in calcineurin/NFAT signaling. *The Journal of neuroscience : the official journal of the Society for Neuroscience*. 29:12957-12969.

Ables, J.L., J.J. Breunig, A.J. Eisch, and P. Rakic. 2011. Not(ch) just development: Notch signalling in the adult brain. *Nature reviews. Neuroscience*. 12:269-283.

Agnihotri, S., A. Wolf, D.M. Munoz, C.J. Smith, A. Gajadhar, A. Restrepo, I.D. Clarke, G.N. Fuller, S. Kesari, P.B. Dirks, C.J. McGlade, W.L. Stanford, K. Aldape, P.S. Mischel, C. Hawkins, and A. Guha. 2011. A GATA4-regulated tumor suppressor network represses formation of malignant human astrocytomas. *The Journal of experimental medicine*. 208:689-702.

Agnihotri, S., A. Wolf, D. Picard, C. Hawkins, and A. Guha. 2009. GATA4 is a regulator of astrocyte cell proliferation and apoptosis in the human and murine central nervous system. *Oncogene*. 28:3033-3046.

Aguzzi, A., B.A. Barres, and M.L. Bennett. 2013. Microglia: scapegoat, saboteur, or something else? *Science*. 339:156-161.

Alagarsamy, S., J. Saugstad, L. Warren, I.M. Mansuy, R.W.t. Gereau, and P.J. Conn. 2005. NMDA-induced potentiation of mGluR5 is mediated by activation of protein phosphatase 2B/calcineurin. *Neuropharmacology*. 49 Suppl 1:135-145.

Albensi, B.C., P.G. Sullivan, M.B. Thompson, S.W. Scheff, and M.P. Mattson. 2000. Cyclosporin ameliorates traumatic brain-injury-induced alterations of hippocampal synaptic plasticity. *Experimental neurology*. 162:385-389.

Alevizopoulos, A., Y. Dusserre, U. Ruegg, and N. Mermod. 1997. Regulation of the transforming growth factor beta-responsive transcription factor CTF-1 by calcineurin and calcium/calmodulin-dependent protein kinase IV. *The Journal of biological chemistry*. 272:23597-23605.

Alevizopoulos, A., Y. Dusserre, M. Tsai-Pflugfelder, T. von der Weid, W. Wahli, and N. Mermod. 1995. A proline-rich TGF-beta-responsive transcriptional activator interacts with histone H3. *Genes & development*. 9:3051-3066.

Alevizopoulos, A., and N. Mermod. 1996. Antagonistic regulation of a proline-rich transcription factor by transforming growth factor beta and tumor necrosis factor alpha. *The Journal of biological chemistry*. 271:29672-29681.

Allen, N.J., and B.A. Barres. 2009. Neuroscience: Glia - more than just brain glue. *Nature*. 457:675-677.

Alqudah, M.A., S. Agarwal, M.S. Al-Keilani, Z.A. Sibenaller, T.C. Ryken, and M. Assem. 2013. NOTCH3 is a prognostic factor that promotes glioma cell proliferation, migration and invasion via activation of CCND1 and EGFR. *PloS one*. 8:e77299.

Altmann, H., W. Wendler, and E.L. Winnacker. 1994. Transcriptional activation by CTF proteins is mediated by a bipartite low-proline domain. *Proceedings of the National Academy of Sciences of the United States of America*. 91:3901-3905.

Amemiya, K., R. Traub, L. Durham, and E.O. Major. 1992. Adjacent nuclear factor-1 and activator protein binding sites in the enhancer of the neurotropic JC virus. A common characteristic of many brain-specific genes. *The Journal of biological chemistry*. 267:14204-14211.

Andrin, C., D. McDonald, K.M. Attwood, A. Rodrigue, S. Ghosh, R. Mirzayans, J.Y. Masson, G. Dellaire, and M.J. Hendzel. 2012. A requirement for polymerized actin in DNA double-strand break repair. *Nucleus*. 3:384-395.

Angelastro, J.M., T.N. Ignatova, V.G. Kukekov, D.A. Steindler, G.B. Stengren, C. Mendelsohn, and L.A. Greene. 2003. Regulated expression of ATF5 is required for the progression of neural progenitor cells to neurons. *The Journal of neuroscience : the official journal of the Society for Neuroscience*. 23:4590-4600.

Angelastro, J.M., J.L. Mason, T.N. Ignatova, V.G. Kukekov, G.B. Stengren, J.E. Goldman, and L.A. Greene. 2005. Downregulation of activating transcription factor 5 is required for differentiation of neural progenitor cells into astrocytes. *The Journal of neuroscience : the official journal of the Society for Neuroscience*. 25:3889-3899.

Anthony, T.E., C. Klein, G. Fishell, and N. Heintz. 2004. Radial glia serve as neuronal progenitors in all regions of the central nervous system. *Neuron*. 41:881-890.

Anthony, T.E., H.A. Mason, T. Gridley, G. Fishell, and N. Heintz. 2005. Brain lipid-binding protein is a direct target of Notch signaling in radial glial cells. *Genes Dev*. 19:1028-1033.

Apt, D., Y. Liu, and H.U. Bernard. 1994. Cloning and functional analysis of spliced isoforms of human nuclear factor I-X: interference with transcriptional activation by NFI/CTF in a cell-type specific manner. *Nucleic acids research*. 22:3825-3833.

Arai, Y., N. Funatsu, K. Numayama-Tsuruta, T. Nomura, S. Nakamura, and N. Osumi. 2005. Role of Fabp7, a downstream gene of Pax6, in the maintenance of neuroepithelial cells during early embryonic development of the rat cortex. *J Neurosci*. 25:9752-9761.

Aramburu, J., A. Rao, and C.B. Klee. 2000. Calcineurin: from structure to function. *Current topics in cellular regulation*. 36:237-295.

Aramburu, J., M.B. Yaffe, C. Lopez-Rodriguez, L.C. Cantley, P.G. Hogan, and A. Rao. 1999. Affinity-driven peptide selection of an NFAT inhibitor more selective than cyclosporin A. *Science*. 285:2129-2133.

Aranguren, X.L., M. Beerens, G. Coppiello, C. Wiese, I. Vandersmissen, A. Lo Nigro, C.M. Verfaillie, M. Gessler, and A. Luttun. 2013. COUP-TFII orchestrates venous and lymphatic endothelial identity by homo- or hetero-dimerisation with PROX1. *Journal of cell science*. 126:1164-1175.

Araque, A., G. Carmignoto, P.G. Haydon, S.H. Oliet, R. Robitaille, and A. Volterra. 2014. Gliotransmitters travel in time and space. *Neuron*. 81:728-739.

Archer, T.K., P. Lefebvre, R.G. Wolford, and G.L. Hager. 1992. Transcription factor loading on the MMTV promoter: a bimodal mechanism for promoter activation. *Science*. 255:1573-1576.

Armentero, M.T., M. Horwitz, and N. Mermod. 1994. Targeting of DNA polymerase to the adenovirus origin of DNA replication by interaction with nuclear factor I. *Proceedings of the National Academy of Sciences of the United States of America*. 91:11537-11541.

Ashburner, M., C.A. Ball, J.A. Blake, D. Botstein, H. Butler, J.M. Cherry, A.P. Davis, K. Dolinski, S.S. Dwight, J.T. Eppig, M.A. Harris, D.P. Hill, L. Issel-Tarver, A. Kasarskis, S. Lewis, J.C. Matese, J.E. Richardson, M. Ringwald, G.M. Rubin, and G. Sherlock. 2000. Gene ontology: tool for the unification of biology. The Gene Ontology Consortium. *Nature genetics*. 25:25-29.

Azzi, J.R., M.H. Sayegh, and S.G. Mallat. 2013. Calcineurin inhibitors: 40 years later, can't live without. *J Immunol*. 191:5785-5791.

Bachoo, R.M., E.A. Maher, K.L. Ligon, N.E. Sharpless, S.S. Chan, M.J. You, Y. Tang, J. DeFrances, E. Stover, R. Weissleder, D.H. Rowitch, D.N. Louis, and R.A. DePinho. 2002. Epidermal growth factor receptor and Ink4a/Arf: convergent mechanisms governing terminal differentiation and transformation along the neural stem cell to astrocyte axis. *Cancer cell*. 1:269-277.

Bachurski, C.J., G.H. Yang, T.A. Currier, R.M. Gronostajski, and D. Hong. 2003. Nuclear factor I/thyroid transcription factor 1 interactions modulate surfactant protein C transcription. *Molecular and cellular biology*. 23:9014-9024.

Baek, J.H., J. Hatakeyama, S. Sakamoto, T. Ohtsuka, and R. Kageyama. 2006. Persistent and high levels of Hes1 expression regulate boundary formation in the developing central nervous system. *Development*. 133:2467-2476.

Bar, E.E., A. Lin, V. Mahairaki, W. Matsui, and C.G. Eberhart. 2010. Hypoxia increases the expression of stem-cell markers and promotes clonogenicity in glioblastoma neurospheres. *The American journal of pathology*. 177:1491-1502.

Barani, I.J., and D.A. Larson. 2015. Radiation therapy of glioblastoma. *Cancer treatment and research*. 163:49-73.

Barker, C.A., M. Chang, K. Beal, and T.A. Chan. 2014. Survival of patients treated with radiation therapy for anaplastic astrocytoma. *Radiology and oncology*. 48:381-386.

Barnabe-Heider, F., J.A. Wasylnka, K.J. Fernandes, C. Porsche, M. Sendtner, D.R. Kaplan, and F.D. Miller. 2005. Evidence that embryonic neurons regulate the onset of cortical gliogenesis via cardiotrophin-1. *Neuron*. 48:253-265.

Barry, G., M. Piper, C. Lindwall, R. Moldrich, S. Mason, E. Little, A. Sarkar, S. Tole, R.M. Gronostajski, and L.J. Richards. 2008. Specific glial populations regulate hippocampal morphogenesis. *The Journal of neuroscience : the official journal of the Society for Neuroscience*. 28:12328-12340.

Baumgartel, K., and I.M. Mansuy. 2012. Neural functions of calcineurin in synaptic plasticity and memory. *Learn Mem*. 19:375-384.

Beals, C.R., N.A. Clipstone, S.N. Ho, and G.R. Crabtree. 1997. Nuclear localization of NF-ATc by a calcineurin-dependent, cyclosporin-sensitive intramolecular interaction. *Genes & development*. 11:824-834.

Beier, D., P. Hau, M. Proescholdt, A. Lohmeier, J. Wischhusen, P.J. Oefner, L. Aigner, A. Brawanski, U. Bogdahn, and C.P. Beier. 2007. CD133(+) and CD133(-) glioblastoma-derived cancer stem cells show differential growth characteristics and molecular profiles. *Cancer research*. 67:4010-4015.

Besnard, F., M. Brenner, Y. Nakatani, R. Chao, H.J. Purohit, and E. Freese. 1991. Multiple interacting sites regulate astrocyte-specific transcription of the human gene for glial fibrillary acidic protein. *J Biol Chem*. 266:18877-18883.

Betancourt, J., S. Katzman, and B. Chen. 2014. Nuclear factor one B regulates neural stem cell differentiation and axonal projection of corticofugal neurons. *The Journal of comparative neurology*. 522:6-35.

Bisgrove, D.A., E.A. Monckton, M. Packer, and R. Godbout. 2000. Regulation of brain fatty acid-binding protein expression by differential phosphorylation of nuclear factor I in malignant glioma cell lines. *The Journal of biological chemistry*. 275:30668-30676.

Bleoo, S., X. Sun, M.J. Hendzel, J.M. Rowe, M. Packer, and R. Godbout. 2001. Association of human DEAD box protein DDX1 with a cleavage stimulation factor

involved in 3'-end processing of pre-MRNA. *Molecular biology of the cell*. 12:3046-3059.

Bloch, O. 2015. Immunotherapy for malignant gliomas. *Cancer treatment and research*. 163:143-158.

Bohnen, N.I., and K. Radhakrishnan. 1997. Cancer of the Nervous System. Blackwell Science, Cambridge.

Bonni, A., Y. Sun, M. Nadal-Vicens, A. Bhatt, D.A. Frank, I. Rozovsky, N. Stahl, G.D. Yancopoulos, and M.E. Greenberg. 1997. Regulation of gliogenesis in the central nervous system by the JAK-STAT signaling pathway. *Science*. 278:477-483.

Borgmeyer, U., J. Nowock, and A.E. Sippel. 1984. The TGGCA-binding protein: a eukaryotic nuclear protein recognizing a symmetrical sequence on double-stranded linear DNA. *Nucleic acids research*. 12:4295-4311.

Borlongan, C.V., G. Yu, N. Matsukawa, L. Xu, D.C. Hess, P.R. Sanberg, and Y. Wang. 2005. Acute functional effects of cyclosporine-A and methylprednisolone treatment in adult rats exposed to transient ischemic stroke. *Life sciences*. 76:1503-1512.

Bosher, J., A. Dawson, and R.T. Hay. 1992. Nuclear factor I is specifically targeted to discrete subnuclear sites in adenovirus type 2-infected cells. *Journal of virology*. 66:3140-3150.

Bosser, R., R. Aligue, D. Guerini, N. Agell, E. Carafoli, and O. Bachs. 1993. Calmodulin can modulate protein phosphorylation in rat liver cells nuclei. *The Journal of biological chemistry*. 268:15477-15483.

Brat, D.J., A.A. Castellano-Sanchez, S.B. Hunter, M. Pecot, C. Cohen, E.H. Hammond, S.N. Devi, B. Kaur, and E.G. Van Meir. 2004. Pseudopalisades in glioblastoma are hypoxic, express extracellular matrix proteases, and are formed by an actively migrating cell population. *Cancer research*. 64:920-927.

Bray, S.J. 2006. Notch signalling: a simple pathway becomes complex. *Nature reviews. Molecular cell biology*. 7:678-689.

Brennan, C.W., R.G. Verhaak, A. McKenna, B. Campos, H. Noushmehr, S.R. Salama, S. Zheng, D. Chakravarty, J.Z. Sanborn, S.H. Berman, R. Beroukhim, B. Bernard, C.J. Wu, G. Genovese, I. Shmulevich, J. Barnholtz-Sloan, L. Zou, R. Vegesna, S.A. Shukla, G. Ciriello, W.K. Yung, W. Zhang, C. Sougnez, T. Mikkelsen, K. Aldape, D.D. Bigner, E.G. Van Meir, M. Prados, A. Sloan, K.L. Black, J. Eschbacher, G. Finocchiaro, W. Friedman, D.W. Andrews, A. Guha, M. Iacocca, B.P. O'Neill, G. Foltz, J. Myers, D.J. Weisenberger, R. Penny, R. Kucherlapati, C.M. Perou, D.N. Hayes, R. Gibbs, M. Marra, G.B. Mills, E. Lander, P. Spellman, R. Wilson, C. Sander, J. Weinstein, M. Meyerson, S. Gabriel, P.W. Laird, D.

Haussler, G. Getz, and L. Chin. 2013. The somatic genomic landscape of glioblastoma. *Cell*. 155:462-477.

Briscoe, J., A. Pierani, T.M. Jessell, and J. Ericson. 2000. A homeodomain protein code specifies progenitor cell identity and neuronal fate in the ventral neural tube. *Cell*. 101:435-445.

Buas, M.F., S. Kabak, and T. Kadesch. 2010. The Notch effector Hey1 associates with myogenic target genes to repress myogenesis. *The Journal of biological chemistry*. 285:1249-1258.

Bueno, O.F., E.B. Brandt, M.E. Rothenberg, and J.D. Molkentin. 2002. Defective T cell development and function in calcineurin A beta -deficient mice. *Proceedings of the National Academy of Sciences of the United States of America*. 99:9398-9403.

Buffo, A., I. Rite, P. Tripathi, A. Lepier, D. Colak, A.P. Horn, T. Mori, and M. Gotz. 2008. Origin and progeny of reactive gliosis: A source of multipotent cells in the injured brain. *Proceedings of the National Academy of Sciences of the United States of America*. 105:3581-3586.

Burgoyne, R.D., and L.P. Haynes. 2014. Sense and specificity in neuronal calcium signalling. *Biochimica et biophysica acta*.

Burkard, N., J. Becher, C. Heindl, L. Neyses, K. Schuh, and O. Ritter. 2005. Targeted proteolysis sustains calcineurin activation. *Circulation*. 111:1045-1053.

Cai, L., E.M. Morrow, and C.L. Cepko. 2000. Misexpression of basic helix-loop-helix genes in the murine cerebral cortex affects cell fate choices and neuronal survival. *Development*. 127:3021-3030.

Campbell, C.E., M. Piper, C. Plachez, Y.T. Yeh, J.S. Baizer, J.M. Osinski, E.D. Litwack, L.J. Richards, and R.M. Gronostajski. 2008. The transcription factor Nfix is essential for normal brain development. *BMC developmental biology*. 8:52.

Cardinale, R., M. Won, A. Choucair, M. Gillin, A. Chakravarti, C. Schultz, L. Souhami, A. Chen, H. Pham, and M. Mehta. 2006. A phase II trial of accelerated radiotherapy using weekly stereotactic conformal boost for supratentorial glioblastoma multiforme: RTOG 0023. *International journal of radiation oncology, biology, physics*. 65:1422-1428.

Carrion, A.M., W.A. Link, F. Ledo, B. Mellstrom, and J.R. Naranjo. 1999. DREAM is a Ca2+-regulated transcriptional repressor. *Nature*. 398:80-84.

Casper, K.B., and K.D. McCarthy. 2006. GFAP-positive progenitor cells produce neurons and oligodendrocytes throughout the CNS. *Molecular and cellular neurosciences*. 31:676-684.

Catania, A., S. Urban, E. Yan, C. Hao, G. Barron, and J. Allalunis-Turner. 2001. Expression and localization of cyclin-dependent kinase 5 in apoptotic human glioma cells. *Neuro-oncology*. 3:89-98.

Cattaneo, E., L. Conti, and C. De-Fraja. 1999. Signalling through the JAK-STAT pathway in the developing brain. *Trends in neurosciences*. 22:365-369.

Cebolla, B., A. Fernandez-Perez, G. Perea, A. Araque, and M. Vallejo. 2008. DREAM mediates cAMP-dependent, Ca2+-induced stimulation of GFAP gene expression and regulates cortical astrogliogenesis. *The Journal of neuroscience : the official journal of the Society for Neuroscience*. 28:6703-6713.

Cebolla, B., and M. Vallejo. 2006. Nuclear factor-I regulates glial fibrillary acidic protein gene expression in astrocytes differentiated from cortical precursor cells. *Journal of neurochemistry*. 97:1057-1070.

Chan, A.Y., S.J. Coniglio, Y.Y. Chuang, D. Michaelson, U.G. Knaus, M.R. Philips, and M. Symons. 2005. Roles of the Rac1 and Rac3 GTPases in human tumor cell invasion. *Oncogene*. 24:7821-7829.

Chaudhry, A.Z., G.E. Lyons, and R.M. Gronostajski. 1997. Expression patterns of the four nuclear factor I genes during mouse embryogenesis indicate a potential role in development. *Developmental dynamics : an official publication of the American Association of Anatomists*. 208:313-325.

Chaudhry, A.Z., A.D. Vitullo, and R.M. Gronostajski. 1998. Nuclear factor I (NFI) isoforms differentially activate simple versus complex NFI-responsive promoters. *The Journal of biological chemistry*. 273:18538-18546.

Chaudhry, A.Z., A.D. Vitullo, and R.M. Gronostajski. 1999. Nuclear factor I-mediated repression of the mouse mammary tumor virus promoter is abrogated by the coactivators p300/CBP and SRC-1. *The Journal of biological chemistry*. 274:7072-7081.

Chedotal, A. 2010. Should I stay or should I go? Becoming a granule cell. *Trends in neurosciences*. 33:163-172.

Chen, J., R.M. McKay, and L.F. Parada. 2012. Malignant glioma: lessons from genomics, mouse models, and stem cells. *Cell*. 149:36-47.

Chen, R., M. Liu, H. Li, Y. Xue, W.N. Ramey, N. He, N. Ai, H. Luo, Y. Zhu, N. Zhou, and Q. Zhou. 2008. PP2B and PP1alpha cooperatively disrupt 7SK snRNP to release P-TEFb for transcription in response to Ca2+ signaling. *Genes & development*. 22:1356-1368.

Chen, R., M.C. Nishimura, S.M. Bumbaca, S. Kharbanda, W.F. Forrest, I.M. Kasman, J.M. Greve, R.H. Soriano, L.L. Gilmour, C.S. Rivers, Z. Modrusan, S. Nacu, S. Guerrero, K.A. Edgar, J.J. Wallin, K. Lamszus, M. Westphal, S. Heim,

C.D. James, S.R. VandenBerg, J.F. Costello, S. Moorefield, C.J. Cowdrey, M. Prados, and H.S. Phillips. 2010. A hierarchy of self-renewing tumor-initiating cell types in glioblastoma. *Cancer cell*. 17:362-375.

Chen, W.J., and R.K. Liem. 1994. Reexpression of glial fibrillary acidic protein rescues the ability of astrocytoma cells to form processes in response to neurons. *J Cell Biol*. 127:813-823.

Chinnaiyan, P., E. Kensicki, G. Bloom, A. Prabhu, B. Sarcar, S. Kahali, S. Eschrich, X. Qu, P. Forsyth, and R. Gillies. 2012. The metabolomic signature of malignant glioma reflects accelerated anabolic metabolism. *Cancer research*. 72:5878-5888.

Chinot, O.L., W. Wick, and T. Cloughesy. 2014. Bevacizumab for newly diagnosed glioblastoma. *The New England journal of medicine*. 370:2049.

Cho, A., Y. Tang, J. Davila, S. Deng, L. Chen, E. Miller, M. Wernig, and I.A. Graef. 2014. Calcineurin signaling regulates neural induction through antagonizing the BMP pathway. *Neuron*. 82:109-124.

Ciechomska, I.A., K. Gabrusiewicz, A.A. Szczepankiewicz, and B. Kaminska. 2013. Endoplasmic reticulum stress triggers autophagy in malignant glioma cells undergoing cyclosporine a-induced cell death. *Oncogene*. 32:1518-1529.

Ciriello, G., E. Cerami, C. Sander, and N. Schultz. 2012. Mutual exclusivity analysis identifies oncogenic network modules. *Genome research*. 22:398-406.

Clark, G.D. 2002. Brain development and the genetics of brain development. *Neurologic clinics*. 20:917-939.

Clarke, K., K. Smith, W.J. Gullick, and A.L. Harris. 2001. Mutant epidermal growth factor receptor enhances induction of vascular endothelial growth factor by hypoxia and insulin-like growth factor-1 via a PI3 kinase dependent pathway. *British journal of cancer*. 84:1322-1329.

Clift, D.E., R.J. Thorn, E.A. Passarelli, M. Kapoor, M.K. LoPiccolo, H.A. Richendrfer, R.M. Colwill, and R. Creton. 2015. Effects of embryonic cyclosporine exposures on brain development and behavior. *Behavioural brain research*. 282:117-124.

Clipstone, N.A., and G.R. Crabtree. 1992. Identification of calcineurin as a key signalling enzyme in T-lymphocyte activation. *Nature*. 357:695-697.

Coghlan, V.M., B.A. Perrino, M. Howard, L.K. Langeberg, J.B. Hicks, W.M. Gallatin, and J.D. Scott. 1995. Association of protein kinase A and protein phosphatase 2B with a common anchoring protein. *Science*. 267:108-111.

Cohen, R.B., M. Sheffery, and C.G. Kim. 1986. Partial purification of a nuclear protein that binds to the CCAAT box of the mouse alpha 1-globin gene. *Molecular and cellular biology*. 6:821-832.

Cooke, D.W., and M.D. Lane. 1999a. Transcription factor NF1 mediates repression of the GLUT4 promoter by cyclic-AMP. *Biochemical and biophysical research communications*. 260:600-604.

Cooke, D.W., and M.D. Lane. 1999b. The transcription factor nuclear factor I mediates repression of the GLUT4 promoter by insulin. *The Journal of biological chemistry*. 274:12917-12924.

Cormack, B., and I. Castano. 2002. Introduction of point mutations into cloned genes. *Methods Enzymol*. 350:199-218.

Cornell-Bell, A.H., S.M. Finkbeiner, M.S. Cooper, and S.J. Smith. 1990. Glutamate induces calcium waves in cultured astrocytes: long-range glial signaling. *Science*. 247:470-473.

Cuddapah, V.A., S. Robel, S. Watkins, and H. Sontheimer. 2014. A neurocentric perspective on glioma invasion. *Nature reviews. Neuroscience*. 15:455-465.

Culican, S.M., N.L. Baumrind, M. Yamamoto, and A.L. Pearlman. 1990. Cortical radial glia: identification in tissue culture and evidence for their transformation to astrocytes. *J Neurosci*. 10:684-692.

Cyert, M.S. 2001. Regulation of nuclear localization during signaling. *The Journal of biological chemistry*. 276:20805-20808.

Czirjak, G., and P. Enyedi. 2006. Targeting of calcineurin to an NFAT-like docking site is required for the calcium-dependent activation of the background K+ channel, TRESK. *The Journal of biological chemistry*. 281:14677-14682.

Czirjak, G., Z.E. Toth, and P. Enyedi. 2004. The two-pore domain K+ channel, TRESK, is activated by the cytoplasmic calcium signal through calcineurin. *The Journal of biological chemistry*. 279:18550-18558.

Dacher, M., S. Gouty, S. Dash, B.M. Cox, and F.S. Nugent. 2013. A-kinase anchoring protein-calcineurin signaling in long-term depression of GABAergic synapses. *The Journal of neuroscience : the official journal of the Society for Neuroscience*. 33:2650-2660.

Dahlqvist, C., A. Blokzijl, G. Chapman, A. Falk, K. Dannaeus, C.F. Ibanez, and U. Lendahl. 2003. Functional Notch signaling is required for BMP4-induced inhibition of myogenic differentiation. *Development*. 130:6089-6099.

das Neves, L., C.S. Duchala, F. Tolentino-Silva, M.A. Haxhiu, C. Colmenares, W.B. Macklin, C.E. Campbell, K.G. Butz, and R.M. Gronostajski. 1999a. Disruption

of the murine nuclear factor I-A gene (Nfia) results in perinatal lethality, hydrocephalus, and agenesis of the corpus callosum. *Proceedings of the National Academy of Sciences of the United States of America*. 96:11946-11951.

das Neves, L., C.S. Duchala, F. Tolentino-Silva, M.A. Haxhiu, C. Colmenares, W.B. Macklin, C.E. Campbell, K.G. Butz, R.M. Gronostajski, and F. Godinho. 1999b. Disruption of the murine nuclear factor I-A gene (Nfia) results in perinatal lethality, hydrocephalus, and agenesis of the corpus callosum. *Proc Natl Acad Sci U S A*. 96:11946-11951.

Davies, K.J., G. Ermak, B.A. Rothermel, M. Pritchard, J. Heitman, J. Ahnn, F. Henrique-Silva, D. Crawford, S. Canaider, P. Strippoli, P. Carinci, K.T. Min, D.S. Fox, K.W. Cunningham, R. Bassel-Duby, E.N. Olson, Z. Zhang, R.S. Williams, H.P. Gerber, M. Perez-Riba, H. Seo, X. Cao, C.B. Klee, J.M. Redondo, L.J. Maltais, E.A. Bruford, S. Povey, J.D. Molkentin, F.D. McKeon, E.J. Duh, G.R. Crabtree, M.S. Cyert, S. de la Luna, and X. Estivill. 2007. Renaming the DSCR1/Adapt78 gene family as RCAN: regulators of calcineurin. *FASEB journal : official publication of the Federation of American Societies for Experimental Biology*. 21:3023-3028.

Dawson, T.M., J.P. Steiner, W.E. Lyons, M. Fotuhi, M. Blue, and S.H. Snyder. 1994. The immunophilins, FK506 binding protein and cyclophilin, are discretely localized in the brain: relationship to calcineurin. *Neuroscience*. 62:569-580.

De Rosa, A., S. Pellegatta, M. Rossi, P. Tunici, L. Magnoni, M.C. Speranza, F. Malusa, V. Miragliotta, E. Mori, G. Finocchiaro, and A. Bakker. 2012. A radial glia gene marker, fatty acid binding protein 7 (FABP7), is involved in proliferation and invasion of glioblastoma cells. *PloS one*. 7:e52113.

DeAngelis, L.M. 2001. Brain tumors. *The New England journal of medicine*. 344:114-123.

Dell'albani, P., M. Rodolico, R. Pellitteri, E. Tricarichi, S.A. Torrisi, S. D'Antoni, M. Zappia, V. Albanese, R. Caltabiano, N. Platania, E. Aronica, and M.V. Catania. 2014. Differential patterns of NOTCH1-4 receptor expression are markers of glioma cell differentiation. *Neuro-oncology*. 16:204-216.

Deltour, I., A. Auvinen, M. Feychting, C. Johansen, L. Klaeboe, R. Sankila, and J. Schuz. 2012. Mobile phone use and incidence of glioma in the Nordic countries 1979-2008: consistency check. *Epidemiology*. 23:301-307.

Deneen, B., R. Ho, A. Lukaszewicz, C.J. Hochstim, R.M. Gronostajski, and D.J. Anderson. 2006. The transcription factor NFIA controls the onset of gliogenesis in the developing spinal cord. *Neuron*. 52:953-968.

Denny, B.J., R.T. Wheelhouse, M.F. Stevens, L.L. Tsang, and J.A. Slack. 1994. NMR and molecular modeling investigation of the mechanism of activation of the

antitumor drug temozolomide and its interaction with DNA. *Biochemistry*. 33:9045-9051.

Deorah, S., C.F. Lynch, Z.A. Sibenaller, and T.C. Ryken. 2006. Trends in brain cancer incidence and survival in the United States: Surveillance, Epidemiology, and End Results Program, 1973 to 2001. *Neurosurgical focus*. 20:E1.

Dhavan, R., and L.H. Tsai. 2001. A decade of CDK5. *Nature reviews. Molecular cell biology*. 2:749-759.

Di Croce, L., R. Koop, P. Venditti, H.M. Westphal, K.P. Nightingale, D.F. Corona, P.B. Becker, and M. Beato. 1999. Two-step synergism between the progesterone receptor and the DNA-binding domain of nuclear factor 1 on MMTV minichromosomes. *Molecular cell*. 4:45-54.

Dick, F.A., and S.M. Rubin. 2013. Molecular mechanisms underlying RB protein function. *Nature reviews. Molecular cell biology*. 14:297-306.

Dignam, J.D., R.M. Lebovitz, and R.G. Roeder. 1983. Accurate transcription initiation by RNA polymerase II in a soluble extract from isolated mammalian nuclei. *Nucleic Acids Res*. 11:1475-1489.

Ding, B., W. Wang, T. Selvakumar, H.S. Xi, H. Zhu, C.W. Chow, J.D. Horton, R.M. Gronostajski, and D.L. Kilpatrick. 2013. Temporal regulation of nuclear factor one occupancy by calcineurin/NFAT governs a voltage-sensitive developmental switch in late maturing neurons. *The Journal of neuroscience : the official journal of the Society for Neuroscience*. 33:2860-2872.

Ding, S., T. Fellin, Y. Zhu, S.Y. Lee, Y.P. Auberson, D.F. Meaney, D.A. Coulter, G. Carmignoto, and P.G. Haydon. 2007. Enhanced astrocytic Ca2+ signals contribute to neuronal excitotoxicity after status epilepticus. *The Journal of neuroscience : the official journal of the Society for Neuroscience*. 27:10674-10684.

Dirks, P.B. 2001. Glioma migration: clues from the biology of neural progenitor cells and embryonic CNS cell migration. *Journal of neuro-oncology*. 53:203-212.

Doetsch, F. 2003a. The glial identity of neural stem cells. *Nature neuroscience*. 6:1127-1134.

Doetsch, F. 2003b. A niche for adult neural stem cells. *Current opinion in genetics & development*. 13:543-550.

Doetsch, F., I. Caille, D.A. Lim, J.M. Garcia-Verdugo, and A. Alvarez-Buylla. 1999a. Subventricular zone astrocytes are neural stem cells in the adult mammalian brain. *Cell*. 97:703-716.

Doetsch, F., J.M. Garcia-Verdugo, and A. Alvarez-Buylla. 1997. Cellular composition and three-dimensional organization of the subventricular germinal

zone in the adult mammalian brain. *The Journal of neuroscience : the official journal of the Society for Neuroscience*. 17:5046-5061.

Doetsch, F., J.M. Garcia-Verdugo, and A. Alvarez-Buylla. 1999b. Regeneration of a germinal layer in the adult mammalian brain. *Proceedings of the National Academy of Sciences of the United States of America*. 96:11619-11624.

Dolecek, T.A., J.M. Propp, N.E. Stroup, and C. Kruchko. 2012. CBTRUS statistical report: primary brain and central nervous system tumors diagnosed in the United States in 2005-2009. *Neuro-oncology*. 14 Suppl 5:v1-49.

Donella-Deana, A., M.H. Krinks, M. Ruzzene, C. Klee, and L.A. Pinna. 1994. Dephosphorylation of phosphopeptides by calcineurin (protein phosphatase 2B). *European journal of biochemistry / FEBS*. 219:109-117.

Donovan, J., A. Kordylewska, Y.N. Jan, and M.F. Utset. 2002. Tetralogy of fallot and other congenital heart defects in Hey2 mutant mice. *Current biology : CB*. 12:1605-1610.

Dooley, A.L., M.M. Winslow, D.Y. Chiang, S. Banerji, N. Stransky, T.L. Dayton, E.L. Snyder, S. Senna, C.A. Whittaker, R.T. Bronson, D. Crowley, J. Barretina, L. Garraway, M. Meyerson, and T. Jacks. 2011. Nuclear factor I/B is an oncogene in small cell lung cancer. *Genes & development*. 25:1470-1475.

Driller, K., A. Pagenstecher, M. Uhl, H. Omran, A. Berlis, A. Grunder, and A.E. Sippel. 2007. Nuclear factor I X deficiency causes brain malformation and severe skeletal defects. *Mol Cell Biol*. 27:3855-3867.

Dubrow, R., and A.S. Darefsky. 2011. Demographic variation in incidence of adult glioma by subtype, United States, 1992-2007. *BMC cancer*. 11:325.

Duffy, S., and B.A. MacVicar. 1996. In vitro ischemia promotes calcium influx and intracellular calcium release in hippocampal astrocytes. *The Journal of neuroscience : the official journal of the Society for Neuroscience*. 16:71-81.

Dunham, C. 2010. Pediatric brain tumors: a histologic and genetic update on commonly encountered entities. *Seminars in diagnostic pathology*. 27:147-159.

Dunn, G.P., M.L. Rinne, J. Wykosky, G. Genovese, S.N. Quayle, I.F. Dunn, P.K. Agarwalla, M.G. Chheda, B. Campos, A. Wang, C. Brennan, K.L. Ligon, F. Furnari, W.K. Cavenee, R.A. Depinho, L. Chin, and W.C. Hahn. 2012. Emerging insights into the molecular and cellular basis of glioblastoma. *Genes & development*. 26:756-784.

Dusserre, Y., and N. Mermod. 1992. Purified cofactors and histone H1 mediate transcriptional regulation by CTF/NF-I. *Molecular and cellular biology*. 12:5228-5237.

Easaw, J.C., W.P. Mason, J. Perry, N. Laperriere, D.D. Eisenstat, R. Del Maestro, K. Belanger, D. Fulton, and D. Macdonald. 2011. Canadian recommendations for the treatment of recurrent or progressive glioblastoma multiforme. *Curr Oncol*. 18:e126-136.

Eastwood, S.L., T. Salih, and P.J. Harrison. 2005. Differential expression of calcineurin A subunit mRNA isoforms during rat hippocampal and cerebellar development. *The European journal of neuroscience*. 22:3017-3024.

el-Deiry, W.S., J.W. Harper, P.M. O'Connor, V.E. Velculescu, C.E. Canman, J. Jackman, J.A. Pietenpol, M. Burrell, D.E. Hill, Y. Wang, and et al. 1994. WAF1/CIP1 is induced in p53-mediated G1 arrest and apoptosis. *Cancer research*. 54:1169-1174.

El Hindy, N., K. Keyvani, A. Pagenstecher, P. Dammann, I.E. Sandalcioglu, U. Sure, and Y. Zhu. 2013. Implications of Dll4-Notch signaling activation in primary glioblastoma multiforme. *Neuro-oncology*. 15:1366-1378.

Emery, B. 2010. Regulation of oligodendrocyte differentiation and myelination. *Science*. 330:779-782.

Eng, L.F. 1985. Glial fibrillary acidic protein (GFAP): the major protein of glial intermediate filaments in differentiated astrocytes. *Journal of neuroimmunology*. 8:203-214.

Eng, L.F., and L.J. Rubinstein. 1978. Contribution of immunohistochemistry to diagnostic problems of human cerebral tumors. *The journal of histochemistry and cytochemistry : official journal of the Histochemistry Society*. 26:513-522.

Engelhard, H.H., H.A. Duncan, and M. Dal Canto. 1997. Molecular characterization of glioblastoma cell differentiation. *Neurosurgery*. 41:886-896; discussion 896-887.

Enz, A., G. Shapiro, A. Chappuis, and A. Dattler. 1994. Nonradioactive assay for protein phosphatase 2B (calcineurin) activity using a partial sequence of the subunit of cAMP-dependent protein kinase as substrate. *Analytical biochemistry*. 216:147-153.

Ermak, G., C.D. Harris, and K.J. Davies. 2002. The DSCR1 (Adapt78) isoform 1 protein calcipressin 1 inhibits calcineurin and protects against acute calcium-mediated stress damage, including transient oxidative stress. *FASEB journal : official publication of the Federation of American Societies for Experimental Biology*. 16:814-824.

Esnault, G., S. Majocchi, D. Martinet, N. Besuchet-Schmutz, J.S. Beckmann, and N. Mermod. 2009. Transcription factor CTF1 acts as a chromatin domain boundary that shields human telomeric genes from silencing. *Molecular and cellular biology*. 29:2409-2418.

Esteller, M., S.R. Hamilton, P.C. Burger, S.B. Baylin, and J.G. Herman. 1999. Inactivation of the DNA repair gene O6-methylguanine-DNA methyltransferase by promoter hypermethylation is a common event in primary human neoplasia. *Cancer research*. 59:793-797.

Fancy, S.P., S.M. Glasgow, M. Finley, D.H. Rowitch, and B. Deneen. 2012. Evidence that nuclear factor IA inhibits repair after white matter injury. *Annals of neurology*. 72:224-233.

Farber, L.H., F.J. Wilson, and D.J. Wolff. 1987. Calmodulin-dependent phosphatases of PC12, GH3, and C6 cells: physical, kinetic, and immunochemical properties. *Journal of neurochemistry*. 49:404-414.

Feng, L., M.E. Hatten, and N. Heintz. 1994. Brain lipid-binding protein (BLBP): a novel signaling system in the developing mammalian CNS. *Neuron*. 12:895-908.

Feng, L., and N. Heintz. 1995. Differentiating neurons activate transcription of the brain lipid-binding protein gene in radial glia through a novel regulatory element. *Development*. 121:1719-1730.

Fernandez, A.M., S. Fernandez, P. Carrero, M. Garcia-Garcia, and I. Torres-Aleman. 2007. Calcineurin in reactive astrocytes plays a key role in the interplay between proinflammatory and anti-inflammatory signals. *The Journal of neuroscience : the official journal of the Society for Neuroscience*. 27:8745-8756.

Ferreira, A., R. Kincaid, and K.S. Kosik. 1993. Calcineurin is associated with the cytoskeleton of cultured neurons and has a role in the acquisition of polarity. *Molecular biology of the cell*. 4:1225-1238.

Fiol, C.J., A.M. Mahrenholz, Y. Wang, R.W. Roeske, and P.J. Roach. 1987. Formation of protein kinase recognition sites by covalent modification of the substrate. Molecular mechanism for the synergistic action of casein kinase II and glycogen synthase kinase 3. *The Journal of biological chemistry*. 262:14042-14048.

Fischer, A., and M. Gessler. 2007. Delta-Notch--and then? Protein interactions and proposed modes of repression by Hes and Hey bHLH factors. *Nucleic acids research*. 35:4583-4596.

Fischer, A., J. Klattig, B. Kneitz, H. Diez, M. Maier, B. Holtmann, C. Englert, and M. Gessler. 2005. Hey basic helix-loop-helix transcription factors are repressors of GATA4 and GATA6 and restrict expression of the GATA target gene ANF in fetal hearts. *Molecular and cellular biology*. 25:8960-8970.

Fischer, A., N. Schumacher, M. Maier, M. Sendtner, and M. Gessler. 2004. The Notch target genes Hey1 and Hey2 are required for embryonic vascular development. *Genes & development*. 18:901-911.

Fischer, A., C. Steidl, T.U. Wagner, E. Lang, P.M. Jakob, P. Friedl, K.P. Knobeloch, and M. Gessler. 2007. Combined loss of Hey1 and HeyL causes congenital heart defects because of impaired epithelial to mesenchymal transition. *Circulation research*. 100:856-863.

Fiveash, J.B., and S.A. Spencer. 2003. Role of radiation therapy and radiosurgery in glioblastoma multiforme. *Cancer J*. 9:222-229.

Fletcher, C.F., N.A. Jenkins, N.G. Copeland, A.Z. Chaudhry, and R.M. Gronostajski. 1999. Exon structure of the nuclear factor I DNA-binding domain from C. elegans to mammals. *Mammalian genome : official journal of the International Mammalian Genome Society*. 10:390-396.

Forsyth, P.A., H. Wong, T.D. Laing, N.B. Rewcastle, D.G. Morris, H. Muzik, K.J. Leco, R.N. Johnston, P.M. Brasher, G. Sutherland, and D.R. Edwards. 1999. Gelatinase-A (MMP-2), gelatinase-B (MMP-9) and membrane type matrix metalloproteinase-1 (MT1-MMP) are involved in different aspects of the pathophysiology of malignant gliomas. *British journal of cancer*. 79:1828-1835.

Frederick, L., X.Y. Wang, G. Eley, and C.D. James. 2000. Diversity and frequency of epidermal growth factor receptor mutations in human glioblastomas. *Cancer research*. 60:1383-1387.

Freeman, M.R., and D.H. Rowitch. 2013. Evolving concepts of gliogenesis: a look way back and ahead to the next 25 years. *Neuron*. 80:613-623.

Friedman, H.S., M.D. Prados, P.Y. Wen, T. Mikkelsen, D. Schiff, L.E. Abrey, W.K. Yung, N. Paleologos, M.K. Nicholas, R. Jensen, J. Vredenburgh, J. Huang, M. Zheng, and T. Cloughesy. 2009. Bevacizumab alone and in combination with irinotecan in recurrent glioblastoma. *Journal of clinical oncology : official journal of the American Society of Clinical Oncology*. 27:4733-4740.

Friedmann-Morvinski, D., E.A. Bushong, E. Ke, Y. Soda, T. Marumoto, O. Singer, M.H. Ellisman, and I.M. Verma. 2012. Dedifferentiation of neurons and astrocytes by oncogenes can induce gliomas in mice. *Science*. 338:1080-1084.

Fruman, D.A., C.B. Klee, B.E. Bierer, and S.J. Burakoff. 1992. Calcineurin phosphatase activity in T lymphocytes is inhibited by FK 506 and cyclosporin A. *Proceedings of the National Academy of Sciences of the United States of America*. 89:3686-3690.

Fuentes, J.J., L. Genesca, T.J. Kingsbury, K.W. Cunningham, M. Perez-Riba, X. Estivill, and S. de la Luna. 2000. DSCR1, overexpressed in Down syndrome, is an inhibitor of calcineurin-mediated signaling pathways. *Human molecular genetics*. 9:1681-1690.

Fukada, S., M. Yamaguchi, H. Kokubo, R. Ogawa, A. Uezumi, T. Yoneda, M.M. Matev, N. Motohashi, T. Ito, A. Zolkiewska, R.L. Johnson, Y. Saga, Y. Miyagoe-

Suzuki, K. Tsujikawa, S. Takeda, and H. Yamamoto. 2011. Hesr1 and Hesr3 are essential to generate undifferentiated quiescent satellite cells and to maintain satellite cell numbers. *Development*. 138:4609-4619.

Fuke, S., N. Minami, H. Kokubo, A. Yoshikawa, H. Yasumatsu, N. Sasagawa, Y. Saga, T. Tsukahara, and S. Ishiura. 2006. Hesr1 knockout mice exhibit behavioral alterations through the dopaminergic nervous system. *Journal of neuroscience research*. 84:1555-1563.

Fukushima, T., H. Takeshima, and H. Kataoka. 2009. Anti-glioma therapy with temozolomide and status of the DNA-repair gene MGMT. *Anticancer research*. 29:4845-4854.

Fulton, D.S., R.C. Urtasun, I. Scott-Brown, E.S. Johnson, B. Mielke, B. Curry, D. Huyser-Wierenga, J. Hanson, and M. Feldstein. 1992. Increasing radiation dose intensity using hyperfractionation in patients with malignant glioma. Final report of a prospective phase I-II dose response study. *Journal of neuro-oncology*. 14:63-72.

Furlong, E.E., T. Rein, and F. Martin. 1996. YY1 and NF1 both activate the human p53 promoter by alternatively binding to a composite element, and YY1 and E1A cooperate to amplify p53 promoter activity. *Molecular and cellular biology*. 16:5933-5945.

Furnari, F.B., T. Fenton, R.M. Bachoo, A. Mukasa, J.M. Stommel, A. Stegh, W.C. Hahn, K.L. Ligon, D.N. Louis, C. Brennan, L. Chin, R.A. DePinho, and W.K. Cavenee. 2007. Malignant astrocytic glioma: genetics, biology, and paths to treatment. *Genes & development*. 21:2683-2710.

Furukawa, T., S. Mukherjee, Z.Z. Bao, E.M. Morrow, and C.L. Cepko. 2000. rax, Hes1, and notch1 promote the formation of Muller glia by postnatal retinal progenitor cells. *Neuron*. 26:383-394.

Gaetani, P., E. Hulleman, D. Levi, M. Quarto, M. Scorsetti, K. Helins, M. Simonelli, P. Colombo, and R. Baena y Rodriguez. 2010. Expression of the transcription factor HEY1 in glioblastoma: a preliminary clinical study. *Tumori*. 96:97-102.

Galli, R., E. Binda, U. Orfanelli, B. Cipelletti, A. Gritti, S. De Vitis, R. Fiocco, C. Foroni, F. Dimeco, and A. Vescovi. 2004. Isolation and characterization of tumorigenic, stem-like neural precursors from human glioblastoma. *Cancer research*. 64:7011-7021.

Garcia-Cozar, F.J., H. Okamura, J.F. Aramburu, K.T. Shaw, L. Pelletier, R. Showalter, E. Villafranca, and A. Rao. 1998. Two-site interaction of nuclear factor of activated T cells with activated calcineurin. *The Journal of biological chemistry*. 273:23877-23883.

Garcia, E., A. Stracher, and D. Jay. 2006. Calcineurin dephosphorylates the C-terminal region of filamin in an important regulatory site: a possible mechanism for filamin mobilization and cell signaling. *Archives of biochemistry and biophysics*. 446:140-150.

Gauthier, A.S., O. Furstoss, T. Araki, R. Chan, B.G. Neel, D.R. Kaplan, and F.D. Miller. 2007. Control of CNS cell-fate decisions by SHP-2 and its dysregulation in Noonan syndrome. *Neuron*. 54:245-262.

Gerber, A.N., T.R. Klesert, D.A. Bergstrom, and S.J. Tapscott. 1997. Two domains of MyoD mediate transcriptional activation of genes in repressive chromatin: a mechanism for lineage determination in myogenesis. *Genes Dev*. 11:436-450.

Gerber, D.J., D. Hall, T. Miyakawa, S. Demars, J.A. Gogos, M. Karayiorgou, and S. Tonegawa. 2003. Evidence for association of schizophrenia with genetic variation in the 8p21.3 gene, PPP3CC, encoding the calcineurin gamma subunit. *Proceedings of the National Academy of Sciences of the United States of America*. 100:8993-8998.

Gessler, M., K.P. Knobeloch, A. Helisch, K. Amann, N. Schumacher, E. Rohde, A. Fischer, and C. Leimeister. 2002. Mouse gridlock: no aortic coarctation or deficiency, but fatal cardiac defects in Hey2 -/- mice. *Current biology : CB*. 12:1601-1604.

Giachino, C., O. Basak, S. Lugert, P. Knuckles, K. Obernier, R. Fiorelli, S. Frank, O. Raineteau, A. Alvarez-Buylla, and V. Taylor. 2014. Molecular diversity subdivides the adult forebrain neural stem cell population. *Stem Cells*. 32:70-84.

Giannone, G., P. Ronde, M. Gaire, J. Haiech, and K. Takeda. 2002. Calcium oscillations trigger focal adhesion disassembly in human U87 astrocytoma cells. *The Journal of biological chemistry*. 277:26364-26371.

Gilmore, E.C., T. Ohshima, A.M. Goffinet, A.B. Kulkarni, and K. Herrup. 1998. Cyclin-dependent kinase 5-deficient mice demonstrate novel developmental arrest in cerebral cortex. *The Journal of neuroscience : the official journal of the Society for Neuroscience*. 18:6370-6377.

Glasgow, S.M., D. Laug, V.S. Brawley, Z. Zhang, A. Corder, Z. Yin, S.T. Wong, X.N. Li, A.E. Foster, N. Ahmed, and B. Deneen. 2013. The miR-223/nuclear factor I-A axis regulates glial precursor proliferation and tumorigenesis in the CNS. *The Journal of neuroscience : the official journal of the Society for Neuroscience*. 33:13560-13568.

Glasgow, S.M., W. Zhu, C.C. Stolt, T.W. Huang, F. Chen, J.J. LoTurco, J.L. Neul, M. Wegner, C. Mohila, and B. Deneen. 2014. Mutual antagonism between Sox10 and NFIA regulates diversification of glial lineages and glioma subtypes. *Nature neuroscience*. 17:1322-1329.

Godbout, R., D.A. Bisgrove, D. Shkolny, and R.S. Day, 3rd. 1998. Correlation of B-FABP and GFAP expression in malignant glioma. *Oncogene*. 16:1955-1962.

Goll, D.E., V.F. Thompson, H. Li, W. Wei, and J. Cong. 2003. The calpain system. *Physiological reviews*. 83:731-801.

Gomes, W.A., M.F. Mehler, and J.A. Kessler. 2003. Transgenic overexpression of BMP4 increases astroglial and decreases oligodendroglial lineage commitment. *Developmental biology*. 255:164-177.

Gooch, J.L., J.J. Toro, R.L. Guler, and J.L. Barnes. 2004. Calcineurin A-alpha but not A-beta is required for normal kidney development and function. *The American journal of pathology*. 165:1755-1765.

Gopalan, S.M., K.M. Wilczynska, B.S. Konik, L. Bryan, and T. Kordula. 2006a. Astrocyte-specific expression of the alpha1-antichymotrypsin and glial fibrillary acidic protein genes requires activator protein-1. *J Biol Chem*. 281:1956-1963.

Gopalan, S.M., K.M. Wilczynska, B.S. Konik, L. Bryan, and T. Kordula. 2006b. Nuclear factor-1-X regulates astrocyte-specific expression of the alpha1-antichymotrypsin and glial fibrillary acidic protein genes. *The Journal of biological chemistry*. 281:13126-13133.

Goto, S., Y. Matsukado, Y. Mihara, N. Inoue, and E. Miyamoto. 1986. The distribution of calcineurin in rat brain by light and electron microscopic immunohistochemistry and enzyme-immunoassay. *Brain research*. 397:161-172.

Gotz, M., and W.B. Huttner. 2005. The cell biology of neurogenesis. *Nature reviews. Molecular cell biology*. 6:777-788.

Gotz, M., S. Sirko, J. Beckers, and M. Irmler. 2015. Reactive astrocytes as neural stem or progenitor cells: In vivo lineage, In vitro potential, and Genome-wide expression analysis. *Glia*.

Grabowska, M.M., A.D. Elliott, D.J. DeGraff, P.D. Anderson, G. Anumanthan, H. Yamashita, Q. Sun, D.B. Friedman, D.L. Hachey, X. Yu, J.H. Sheehan, J.M. Ahn, G.V. Raj, D.W. Piston, R.M. Gronostajski, and R.J. Matusik. 2014. NFI transcription factors interact with FOXA1 to regulate prostate-specific gene expression. *Mol Endocrinol*. 28:949-964.

Graef, I.A., F. Wang, F. Charron, L. Chen, J. Neilson, M. Tessier-Lavigne, and G.R. Crabtree. 2003. Neurotrophins and netrins require calcineurin/NFAT signaling to stimulate outgrowth of embryonic axons. *Cell*. 113:657-670.

Griffith, J.P., J.L. Kim, E.E. Kim, M.D. Sintchak, J.A. Thomson, M.J. Fitzgibbon, M.A. Fleming, P.R. Caron, K. Hsiao, and M.A. Navia. 1995. X-ray structure of calcineurin inhibited by the immunophilin-immunosuppressant FKBP12-FK506 complex. *Cell*. 82:507-522.

Gronostajski, R.M. 1986. Analysis of nuclear factor I binding to DNA using degenerate oligonucleotides. *Nucleic acids research*. 14:9117-9132.

Gronostajski, R.M. 1987. Site-specific DNA binding of nuclear factor I: effect of the spacer region. *Nucleic Acids Res*. 15:5545-5559.

Gronostajski, R.M. 2000. Roles of the NFI/CTF gene family in transcription and development. *Gene*. 249:31-45.

Gronostajski, R.M., S. Adhya, K. Nagata, R.A. Guggenheimer, and J. Hurwitz. 1985. Site-specific DNA binding of nuclear factor I: analyses of cellular binding sites. *Molecular and cellular biology*. 5:964-971.

Grunder, A., T.T. Ebel, M. Mallo, G. Schwarzkopf, T. Shimizu, A.E. Sippel, and H. Schrewe. 2002. Nuclear factor I-B (Nfib) deficient mice have severe lung hypoplasia. *Mechanisms of development*. 112:69-77.

Grunder, A., F. Qian, T.T. Ebel, A. Mincheva, P. Lichter, U. Kruse, and A.E. Sippel. 2003. Genomic organization, splice products and mouse chromosomal localization of genes for transcription factor Nuclear Factor One. *Gene*. 304:171-181.

Guichet, P.O., S. Guelfi, M. Teigell, L. Hoppe, N. Bakalara, L. Bauchet, H. Duffau, K. Lamszus, B. Rothhut, and J.P. Hugnot. 2015. Notch1 stimulation induces a vascularization switch with pericyte-like cell differentiation of glioblastoma stem cells. *Stem Cells*. 33:21-34.

Hallhuber, M., N. Burkard, R. Wu, M.H. Buch, S. Engelhardt, L. Hein, L. Neyses, K. Schuh, and O. Ritter. 2006. Inhibition of nuclear import of calcineurin prevents myocardial hypertrophy. *Circulation research*. 99:626-635.

Hamilton, J.D., M. Rapp, T. Schneiderhan, M. Sabel, A. Hayman, A. Scherer, P. Kropil, W. Budach, P. Gerber, U. Kretschmar, S. Prabhu, L.E. Ginsberg, E. Bolke, and C. Matuschek. 2014. Glioblastoma multiforme metastasis outside the CNS: three case reports and possible mechanisms of escape. *Journal of clinical oncology : official journal of the American Society of Clinical Oncology*. 32:e80-84.

Hamza, M.A., and M. Gilbert. 2014. Targeted therapy in gliomas. *Current oncology reports*. 16:379.

Hanahan, D., and R.A. Weinberg. 2011. Hallmarks of cancer: the next generation. *Cell*. 144:646-674.

Hansen, D.V., J.H. Lui, P.R. Parker, and A.R. Kriegstein. 2010. Neurogenic radial glia in the outer subventricular zone of human neocortex. *Nature*. 464:554-561.

Hardesty, D.A., and N. Sanai. 2012. The value of glioma extent of resection in the modern neurosurgical era. *Frontiers in neurology*. 3:140.

Harris, L., C. Dixon, K. Cato, Y.H. Heng, N.D. Kurniawan, J.F. Ullmann, A.L. Janke, R.M. Gronostajski, L.J. Richards, T.H. Burne, and M. Piper. 2013. Heterozygosity for nuclear factor one x affects hippocampal-dependent behaviour in mice. *PloS one*. 8:e65478.

Harris, L., L.A. Genovesi, R.M. Gronostajski, B.J. Wainwright, and M. Piper. 2015. Nuclear factor one transcription factors: Divergent functions in developmental versus adult stem cell populations. *Developmental dynamics : an official publication of the American Association of Anatomists*. 244:227-238.

Hashimoto, T., T. Kawamata, N. Saito, M. Sasaki, M. Nakai, S. Niu, T. Taniguchi, A. Terashima, M. Yasuda, K. Maeda, and C. Tanaka. 1998. Isoform-specific redistribution of calcineurin A alpha and A beta in the hippocampal CA1 region of gerbils after transient ischemia. *Journal of neurochemistry*. 70:1289-1298.

He, F., W. Ge, K. Martinowich, S. Becker-Catania, V. Coskun, W. Zhu, H. Wu, D. Castro, F. Guillemot, G. Fan, J. de Vellis, and Y.E. Sun. 2005. A positive autoregulatory loop of Jak-STAT signaling controls the onset of astrogliogenesis. *Nature neuroscience*. 8:616-625.

Hebbar, P.B., and T.K. Archer. 2007. Chromatin-dependent cooperativity between site-specific transcription factors in vivo. *The Journal of biological chemistry*. 282:8284-8291.

Hebbar, P.B., and T.K. Archer. 2008. Altered histone H1 stoichiometry and an absence of nucleosome positioning on transfected DNA. *J Biol Chem*. 283:4595-4601.

Hegarty, S.V., G.W. O'Keeffe, and A.M. Sullivan. 2013. BMP-Smad 1/5/8 signalling in the development of the nervous system. *Progress in neurobiology*. 109:28-41.

Hegi, M.E., A.C. Diserens, T. Gorlia, M.F. Hamou, N. de Tribolet, M. Weller, J.M. Kros, J.A. Hainfellner, W. Mason, L. Mariani, J.E. Bromberg, P. Hau, R.O. Mirimanoff, J.G. Cairncross, R.C. Janzer, and R. Stupp. 2005. MGMT gene silencing and benefit from temozolomide in glioblastoma. *The New England journal of medicine*. 352:997-1003.

Heisig, J., D. Weber, E. Englberger, A. Winkler, S. Kneitz, W.K. Sung, E. Wolf, M. Eilers, C.L. Wei, and M. Gessler. 2012. Target gene analysis by microarrays and chromatin immunoprecipitation identifies HEY proteins as highly redundant bHLH repressors. *PLoS genetics*. 8:e1002728.

Heng, Y.H., R.C. McLeay, T.J. Harvey, A.G. Smith, G. Barry, K. Cato, C. Plachez, E. Little, S. Mason, C. Dixon, R.M. Gronostajski, T.L. Bailey, L.J. Richards, and M. Piper. 2014. NFIX regulates neural progenitor cell differentiation during hippocampal morphogenesis. *Cereb Cortex*. 24:261-279.

Hermanson, O., K. Jepsen, and M.G. Rosenfeld. 2002. N-CoR controls differentiation of neural stem cells into astrocytes. *Nature*. 419:934-939.

Hirabayashi, Y., N. Suzki, M. Tsuboi, T.A. Endo, T. Toyoda, J. Shinga, H. Koseki, M. Vidal, and Y. Gotoh. 2009. Polycomb limits the neurogenic competence of neural precursor cells to promote astrogenic fate transition. *Neuron*. 63:600-613.

Hirata, H., S. Yoshiura, T. Ohtsuka, Y. Bessho, T. Harada, K. Yoshikawa, and R. Kageyama. 2002. Oscillatory expression of the bHLH factor Hes1 regulated by a negative feedback loop. *Science*. 298:840-843.

Hirt, B. 1967. Selective extraction of polyoma DNA from infected mouse cell cultures. *J Mol Biol*. 26:365-369.

Hitoshi, S., T. Alexson, V. Tropepe, D. Donoviel, A.J. Elia, J.S. Nye, R.A. Conlon, T.W. Mak, A. Bernstein, and D. van der Kooy. 2002. Notch pathway molecules are essential for the maintenance, but not the generation, of mammalian neural stem cells. *Genes & development*. 16:846-858.

Hogan, P.G., L. Chen, J. Nardone, and A. Rao. 2003. Transcriptional regulation by calcium, calcineurin, and NFAT. *Genes & development*. 17:2205-2232.

Hogan, P.G., and H. Li. 2005. Calcineurin. *Current biology : CB*. 15:R442-443.

Holmfeldt, P., J. Pardieck, A.C. Saulsberry, S.K. Nandakumar, D. Finkelstein, J.T. Gray, D.A. Persons, and S. McKinney-Freeman. 2013. Nfix is a novel regulator of murine hematopoietic stem and progenitor cell survival. *Blood*. 122:2987-2996.

Honda, R., H. Tanaka, and H. Yasuda. 1997. Oncoprotein MDM2 is a ubiquitin ligase E3 for tumor suppressor p53. *FEBS letters*. 420:25-27.

Horn, H.F., and K.H. Vousden. 2007. Coping with stress: multiple ways to activate p53. *Oncogene*. 26:1306-1316.

Hornbeck, P.V., I. Chabra, J.M. Kornhauser, E. Skrzypek, and B. Zhang. 2004. PhosphoSite: A bioinformatics resource dedicated to physiological protein phosphorylation. *Proteomics*. 4:1551-1561.

Hottinger, A.F., and Y. Khakoo. 2009. Neurooncology of familial cancer syndromes. *Journal of child neurology*. 24:1526-1535.

Hsu, Y.C., J. Osinski, C.E. Campbell, E.D. Litwack, D. Wang, S. Liu, C.J. Bachurski, and R.M. Gronostajski. 2011. Mesenchymal nuclear factor I B regulates cell proliferation and epithelial differentiation during lung maturation. *Developmental biology*. 354:242-252.

Huang, H.S., M. Nagane, C.K. Klingbeil, H. Lin, R. Nishikawa, X.D. Ji, C.M. Huang, G.N. Gill, H.S. Wiley, and W.K. Cavenee. 1997. The enhanced tumorigenic activity

of a mutant epidermal growth factor receptor common in human cancers is mediated by threshold levels of constitutive tyrosine phosphorylation and unattenuated signaling. *The Journal of biological chemistry*. 272:2927-2935.

Huang, W., J.B. Fileta, A. Dobberfuhl, T. Filippopolous, Y. Guo, G. Kwon, and C.L. Grosskreutz. 2005. Calcineurin cleavage is triggered by elevated intraocular pressure, and calcineurin inhibition blocks retinal ganglion cell death in experimental glaucoma. *Proceedings of the National Academy of Sciences of the United States of America*. 102:12242-12247.

Hulleman, E., M. Quarto, R. Vernell, G. Masserdotti, E. Colli, J.M. Kros, D. Levi, P. Gaetani, P. Tunici, G. Finocchiaro, R.R. Baena, M. Capra, and K. Helin. 2009. A role for the transcription factor HEY1 in glioblastoma. *Journal of cellular and molecular medicine*. 13:136-146.

Imayoshi, I., and R. Kageyama. 2014. bHLH factors in self-renewal, multipotency, and fate choice of neural progenitor cells. *Neuron*. 82:9-23.

Inoue, T., T. Tamura, T. Furuichi, and K. Mikoshiba. 1990. Isolation of complementary DNAs encoding a cerebellum-enriched nuclear factor I family that activates transcription from the mouse myelin basic protein promoter. *J Biol Chem*. 265:19065-19070.

Irshad, K., S.K. Mohapatra, C. Srivastava, H. Garg, S. Mishra, B. Dikshit, C. Sarkar, D. Gupta, P.S. Chandra, P. Chattopadhyay, S. Sinha, and K. Chosdol. 2015. A combined gene signature of hypoxia and notch pathway in human glioblastoma and its prognostic relevance. *PloS one*. 10:e0118201.

Ishiuchi, S., Y. Yoshida, K. Sugawara, M. Aihara, T. Ohtani, T. Watanabe, N. Saito, K. Tsuzuki, H. Okado, A. Miwa, Y. Nakazato, and S. Ozawa. 2007. Ca2+-permeable AMPA receptors regulate growth of human glioblastoma via Akt activation. *The Journal of neuroscience : the official journal of the Society for Neuroscience*. 27:7987-8001.

Iso, T., G. Chung, Y. Hamamori, and L. Kedes. 2002. HERP1 is a cell type-specific primary target of Notch. *The Journal of biological chemistry*. 277:6598-6607.

Iso, T., V. Sartorelli, G. Chung, T. Shichinohe, L. Kedes, and Y. Hamamori. 2001a. HERP, a new primary target of Notch regulated by ligand binding. *Molecular and cellular biology*. 21:6071-6079.

Iso, T., V. Sartorelli, C. Poizat, S. Iezzi, H.Y. Wu, G. Chung, L. Kedes, and Y. Hamamori. 2001b. HERP, a novel heterodimer partner of HES/E(spl) in Notch signaling. *Molecular and cellular biology*. 21:6080-6089.

Jackson, S.P., J.J. MacDonald, S. Lees-Miller, and R. Tjian. 1990. GC box binding induces phosphorylation of Sp1 by a DNA-dependent protein kinase. *Cell*. 63:155-165.

Jackson, S.P., and R. Tjian. 1988. O-glycosylation of eukaryotic transcription factors: implications for mechanisms of transcriptional regulation. *Cell*. 55:125-133.

Jacques, T.S., A. Swales, M.J. Brzozowski, N.V. Henriquez, J.M. Linehan, Z. Mirzadeh, O.M. C, H. Naumann, A. Alvarez-Buylla, and S. Brandner. 2010. Combinations of genetic mutations in the adult neural stem cell compartment determine brain tumour phenotypes. *The EMBO journal*. 29:222-235.

Jain, J., P.G. McCaffrey, Z. Miner, T.K. Kerppola, J.N. Lambert, G.L. Verdine, T. Curran, and A. Rao. 1993. The T-cell transcription factor NFATp is a substrate for calcineurin and interacts with Fos and Jun. *Nature*. 365:352-355.

Jain, R.K., E. di Tomaso, D.G. Duda, J.S. Loeffler, A.G. Sorensen, and T.T. Batchelor. 2007. Angiogenesis in brain tumours. *Nature reviews. Neuroscience*. 8:610-622.

Jalali, A., A.G. Bassuk, L. Kan, N. Israsena, A. Mukhopadhyay, T. McGuire, and J.A. Kessler. 2011. HeyL promotes neuronal differentiation of neural progenitor cells. *Journal of neuroscience research*. 89:299-309.

Janbazian, L., J. Karamchandani, and S. Das. 2014. Mouse models of glioblastoma: lessons learned and questions to be answered. *Journal of neuro-oncology*. 118:1-8.

Jeon, H.M., X. Jin, J.S. Lee, S.Y. Oh, Y.W. Sohn, H.J. Park, K.M. Joo, W.Y. Park, D.H. Nam, R.A. DePinho, L. Chin, and H. Kim. 2008. Inhibitor of differentiation 4 drives brain tumor-initiating cell genesis through cyclin E and notch signaling. *Genes & development*. 22:2028-2033.

Jessell, T.M. 2000. Neuronal specification in the spinal cord: inductive signals and transcriptional codes. *Nature reviews. Genetics*. 1:20-29.

Jiang, H., F. Xiong, S. Kong, T. Ogawa, M. Kobayashi, and J.O. Liu. 1997. Distinct tissue and cellular distribution of two major isoforms of calcineurin. *Molecular immunology*. 34:663-669.

Johansson, E.M., M. Kannius-Janson, G. Bjursell, and J. Nilsson. 2003. The p53 tumor suppressor gene is regulated in vivo by nuclear factor 1-C2 in the mouse mammary gland during pregnancy. *Oncogene*. 22:6061-6070.

Jones, K.A., J.T. Kadonaga, P.J. Rosenfeld, T.J. Kelly, and R. Tjian. 1987. A cellular DNA-binding protein that activates eukaryotic transcription and DNA replication. *Cell*. 48:79-89.

Jones, K.A., K.R. Yamamoto, and R. Tjian. 1985. Two distinct transcription factors bind to the HSV thymidine kinase promoter in vitro. *Cell*. 42:559-572.

Jordan, J.T., and P.Y. Wen. 2015. Novel chemotherapeutic approaches in adult high-grade gliomas. *Cancer treatment and research*. 163:117-142.

Josephson, R., T. Muller, J. Pickel, S. Okabe, K. Reynolds, P.A. Turner, A. Zimmer, and R.D. McKay. 1998. POU transcription factors control expression of CNS stem cell-specific genes. *Development*. 125:3087-3100.

Jung, S., H. Yang, B.S. Kim, K. Chu, S.K. Lee, and D. Jeon. 2012. The immunosuppressant cyclosporin A inhibits recurrent seizures in an experimental model of temporal lobe epilepsy. *Neuroscience letters*. 529:133-138.

Jurado, S., V. Biou, and R.C. Malenka. 2010. A calcineurin/AKAP complex is required for NMDA receptor-dependent long-term depression. *Nature neuroscience*. 13:1053-1055.

Kakalis, L.T., M. Kennedy, R. Sikkink, F. Rusnak, and I.M. Armitage. 1995. Characterization of the calcium-binding sites of calcineurin B. *FEBS letters*. 362:55-58.

Kaloshi, G., K. Mokhtari, C. Carpentier, S. Taillibert, J. Lejeune, Y. Marie, J.Y. Delattre, R. Godbout, and M. Sanson. 2007. FABP7 expression in glioblastomas: relation to prognosis, invasion and EGFR status. *J Neurooncol*. 84:245-248.

Kamnasaran, D., B. Qian, C. Hawkins, W.L. Stanford, and A. Guha. 2007. GATA6 is an astrocytoma tumor suppressor gene identified by gene trapping of mouse glioma model. *Proceedings of the National Academy of Sciences of the United States of America*. 104:8053-8058.

Kang, P., H.K. Lee, S.M. Glasgow, M. Finley, T. Donti, Z.B. Gaber, B.H. Graham, A.E. Foster, B.G. Novitch, R.M. Gronostajski, and B. Deneen. 2012. Sox9 and NFIA coordinate a transcriptional regulatory cascade during the initiation of gliogenesis. *Neuron*. 74:79-94.

Kaur, B., F.W. Khwaja, E.A. Severson, S.L. Matheny, D.J. Brat, and E.G. Van Meir. 2005. Hypoxia and the hypoxia-inducible-factor pathway in glioma growth and angiogenesis. *Neuro-oncology*. 7:134-153.

Kaur, B., C. Tan, D.J. Brat, D.E. Post, and E.G. Van Meir. 2004. Genetic and hypoxic regulation of angiogenesis in gliomas. *Journal of neuro-oncology*. 70:229-243.

Kawahara, T., E. Kashiwagi, H. Ide, Y. Li, Y. Zheng, H. Ishiguro, and H. Miyamoto. 2015a. The role of NFATc1 in prostate cancer progression: cyclosporine A and tacrolimus inhibit cell proliferation, migration, and invasion. *The Prostate*. 75:573-584.

Kawahara, T., E. Kashiwagi, H. Ide, Y. Li, Y. Zheng, Y. Miyamoto, G.J. Netto, H. Ishiguro, and H. Miyamoto. 2015b. Cyclosporine A and tacrolimus inhibit bladder cancer growth through down-regulation of NFATc1. *Oncotarget*. 6:1582-1593.

Kawamura, H., K. Nagata, Y. Masamune, and Y. Nakanishi. 1993. Phosphorylation of NF-I in vitro by cdc2 kinase. *Biochemical and biophysical research communications*. 192:1424-1431.

Kayyali, U.S., W. Zhang, A.G. Yee, J.G. Seidman, and H. Potter. 1997. Cytoskeletal changes in the brains of mice lacking calcineurin A alpha. *Journal of neurochemistry*. 68:1668-1678.

Kilka, S., F. Erdmann, A. Migdoll, G. Fischer, and M. Weiwad. 2009. The proline-rich N-terminal sequence of calcineurin Abeta determines substrate binding. *Biochemistry*. 48:1900-1910.

Kilpatrick, D.L., W. Wang, R. Gronostajski, and E.D. Litwack. 2012. Nuclear factor I and cerebellar granule neuron development: an intrinsic-extrinsic interplay. *Cerebellum*. 11:41-49.

Kim, D., B.P. Fiske, K. Birsoy, E. Freinkman, K. Kami, R.L. Possemato, Y. Chudnovsky, M.E. Pacold, W.W. Chen, J.R. Cantor, L.M. Shelton, D.Y. Gui, M. Kwon, S.H. Ramkissoon, K.L. Ligon, S.W. Kang, M. Snuderl, M.G. Vander Heiden, and D.M. Sabatini. 2015. SHMT2 drives glioma cell survival in ischaemia but imposes a dependence on glycine clearance. *Nature*. 520:363-367.

Kim, T.K., and R.G. Roeder. 1994. Involvement of the basic repeat domain of TATA-binding protein (TBP) in transcription by RNA polymerases I, II, and III. *The Journal of biological chemistry*. 269:4891-4894.

Kim, T.Y., S. Zhong, C.R. Fields, J.H. Kim, and K.D. Robertson. 2006. Epigenomic profiling reveals novel and frequent targets of aberrant DNA methylation-mediated silencing in malignant glioma. *Cancer research*. 66:7490-7501.

Kingsbury, T.J., L.L. Bambrick, C.D. Roby, and B.K. Krueger. 2007. Calcineurin activity is required for depolarization-induced, CREB-dependent gene transcription in cortical neurons. *Journal of neurochemistry*. 103:761-770.

Kingsbury, T.J., and K.W. Cunningham. 2000. A conserved family of calcineurin regulators. *Genes & development*. 14:1595-1604.

Kissinger, C.R., H.E. Parge, D.R. Knighton, C.T. Lewis, L.A. Pelletier, A. Tempczyk, V.J. Kalish, K.D. Tucker, R.E. Showalter, E.W. Moomaw, and et al. 1995. Crystal structures of human calcineurin and the human FKBP12-FK506-calcineurin complex. *Nature*. 378:641-644.

Klee, C.B., T.H. Crouch, and M.H. Krinks. 1979. Calcineurin: a calcium- and calmodulin-binding protein of the nervous system. *Proceedings of the National Academy of Sciences of the United States of America*. 76:6270-6273.

Klee, C.B., G.F. Draetta, and M.J. Hubbard. 1988. Calcineurin. *Advances in enzymology and related areas of molecular biology*. 61:149-200.

Klee, C.B., H. Ren, and X. Wang. 1998. Regulation of the calmodulin-stimulated protein phosphatase, calcineurin. *The Journal of biological chemistry*. 273:13367-13370.

Kleihues, P., W.K. Cavenee, and International Agency for Research on Cancer. 2000. Pathology and genetics of tumours of the nervous system. IARC Press, Lyon. 314 p. pp.

Kleihues, P., and L.H. Sobin. 2000. World Health Organization classification of tumors. *Cancer*. 88:2887.

Kleihues, P., F. Soylemezoglu, B. Schauble, B.W. Scheithauer, and P.C. Burger. 1995. Histopathology, classification, and grading of gliomas. *Glia*. 15:211-221.

Knudsen, E.S., and J.Y. Wang. 2010. Targeting the RB-pathway in cancer therapy. *Clinical cancer research : an official journal of the American Association for Cancer Research*. 16:1094-1099.

Kodama, T., E. Ikeda, A. Okada, T. Ohtsuka, M. Shimoda, T. Shiomi, K. Yoshida, M. Nakada, E. Ohuchi, and Y. Okada. 2004. ADAM12 is selectively overexpressed in human glioblastomas and is associated with glioblastoma cell proliferation and shedding of heparin-binding epidermal growth factor. *The American journal of pathology*. 165:1743-1753.

Kokubo, H., Y. Lun, and R.L. Johnson. 1999. Identification and expression of a novel family of bHLH cDNAs related to Drosophila hairy and enhancer of split. *Biochemical and biophysical research communications*. 260:459-465.

Koster, M., T. Frahm, and H. Hauser. 2005. Nucleocytoplasmic shuttling revealed by FRAP and FLIP technologies. *Current opinion in biotechnology*. 16:28-34.

Krebs, C.J., B. Dey, and G. Kumar. 1996. The cerebellum-enriched form of nuclear factor I is functionally different from ubiquitous nuclear factor I in glial-specific promoter regulation. *Journal of neurochemistry*. 66:1354-1361.

Kriegstein, A., and A. Alvarez-Buylla. 2009. The glial nature of embryonic and adult neural stem cells. *Annual review of neuroscience*. 32:149-184.

Kruse, U., F. Qian, and A.E. Sippel. 1991. Identification of a fourth nuclear factor I gene in chicken by cDNA cloning: NFI-X. *Nucleic acids research*. 19:6641.

Kruse, U., and A.E. Sippel. 1994a. The genes for transcription factor nuclear factor I give rise to corresponding splice variants between vertebrate species. *Journal of molecular biology*. 238:860-865.

Kruse, U., and A.E. Sippel. 1994b. Transcription factor nuclear factor I proteins form stable homo- and heterodimers. *FEBS letters*. 348:46-50.

Kubbutat, M.H., S.N. Jones, and K.H. Vousden. 1997. Regulation of p53 stability by Mdm2. *Nature*. 387:299-303.

Kumar, K.U., A. Pater, and M.M. Pater. 1993. Human JC virus perfect palindromic nuclear factor 1-binding sequences important for glial cell-specific expression in differentiating embryonal carcinoma cells. *J Virol*. 67:572-576.

Kuno, T., H. Mukai, A. Ito, C.D. Chang, K. Kishima, N. Saito, and C. Tanaka. 1992. Distinct cellular expression of calcineurin A alpha and A beta in rat brain. *Journal of neurochemistry*. 58:1643-1651.

Kurtz, A., A. Zimmer, F. Schnutgen, G. Bruning, F. Spener, and T. Muller. 1994. The expression pattern of a novel gene encoding brain-fatty acid binding protein correlates with neuronal and glial cell development. *Development*. 120:2637-2649.

Kwon, C.H., D. Zhao, J. Chen, S. Alcantara, Y. Li, D.K. Burns, R.P. Mason, E.Y. Lee, H. Wu, and L.F. Parada. 2008. Pten haploinsufficiency accelerates formation of high-grade astrocytomas. *Cancer research*. 68:3286-3294.

Lajoie, M., Y.C. Hsu, R.M. Gronostajski, and T.L. Bailey. 2014. An overlapping set of genes is regulated by both NFIB and the glucocorticoid receptor during lung maturation. *BMC genomics*. 15:231.

Lalioti, V., G. Muruais, A. Dinarina, J. van Damme, J. Vandekerckhove, and I.V. Sandoval. 2009. The atypical kinase Cdk5 is activated by insulin, regulates the association between GLUT4 and E-Syt1, and modulates glucose transport in 3T3-L1 adipocytes. *Proceedings of the National Academy of Sciences of the United States of America*. 106:4249-4253.

Langlois, A., S. Lee, D.S. Kim, P.B. Dirks, and J.T. Rutka. 2002. p16(ink4a) and retinoic acid modulate rhoA and GFAP expression during induction of a stellate phenotype in U343 MG-A astrocytoma cells. *Glia*. 40:85-94.

Larrivee, B., C. Prahst, E. Gordon, R. del Toro, T. Mathivet, A. Duarte, M. Simons, and A. Eichmann. 2012. ALK1 signaling inhibits angiogenesis by cooperating with the Notch pathway. *Developmental cell*. 22:489-500.

Larson, D.A., P.H. Gutin, S.A. Leibel, T.L. Phillips, P.K. Sneed, and W.M. Wara. 1990. Stereotaxic irradiation of brain tumors. *Cancer*. 65:792-799.

Lavery, K., S. Hawley, P. Swain, R. Rooney, D. Falb, and M.H. Alaoui-Ismaili. 2009. New insights into BMP-7 mediated osteoblastic differentiation of primary human mesenchymal stem cells. *Bone*. 45:27-41.

Leahy, P., D.R. Crawford, G. Grossman, R.M. Gronostajski, and R.W. Hanson. 1999. CREB binding protein coordinates the function of multiple transcription factors including nuclear factor I to regulate phosphoenolpyruvate carboxykinase (GTP) gene transcription. *The Journal of biological chemistry*. 274:8813-8822.

Leclerc, C., I. Neant, and M. Moreau. 2011. Early neural development in vertebrates is also a matter of calcium. *Biochimie*. 93:2102-2111.

Lee, C.W., J.C. Ferreon, A.C. Ferreon, M. Arai, and P.E. Wright. 2010. Graded enhancement of p53 binding to CREB-binding protein (CBP) by multisite phosphorylation. *Proceedings of the National Academy of Sciences of the United States of America*. 107:19290-19295.

Lee, D.S., J.T. Park, H.M. Kim, J.S. Ko, H.H. Son, R.M. Gronostajski, M.I. Cho, P.H. Choung, and J.C. Park. 2009. Nuclear factor I-C is essential for odontogenic cell proliferation and odontoblast differentiation during tooth root development. *The Journal of biological chemistry*. 284:17293-17303.

Lee, J.S., J. Xiao, P. Patel, J. Schade, J. Wang, B. Deneen, A. Erdreich-Epstein, and H.R. Song. 2014. A novel tumor-promoting role for nuclear factor IA in glioblastomas is mediated through negative regulation of p53, p21, and PAI1. *Neuro-oncology*. 16:191-203.

Leegwater, P.A., P.C. van der Vliet, R.A. Rupp, J. Nowock, and A.E. Sippel. 1986. Functional homology between the sequence-specific DNA-binding proteins nuclear factor I from HeLa cells and the TGGCA protein from chicken liver. *The EMBO journal*. 5:381-386.

Lehtinen, M.K., Z. Yuan, P.R. Boag, Y. Yang, J. Villen, E.B. Becker, S. DiBacco, N. de la Iglesia, S. Gygi, T.K. Blackwell, and A. Bonni. 2006. A conserved MST-FOXO signaling pathway mediates oxidative-stress responses and extends life span. *Cell*. 125:987-1001.

Leimeister, C., A. Externbrink, B. Klamt, and M. Gessler. 1999. Hey genes: a novel subfamily of hairy- and Enhancer of split related genes specifically expressed during mouse embryogenesis. *Mechanisms of development*. 85:173-177.

Leimeister, C., N. Schumacher, C. Steidl, and M. Gessler. 2000. Analysis of HeyL expression in wild-type and Notch pathway mutant mouse embryos. *Mechanisms of development*. 98:175-178.

Lewis, R.A., L.P. Gerson, K.A. Axelson, V.M. Riccardi, and R.P. Whitford. 1984. von Recklinghausen neurofibromatosis. II. Incidence of optic gliomata. *Ophthalmology*. 91:929-935.

Li, A., J. Walling, Y. Kotliarov, A. Center, M.E. Steed, S.J. Ahn, M. Rosenblum, T. Mikkelsen, J.C. Zenklusen, and H.A. Fine. 2008. Genomic changes and gene expression profiles reveal that established glioma cell lines are poorly representative of primary human gliomas. *Molecular cancer research : MCR*. 6:21-30.

Li, H., A. Rao, and P.G. Hogan. 2011. Interaction of calcineurin with substrates and targeting proteins. *Trends in cell biology*. 21:91-103.

Li, X., J.M. Newbern, Y. Wu, M. Morgan-Smith, J. Zhong, J. Charron, and W.D. Snider. 2012. MEK Is a Key Regulator of Gliogenesis in the Developing Brain. *Neuron*. 75:1035-1050.

Liang, Y., A.W. Bollen, K.D. Aldape, and N. Gupta. 2006. Nuclear FABP7 immunoreactivity is preferentially expressed in infiltrative glioma and is associated with poor prognosis in EGFR-overexpressing glioblastoma. *BMC cancer*. 6:97.

Liang, Y., M. Diehn, N. Watson, A.W. Bollen, K.D. Aldape, M.K. Nicholas, K.R. Lamborn, M.S. Berger, D. Botstein, P.O. Brown, and M.A. Israel. 2005. Gene expression profiling reveals molecularly and clinically distinct subtypes of glioblastoma multiforme. *Proceedings of the National Academy of Sciences of the United States of America*. 102:5814-5819.

Lindberg, N., Y. Jiang, Y. Xie, H. Bolouri, M. Kastemar, T. Olofsson, E.C. Holland, and L. Uhrbom. 2014. Oncogenic signaling is dominant to cell of origin and dictates astrocytic or oligodendroglial tumor development from oligodendrocyte precursor cells. *The Journal of neuroscience : the official journal of the Society for Neuroscience*. 34:14644-14651.

Little, M.P., P. Rajaraman, R.E. Curtis, S.S. Devesa, P.D. Inskip, D.P. Check, and M.S. Linet. 2012. Mobile phone use and glioma risk: comparison of epidemiological study results with incidence trends in the United States. *BMJ*. 344:e1147.

Liu, C., J.C. Sage, M.R. Miller, R.G. Verhaak, S. Hippenmeyer, H. Vogel, O. Foreman, R.T. Bronson, A. Nishiyama, L. Luo, and H. Zong. 2011. Mosaic analysis with double markers reveals tumor cell of origin in glioma. *Cell*. 146:209-221.

Liu, C., and H. Zong. 2012. Developmental origins of brain tumors. *Current opinion in neurobiology*. 22:844-849.

Liu, F., I. Grundke-Iqbal, K. Iqbal, Y. Oda, K. Tomizawa, and C.X. Gong. 2005a. Truncation and activation of calcineurin A by calpain I in Alzheimer disease brain. *The Journal of biological chemistry*. 280:37755-37762.

Liu, J., M.W. Albers, T.J. Wandless, S. Luan, D.G. Alberg, P.J. Belshaw, P. Cohen, C. MacKintosh, C.B. Klee, and S.L. Schreiber. 1992. Inhibition of T cell signaling by immunophilin-ligand complexes correlates with loss of calcineurin phosphatase activity. *Biochemistry*. 31:3896-3901.

Liu, J., J.D. Farmer, Jr., W.S. Lane, J. Friedman, I. Weissman, and S.L. Schreiber. 1991. Calcineurin is a common target of cyclophilin-cyclosporin A and FKBP-FK506 complexes. *Cell*. 66:807-815.

Liu, J., E.S. Masuda, L. Tsuruta, N. Arai, and K. Arai. 1999. Two independent calcineurin-binding regions in the N-terminal domain of murine NF-ATx1 recruit calcineurin to murine NF-ATx1. *J Immunol*. 162:4755-4761.

Liu, L., J. Zhang, J. Yuan, Y. Dang, C. Yang, X. Chen, J. Xu, and L. Yu. 2005b. Characterization of a human regulatory subunit of protein phosphatase 3 gene (PPP3RL) expressed specifically in testis. *Molecular biology reports*. 32:41-45.

Liu, T., Y. Gao, K. Sakamoto, T. Minamizato, K. Furukawa, T. Tsukazaki, Y. Shibata, K. Bessho, T. Komori, and A. Yamaguchi. 2007. BMP-2 promotes differentiation of osteoblasts and chondroblasts in Runx2-deficient cell lines. *Journal of cellular physiology*. 211:728-735.

Lois, C., J.M. Garcia-Verdugo, and A. Alvarez-Buylla. 1996. Chain migration of neuronal precursors. *Science*. 271:978-981.

Louis, D.N. 1994. The p53 gene and protein in human brain tumors. *Journal of neuropathology and experimental neurology*. 53:11-21.

Louis, D.N., Deutsches Krebsforschungszentrum Heidelberg., International Agency for Research on Cancer., and World Health Organization. 2007. WHO classification of tumours of the central nervous system. *In* World Health Organization classification of tumours. Distributed by WHO Press, World Health Organization, Geneva, Switzerland. 309 p.

Lu, W., F. Quintero-Rivera, Y. Fan, F.S. Alkuraya, D.J. Donovan, Q. Xi, A. Turbe-Doan, Q.G. Li, C.G. Campbell, A.L. Shanske, E.H. Sherr, A. Ahmad, R. Peters, B. Rilliet, P. Parvex, A.G. Bassuk, D.J. Harris, H. Ferguson, C. Kelly, C.A. Walsh, R.M. Gronostajski, K. Devriendt, A. Higgins, A.H. Ligon, B.J. Quade, C.C. Morton, J.F. Gusella, and R.L. Maas. 2007. NFIA haploinsufficiency is associated with a CNS malformation syndrome and urinary tract defects. *PLoS genetics*. 3:e80.

Lu, Y.M., I.M. Mansuy, E.R. Kandel, and J. Roder. 2000. Calcineurin-mediated LTD of GABAergic inhibition underlies the increased excitability of CA1 neurons associated with LTP. *Neuron*. 26:197-205.

Lun, M., E. Lok, S. Gautam, E. Wu, and E.T. Wong. 2011. The natural history of extracranial metastasis from glioblastoma multiforme. *Journal of neuro-oncology*. 105:261-273.

Lyons, S.A., W.J. Chung, A.K. Weaver, T. Ogunrinu, and H. Sontheimer. 2007. Autocrine glutamate signaling promotes glioma cell invasion. *Cancer research*. 67:9463-9471.

Macian, F. 2005. NFAT proteins: key regulators of T-cell development and function. *Nature reviews. Immunology*. 5:472-484.

Maier, M.M., and M. Gessler. 2000. Comparative analysis of the human and mouse Hey1 promoter: Hey genes are new Notch target genes. *Biochemical and biophysical research communications*. 275:652-660.

Major, E.O., K. Amemiya, G. Elder, and S.A. Houff. 1990. Glial cells of the human developing brain and B cells of the immune system share a common DNA binding factor for recognition of the regulatory sequences of the human polyomavirus, JCV. *J Neurosci Res*. 27:461-471.

Malatesta, P., M.A. Hack, E. Hartfuss, H. Kettenmann, W. Klinkert, F. Kirchhoff, and M. Gotz. 2003. Neuronal or glial progeny: regional differences in radial glia fate. *Neuron*. 37:751-764.

Malatesta, P., E. Hartfuss, and M. Gotz. 2000. Isolation of radial glial cells by fluorescent-activated cell sorting reveals a neuronal lineage. *Development*. 127:5253-5263.

Malik, N., X. Wang, S. Shah, A.G. Efthymiou, B. Yan, S. Heman-Ackah, M. Zhan, and M. Rao. 2014. Comparison of the gene expression profiles of human fetal cortical astrocytes with pluripotent stem cell derived neural stem cells identifies human astrocyte markers and signaling pathways and transcription factors active in human astrocytes. *PloS one*. 9:e96139.

Manicassamy, S., S. Gupta, Z. Huang, J.D. Molkentin, W. Shang, and Z. Sun. 2008. Requirement of calcineurin a beta for the survival of naive T cells. *J Immunol*. 180:106-112.

Marko, N.F., and R.J. Weil. 2012. The molecular biology of WHO grade I astrocytomas. *Neuro-oncology*. 14:1424-1431.

Martinez-Martinez, S., L. Genesca, A. Rodriguez, A. Raya, E. Salichs, F. Were, M.D. Lopez-Maderuelo, J.M. Redondo, and S. de la Luna. 2009. The RCAN carboxyl end mediates calcineurin docking-dependent inhibition via a site that dictates binding to substrates and regulators. *Proceedings of the National Academy of Sciences of the United States of America*. 106:6117-6122.

Martinez, R., J.I. Martin-Subero, V. Rohde, M. Kirsch, M. Alaminos, A.F. Fernandez, S. Ropero, G. Schackert, and M. Esteller. 2009. A microarray-based DNA methylation study of glioblastoma multiforme. *Epigenetics : official journal of the DNA Methylation Society*. 4:255-264.

Martynoga, B., J.L. Mateo, B. Zhou, J. Andersen, A. Achimastou, N. Urban, D. van den Berg, D. Georgopoulou, S. Hadjur, J. Wittbrodt, L. Ettwiller, M. Piper, R.M. Gronostajski, and F. Guillemot. 2013. Epigenomic enhancer annotation reveals a

key role for NFIX in neural stem cell quiescence. *Genes & development*. 27:1769-1786.

Mason, J.L., J.M. Angelastro, T.N. Ignatova, V.G. Kukekov, G. Lin, L.A. Greene, and J.E. Goldman. 2005. ATF5 regulates the proliferation and differentiation of oligodendrocytes. *Molecular and cellular neurosciences*. 29:372-380.

Mason, S., M. Piper, R.M. Gronostajski, and L.J. Richards. 2009. Nuclear factor one transcription factors in CNS development. *Molecular neurobiology*. 39:10-23.

Mason, W.P., R.D. Maestro, D. Eisenstat, P. Forsyth, D. Fulton, N. Laperriere, D. Macdonald, J. Perry, and B. Thiessen. 2007. Canadian recommendations for the treatment of glioblastoma multiforme. *Curr Oncol*. 14:110-117.

Masood, K., F. Besnard, Y. Su, and M. Brenner. 1993. Analysis of a segment of the human glial fibrillary acidic protein gene that directs astrocyte-specific transcription. *J Neurochem*. 61:160-166.

Mateo, J.L., D.L. van den Berg, M. Haeussler, D. Drechsel, Z.B. Gaber, D.S. Castro, P. Robson, G.E. Crawford, P. Flicek, L. Ettwiller, J. Wittbrodt, F. Guillemot, and B. Martynoga. 2015. Characterization of the neural stem cell gene regulatory network identifies OLIG2 as a multifunctional regulator of self-renewal. *Genome research*. 25:41-56.

Matsuda, S., F. Shibasaki, K. Takehana, H. Mori, E. Nishida, and S. Koyasu. 2000. Two distinct action mechanisms of immunophilin-ligand complexes for the blockade of T-cell activation. *EMBO reports*. 1:428-434.

Matsuda, T., K. Takuma, S. Asano, Y. Kishida, H. Nakamura, K. Mori, S. Maeda, and A. Baba. 1998. Involvement of calcineurin in Ca2+ paradox-like injury of cultured rat astrocytes. *Journal of neurochemistry*. 70:2004-2011.

McManus, M.F., L.C. Chen, I. Vallejo, and M. Vallejo. 1999. Astroglial differentiation of cortical precursor cells triggered by activation of the cAMP-dependent signaling pathway. *The Journal of neuroscience : the official journal of the Society for Neuroscience*. 19:9004-9015.

Mellai, M., O. Monzeglio, A. Piazzi, V. Caldera, L. Annovazzi, P. Cassoni, G. Valente, S. Cordera, C. Mocellini, and D. Schiffer. 2012. MGMT promoter hypermethylation and its associations with genetic alterations in a series of 350 brain tumors. *Journal of neuro-oncology*. 107:617-631.

Merkle, F.T., A.D. Tramontin, J.M. Garcia-Verdugo, and A. Alvarez-Buylla. 2004. Radial glia give rise to adult neural stem cells in the subventricular zone. *Proceedings of the National Academy of Sciences of the United States of America*. 101:17528-17532.

Mermod, N., E.A. O'Neill, T.J. Kelly, and R. Tjian. 1989. The proline-rich transcriptional activator of CTF/NF-I is distinct from the replication and DNA binding domain. *Cell*. 58:741-753.

Messina, G., S. Biressi, S. Monteverde, A. Magli, M. Cassano, L. Perani, E. Roncaglia, E. Tagliafico, L. Starnes, C.E. Campbell, M. Grossi, D.J. Goldhamer, R.M. Gronostajski, and G. Cossu. 2010. Nfix regulates fetal-specific transcription in developing skeletal muscle. *Cell*. 140:554-566.

Mi, H., A. Muruganujan, and P.D. Thomas. 2013. PANTHER in 2013: modeling the evolution of gene function, and other gene attributes, in the context of phylogenetic trees. *Nucleic acids research*. 41:D377-386.

Miller, F.D., and A.S. Gauthier. 2007. Timing is everything: making neurons versus glia in the developing cortex. *Neuron*. 54:357-369.

Minty, A.J., M. Caravatti, B. Robert, A. Cohen, P. Daubas, A. Weydert, F. Gros, and M.E. Buckingham. 1981. Mouse actin messenger RNAs. Construction and characterization of a recombinant plasmid molecule containing a complementary DNA transcript of mouse alpha-actin mRNA. *J Biol Chem*. 256:1008-1014.

Mita, R., M.J. Beaulieu, C. Field, and R. Godbout. 2010. Brain fatty acid-binding protein and omega-3/omega-6 fatty acids: mechanistic insight into malignant glioma cell migration. *The Journal of biological chemistry*. 285:37005-37015.

Mita, R., J.E. Coles, D.D. Glubrecht, R. Sung, X. Sun, and R. Godbout. 2007. B-FABP-expressing radial glial cells: the malignant glioma cell of origin? *Neoplasia*. 9:734-744.

Miyamoto, Y., J. Yamauchi, J.R. Chan, A. Okada, Y. Tomooka, S. Hisanaga, and A. Tanoue. 2007. Cdk5 regulates differentiation of oligodendrocyte precursor cells through the direct phosphorylation of paxillin. *Journal of cell science*. 120:4355-4366.

Moon, H.G., K.T. Hwang, J.A. Kim, H.S. Kim, M.J. Lee, E.M. Jung, E. Ko, W. Han, and D.Y. Noh. 2011. NFIB is a potential target for estrogen receptor-negative breast cancers. *Molecular oncology*. 5:538-544.

Morita, M., N. Kozuka, R. Itofusa, M. Yukawa, and Y. Kudo. 2005. Autocrine activation of EGF receptor promotes oscillation of glutamate-induced calcium increase in astrocytes cultured in rat cerebral cortex. *Journal of neurochemistry*. 95:871-879.

Morrison, S.J., S.E. Perez, Z. Qiao, J.M. Verdi, C. Hicks, G. Weinmaster, and D.J. Anderson. 2000. Transient Notch activation initiates an irreversible switch from neurogenesis to gliogenesis by neural crest stem cells. *Cell*. 101:499-510.

Mukhopadhyay, S.S., S.L. Wyszomierski, R.M. Gronostajski, and J.M. Rosen. 2001. Differential interactions of specific nuclear factor I isoforms with the glucocorticoid receptor and STAT5 in the cooperative regulation of WAP gene transcription. *Molecular and cellular biology*. 21:6859-6869.

Muramatsu, T., P.R. Giri, S. Higuchi, and R.L. Kincaid. 1992. Molecular cloning of a calmodulin-dependent phosphatase from murine testis: identification of a developmentally expressed nonneural isoenzyme. *Proceedings of the National Academy of Sciences of the United States of America*. 89:529-533.

Muramatsu, T., and R.L. Kincaid. 1992. Molecular cloning and chromosomal mapping of the human gene for the testis-specific catalytic subunit of calmodulin-dependent protein phosphatase (calcineurin A). *Biochemical and biophysical research communications*. 188:265-271.

Murphy, K.G., J.D. Hatton, and H.S. U. 1998. Role of glial fibrillary acidic protein expression in the biology of human glioblastoma U-373MG cells. *J Neurosurg*. 89:997-1006.

Murtagh, J., F. Martin, and R.M. Gronostajski. 2003. The Nuclear Factor I (NFI) gene family in mammary gland development and function. *Journal of mammary gland biology and neoplasia*. 8:241-254.

Nagata, K., R.A. Guggenheimer, T. Enomoto, J.H. Lichy, and J. Hurwitz. 1982. Adenovirus DNA replication in vitro: identification of a host factor that stimulates synthesis of the preterminal protein-dCMP complex. *Proceedings of the National Academy of Sciences of the United States of America*. 79:6438-6442.

Nagata, K., R.A. Guggenheimer, and J. Hurwitz. 1983. Specific binding of a cellular DNA replication protein to the origin of replication of adenovirus DNA. *Proceedings of the National Academy of Sciences of the United States of America*. 80:6177-6181.

Naka, H., S. Nakamura, T. Shimazaki, and H. Okano. 2008. Requirement for COUP-TFI and II in the temporal specification of neural stem cells in CNS development. *Nature neuroscience*. 11:1014-1023.

Nakada, M., S. Nakada, T. Demuth, N.L. Tran, D.B. Hoelzinger, and M.E. Berens. 2007. Molecular targets of glioma invasion. *Cellular and molecular life sciences : CMLS*. 64:458-478.

Nakagawa, O., D.G. McFadden, M. Nakagawa, H. Yanagisawa, T. Hu, D. Srivastava, and E.N. Olson. 2000. Members of the HRT family of basic helix-loop-helix proteins act as transcriptional repressors downstream of Notch signaling. *Proceedings of the National Academy of Sciences of the United States of America*. 97:13655-13660.

Nakagawa, O., M. Nakagawa, J.A. Richardson, E.N. Olson, and D. Srivastava. 1999. HRT1, HRT2, and HRT3: a new subclass of bHLH transcription factors marking specific cardiac, somitic, and pharyngeal arch segments. *Developmental biology*. 216:72-84.

Nakashima, K., T. Takizawa, W. Ochiai, M. Yanagisawa, T. Hisatsune, M. Nakafuku, K. Miyazono, T. Kishimoto, R. Kageyama, and T. Taga. 2001. BMP2-mediated alteration in the developmental pathway of fetal mouse brain cells from neurogenesis to astrocytogenesis. *Proceedings of the National Academy of Sciences of the United States of America*. 98:5868-5873.

Nakashima, K., M. Yanagisawa, H. Arakawa, N. Kimura, T. Hisatsune, M. Kawabata, K. Miyazono, and T. Taga. 1999. Synergistic signaling in fetal brain by STAT3-Smad1 complex bridged by p300. *Science*. 284:479-482.

Namihira, M., J. Kohyama, K. Semi, T. Sanosaka, B. Deneen, T. Taga, and K. Nakashima. 2009. Committed neuronal precursors confer astrocytic potential on residual neural precursor cells. *Developmental cell*. 16:245-255.

Namihira, M., K. Nakashima, and T. Taga. 2004. Developmental stage dependent regulation of DNA methylation and chromatin modification in a immature astrocyte specific gene promoter. *FEBS letters*. 572:184-188.

Nandhu, M.S., B. Hu, S.E. Cole, A. Erdreich-Epstein, D.J. Rodriguez-Gil, and M.S. Viapiano. 2014. Novel paracrine modulation of Notch-DLL4 signaling by fibulin-3 promotes angiogenesis in high-grade gliomas. *Cancer research*. 74:5435-5448.

Narita, Y., M. Nagane, K. Mishima, H.J. Huang, F.B. Furnari, and W.K. Cavenee. 2002. Mutant epidermal growth factor receptor signaling down-regulates p27 through activation of the phosphatidylinositol 3-kinase/Akt pathway in glioblastomas. *Cancer research*. 62:6764-6769.

Nedergaard, M., J.J. Rodriguez, and A. Verkhratsky. 2010. Glial calcium and diseases of the nervous system. *Cell calcium*. 47:140-149.

Neglia, J.P., A.T. Meadows, L.L. Robison, T.H. Kim, W.A. Newton, F.B. Ruymann, H.N. Sather, and G.D. Hammond. 1991. Second neoplasms after acute lymphoblastic leukemia in childhood. *The New England journal of medicine*. 325:1330-1336.

Nelson, D.F., M. Diener-West, J. Horton, C.H. Chang, D. Schoenfeld, and J.S. Nelson. 1988. Combined modality approach to treatment of malignant gliomas--re-evaluation of RTOG 7401/ECOG 1374 with long-term follow-up: a joint study of the Radiation Therapy Oncology Group and the Eastern Cooperative Oncology Group. *NCI monographs : a publication of the National Cancer Institute*:279-284.

Nery, S., H. Wichterle, and G. Fishell. 2001. Sonic hedgehog contributes to oligodendrocyte specification in the mammalian forebrain. *Development*. 128:527-540.

Newlands, E.S., M.F. Stevens, S.R. Wedge, R.T. Wheelhouse, and C. Brock. 1997. Temozolomide: a review of its discovery, chemical properties, pre-clinical development and clinical trials. *Cancer treatment reviews*. 23:35-61.

Nilsson, J., G. Bjursell, and M. Kannius-Janson. 2006. Nuclear Jak2 and transcription factor NF1-C2: a novel mechanism of prolactin signaling in mammary epithelial cells. *Molecular and cellular biology*. 26:5663-5674.

Nilsson, J., K. Helou, A. Kovacs, P.O. Bendahl, G. Bjursell, M. Ferno, P. Carlsson, and M. Kannius-Janson. 2010. Nuclear Janus-activated kinase 2/nuclear factor 1-C2 suppresses tumorigenesis and epithelial-to-mesenchymal transition by repressing Forkhead box F1. *Cancer research*. 70:2020-2029.

Noctor, S.C., A.C. Flint, T.A. Weissman, W.S. Wong, B.K. Clinton, and A.R. Kriegstein. 2002. Dividing precursor cells of the embryonic cortical ventricular zone have morphological and molecular characteristics of radial glia. *The Journal of neuroscience : the official journal of the Society for Neuroscience*. 22:3161-3173.

Norris, C.M., I. Kadish, E.M. Blalock, K.C. Chen, V. Thibault, N.M. Porter, P.W. Landfield, and S.D. Kraner. 2005. Calcineurin triggers reactive/inflammatory processes in astrocytes and is upregulated in aging and Alzheimer's models. *The Journal of neuroscience : the official journal of the Society for Neuroscience*. 25:4649-4658.

Noushmehr, H., D.J. Weisenberger, K. Diefes, H.S. Phillips, K. Pujara, B.P. Berman, F. Pan, C.E. Pelloski, E.P. Sulman, K.P. Bhat, R.G. Verhaak, K.A. Hoadley, D.N. Hayes, C.M. Perou, H.K. Schmidt, L. Ding, R.K. Wilson, D. Van Den Berg, H. Shen, H. Bengtsson, P. Neuvial, L.M. Cope, J. Buckley, J.G. Herman, S.B. Baylin, P.W. Laird, and K. Aldape. 2010. Identification of a CpG island methylator phenotype that defines a distinct subgroup of glioma. *Cancer cell*. 17:510-522.

O'Brien, R.M., E.L. Noisin, A. Suwanichkul, T. Yamasaki, P.C. Lucas, J.C. Wang, D.R. Powell, and D.K. Granner. 1995. Hepatic nuclear factor 3- and hormone-regulated expression of the phosphoenolpyruvate carboxykinase and insulin-like growth factor-binding protein 1 genes. *Molecular and cellular biology*. 15:1747-1758.

Oh, M.C., J.M. Kim, M. Safaee, G. Kaur, M.Z. Sun, R. Kaur, A. Celli, T.M. Mauro, and A.T. Parsa. 2012. Overexpression of calcium-permeable glutamate receptors in glioblastoma derived brain tumor initiating cells. *PloS one*. 7:e47846.

Oh, T., E.T. Sayegh, S. Fakurnejad, D. Oyon, J.B. Lamano, J.D. DiDomenico, O. Bloch, and A.T. Parsa. 2015. Vaccine therapies in malignant glioma. *Current neurology and neuroscience reports*. 15:508.

Ohgaki, H. 2009. Epidemiology of brain tumors. *Methods Mol Biol*. 472:323-342.

Ohgaki, H., and P. Kleihues. 2005a. Epidemiology and etiology of gliomas. *Acta neuropathologica*. 109:93-108.

Ohgaki, H., and P. Kleihues. 2005b. Population-based studies on incidence, survival rates, and genetic alterations in astrocytic and oligodendroglial gliomas. *Journal of neuropathology and experimental neurology*. 64:479-489.

Ohshima, T., J.M. Ward, C.G. Huh, G. Longenecker, Veeranna, H.C. Pant, R.O. Brady, L.J. Martin, and A.B. Kulkarni. 1996. Targeted disruption of the cyclin-dependent kinase 5 gene results in abnormal corticogenesis, neuronal pathology and perinatal death. *Proceedings of the National Academy of Sciences of the United States of America*. 93:11173-11178.

Ohtsuka, T., M. Sakamoto, F. Guillemot, and R. Kageyama. 2001. Roles of the basic helix-loop-helix genes Hes1 and Hes5 in expansion of neural stem cells of the developing brain. *The Journal of biological chemistry*. 276:30467-30474.

Okamura, H., J. Aramburu, C. Garcia-Rodriguez, J.P. Viola, A. Raghavan, M. Tahiliani, X. Zhang, J. Qin, P.G. Hogan, and A. Rao. 2000. Concerted dephosphorylation of the transcription factor NFAT1 induces a conformational switch that regulates transcriptional activity. *Molecular cell*. 6:539-550.

Okano, H., and S. Temple. 2009. Cell types to order: temporal specification of CNS stem cells. *Current opinion in neurobiology*. 19:112-119.

Oliveria, S.F., M.L. Dell'Acqua, and W.A. Sather. 2007. AKAP79/150 anchoring of calcineurin controls neuronal L-type Ca2+ channel activity and nuclear signaling. *Neuron*. 55:261-275.

Onoyama, Y., M. Abe, E. Yabumoto, T. Sakamoto, and T. Nishidai. 1976. Radiation therapy in the treatment of glioblastoma. *AJR. American journal of roentgenology*. 126:481-492.

Osada, S., T. Matsubara, S. Daimon, Y. Terazu, M. Xu, T. Nishihara, and M. Imagawa. 1999. Expression, DNA-binding specificity and transcriptional regulation of nuclear factor 1 family proteins from rat. *The Biochemical journal*. 342 (Pt 1):189-198.

Ostrom, Q.T., L. Bauchet, F.G. Davis, I. Deltour, J.L. Fisher, C.E. Langer, M. Pekmezci, J.A. Schwartzbaum, M.C. Turner, K.M. Walsh, M.R. Wrensch, and J.S. Barnholtz-Sloan. 2014a. The epidemiology of glioma in adults: a "state of the science" review. *Neuro-oncology*. 16:896-913.

Ostrom, Q.T., Y. Chen, M.d.B. P, A. Ondracek, P. Farah, H. Gittleman, Y. Wolinsky, C. Kruchko, M.L. Cohen, D.J. Brat, and J.S. Barnholtz-Sloan. 2014b. The descriptive epidemiology of atypical teratoid/rhabdoid tumors in the United States, 2001-2010. *Neuro-oncology*. 16:1392-1399.

Ouellet, S., F. Vigneault, M. Lessard, S. Leclerc, R. Drouin, and S.L. Guerin. 2006. Transcriptional regulation of the cyclin-dependent kinase inhibitor 1A (p21) gene by NFI in proliferating human cells. *Nucleic acids research*. 34:6472-6487.

Panatier, A., J. Vallee, M. Haber, K.K. Murai, J.C. Lacaille, and R. Robitaille. 2011. Astrocytes are endogenous regulators of basal transmission at central synapses. *Cell*. 146:785-798.

Park, D., A.P. Xiang, L. Zhang, F.F. Mao, N.M. Walton, S.S. Choi, and B.T. Lahn. 2009. The radial glia antibody RC2 recognizes a protein encoded by Nestin. *Biochemical and biophysical research communications*. 382:588-592.

Park, S., M. Uesugi, and G.L. Verdine. 2000. A second calcineurin binding site on the NFAT regulatory domain. *Proceedings of the National Academy of Sciences of the United States of America*. 97:7130-7135.

Parsa, A.T., S. Wachhorst, K.R. Lamborn, M.D. Prados, M.W. McDermott, M.S. Berger, and S.M. Chang. 2005. Prognostic significance of intracranial dissemination of glioblastoma multiforme in adults. *Journal of neurosurgery*. 102:622-628.

Parsons, D.W., S. Jones, X. Zhang, J.C. Lin, R.J. Leary, P. Angenendt, P. Mankoo, H. Carter, I.M. Siu, G.L. Gallia, A. Olivi, R. McLendon, B.A. Rasheed, S. Keir, T. Nikolskaya, Y. Nikolsky, D.A. Busam, H. Tekleab, L.A. Diaz, Jr., J. Hartigan, D.R. Smith, R.L. Strausberg, S.K. Marie, S.M. Shinjo, H. Yan, G.J. Riggins, D.D. Bigner, R. Karchin, N. Papadopoulos, G. Parmigiani, B. Vogelstein, V.E. Velculescu, and K.W. Kinzler. 2008. An integrated genomic analysis of human glioblastoma multiforme. *Science*. 321:1807-1812.

Patel, A.P., I. Tirosh, J.J. Trombetta, A.K. Shalek, S.M. Gillespie, H. Wakimoto, D.P. Cahill, B.V. Nahed, W.T. Curry, R.L. Martuza, D.N. Louis, O. Rozenblatt-Rosen, M.L. Suva, A. Regev, and B.E. Bernstein. 2014. Single-cell RNA-seq highlights intratumoral heterogeneity in primary glioblastoma. *Science*. 344:1396-1401.

Paulson, M., S. Pisharody, L. Pan, S. Guadagno, A.L. Mui, and D.E. Levy. 1999. Stat protein transactivation domains recruit p300/CBP through widely divergent sequences. *The Journal of biological chemistry*. 274:25343-25349.

Pereira, J.D., S.N. Sansom, J. Smith, M.W. Dobenecker, A. Tarakhovsky, and F.J. Livesey. 2010. Ezh2, the histone methyltransferase of PRC2, regulates the balance between self-renewal and differentiation in the cerebral cortex.

Proceedings of the National Academy of Sciences of the United States of America. 107:15957-15962.

Petrik, D., S. Yun, S.E. Latchney, S. Kamrudin, J.A. LeBlanc, J.A. Bibb, and A.J. Eisch. 2013. Early postnatal in vivo gliogenesis from nestin-lineage progenitors requires cdk5. *PloS one*. 8:e72819.

Phillips, C., M. Guiney, J. Smith, P. Hughes, K. Narayan, and G. Quong. 2003. A randomized trial comparing 35Gy in ten fractions with 60Gy in 30 fractions of cerebral irradiation for glioblastoma multiforme and older patients with anaplastic astrocytoma. *Radiotherapy and oncology : journal of the European Society for Therapeutic Radiology and Oncology*. 68:23-26.

Phillips, H.S., S. Kharbanda, R. Chen, W.F. Forrest, R.H. Soriano, T.D. Wu, A. Misra, J.M. Nigro, H. Colman, L. Soroceanu, P.M. Williams, Z. Modrusan, B.G. Feuerstein, and K. Aldape. 2006. Molecular subclasses of high-grade glioma predict prognosis, delineate a pattern of disease progression, and resemble stages in neurogenesis. *Cancer cell*. 9:157-173.

Piccirillo, S.G., B.A. Reynolds, N. Zanetti, G. Lamorte, E. Binda, G. Broggi, H. Brem, A. Olivi, F. Dimeco, and A.L. Vescovi. 2006. Bone morphogenetic proteins inhibit the tumorigenic potential of human brain tumour-initiating cells. *Nature*. 444:761-765.

Pierfelice, T., L. Alberi, and N. Gaiano. 2011. Notch in the vertebrate nervous system: an old dog with new tricks. *Neuron*. 69:840-855.

Pillai, S., P. Dasgupta, and S.P. Chellappan. 2009. Chromatin immunoprecipitation assays: analyzing transcription factor binding and histone modifications in vivo. *Methods Mol Biol*. 523:323-339.

Pinto, L., and M. Gotz. 2007. Radial glial cell heterogeneity--the source of diverse progeny in the CNS. *Progress in neurobiology*. 83:2-23.

Piper, M., G. Barry, T.J. Harvey, R. McLeay, A.G. Smith, L. Harris, S. Mason, B.W. Stringer, B.W. Day, N.R. Wray, R.M. Gronostajski, T.L. Bailey, A.W. Boyd, and L.J. Richards. 2014. NFIB-mediated repression of the epigenetic factor Ezh2 regulates cortical development. *The Journal of neuroscience : the official journal of the Society for Neuroscience*. 34:2921-2930.

Piper, M., G. Barry, J. Hawkins, S. Mason, C. Lindwall, E. Little, A. Sarkar, A.G. Smith, R.X. Moldrich, G.M. Boyle, S. Tole, R.M. Gronostajski, T.L. Bailey, and L.J. Richards. 2010. NFIA controls telencephalic progenitor cell differentiation through repression of the Notch effector Hes1. *The Journal of neuroscience : the official journal of the Society for Neuroscience*. 30:9127-9139.

Piper, M., L. Harris, G. Barry, Y.H. Heng, C. Plachez, R.M. Gronostajski, and L.J. Richards. 2011. Nuclear factor one X regulates the development of multiple cellular

populations in the postnatal cerebellum. *The Journal of comparative neurology*. 519:3532-3548.

Plachez, C., K. Cato, R.C. McLeay, Y.H. Heng, T.L. Bailey, R.M. Gronostajski, L.J. Richards, A.C. Puche, and M. Piper. 2012. Expression of nuclear factor one A and -B in the olfactory bulb. *The Journal of comparative neurology*. 520:3135-3149.

Potter, N.E., K. Phipps, W. Harkness, R. Hayward, D. Thompson, T.S. Jacques, B. Harding, D.G. Thomas, J. Rees, J.L. Darling, and T.J. Warr. 2009. Astrocytoma derived short-term cell cultures retain molecular signatures characteristic of the tumour in situ. *Experimental cell research*. 315:2835-2846.

Prado, F., G. Vicent, C. Cardalda, and M. Beato. 2002. Differential role of the proline-rich domain of nuclear factor 1-C splice variants in DNA binding and transactivation. *The Journal of biological chemistry*. 277:16383-16390.

Prados, M.D., W.M. Wara, P.K. Sneed, M. McDermott, S.M. Chang, J. Rabbitt, M. Page, M. Malec, R.L. Davis, P.H. Gutin, K. Lamborn, C.B. Wilson, T.L. Phillips, and D.A. Larson. 2001. Phase III trial of accelerated hyperfractionation with or without difluromethylornithine (DFMO) versus standard fractionated radiotherapy with or without DFMO for newly diagnosed patients with glioblastoma multiforme. *International journal of radiation oncology, biology, physics*. 49:71-77.

Prakriya, M. 2009. The molecular physiology of CRAC channels. *Immunological reviews*. 231:88-98.

Pufall, M.A., G.M. Lee, M.L. Nelson, H.S. Kang, A. Velyvis, L.E. Kay, L.P. McIntosh, and B.J. Graves. 2005. Variable control of Ets-1 DNA binding by multiple phosphates in an unstructured region. *Science*. 309:142-145.

Pujol, M.J., R. Bosser, M. Vendrell, J. Serratosa, and O. Bachs. 1993. Nuclear calmodulin-binding proteins in rat neurons. *Journal of neurochemistry*. 60:1422-1428.

Purow, B.W., R.M. Haque, M.W. Noel, Q. Su, M.J. Burdick, J. Lee, T. Sundaresan, S. Pastorino, J.K. Park, I. Mikolaenko, D. Maric, C.G. Eberhart, and H.A. Fine. 2005. Expression of Notch-1 and its ligands, Delta-like-1 and Jagged-1, is critical for glioma cell survival and proliferation. *Cancer research*. 65:2353-2363.

Pyrzynska, B., A. Lis, G. Mosieniak, and B. Kaminska. 2001. Cyclosporin A-sensitive signaling pathway involving calcineurin regulates survival of reactive astrocytes. *Neurochemistry international*. 38:409-415.

Qian, F., U. Kruse, P. Lichter, and A.E. Sippel. 1995. Chromosomal localization of the four genes (NFIA, B, C, and X) for the human transcription factor nuclear factor I by FISH. *Genomics*. 28:66-73.

Qiang, L., T. Wu, H.W. Zhang, N. Lu, R. Hu, Y.J. Wang, L. Zhao, F.H. Chen, X.T. Wang, Q.D. You, and Q.L. Guo. 2012. HIF-1alpha is critical for hypoxia-mediated maintenance of glioblastoma stem cells by activating Notch signaling pathway. *Cell death and differentiation*. 19:284-294.

Quinones-Hinojosa, A., and K. Chaichana. 2007. The human subventricular zone: a source of new cells and a potential source of brain tumors. *Experimental neurology*. 205:313-324.

Rajan, P., and R.D. McKay. 1998. Multiple routes to astrocytic differentiation in the CNS. *The Journal of neuroscience : the official journal of the Society for Neuroscience*. 18:3620-3629.

Rakic, P. 1972. Mode of cell migration to the superficial layers of fetal monkey neocortex. *The Journal of comparative neurology*. 145:61-83.

Ramasamy, S.K., and N. Lenka. 2010. Notch exhibits ligand bias and maneuvers stage-specific steering of neural differentiation in embryonic stem cells. *Molecular and cellular biology*. 30:1946-1957.

Rao, J.S. 2003. Molecular mechanisms of glioma invasiveness: the role of proteases. *Nature reviews. Cancer*. 3:489-501.

Reitman, Z.J., D.W. Parsons, and H. Yan. 2010. IDH1 and IDH2: not your typical oncogenes. *Cancer cell*. 17:215-216.

Rich, J.N., C. Guo, R.E. McLendon, D.D. Bigner, X.F. Wang, and C.M. Counter. 2001. A genetically tractable model of human glioma formation. *Cancer research*. 61:3556-3560.

Ritter, O., S. Hack, K. Schuh, N. Rothlein, A. Perrot, K.J. Osterziel, H.D. Schulte, and L. Neyses. 2002. Calcineurin in human heart hypertrophy. *Circulation*. 105:2265-2269.

Rodriguez, A., J. Roy, S. Martinez-Martinez, M.D. Lopez-Maderuelo, P. Nino-Moreno, L. Orti, D. Pantoja-Uceda, A. Pineda-Lucena, M.S. Cyert, and J.M. Redondo. 2009. A conserved docking surface on calcineurin mediates interaction with substrates and immunosuppressants. *Molecular cell*. 33:616-626.

Romao, L.F., O. Sousa Vde, V.M. Neto, and F.C. Gomes. 2008. Glutamate activates GFAP gene promoter from cultured astrocytes through TGF-beta1 pathways. *J Neurochem*. 106:746-756.

Ross, S.E., M.E. Greenberg, and C.D. Stiles. 2003. Basic helix-loop-helix factors in cortical development. *Neuron*. 39:13-25.

Rothermel, B., R.B. Vega, J. Yang, H. Wu, R. Bassel-Duby, and R.S. Williams. 2000. A protein encoded within the Down syndrome critical region is enriched in

striated muscles and inhibits calcineurin signaling. *The Journal of biological chemistry*. 275:8719-8725.

Roulet, E., P. Bucher, R. Schneider, E. Wingender, Y. Dusserre, T. Werner, and N. Mermod. 2000. Experimental analysis and computer prediction of CTF/NFI transcription factor DNA binding sites. *Journal of molecular biology*. 297:833-848.

Rowitch, D.H., and A.R. Kriegstein. 2010. Developmental genetics of vertebrate glial-cell specification. *Nature*. 468:214-222.

Roy, R.J., P. Gosselin, and S.L. Guerin. 1991. A short protocol for micro-purification of nuclear proteins from whole animal tissue. *BioTechniques*. 11:770-777.

Rupp, R.A., U. Kruse, G. Multhaup, U. Gobel, K. Beyreuther, and A.E. Sippel. 1990. Chicken NFI/TGGCA proteins are encoded by at least three independent genes: NFI-A, NFI-B and NFI-C with homologues in mammalian genomes. *Nucleic acids research*. 18:2607-2616.

Rusnak, F., and P. Mertz. 2000. Calcineurin: form and function. *Physiological reviews*. 80:1483-1521.

Rutka, J.T., S.L. Hubbard, K. Fukuyama, K. Matsuzawa, P.B. Dirks, and L.E. Becker. 1994. Effects of antisense glial fibrillary acidic protein complementary DNA on the growth, invasion, and adhesion of human astrocytoma cells. *Cancer Res*. 54:3267-3272.

Rutka, J.T., and S.L. Smith. 1993. Transfection of human astrocytoma cells with glial fibrillary acidic protein complementary DNA: analysis of expression, proliferation, and tumorigenicity. *Cancer Res*. 53:3624-3631.

Sakamoto, M., H. Hirata, T. Ohtsuka, Y. Bessho, and R. Kageyama. 2003. The basic helix-loop-helix genes Hesr1/Hey1 and Hesr2/Hey2 regulate maintenance of neural precursor cells in the brain. *The Journal of biological chemistry*. 278:44808-44815.

Sakata, Y., C.N. Kamei, H. Nakagami, R. Bronson, J.K. Liao, and M.T. Chin. 2002. Ventricular septal defect and cardiomyopathy in mice lacking the transcription factor CHF1/Hey2. *Proceedings of the National Academy of Sciences of the United States of America*. 99:16197-16202.

Salazar, O.M., P. Rubin, M.L. Feldstein, and R. Pizzutiello. 1979. High dose radiation therapy in the treatment of malignant gliomas: final report. *International journal of radiation oncology, biology, physics*. 5:1733-1740.

Sama, M.A., D.M. Mathis, J.L. Furman, H.M. Abdul, I.A. Artiushin, S.D. Kraner, and C.M. Norris. 2008. Interleukin-1beta-dependent signaling between astrocytes

and neurons depends critically on astrocytic calcineurin/NFAT activity. *The Journal of biological chemistry*. 283:21953-21964.

Sanai, N., A. Alvarez-Buylla, and M.S. Berger. 2005. Neural stem cells and the origin of gliomas. *The New England journal of medicine*. 353:811-822.

Sanai, N., and M.S. Berger. 2008. Glioma extent of resection and its impact on patient outcome. *Neurosurgery*. 62:753-764; discussion 264-756.

Sanderson, J.L., J.A. Gorski, E.S. Gibson, P. Lam, R.K. Freund, W.S. Chick, and M.L. Dell'Acqua. 2012. AKAP150-anchored calcineurin regulates synaptic plasticity by limiting synaptic incorporation of Ca2+-permeable AMPA receptors. *The Journal of neuroscience : the official journal of the Society for Neuroscience*. 32:15036-15052.

Sanna, B., E.B. Brandt, R.A. Kaiser, P. Pfluger, S.A. Witt, T.R. Kimball, E. van Rooij, L.J. De Windt, M.E. Rothenberg, M.H. Tschop, S.C. Benoit, and J.D. Molkentin. 2006. Modulatory calcineurin-interacting proteins 1 and 2 function as calcineurin facilitators in vivo. *Proceedings of the National Academy of Sciences of the United States of America*. 103:7327-7332.

Santella, L., and E. Carafoli. 1997. Calcium signaling in the cell nucleus. *FASEB journal : official publication of the Federation of American Societies for Experimental Biology*. 11:1091-1109.

Santoro, C., N. Mermod, P.C. Andrews, and R. Tjian. 1988. A family of human CCAAT-box-binding proteins active in transcription and DNA replication: cloning and expression of multiple cDNAs. *Nature*. 334:218-224.

Satoh, S., T. Noaki, T. Ishigure, S. Osada, M. Imagawa, N. Miura, K. Yamada, and T. Noguchi. 2005. Nuclear factor 1 family members interact with hepatocyte nuclear factor 1alpha to synergistically activate L-type pyruvate kinase gene transcription. *The Journal of biological chemistry*. 280:39827-39834.

Scheer, N., A. Groth, S. Hans, and J.A. Campos-Ortega. 2001. An instructive function for Notch in promoting gliogenesis in the zebrafish retina. *Development*. 128:1099-1107.

Schmechel, D.E., and P. Rakic. 1979. A Golgi study of radial glial cells in developing monkey telencephalon: morphogenesis and transformation into astrocytes. *Anat Embryol (Berl)*. 156:115-152.

Scholze, A.R., L.C. Foo, S. Mulinyawe, and B.A. Barres. 2014. BMP signaling in astrocytes downregulates EGFR to modulate survival and maturation. *PloS one*. 9:e110668.

Schwartz, N., A. Schohl, and E.S. Ruthazer. 2009. Neural activity regulates synaptic properties and dendritic structure in vivo through calcineurin/NFAT signaling. *Neuron*. 62:655-669.

Scott, C.E., S.L. Wynn, A. Sesay, C. Cruz, M. Cheung, M.V. Gomez Gaviro, S. Booth, B. Gao, K.S. Cheah, R. Lovell-Badge, and J. Briscoe. 2010. SOX9 induces and maintains neural stem cells. *Nature neuroscience*. 13:1181-1189.

Scrideli, C.A., C.G. Carlotti, Jr., O.K. Okamoto, V.S. Andrade, M.A. Cortez, F.J. Motta, A.K. Lucio-Eterovic, L. Neder, S. Rosemberg, S.M. Oba-Shinjo, S.K. Marie, and L.G. Tone. 2008. Gene expression profile analysis of primary glioblastomas and non-neoplastic brain tissue: identification of potential target genes by oligonucleotide microarray and real-time quantitative PCR. *Journal of neuro-oncology*. 88:281-291.

Serfling, E., F. Berberich-Siebelt, S. Chuvpilo, E. Jankevics, S. Klein-Hessling, T. Twardzik, and A. Avots. 2000. The role of NF-AT transcription factors in T cell activation and differentiation. *Biochimica et biophysica acta*. 1498:1-18.

Shapiro, W.R., S.B. Green, P.C. Burger, M.S. Mahaley, Jr., R.G. Selker, J.C. VanGilder, J.T. Robertson, J. Ransohoff, J. Mealey, Jr., T.A. Strike, and et al. 1989. Randomized trial of three chemotherapy regimens and two radiotherapy regimens and two radiotherapy regimens in postoperative treatment of malignant glioma. Brain Tumor Cooperative Group Trial 8001. *Journal of neurosurgery*. 71:1-9.

Sharff, K.A., W.X. Song, X. Luo, N. Tang, J. Luo, J. Chen, Y. Bi, B.C. He, J. Huang, X. Li, W. Jiang, G.H. Zhu, Y. Su, Y. He, J. Shen, Y. Wang, L. Chen, G.W. Zuo, B. Liu, X. Pan, R.R. Reid, H.H. Luu, R.C. Haydon, and T.C. He. 2009. Hey1 basic helix-loop-helix protein plays an important role in mediating BMP9-induced osteogenic differentiation of mesenchymal progenitor cells. *The Journal of biological chemistry*. 284:649-659.

Sharma, R.R., D.P. Singh, A. Pathak, N. Khandelwal, C.M. Sehgal, R. Kapoor, S. Ghoshal, F.D. Patel, and S.C. Sharma. 2003. Local control of high-grade gliomas with limited volume irradiation versus whole brain irradiation. *Neurology India*. 51:512-517.

Shaw, K.T., A.M. Ho, A. Raghavan, J. Kim, J. Jain, J. Park, S. Sharma, A. Rao, and P.G. Hogan. 1995. Immunosuppressive drugs prevent a rapid dephosphorylation of transcription factor NFAT1 in stimulated immune cells. *Proceedings of the National Academy of Sciences of the United States of America*. 92:11205-11209.

Shibasaki, F., U. Hallin, and H. Uchino. 2002. Calcineurin as a multifunctional regulator. *Journal of biochemistry*. 131:1-15.

Shibasaki, F., and F. McKeon. 1995. Calcineurin functions in Ca(2+)-activated cell death in mammalian cells. *The Journal of cell biology*. 131:735-743.

Shibasaki, F., E.R. Price, D. Milan, and F. McKeon. 1996. Role of kinases and the phosphatase calcineurin in the nuclear shuttling of transcription factor NF-AT4. *Nature*. 382:370-373.

Shieh, S.Y., M. Ikeda, Y. Taya, and C. Prives. 1997. DNA damage-induced phosphorylation of p53 alleviates inhibition by MDM2. *Cell*. 91:325-334.

Shimojo, H., T. Ohtsuka, and R. Kageyama. 2008. Oscillations in notch signaling regulate maintenance of neural progenitors. *Neuron*. 58:52-64.

Shin, H.Y., Y.H. Hong, S.S. Jang, H.G. Chae, S.L. Paek, H.E. Moon, D.G. Kim, J. Kim, S.H. Paek, and S.J. Kim. 2010. A role of canonical transient receptor potential 5 channel in neuronal differentiation from A2B5 neural progenitor cells. *PloS one*. 5:e10359.

Shu, T., K.G. Butz, C. Plachez, R.M. Gronostajski, and L.J. Richards. 2003. Abnormal development of forebrain midline glia and commissural projections in Nfia knock-out mice. *The Journal of neuroscience : the official journal of the Society for Neuroscience*. 23:203-212.

Siebzehnrubl, F.A., B.A. Reynolds, A. Vescovi, D.A. Steindler, and L.P. Deleyrolle. 2011. The origins of glioma: E Pluribus Unum? *Glia*. 59:1135-1147.

Simpson, J.R., J. Horton, C. Scott, W.J. Curran, P. Rubin, J. Fischbach, S. Isaacson, M. Rotman, S.O. Asbell, J.S. Nelson, and et al. 1993. Influence of location and extent of surgical resection on survival of patients with glioblastoma multiforme: results of three consecutive Radiation Therapy Oncology Group (RTOG) clinical trials. *International journal of radiation oncology, biology, physics*. 26:239-244.

Singh, S.K., R. Bhardwaj, K.M. Wilczynska, C.I. Dumur, and T. Kordula. 2011a. A complex of nuclear factor I-X3 and STAT3 regulates astrocyte and glioma migration through the secreted glycoprotein YKL-40. *The Journal of biological chemistry*. 286:39893-39903.

Singh, S.K., I.D. Clarke, M. Terasaki, V.E. Bonn, C. Hawkins, J. Squire, and P.B. Dirks. 2003. Identification of a cancer stem cell in human brain tumors. *Cancer research*. 63:5821-5828.

Singh, S.K., K.M. Wilczynska, A. Grzybowski, J. Yester, B. Osrah, L. Bryan, S. Wright, I. Griswold-Prenner, and T. Kordula. 2011b. The unique transcriptional activation domain of nuclear factor-I-X3 is critical to specifically induce marker gene expression in astrocytes. *The Journal of biological chemistry*. 286:7315-7326.

Skardelly, M., A. Glien, C. Groba, N. Schlichting, M. Kamprad, J. Meixensberger, and J. Milosevic. 2013. The influence of immunosuppressive drugs on neural stem/progenitor cell fate in vitro. *Experimental cell research*. 319:3170-3181.

Somasundaram, A., A.K. Shum, H.J. McBride, J.A. Kessler, S. Feske, R.J. Miller, and M. Prakriya. 2014. Store-operated CRAC channels regulate gene expression and proliferation in neural progenitor cells. *The Journal of neuroscience : the official journal of the Society for Neuroscience*. 34:9107-9123.

Song, H.R., I. Gonzalez-Gomez, G.S. Suh, D.L. Commins, R. Sposto, F.H. Gilles, B. Deneen, and A. Erdreich-Epstein. 2010. Nuclear factor IA is expressed in astrocytomas and is associated with improved survival. *Neuro-oncology*. 12:122-132.

Souhami, L., W. Seiferheld, D. Brachman, E.B. Podgorsak, M. Werner-Wasik, R. Lustig, C.J. Schultz, W. Sause, P. Okunieff, J. Buckner, L. Zamorano, M.P. Mehta, and W.J. Curran, Jr. 2004. Randomized comparison of stereotactic radiosurgery followed by conventional radiotherapy with carmustine to conventional radiotherapy with carmustine for patients with glioblastoma multiforme: report of Radiation Therapy Oncology Group 93-05 protocol. *International journal of radiation oncology, biology, physics*. 60:853-860.

Steele-Perkins, G., K.G. Butz, G.E. Lyons, M. Zeichner-David, H.J. Kim, M.I. Cho, and R.M. Gronostajski. 2003. Essential role for NFI-C/CTF transcription-replication factor in tooth root development. *Molecular and cellular biology*. 23:1075-1084.

Steele-Perkins, G., C. Plachez, K.G. Butz, G. Yang, C.J. Bachurski, S.L. Kinsman, E.D. Litwack, L.J. Richards, and R.M. Gronostajski. 2005. The transcription factor gene Nfib is essential for both lung maturation and brain development. *Molecular and cellular biology*. 25:685-698.

Steiner, J.P., T.M. Dawson, M. Fotuhi, C.E. Glatt, A.M. Snowman, N. Cohen, and S.H. Snyder. 1992. High brain densities of the immunophilin FKBP colocalized with calcineurin. *Nature*. 358:584-587.

Stemmer, P.M., and C.B. Klee. 1994. Dual calcium ion regulation of calcineurin by calmodulin and calcineurin B. *Biochemistry*. 33:6859-6866.

Stiles, C.D., and D.H. Rowitch. 2008. Glioma stem cells: a midterm exam. *Neuron*. 58:832-846.

Stiles, J. 2008. The fundamentals of brain development : integrating nature and nurture. Harvard University Press, Cambridge, Mass. xii, 421 p. pp.

Stiles, J., and T.L. Jernigan. 2010. The basics of brain development. *Neuropsychology review*. 20:327-348.

Stockhausen, M.T., K. Kristoffersen, and H.S. Poulsen. 2010. The functional role of Notch signaling in human gliomas. *Neuro-oncology*. 12:199-211.

Stolt, C.C., P. Lommes, E. Sock, M.C. Chaboissier, A. Schedl, and M. Wegner. 2003. The Sox9 transcription factor determines glial fate choice in the developing spinal cord. *Genes & development*. 17:1677-1689.

Stolt, C.C., S. Rehberg, M. Ader, P. Lommes, D. Riethmacher, M. Schachner, U. Bartsch, and M. Wegner. 2002. Terminal differentiation of myelin-forming oligodendrocytes depends on the transcription factor Sox10. *Genes & development*. 16:165-170.

Stummer, W., H.J. Reulen, T. Meinel, U. Pichlmeier, W. Schumacher, J.C. Tonn, V. Rohde, F. Oppel, B. Turowski, C. Woiciechowsky, K. Franz, and T. Pietsch. 2008. Extent of resection and survival in glioblastoma multiforme: identification of and adjustment for bias. *Neurosurgery*. 62:564-576; discussion 564-576.

Stupp, R., M. Gander, S. Leyvraz, and E. Newlands. 2001. Current and future developments in the use of temozolomide for the treatment of brain tumours. *The Lancet. Oncology*. 2:552-560.

Stupp, R., M.E. Hegi, T. Gorlia, S.C. Erridge, J. Perry, Y.K. Hong, K.D. Aldape, B. Lhermitte, T. Pietsch, D. Grujicic, J.P. Steinbach, W. Wick, R. Tarnawski, D.H. Nam, P. Hau, A. Weyerbrock, M.J. Taphoorn, C.C. Shen, N. Rao, L. Thurzo, U. Herrlinger, T. Gupta, R.D. Kortmann, K. Adamska, C. McBain, A.A. Brandes, J.C. Tonn, O. Schnell, T. Wiegel, C.Y. Kim, L.B. Nabors, D.A. Reardon, M.J. van den Bent, C. Hicking, A. Markivskyy, M. Picard, and M. Weller. 2014. Cilengitide combined with standard treatment for patients with newly diagnosed glioblastoma with methylated MGMT promoter (CENTRIC EORTC 26071-22072 study): a multicentre, randomised, open-label, phase 3 trial. *The Lancet. Oncology*. 15:1100-1108.

Stupp, R., M.E. Hegi, W.P. Mason, M.J. van den Bent, M.J. Taphoorn, R.C. Janzer, S.K. Ludwin, A. Allgeier, B. Fisher, K. Belanger, P. Hau, A.A. Brandes, J. Gijtenbeek, C. Marosi, C.J. Vecht, K. Mokhtari, P. Wesseling, S. Villa, E. Eisenhauer, T. Gorlia, M. Weller, D. Lacombe, J.G. Cairncross, and R.O. Mirimanoff. 2009. Effects of radiotherapy with concomitant and adjuvant temozolomide versus radiotherapy alone on survival in glioblastoma in a randomised phase III study: 5-year analysis of the EORTC-NCIC trial. *The Lancet. Oncology*. 10:459-466.

Stupp, R., W.P. Mason, M.J. van den Bent, M. Weller, B. Fisher, M.J. Taphoorn, K. Belanger, A.A. Brandes, C. Marosi, U. Bogdahn, J. Curschmann, R.C. Janzer, S.K. Ludwin, T. Gorlia, A. Allgeier, D. Lacombe, J.G. Cairncross, E. Eisenhauer, and R.O. Mirimanoff. 2005. Radiotherapy plus concomitant and adjuvant temozolomide for glioblastoma. *The New England journal of medicine*. 352:987-996.

Suk, H.Y., C. Zhou, T.T. Yang, H. Zhu, R.Y. Yu, O. Olabisi, X. Yang, D. Brancho, J.Y. Kim, P.E. Scherer, P.G. Frank, M.P. Lisanti, J.W. Calvert, D.J. Lefer, J.D. Molkentin, A. Ghigo, E. Hirsch, J. Jin, and C.W. Chow. 2013. Ablation of calcineurin Abeta reveals hyperlipidemia and signaling cross-talks with phosphodiesterases. *The Journal of biological chemistry*. 288:3477-3488.

Sumner, C., T. Shinohara, L. Durham, R. Traub, E.O. Major, and K. Amemiya. 1996. Expression of multiple classes of the nuclear factor-1 family in the developing human brain: differential expression of two classes of NF-1 genes. *Journal of neurovirology*. 2:87-100.

Sun, J., C.N. Kamei, M.D. Layne, M.K. Jain, J.K. Liao, M.E. Lee, and M.T. Chin. 2001a. Regulation of myogenic terminal differentiation by the hairy-related transcription factor CHF2. *The Journal of biological chemistry*. 276:18591-18596.

Sun, L., H.C. Blair, Y. Peng, N. Zaidi, O.A. Adebanjo, X.B. Wu, X.Y. Wu, J. Iqbal, S. Epstein, E. Abe, B.S. Moonga, and M. Zaidi. 2005. Calcineurin regulates bone formation by the osteoblast. *Proceedings of the National Academy of Sciences of the United States of America*. 102:17130-17135.

Sun, Y., M. Nadal-Vicens, S. Misono, M.Z. Lin, A. Zubiaga, X. Hua, G. Fan, and M.E. Greenberg. 2001b. Neurogenin promotes neurogenesis and inhibits glial differentiation by independent mechanisms. *Cell*. 104:365-376.

Swerdlow, A.J., M. Feychting, A.C. Green, L.K. Leeka Kheifets, and D.A. Savitz. 2011. Mobile phones, brain tumors, and the interphone study: where are we now? *Environmental health perspectives*. 119:1534-1538.

Takata, T., and F. Ishikawa. 2003. Human Sir2-related protein SIRT1 associates with the bHLH repressors HES1 and HEY2 and is involved in HES1- and HEY2-mediated transcriptional repression. *Biochemical and biophysical research communications*. 301:250-257.

Takebayashi, K., Y. Sasai, Y. Sakai, T. Watanabe, S. Nakanishi, and R. Kageyama. 1994. Structure, chromosomal locus, and promoter analysis of the gene encoding the mouse helix-loop-helix factor HES-1. Negative autoregulation through the multiple N box elements. *The Journal of biological chemistry*. 269:5150-5156.

Takizawa, T., K. Nakashima, M. Namihira, W. Ochiai, A. Uemura, M. Yanagisawa, N. Fujita, M. Nakao, and T. Taga. 2001. DNA methylation is a critical cell-intrinsic determinant of astrocyte differentiation in the fetal brain. *Developmental cell*. 1:749-758.

Taylor, M.K., K. Yeager, and S.J. Morrison. 2007. Physiological Notch signaling promotes gliogenesis in the developing peripheral and central nervous systems. *Development*. 134:2435-2447.

Tidow, H., and P. Nissen. 2013. Structural diversity of calmodulin binding to its target sites. *The FEBS journal*. 280:5551-5565.

Tie, X., S. Han, L. Meng, Y. Wang, and A. Wu. 2013. NFAT1 is highly expressed in, and regulates the invasion of, glioblastoma multiforme cells. *PloS one*. 8:e66008.

Toledo, F., and G.M. Wahl. 2006. Regulating the p53 pathway: in vitro hypotheses, in vivo veritas. *Nature reviews. Cancer*. 6:909-923.

Truax, A.D., and S.F. Greer. 2012. ChIP and Re-ChIP assays: investigating interactions between regulatory proteins, histone modifications, and the DNA sequences to which they bind. *Methods Mol Biol*. 809:175-188.

Turcan, S., D. Rohle, A. Goenka, L.A. Walsh, F. Fang, E. Yilmaz, C. Campos, A.W. Fabius, C. Lu, P.S. Ward, C.B. Thompson, A. Kaufman, O. Guryanova, R. Levine, A. Heguy, A. Viale, L.G. Morris, J.T. Huse, I.K. Mellinghoff, and T.A. Chan. 2012. IDH1 mutation is sufficient to establish the glioma hypermethylator phenotype. *Nature*. 483:479-483.

Ueki, K., T. Muramatsu, and R.L. Kincaid. 1992. Structure and expression of two isoforms of the murine calmodulin-dependent protein phosphatase regulatory subunit (calcineurin B). *Biochemical and biophysical research communications*. 187:537-543.

Uhrbom, L., M. Kastemar, F.K. Johansson, B. Westermark, and E.C. Holland. 2005. Cell type-specific tumor suppression by Ink4a and Arf in Kras-induced mouse gliomagenesis. *Cancer research*. 65:2065-2069.

van der Meulen, J.D., H.J. Houthoff, and E.J. Ebels. 1978. Glial fibrillary acidic protein in human gliomas. *Neuropathol Appl Neurobiol*. 4:177-190.

Vanderklish, P.W., and B.A. Bahr. 2000. The pathogenic activation of calpain: a marker and mediator of cellular toxicity and disease states. *International journal of experimental pathology*. 81:323-339.

Vega, R.B., B.A. Rothermel, C.J. Weinheimer, A. Kovacs, R.H. Naseem, R. Bassel-Duby, R.S. Williams, and E.N. Olson. 2003. Dual roles of modulatory calcineurin-interacting protein 1 in cardiac hypertrophy. *Proceedings of the National Academy of Sciences of the United States of America*. 100:669-674.

Verhaak, R.G., K.A. Hoadley, E. Purdom, V. Wang, Y. Qi, M.D. Wilkerson, C.R. Miller, L. Ding, T. Golub, J.P. Mesirov, G. Alexe, M. Lawrence, M. O'Kelly, P. Tamayo, B.A. Weir, S. Gabriel, W. Winckler, S. Gupta, L. Jakkula, H.S. Feiler, J.G. Hodgson, C.D. James, J.N. Sarkaria, C. Brennan, A. Kahn, P.T. Spellman, R.K. Wilson, T.P. Speed, J.W. Gray, M. Meyerson, G. Getz, C.M. Perou, and D.N. Hayes. 2010. Integrated genomic analysis identifies clinically relevant subtypes of

glioblastoma characterized by abnormalities in PDGFRA, IDH1, EGFR, and NF1. *Cancer cell*. 17:98-110.

Vinade, L., C.A. Goncalves, S. Wofchuk, C. Gottfried, and R. Rodnight. 1997. Evidence for a role for calcium ions in the dephosphorylation of glial fibrillary acidic protein (GFAP) in immature hippocampal slices and in astrocyte cultures from the rat. *Brain research. Developmental brain research*. 104:11-17.

Volterra, A., N. Liaudet, and I. Savtchouk. 2014. Astrocyte Ca(2)(+) signalling: an unexpected complexity. *Nature reviews. Neuroscience*. 15:327-335.

Vousden, K.H., and C. Prives. 2009. Blinded by the Light: The Growing Complexity of p53. *Cell*. 137:413-431.

Walker, M.D., E. Alexander, Jr., W.E. Hunt, C.M. Leventhal, M.S. Mahaley, Jr., J. Mealey, H.A. Norrell, G. Owens, J. Ransohoff, C.B. Wilson, and E.A. Gehan. 1976. Evaluation of mithramycin in the treatment of anaplastic gliomas. *Journal of neurosurgery*. 44:655-667.

Walker, M.D., E. Alexander, Jr., W.E. Hunt, C.S. MacCarty, M.S. Mahaley, Jr., J. Mealey, Jr., H.A. Norrell, G. Owens, J. Ransohoff, C.B. Wilson, E.A. Gehan, and T.A. Strike. 1978. Evaluation of BCNU and/or radiotherapy in the treatment of anaplastic gliomas. A cooperative clinical trial. *Journal of neurosurgery*. 49:333-343.

Walker, M.D., S.B. Green, D.P. Byar, E. Alexander, Jr., U. Batzdorf, W.H. Brooks, W.E. Hunt, C.S. MacCarty, M.S. Mahaley, Jr., J. Mealey, Jr., G. Owens, J. Ransohoff, 2nd, J.T. Robertson, W.R. Shapiro, K.R. Smith, Jr., C.B. Wilson, and T.A. Strike. 1980. Randomized comparisons of radiotherapy and nitrosoureas for the treatment of malignant glioma after surgery. *The New England journal of medicine*. 303:1323-1329.

Wang, J., J. Bushman, X. Wang, M. Mayer-Proschel, M. Johnson, and M. Noble. 2013. Oligodendrocyte/type-2 astrocyte progenitor cells and glial-restricted precursor cells generate different tumor phenotypes in response to the identical oncogenes. *The Journal of neuroscience : the official journal of the Society for Neuroscience*. 33:16805-16817.

Wang, J., S.U. Pol, A.K. Haberman, C. Wang, M.A. O'Bara, and F.J. Sim. 2014. Transcription factor induction of human oligodendrocyte progenitor fate and differentiation. *Proceedings of the National Academy of Sciences of the United States of America*. 111:E2885-2894.

Wang, L., Z. Wang, J. Li, W. Zhang, F. Ren, and W. Yue. 2015. NFATc1 activation promotes the invasion of U251 human glioblastoma multiforme cells through COX-2. *International journal of molecular medicine*. 35:1333-1340.

Wang, M., T. Wang, S. Liu, D. Yoshida, and A. Teramoto. 2003. The expression of matrix metalloproteinase-2 and -9 in human gliomas of different pathological grades. *Brain tumor pathology*. 20:65-72.

Wang, M.G., H. Yi, D. Guerini, C.B. Klee, and O.W. McBride. 1996. Calcineurin A alpha (PPP3CA), calcineurin A beta (PPP3CB) and calcineurin B (PPP3R1) are located on human chromosomes 4, 10q21-->q22 and 2p16-->p15 respectively. *Cytogenetics and cell genetics*. 72:236-241.

Wang, W., J.E. Crandall, E.D. Litwack, R.M. Gronostajski, and D.L. Kilpatrick. 2010. Targets of the nuclear factor I regulon involved in early and late development of postmitotic cerebellar granule neurons. *Journal of neuroscience research*. 88:258-265.

Wang, W., D. Mullikin-Kilpatrick, J.E. Crandall, R.M. Gronostajski, E.D. Litwack, and D.L. Kilpatrick. 2007. Nuclear factor I coordinates multiple phases of cerebellar granule cell development via regulation of cell adhesion molecules. *The Journal of neuroscience : the official journal of the Society for Neuroscience*. 27:6115-6127.

Wang, W., Y. Shin, M. Shi, and D.L. Kilpatrick. 2011. Temporal control of a dendritogenesis-linked gene via REST-dependent regulation of nuclear factor I occupancy. *Molecular biology of the cell*. 22:868-879.

Wang, W., R.E. Stock, R.M. Gronostajski, Y.W. Wong, M. Schachner, and D.L. Kilpatrick. 2004. A role for nuclear factor I in the intrinsic control of cerebellar granule neuron gene expression. *The Journal of biological chemistry*. 279:53491-53497.

Warburg, O. 1956a. On respiratory impairment in cancer cells. *Science*. 124:269-270.

Warburg, O. 1956b. On the origin of cancer cells. *Science*. 123:309-314.

Ward, P.S., J. Patel, D.R. Wise, O. Abdel-Wahab, B.D. Bennett, H.A. Coller, J.R. Cross, V.R. Fantin, C.V. Hedvat, A.E. Perl, J.D. Rabinowitz, M. Carroll, S.M. Su, K.A. Sharp, R.L. Levine, and C.B. Thompson. 2010. The common feature of leukemia-associated IDH1 and IDH2 mutations is a neomorphic enzyme activity converting alpha-ketoglutarate to 2-hydroxyglutarate. *Cancer cell*. 17:225-234.

Watts, G.S., R.O. Pieper, J.F. Costello, Y.M. Peng, W.S. Dalton, and B.W. Futscher. 1997. Methylation of discrete regions of the O6-methylguanine DNA methyltransferase (MGMT) CpG island is associated with heterochromatinization of the MGMT transcription start site and silencing of the gene. *Molecular and cellular biology*. 17:5612-5619.

Weber, D., C. Wiese, and M. Gessler. 2014. Hey bHLH transcription factors. *Current topics in developmental biology*. 110:285-315.

Wendler, W., H. Altmann, and E. Ludwig-Winnacker. 1994. Transcriptional activation of NFI/CTF1 depends on a sequence motif strongly related to the carboxyterminal domain of RNA polymerase II. *Nucleic acids research*. 22:2601-2603.

Westphal, M., and K. Lamszus. 2011. The neurobiology of gliomas: from cell biology to the development of therapeutic approaches. *Nature reviews. Neuroscience*. 12:495-508.

Withers, H.R., L.J. Peters, H.D. Thames, and G.H. Fletcher. 1982. Hyperfractionation. *International journal of radiation oncology, biology, physics*. 8:1807-1809.

Woltje, K., M. Jabs, and A. Fischer. 2015. Serum induces transcription of Hey1 and Hey2 genes by Alk1 but not Notch signaling in endothelial cells. *PloS one*. 10:e0120547.

Wong, Y.W., C. Schulze, T. Streichert, R.M. Gronostajski, M. Schachner, and T. Tilling. 2007. Gene expression analysis of nuclear factor I-A deficient mice indicates delayed brain maturation. *Genome biology*. 8:R72.

Wu, H.Y., K. Tomizawa, Y. Oda, F.Y. Wei, Y.F. Lu, M. Matsushita, S.T. Li, A. Moriwaki, and H. Matsui. 2004. Critical role of calpain-mediated cleavage of calcineurin in excitotoxic neurodegeneration. *The Journal of biological chemistry*. 279:4929-4940.

Wu, M., M. Hernandez, S. Shen, J.K. Sabo, D. Kelkar, J. Wang, R. O'Leary, G.R. Phillips, H.S. Cate, and P. Casaccia. 2012. Differential modulation of the oligodendrocyte transcriptome by sonic hedgehog and bone morphogenetic protein 4 via opposing effects on histone acetylation. *The Journal of neuroscience : the official journal of the Society for Neuroscience*. 32:6651-6664.

Wu, Y., Y. Liu, E.M. Levine, and M.S. Rao. 2003. Hes1 but not Hes5 regulates an astrocyte versus oligodendrocyte fate choice in glial restricted precursors. *Developmental dynamics : an official publication of the American Association of Anatomists*. 226:675-689.

Xiao, A., H. Wu, P.P. Pandolfi, D.N. Louis, and T. Van Dyke. 2002. Astrocyte inactivation of the pRb pathway predisposes mice to malignant astrocytoma development that is accelerated by PTEN mutation. *Cancer cell*. 1:157-168.

Xiao, A., C. Yin, C. Yang, A. Di Cristofano, P.P. Pandolfi, and T. Van Dyke. 2005. Somatic induction of Pten loss in a preclinical astrocytoma model reveals major roles in disease progression and avenues for target discovery and validation. *Cancer research*. 65:5172-5180.

Xiao, H., J.T. Lis, J. Greenblatt, and J.D. Friesen. 1994. The upstream activator CTF/NF1 and RNA polymerase II share a common element involved in transcriptional activation. *Nucleic acids research*. 22:1966-1973.

Xie, Z., B. Lei, Q. Huang, J. Deng, M. Wu, W. Shen, and Y. Cheng. 2012. Neuroprotective effect of Cyclosporin A on the development of early brain injury in a subarachnoid hemorrhage model: a pilot study. *Brain research*. 1472:113-123.

Xu, P., S. Yu, R. Jiang, C. Kang, G. Wang, H. Jiang, and P. Pu. 2009. Differential expression of Notch family members in astrocytomas and medulloblastomas. *Pathology oncology research : POR*. 15:703-710.

Xu, W., H. Yang, Y. Liu, Y. Yang, P. Wang, S.H. Kim, S. Ito, C. Yang, M.T. Xiao, L.X. Liu, W.Q. Jiang, J. Liu, J.Y. Zhang, B. Wang, S. Frye, Y. Zhang, Y.H. Xu, Q.Y. Lei, K.L. Guan, S.M. Zhao, and Y. Xiong. 2011. Oncometabolite 2-hydroxyglutarate is a competitive inhibitor of alpha-ketoglutarate-dependent dioxygenases. *Cancer cell*. 19:17-30.

Yakel, J.L. 1997. Calcineurin regulation of synaptic function: from ion channels to transmitter release and gene transcription. *Trends in pharmacological sciences*. 18:124-134.

Yamamoto, M., R. Sawaya, S. Mohanam, A.K. Bindal, J.M. Bruner, K. Oka, V.H. Rao, M. Tomonaga, G.L. Nicolson, and J.S. Rao. 1994a. Expression and localization of urokinase-type plasminogen activator in human astrocytomas in vivo. *Cancer research*. 54:3656-3661.

Yamamoto, M., R. Sawaya, S. Mohanam, V.H. Rao, J.M. Bruner, G.L. Nicolson, and J.S. Rao. 1994b. Expression and localization of urokinase-type plasminogen activator receptor in human gliomas. *Cancer research*. 54:5016-5020.

Yan, H., D.W. Parsons, G. Jin, R. McLendon, B.A. Rasheed, W. Yuan, I. Kos, I. Batinic-Haberle, S. Jones, G.J. Riggins, H. Friedman, A. Friedman, D. Reardon, J. Herndon, K.W. Kinzler, V.E. Velculescu, B. Vogelstein, and D.D. Bigner. 2009. IDH1 and IDH2 mutations in gliomas. *The New England journal of medicine*. 360:765-773.

Yang, B.S., J.D. Gilbert, and S.O. Freytag. 1993. Overexpression of Myc suppresses CCAAT transcription factor/nuclear factor 1-dependent promoters in vivo. *Molecular and cellular biology*. 13:3093-3102.

Yang, S.A., and C.B. Klee. 2000. Low affinity Ca2+-binding sites of calcineurin B mediate conformational changes in calcineurin A. *Biochemistry*. 39:16147-16154.

Yang, T.T., R.Y. Yu, A. Agadir, G.J. Gao, R. Campos-Gonzalez, C. Tournier, and C.W. Chow. 2008. Integration of protein kinases mTOR and extracellular signal-regulated kinase 5 in regulating nucleocytoplasmic localization of NFATc4. *Molecular and cellular biology*. 28:3489-3501.

Yang, Y., H. Wang, J. Zhang, F. Luo, K. Herrup, J.A. Bibb, R. Lu, and R.H. Miller. 2013. Cyclin dependent kinase 5 is required for the normal development of oligodendrocytes and myelin formation. *Developmental biology*. 378:94-106.

Zanotti, S., and E. Canalis. 2013. Hairy and Enhancer of Split-related with YRPW motif (HEY)2 regulates bone remodeling in mice. *The Journal of biological chemistry*. 288:21547-21557.

Zavadil, J., L. Cermak, N. Soto-Nieves, and E.P. Bottinger. 2004. Integration of TGF-beta/Smad and Jagged1/Notch signalling in epithelial-to-mesenchymal transition. *The EMBO journal*. 23:1155-1165.

Zhang, B.W., G. Zimmer, J. Chen, D. Ladd, E. Li, F.W. Alt, G. Wiederrecht, J. Cryan, E.A. O'Neill, C.E. Seidman, A.K. Abbas, and J.G. Seidman. 1996. T cell responses in calcineurin A alpha-deficient mice. *The Journal of experimental medicine*. 183:413-420.

Zhang, X.P., G. Zheng, L. Zou, H.L. Liu, L.H. Hou, P. Zhou, D.D. Yin, Q.J. Zheng, L. Liang, S.Z. Zhang, L. Feng, L.B. Yao, A.G. Yang, H. Han, and J.Y. Chen. 2008. Notch activation promotes cell proliferation and the formation of neural stem cell-like colonies in human glioma cells. *Molecular and cellular biochemistry*. 307:101-108.

Zheng, H., H. Ying, H. Yan, A.C. Kimmelman, D.J. Hiller, A.J. Chen, S.R. Perry, G. Tonon, G.C. Chu, Z. Ding, J.M. Stommel, K.L. Dunn, R. Wiedemeyer, M.J. You, C. Brennan, Y.A. Wang, K.L. Ligon, W.H. Wong, L. Chin, and R.A. DePinho. 2008. p53 and Pten control neural and glioma stem/progenitor cell renewal and differentiation. *Nature*. 455:1129-1133.

Zhou, Q., and D.J. Anderson. 2002. The bHLH transcription factors OLIG2 and OLIG1 couple neuronal and glial subtype specification. *Cell*. 109:61-73.

Zhu, H., J. Acquaviva, P. Ramachandran, A. Boskovitz, S. Woolfenden, R. Pfannl, R.T. Bronson, J.W. Chen, R. Weissleder, D.E. Housman, and A. Charest. 2009. Oncogenic EGFR signaling cooperates with loss of tumor suppressor gene functions in gliomagenesis. *Proceedings of the National Academy of Sciences of the United States of America*. 106:2712-2716.

Zhu, Y., F. Guignard, D. Zhao, L. Liu, D.K. Burns, R.P. Mason, A. Messing, and L.F. Parada. 2005. Early inactivation of p53 tumor suppressor gene cooperating with NF1 loss induces malignant astrocytoma. *Cancer cell*. 8:119-130.

Zhu, Y., and L.F. Parada. 2001. Neurofibromin, a tumor suppressor in the nervous system. *Experimental cell research*. 264:19-28.

Zhu, Y., and L.F. Parada. 2002. The molecular and genetic basis of neurological tumours. *Nature reviews. Cancer*. 2:616-626.

Zhuo, M., W. Zhang, H. Son, I. Mansuy, R.A. Sobel, J. Seidman, and E.R. Kandel. 1999. A selective role of calcineurin aalpha in synaptic depotentiation in hippocampus. *Proceedings of the National Academy of Sciences of the United States of America*. 96:4650-4655.